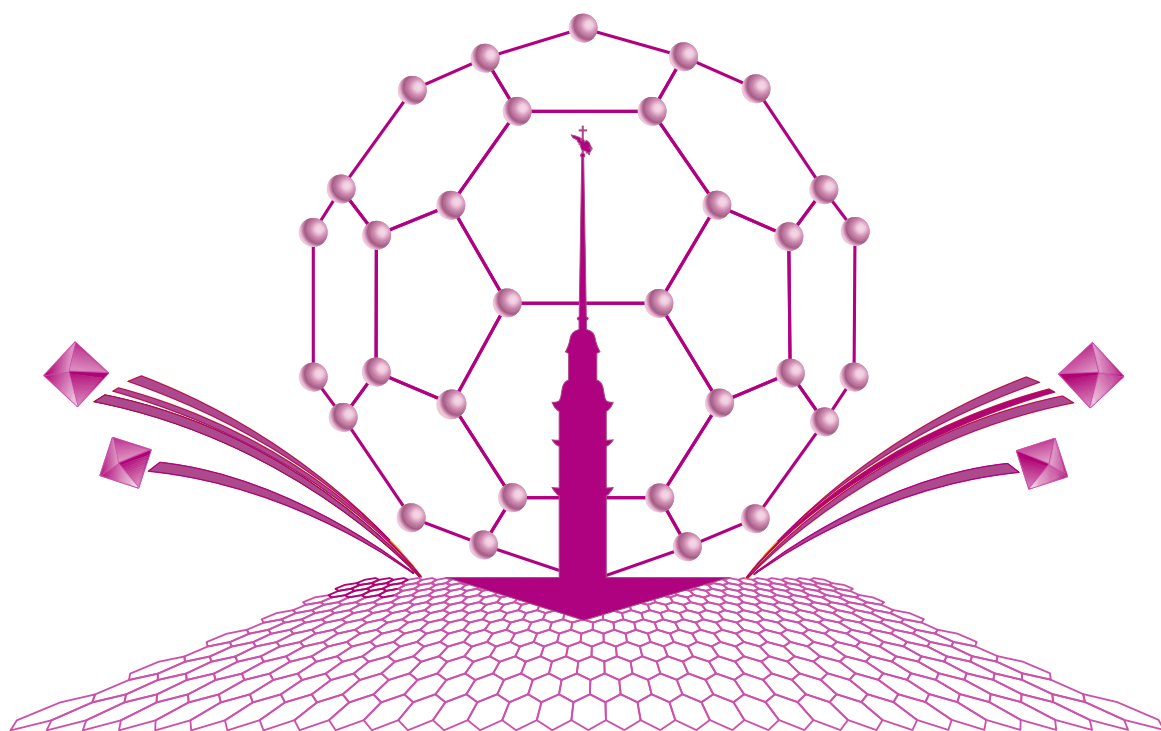


Book of Abstracts

**15th International Conference
Advanced Carbon
Nanostructures**



ACNS'2021

June 28 – July 2, 2021
St Petersburg, Russia

Book of Abstracts

15th International Conference “Advanced Carbon Nanostructures” ACNS’2021

June 28 - July 2, 2021
Saint-Petersburg, Russia

**Book of Abstracts of the 15th International Conference
“Advanced Carbon Nanostructures” (ACNS’2021)
Saint-Petersburg, Russia, June 28 - July 2, 2021
Online Conference**

ISBN 978-5-93634-069-7

Scientific editors: Artur Dideikin, Alexander Meilakhs
Layout: Larisa Zaitseva, Andrey Trofimuk
Design: Vadim Siklitsky

Organizers

- Ioffe Institute, St. Petersburg, *Russia*
- National Research Center "Kurchatov Institute", Moscow, *Russia*
- Petersburg Nuclear Physics Institute named by B.P.Konstantinov of NRC «Kurchatov Institute», St. Petersburg, *Russia*
- St. Petersburg State Institute of Technology, St. Petersburg, *Russia*
- Alferov University, St. Petersburg, *Russia*

in association with Travel Agency "OOO ANDERS"

Partners and Sponsors

- Fund for Infrastructure and Educational Programs
- AVRORA Measuring Technologies

International Advisory Committee

F. Banhart	University of Strasbourg, <i>France</i>
F. Cataldo	Actinium Chemical Research Institute, <i>Italy</i>
L. Echegoyen	University of Texas at El Paso, <i>USA</i>
T. Enoki	Tokyo Institute of Technology, <i>Japan</i>
D. Gruen	Argonne National Laboratory, <i>USA</i>
R. Kalish	Israel Institute of Technology, Technion, <i>Israel</i>
H. Murayama	The KAITEKI Institute, Inc., <i>Japan</i>
E. Osawa	NanoCarbon Research Institute Co., Ltd., <i>Japan</i>
O. Williams	Cardiff University, <i>UK</i>

International Program Committee

Artur T. Dideikin	Chair , Ioffe Institute, <i>Russia</i>
Alexander Meilakhs	Secretary , Ioffe Institute, <i>Russia</i>
Andrey Trofimuk	Secretary Assistant , Ioffe Institute, <i>Russia</i>
V.L. Aksenov	Joint Institute for Nuclear Research, <i>Russia</i>
A.E. Aleksensky	Ioffe Institute, <i>Russia</i>
M.V. Baidakova	Ioffe Institute, <i>Russia</i>
M. Brzhezinskaya	Helmholtz-Zentrum Berlin, <i>Germany</i>
V.Yu. Dolmatov	Federal State Unitary Enterprise "Special Design and Technological Office "Technolog", <i>Russia</i>
A.V. Eletskii	National Research Center "Kurchatov Institute", <i>Russia</i>
M.V. Korobov	Moscow State University, <i>Russia</i>
S.V. Kozyrev	Center for Advanced Studies of Peter the Great St. Petersburg Polytechnic University, <i>Russia</i>
A. Krashennnikov	Helmholtz-Zentrum Dresden-Rossendorf, <i>Germany</i>
I.I. Kulakova	Moscow State University, <i>Russia</i>
I.V. Murin	St. Petersburg University, <i>Russia</i>
A.V. Okotrub	Nikolaev Institute of Inorganic Chemistry SB RAS, <i>Russia</i>
L.B. Piotrovsky	Institute of Experimental Medicine, <i>Russia</i>
O.A. Shenderova	Adamas Nanotechnologies, <i>USA</i>
A.M. Shikin	St. Petersburg State University, <i>Russia</i>
V.I. Sokolov	A.N. Nesmeyanov Institute of Organoelement Compounds RAS, <i>Russia</i>
A.P. Vozniakovskii	Federal State Unitary Enterprise Scientific Research Institute for Synthetic Rubber, <i>Russia</i>
A.Ya. Vul'	Ioffe Institute, <i>Russia</i>

Organizing Committee

Alexander Ya. Vul'	Conference Chair , Ioffe Institute, <i>Russia</i>
Konstantin Reich	Deputy Chair , Ioffe Institute, <i>Russia</i>
Irina V. Vorobyova	Secretary , Ioffe Institute, <i>Russia</i>
B.B. Chaivanov	National Research Center "Kurchatov Institute", <i>Russia</i>
P.N. Brunkov	Ioffe Institute, <i>Russia</i>
A.Yu. Egorov	Alferov University, <i>Russia</i>
I.L. Eremenko	Kurnakov Institute of General and Inorganic Chemistry, <i>Russia</i>
S.V. Kalyuzhnyi	RUSNANO, <i>Russia</i>
V.V. Kveder	Institute of Solid State Physics RAS, <i>Russia</i>
S. V. Sarantseva	Petersburg Nuclear Physics Institute named by B.P.Konstantinov of NRC «Kurchatov Institute», <i>Russia</i>
A.P. Shevchik	St. Petersburg State Institute of Technology, <i>Russia</i>

Timetable

	GMT+3	
Monday, June 28	11.00-11.15	<i>Opening</i>
	11.15-12.15	Online session: Graphene & Related Materials (O1-1)
	12.15-13.15	Online session: Graphene & Related Materials (O1-2)
	13.15-14.00	<i>Lunch time</i>
	14.00-15.00	Online session: Graphene & Related Materials (O1-3)
	15.00-16.00	Online session: Graphene & Related Materials (O1-4)
	16.00-16.15	<i>Break</i>
	16.15-17.15	Online session: Graphene & Related Materials (O1-6)
	17.15-18.15	Online session: Graphene & Related Materials (O1-6)
	18.15-19.15	Plenary lecture: Dieter M. Gruen (I-01)
Tuesday, June 29	11.00-11.45	Invited lecture: Chris Ewels (I-02)
	11.45-12.45	Online session: Carbon Nanostructures (O2-1)
	12.45-13.00	<i>Break</i>
	13.00-14.00	Online session: Carbon Nanostructures (O2-2)
	14.00-14.45	Invited lecture: Raul Arenal (I-03)
	14.45-15.30	<i>Lunch time</i>
	15.30-16.30	Online session: Carbon Nanostructures (O2-3)
	16.30-17.15	Invited lecture: David Tomanek (I-04)
	17.15-18.15	Online session: Carbon Nanotubes (O2-4)
	18.15-18.30	<i>Break</i>
	18.30-19.30	Online session: Carbon Nanotubes (O2-5)
19.30-20.15	Invited lecture: Boris Yakobson (I-05)	
Wednesday, June 30	The 7th one-day Conference-School of Young Scientists "Advanced Carbon Nanostructures and Methods of their Diagnostics"	
	11.00-11.15	<i>Opening</i>
	11.15-12.00	Invited lecture: Viktor Vins (I-06)
	12.00-13.00	Online session: Reports of young scientists (Y3-1)
	13.00-13.45	Invited lecture: Valerii Dolmatov (I-07)
	13.45-14.00	<i>Break</i>
	14.00-14.45	Invited lecture: Sergey Lermontov (I-08)
	14.45-15.30	<i>Lunch time</i>
	15.30-16.15	Invited lecture: Egor Lychagin (I-09)
	16.15-17.15	Online session: Reports of young scientists (Y3-2)
	17.15-18.00	Invited lecture: Aleksandra Siklitckaia (I-10)
	18.00-18.15	<i>Break</i>
	18.15-19.00	Invited lecture: Alexander Vasiliev (I-11)
	19.00-20.00	Online session: Reports of young scientists (Y3-3)
20.00-20.15	<i>Closing remarks</i>	
Thursday, July 01	11.00-11.45	Invited lecture: Andrey Knizhnik (I-12)
	11.45-12.45	Online session: Nanodiamond Particles (O4-1)
	12.45-13.30	Invited lecture: Stepan Stehlik (I-13)
	13.30-14.30	Online session: Nanodiamond Particles (O4-2)
	14.30-15.15	<i>Lunch time</i>
	15.15-16.00	Invited lecture: Ken Haenen (I-14)
	16.00-17.00	Online session: Nanodiamond Particles (O4-3)
	17.00-18.00	Online session: Fullerenes (O4-4)
	18.00-18.15	<i>Break</i>
	18.15-19.15	Online session: Fullerenes (O4-5)
19.15-20.00	Invited lecture: Cami Jan (I-15)	
Friday, July 02	11.00-11.45	Invited lecture: Cecilia Ménard-Moyon (I-16)
	11.45-12.45	Online session: Applications of Nanocarbons (O5-1)
	12.45-13.00	<i>Break</i>
	13.00-13.15	Invited speaker: Sergey Kulikov (I-17)
	13.15-14.00	<i>Lunch time</i>
	14.00-15.00	Online session: Applications of Nanocarbons (O5-2)
15.00-15.30	<i>Closing remarks</i>	

Invited Lectures

Solar cells based on graphene's quantum electrodynamic properties

*Gruen D.M.*¹

dietergruen@comcast.net

¹ Argonne Distinguished Fellow, Emeritus

Single junction solar cells such as silicon cells are subject to the Shockley/Queisser conversion efficiency limit of 32%. Remarkably, multijunction multi semiconductor/tunnel solar cells were developed over the years that have in fact achieved conversion efficiencies near 50%. Unfortunately, these cells suffer from fabrication costs so high as to prevent their deployment in solar power applications. Still, global access to low cost high conversion efficiency solar cells becomes ever more pressing day by day.

Attempts at the creation of "hot carrier" solar cells with theoretical efficiencies up to 86% originated with the inception of that concept 40 years ago. The energies of "hot carriers" are of course far above thermal equilibrium. Thus, they must be extracted using exquisitely timed sequential processes to be charge separated at a junction within femtoseconds after photoexcitation. It is essential that extraction occur before phonon emission leads to lattice thermalization in order successfully to convert most of the absorbed photon energy to electricity. Traditional semiconductors do not appear to lend themselves to "hot carrier" solar cell applications. Their relatively low opacities and carrier mobilities require time regimes too long, on the order of picoseconds, for "hot carrier" extraction to be carried out.

The discovery of graphene has provided a novel substance, Dirac matter, with optical and electrical properties that can, in principle, largely overcome these limitations. Graphene's opacity, larger on a per atom basis than that of any other substance, is determined by the fine structure constant and is wavelength independent. Graphene electrons behave like massless Fermions with near relativistic velocities. In addition, "hot carriers" in graphene have exceptionally long lifetimes because of the so-called "phonon bottleneck" thus facilitating extraction before thermalization processes take over.

The use of graphene as the absorber in a solar cell is accomplished using a 2D/1D van der Waals heterostructure. High aspect ratio ZnO nanowires are clad with single layer graphene produced by the self-limited thermal decomposition of polyaromatic hydrocarbons. Such prototype cells display an open circuit potential of 2 eV and short circuit currents of one milliamp/cm² when irradiated with simulated AMG 1.5 sunlight. The uniquely high cell voltage exceeds that of silicon cells by a factor of about four. Reduction of the cell series resistance is expected to result in an increase in current to a modest 25 ma/cm². At the completion of a performance optimization stage, common for new types of solar cells, PCE's larger than 50% would indicate that a solar cell with "hot carrier" properties has been achieved.

The choice of the SLG/ZnO nanowire architecture finds support in a considerable number of detailed experimental and theoretical studies of the electronic structure at the junction formed between these two materials. Importantly, when in contact with an electron acceptor, the work function of ZnO has been shown to increase by more than two volts. The resulting large work function difference thus enables the highly energetic carriers to transit in attoseconds from graphene to the bottom of the ZnO conduction band. The attractive interaction between ZnO and graphene has been revealed to be dipole-induced dipole in nature by several density functional calculations. The attractive van der Waals forces preserve intact the quantum electrodynamic structure of graphene. Although ZnO is a wide band-gap material, it has a very sizable surface electrical conductivity which has been found strongly to increase with decreasing nanowire diameter. Selective doping during growth leads to surface metallic conductivity. Further discussion of ZnO nanowire properties is beyond the scope of this abstract.

Forming the Void: Folding, Twisting and Collapsing Carbon

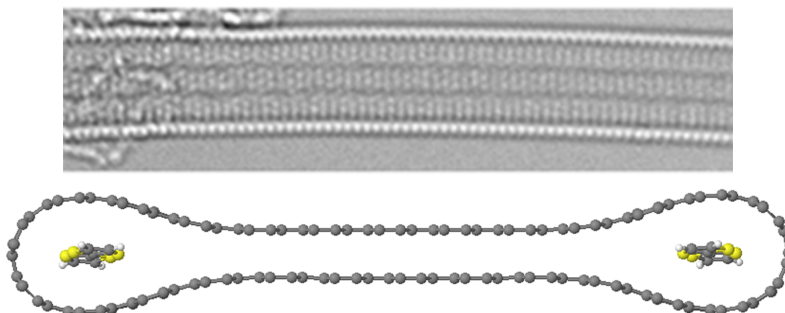
*Ewels C.P.*¹

chris.ewels@cnr-immn.fr

¹ Institut des Matériaux Jean Rouxel (IMN), CNRS / University of Nantes, Nantes, France

Carbon nano-objects can often be conceived as carbon sheets distorted, folded, rolled or coned in different ways. However, it is interesting to examine the inverse and consider not the objects themselves but the void spaces they create. There are a number of ways carbon can be used to confine other materials, either modifying bulk behavior or inducing unique low-dimensional change in the materials they are hosting.

In this talk I will compare edge and buckle (dislocation) formation in graphite [1,2] with behavior in individual nano-objects. Conventional study of nanotubes assumes circular cross-section central cavities, but many other cavity types are possible in these unusual materials, depending on their size and production method [3,4]. I will explore some possibilities to exploit the resultant void spaces, notably the formation of new 1D material phases of intercalants such as phosphorus [5]. Via a combination of theory and experiment we show that encapsulation within intermediate diameter cavities (1.5-2.5 nm) results in red phosphorus-like chain formation, and from this are able to build up a low-dimensional phase diagram for phosphorus constrained in carbon cavities. Finally, if there is time I will extend the talk to the formation of 0D voids in carbon, namely new DFT predictions concerning formation and destruction pathways in ultra-small fullerenes, of relevance to the interstellar medium [6,7].



(top) Experimental image of phosphorus filled single walled carbon nanotube (bottom) collapsed carbon nanotube with filling of the edge cavities.

References

1. M. I. Heggie, I. Suarez-Martinez, C. Davidson, G. Haffenden, *J. Nucl. Mater.* (2011) **413**, 150-155.
2. J. G. McHugh, P. Mouratidis, A. Impellizzeri, K. Jolley, D. Erbahar, C. P. Ewels, in preparation (2021).
3. A. Cefas Torres Dias, M. Monthieux, A. Penicaud, A. Impellizzeri, E. Pichaut, C. Ewels, in preparation (2021).
4. E. Picheau, A. Impellizzeri, D. Rybkovskiy, M. Bayle, J.-Y. Mevellec, F. Hof, H. Saadoui, L. Noé, A. Dias Torres, J.-L. Duvail, M. Monthieux, B. Humbert, P. Puech, C. P. Ewels, A. Pénicaud, *ACS Nano* (2021) **15**, 596-603; *Phys. Rev. B* (2019) **100**, 115410.
5. V. O. Koroteev, D. Rybovskiy, A. Impellizzeri, A. A. Vorfolomeeva, A. V. Okotrub, A. L. Chuvilin, L. G. Bulusheva, C. P. Ewels, in preparation (2021).
6. Y. Tanuma, P. Dunk, T. Maekawa, C. P. Ewels, in preparation (2021).
7. Full publication list available with pdf links from www.ewels.info

Structural and chemical analyses at the atomic scale of carbon nanomaterials

Arenal R.^{1,2,3}

arenal@unizar.es

¹ Instituto de Nanociencia y Materiales de Aragon (INMA), CSIC-Universidad de Zaragoza, 50009 Zaragoza, Spain

² Laboratorio de Microscopias Avanzadas, Universidad de Zaragoza, 50018 Zaragoza, Spain

³ ARAID Foundation, 50018 Zaragoza, Spain

Detailed structural and chemical composition analyses, at the atomic scale, of nanomaterials are required in order to determine their impact on the properties of such objects. Transmission electron microscopy (TEM) and in particular, spatially-resolved electron energy loss spectroscopy (SR-EELS) developed in an aberration-corrected TEM, is the most powerful technique to get this information. Indeed, having access to a close to 1 angstrom electron probe, the atomic configuration of these nanomaterials can be obtained [1-8].

In this communication, I will present a selection of recent works involving all these matters. These works will concern the study of the atomic structure & configuration of 1D and 2D atomically thin nanostructures (including nanotubes & graphene/graphene-like material in pristine and hybrid forms) as well as the opto-electronic properties studies carried out via EELS measurements [1-7]. These works will illustrate the excellent capabilities offered by the use of a Cs probe-corrected (S)TEM, combined with the use of a monochromator, to study these properties within a very good spatial resolution. Furthermore, I will also present some recent in-situ TEM-EELS studies showing how powerful this approach can be for allowing the simultaneous measurement of various physical and chemical features of high interest for the study of different phenomena as the reduction of graphene oxide (GO) thin films [6,7].

References

1. R. Arenal, L. Alvarez, J.-L. Bantignies, To be submitted.
2. R. Arenal, A. Lopez-Bezanilla, ACS Nano 8, 8419 (2014).
3. M. Serra, R. Arenal, R. Tenne, Nanoscale 11, 8073 (2019).
4. A. Setaro, M. Adeli, M. Glaeske, D. Przyrembel, T. Bisswanger, G. Gordeev, M. Weinelt, R. Arenal, R. Haag, S. Reich, Nature Comm. 8, 14281 (2017).
5. R. Canton-Vitoria, T. Scharl, A. Stergiou, A. Cadranel, R. Arenal, D.M. Guldi, N. Tagmatarchis, "Angewandte 59, 3976 (2019).
6. M. Pelaez-Fernandez, A. Bermejo-Solis, A.M. Benito, W.K. Maser, R. Arenal, Carbon 178, 477 (2021).
7. S. Hettler, D. Sebastian, M. Pelaez-Fernandez, A.M. Benito, W.K. Maser, R. Arenal, 2D Materials 8, 031001 (2021).
8. The research leading to these results has received funding from the EU under Grant Agreements 823717 "ESTEEM3" and 881603 Graphene Flagship as well as from the Spanish MICINN (PID2019-104739GB-100/AEI/10.13039/501100011033).

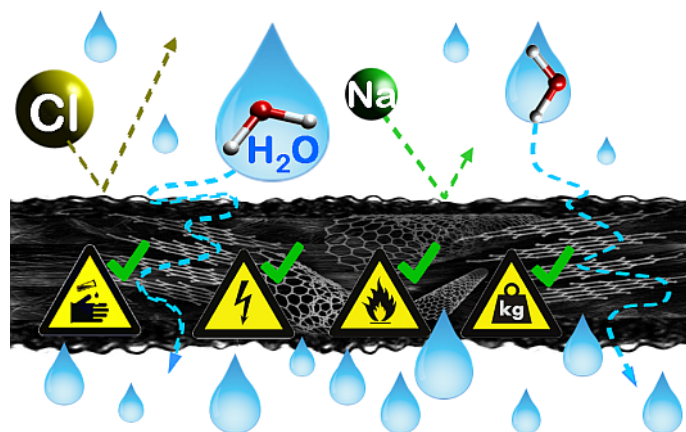
Water! Water!^{*,2}

*Tomanek D.*¹

tomanek@msu.edu

¹ Michigan State University

Whereas water itself is bountiful on Earth, much of it requires treatment to make it suitable for human consumption. Lack of potable water is currently the leading cause of death, ahead of any disease. Recent progress in fabricating nanostructured carbon allotropes may bring a long-awaited paradigm shift in designing membranes that would make efficient desalination of salt water and filtration of contaminated water possible. A previously unexplored membrane design² based on a unique layered assembly of carbon nanostructures including graphite oxide (GO), buckypaper consisting of carbon nanotubes, and a strong carbon fabric should provide high mechanical strength and thermal stability, resilience to harsh chemical cleaning agents and electrical conductivity, thus addressing major shortcomings of commercial reverse osmosis membranes. Microscopic insight into the critical permeation of water molecules in-between GO layers and across in-layer vacancy defects in graphitic carbon can be obtained using *ab initio* density functional theory calculations. Results of these computational studies elucidate the reason for selective rejection of solvated Na^+ ions in an optimized layered all-carbon membrane.



Design and advantages of an all-carbon membrane for water desalination and filtration.

References

^{*} In collaboration with Andrii Kyrylchuk. Partly funded by the NSF/AFOSR EFRI 2-DARE grant number EFMA-1433459 and the Fulbright Foundation.

² David Tomanek and Andrii Kyrylchuk, *Designing an All-Carbon Membrane for Water Desalination*, *Phys. Rev. Applied* **12**, 024054 (2019).

1D-carbon nanotubes and 2D-layers synthesis, insights from thermodynamics to kinetics

*Yakobson B.I.*¹, *Bets K.V.*¹

kb13@rice.edu

¹ Rice University, Houston, TX 77005, USA

There is no unified, synthetic theory of nanotube or 2D-materials growth, no “ToE”. Perhaps never will be, yet useful progress can be achieved. By embracing old ideas of Burton–Cabrera–Frank, we once introduced a dislocation-growth model for nanotubes [PNAS 106, 2506, 2009], a seed for later nanoreactor approach [PNAS 109, 15136, 2012], allowing one to use DFT computations for 2D-material growth kinetics or emerging shapes. It works well in many cases but not all, leaving plenty of room for creativity. We will discuss things new -- since just before the “Covid era” -- from nanotube-edge evolutions [ACS Nano, 13, 8836, 2019], complementarity in lateral epitaxy [Nano Lett., 19, 2027, 2019; Nature, 579, 219, 2020] and flash-synthesis of graphene [Nature, 577, 647, 2020]. to chemically induced graphene → diamond transformation (“no pressure–good science”, as AVS T-shirts once claimed) [Small, 16, 2004782, 2020], and if time permits possibly new physics achievable in hetero-bilayers [Nat. Comm. 11, 2989, 2020 || Nano Lett. 21, 785, 2020 || JACS 143, 350, 2021], and even about machine learning (ML) about CNT [K. Bets, A. Kutana, P. O'Driscoll, BIY, in progress].

Engineering of atomic defects in the crystal structure of diamond

*Vins V.G.*¹

vgvins@gmail.com

¹ LLC VELMAN, Novosibirsk, Russia

The regularities of the transformation of atomic defects in the structure of laboratory-grown and natural diamonds have been studied under two main methods of exposure: radiation damage and high-temperature annealing, which provide almost exhaustive possibilities for controlling defects in diamond. As a result, a material with a given set of properties can be obtained, which is promising for various ultra high-tech applications.

Theory and practice of detonation synthesis of nanodiamond, its properties and application.

*Dolmatov V.Yu.*¹

diamondcentre@mail.ru

¹ Federal State Unitary Enterprise "Special Design and Technological Bureau "Technolog", St. Petersburg, Russia

The review lecture shows the existing models of the structure of detonation nanodiamonds (DND), images of various types of DND depending on the initial explosives (HE), considers the basics of explosive decomposition of explosives, the parameters affecting the DND yield. The modern concepts of the possible mechanisms of the formation of nanodiamonds are shown. The concept of specific power of explosives, the possibility of predictive estimation of the DND yield during explosive explosion, depending on the detonation velocity, specific power and pressure in the Chapman-Jouguet plane, has been introduced. The process of DND synthesis from individual, binary and triple explosive charges is shown, the optimal economical range of DND yield is set at 6.0 - 8.2% wt. Various versions of DND doping with boron, phosphorus, lithium, and silicon are given.

Comparative characteristics of diamonds of static and detonation synthesis, compositions of crude detonation carbon (diamond blend, DB) and DND, sizes of diamond cores are presented. The identity of DND was shown regardless of the explosives used and the synthesis conditions. The volume of the DND cluster and the primary "indestructible aggregate" was determined to be $3.5 \cdot 10^6 \text{ \AA}^3$.

The diversity of DND applications is shown: galvanic processes (with chromium, nickel, aluminum and other metals), the physical and mechanical characteristics of coatings are given, the results of polishing various DND materials, the effects of DND use in polymer compositions, fuel systems, an increase in crop yields are given, the effect of using DB and DND in lubricating compositions. The main directions of using DND in medicine, biology, cosmetology are given.

It has been shown that DND act as classical antioxidants, affecting malignant tumors. Data on the removal of DND from the body are presented; the lungs are the most effective organ for this purpose.

Summarizing conclusions on all areas of research and application of DND are presented.

Carbon Aerogels - Synthesis, Properties, Application

*Lermontov S.A.*¹

lermontov52@yandex.ru

¹ Institute of Physiologically Active Compounds, RAS

Aerogels are new mesoporous materials with a large specific surface area (more than 1000 m²/g), high porosity (95-99%), and low density. The pore size in aerogels (AG), as a rule, lies in the range of 2-20 nm. According to their composition, aerogels are divided into oxide (SiO₂, Al₂O₃, TiO₂, etc.), organic (resorcinol-formaldehyde, carbohydrate, polyolefin - for example, based on ultra-high molecular weight polyethylene UHMWPE), hybrid aerogels.

Electrically conductive carbon aerogels (C-AG), which consist of disordered graphene fragments, play a special role. These materials can be used as electrodes in chemical current sources, sorbents, catalysts, and materials that absorb electromagnetic radiation (EMR).

The report will describe the basic principles and methods for the synthesis of aerogels, including C-AG. It is supposed to provide information on methods for studying the structure of AG, the dependence of their properties on the conditions of obtaining. Information on the preparation and properties of composite materials based on aerogels, including C-AG, will be presented.

Neutron activation analysis for diagnostics of advanced carbon nanomaterials

*Lychagin E.V.*¹

lychag@nf.jinr.ru

¹Joint Institute for Nuclear Research, Frank Laboratory of Neutron Physics, Dubna, Moscow region, Russia.

Carbon nanomaterials comprise the large part of surface atoms and most often contain significant amounts of impurity atoms or radicals. These impurities may occur both in the process of producing and special processing of nanostructures. Sometimes the occurrence of these impurities significantly limits the possibility of using nanostructures when solving specific tasks.

For example, nanodiamond powder is extremely attractive to use as a material for very cold neutron (VCN) reflectors [1, 2]. To date, there are no such reflectors in physical tools. The development of such reflectors will allow to significantly increase the amount of VCNs on extracted neutron beams, which will expand the range of neutron research both in studying the condensed matter physics and fundamental research. Impurity atoms with large neutron capture cross sections or activation cross sections can significantly degrade the property of such a material.

To quantitatively determine the elemental composition of impurities in nanodiamond powder and to develop a technique for its purification, it was natural to use the neutron activation analysis method. This nuclear physics method has been widely used as a powerful analytical method for multielement analysis in various fields of science (see, for example, [3]). The method also turned out to be a very productive tool for studying impurities in nanodiamonds. Carbon, which is the main element of the sample "matrix", is not activated on the one hand (i.e., it does not generate background signals), and it allows the use of carbon gamma lines to determine the concentration of impurities using a relative method when measuring the intensities of prompt gamma quanta on the other hand.

The features of the neutron activation analysis and its variety - prompt gamma quanta analysis illustrated by studies of impurities in detonation synthesis nanodiamond powders and the search for a technology for their purification will be presented in the lecture.

References

1. V. Nesvizhevsky, E.V.Lychagin, A.Yu.Musychka, A.V.Strelkov, G. Pignol, K.V. Protasov "The reflection of very cold neutrons from diamond powder nanoparticles" // Nuclear Instruments and Methods in Physics Research Section A: Accelerators, Spectrometers, Detectors and Associated Equipment **595**, (2008) 631-636 DOI: 10.1016/j.nima.2008.07.149
2. Lychagin E.V., Muzychka A.Yu., Nekhaev G.V., Nesvizhevsky V.V., Pignol G., Protasov K.V., Strelkov A.V. "Storage of very cold neutrons in a trap with nano-structured walls" // Physics Letters B **679** (2009) 186-190 <https://doi.org/10.1016/j.physletb.2009.07.030>
3. Frontasyeva M.V. «Neutron Activation Analysis in the Life Sciences» // Physics of Elementary Particles and Atomic Nuclei T.42, B.2 (2011) 635 (in Russian) http://www1.jinr.ru/Pepan/2011_v42/v-42-2/05_fron.pdf

Modelling the carbonaceous nanostructures: modern advances

*Siklitskaya A.*¹, *Kubas A.*¹, *Lewandowska-Andralojc A.*^{2,3}

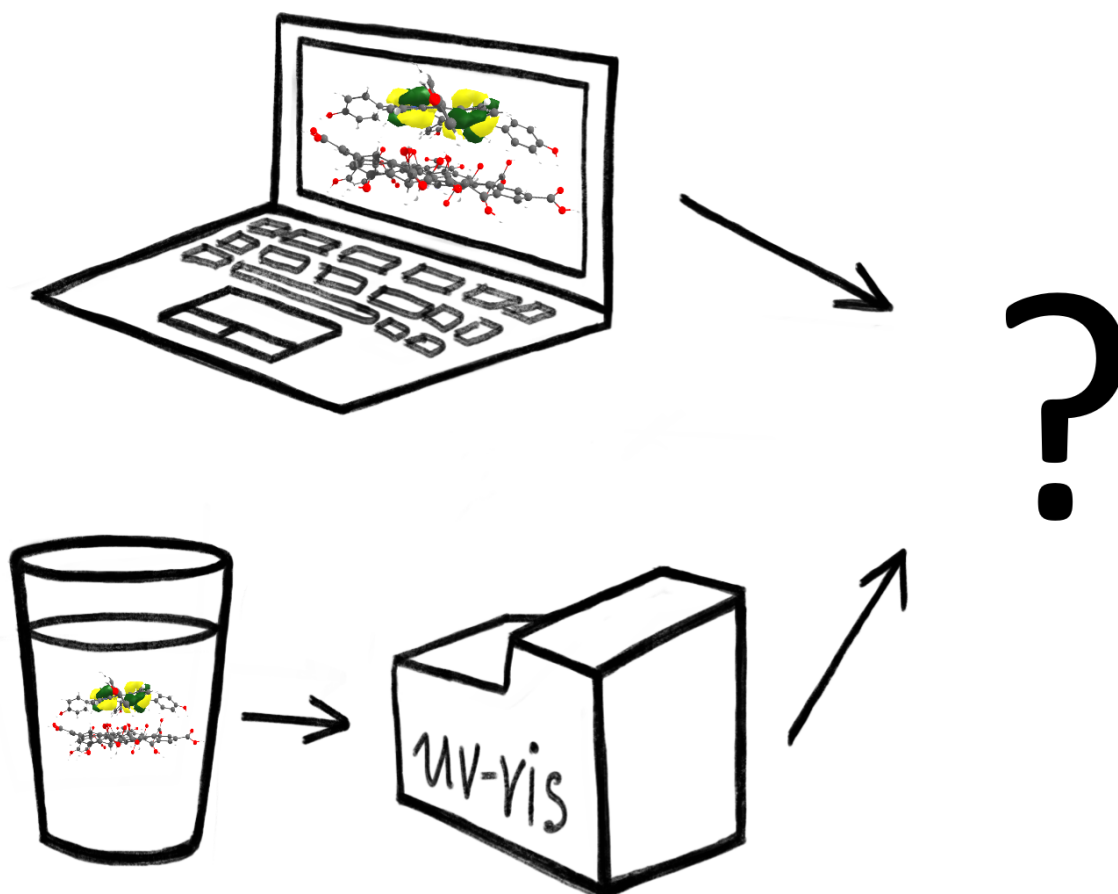
asiklit@ichf.edu.pl

¹ Institute of Physical Chemistry Polish Academy of Sciences, Kasprzaka 44/52, 01-224, Warsaw, Poland

² Faculty of Chemistry, Adam Mickiewicz University, Uniwersytetu Poznanskiego 8, 61-614, Poznan, Poland

³ Center for Advanced Technology, Adam Mickiewicz University, Uniwersytetu Poznanskiego 10, 61-614, Poznan, Poland

Carbonaceous materials include graphene, fullerenes, nanodiamonds and all the allotropic variants of this unique element. This lecture will be a hands-on about the practical possibilities of the modern computational techniques starting from the molecular dynamics up to high-end quantum chemical calculations. We will discuss the UV-vis spectra, efficient geometry optimization and the limitations of the above mentioned methods[1].



References

1. "Lerf-Klinowski-type models of graphene oxide and reduced graphene oxide are robust in analyzing non-covalent functionalization with porphyrins", *Scientific Reports* **volume 11**, Article number: 7977 (2021), <https://www.nature.com/articles/s41598-021-86880-1>

Transmission electron microscopy in the study of carbon-based nanostructures.

Vasiliev A.L.^{1,2}

a.vasiliev56@gmail.com

¹ National Research Centre "Kurchatov Institute"

² Shubnikov Institute of Crystallography of Federal Scientific Research Centre "Crystallography and Photonics" of Russian Academy of Sciences, Moscow, Russia

Transmission electron microscopy (TEM) and scanning transmission electron microscopy (STEM) traditionally occupies an important place in the study of various nanomaterials, including carbon allotropes. Carbon nanomaterials represent the full spectrum of nanomaterials 1D - single-walled carbon nanotubes, 2D - graphene and a wide range of 3D materials - diamonds, multi-walled nanotubes, graphite fibers. A comprehensive study of all these materials is possible only due to recent technical progress in S/TEM instruments and methods. First of all that is the aberration-corrected (AC) S/TEM, which allowed one to use relatively low accelerating voltage. The lower down the accelerating voltage is important because strong knock-on damages occur at typical for electron microscopes accelerating voltage of 200-300 kV. With the development of AC STEM atomic resolution can be achieved together with uncomplicated image interpretation. AC STEM with the registration of electrons with a high angle annular dark field detector (HAADF) allowed determining the structure of one-dimensional crystal inside the single-wall carbon nanotubes. In this way, the size-dependent structure relations between one-dimensional PbTe nanocrystals and carbon nanotube containers in the diameter range of 2.0–1.25 nm using AC TEM were established [1]. Upon decrease of the confining volume, one-dimensional crystals reveal one-dimensional superstructures with nanometer-scale atomic density modulations together with the possible appearance of the electron density wave. Another example of AC HR TEM exploration is the study of diffusion kinetics by "atoms count" using ZnTe and CuI transport through single defects in a single-wall carbon nanotube [2]. The carbon vacancy pairs in sp²-carbon layer were found as an effective way of matter transport. HAADF STEM technique is used in the study of graphene materials with carbon atoms substituted by nitrogen or oxygen atoms [3]. Another trend in modern electron microscopy is cryogenic TEM (Cryo-TEM). Cryo-TEM together with the low dose technique possesses the 3D reconstruction of not only biological macromolecules but also hydrosols of detonation nanodiamonds (DND). The experimental results obtained by Cryo-Electron Tomography explain the unusual rheological properties based on the network formation due to faceted DND particle interactions [4].

References

1. A. Eliseev, N.S. Falaleev, N.I. Verbitskiy, A.A. Volykhov, L.V. Yashina, A.S. Kumskov, V.G. Zhigalina, A.L. Vasiliev, A.V. Lukashin, J. Sloan, N.A. Kiselev Nano letters (2017) **17**, 805.
2. A. Eliseev, A.S. Kumskov, N.S. Falaleev, V.G. Zhigalina, A.A. Eliseev, A.A. Mitrofanov, D.I. Petukhov, A.L. Vasiliev, and N. A. Kiselev The Journal of Physical Chemistry C (2017) **121**, 23669.
3. Hofer, V. Skákalová, T. Görlich, M. Tripathi, A. Mittelberger, C. Mangler, M.R.A. Monazam, T. Susi, J. Kotakoski and J.C. Meyer Nat. Commun. (2019) **10**, 4570
4. M. Kuznetsov, S.I. Belousov, R.A. Kamyshinsky, A.L. Vasiliev, S.N. Chvalun, E.B. Yudina, A.Ya. Vul Carbon (2021) **174**, 138.

Theoretical modeling of structure and properties of detonation nanodiamonds

*Knizhnik A.A.*¹

knizhnik@kintech.ru

¹ NRC "Kurchatov Institute", Moscow, Russia

Diamond nanoparticles (nanodiamonds, ND) are attracting significant interest due to their excellent mechanical and optical properties, high surface areas, tunable surface structures and non-toxicity. These properties open great perspectives in different technical and medical applications of ND nanostructures. In this work we discuss theoretical modeling of fundamental properties of ND systems, starting from individual particles and up to properties of final ND materials.

At first, we describe available atomistic models of the ND particles, and show how these models determine electronic and optical properties of ND particles based on the results of first-principles calculations. In particular, we stress the role of structural defects on the electronic and optical properties of ND materials. Then we discuss surface chemical activity of nanodiamond particles, and compare it with graphene-based counterparts.

Finally, we present an analysis of structural organization and interaction mechanisms of nanodiamond particles in hydrosols. Using first-principles calculations and macroscopic model we describe an interplay between Coulomb and van der Waals attractions in ND ensembles, which can result in formation of chain-like ND aggregates.

Smaller than usual: preparation, properties, and size effects in sub-5 nm nanodiamonds

*Stehlik S.*¹

stehlik@fzu.cz

¹ Institute of Physics of the Czech Academy of Sciences, Prague, Czech Republic

Diamond nanoparticles, so called nanodiamonds (NDs), translate extraordinary properties of diamond to nanoscale which extend their applications ranging from lubrication to drug delivery [1]. NDs produced by detonation and HPHT techniques are readily available in the 5-100 nm mean-size range having properties similar to the bulk. In the sub-5 nm range, theoretical predictions indicate structural changes, as well as pronounced phonon confinement effects.

In this talk, we review recent advances in the preparation of as small as 1-2 nm NDs of both detonation and HPHT origin by a controllable size reduction via oxidative etching in air [2-4]. HRTEM measurements confirm a stable diamond crystalline structure down to 1 nm [4].

We have found that identification of the nano-sized particle distribution by only a single analytic technique might be problematic and, in some cases, can lead to incorrect and misleading results. Here, a combination of different analytic methods such as DLS, AUC, TEM, SAXS and XRD significantly helps to provide more accurate data and understand the measured characteristics and deviations. Key factors and relations are highlighted concerning the used techniques.

Comparison of Raman spectra at the sub-5 nm scale reveals clear differences between the DND and HPHT NDs and limitations of current phonon confinement models for the size distribution analysis. We have found that diamond core size, structural (im)perfections, and temperature (in)stability due to laser irradiation are key features reflected in the particular NDs' Raman spectrum. The first time observed low-frequency (20–200 cm⁻¹) Raman scattering signals may correspond to "breathing" modes of NDs as these signals exhibit a clear size dependence. Thus, this Raman scattering may provide another way for the size distribution of NDs [5].

Finally, we demonstrate how to apply the 2 nm hydrogenated H-DNDs with positive zeta potential to form homogeneous, ultra-thin, extremely dense (1.3×10^{13} cm⁻²) and smooth (RMS < 1 nm) nucleation layer for growing as thin as 5.5 nm nanocrystalline diamond films with surface-switchable On/Off photoluminescence of SiV centers [6].

References

1. N. Nunn, M. Torelli, G. McGuire, O. Shenderova, *Curr. Opin. Solid State Mater. Sci.* (2017) **21**, 1–9.
2. S. Stehlik, D. Miliaieva, M. Varga, A. Kromka, B. Rezek, *MRS Adv.* (2016) **1**, 1067–1073.
3. S. Stehlik, M. Varga, M. Ledinsky, D. Miliaieva, H. Kozak, V. Skakalova, C. Mangler, T.J. Pennycook, J.C. Meyer, A. Kromka, B. Rezek, *Sci. Rep.* (2016) **6**, 38419.
4. S. Stehlik, M. Varga, M. Ledinsky, V. Jirasek, A. Artemenko, H. Kozak, L. Ondic, V. Skakalova, G. Argentero, T. Pennycook, J.C. Meyer, A. Fejfar, A. Kromka, B. Rezek, *J. Phys. Chem. C.* (2015) **119**, 27708–27720.
5. S. Stehlik, M. Mermoux, B. Schummer, O. Vanek, K. Kolarova, P. Stenclova, A. Vlk, M. Ledinsky, R. Pfeifer, O. Romanyuk, I. Gordeev, F. Roussel-Dherbey, Z. Nemeckova, J. Henych, P. Bezducka, A. Kromka, B. Rezek, *J. Phys. Chem. C.* (2021) **125**, 5647–5669.
6. S. Stehlik, M. Varga, P. Stenclova, L. Ondic, M. Ledinsky, J. Pangrac, O. Vanek, J. Lipov, A. Kromka, B. Rezek, *ACS Appl. Mater. Interfaces.* (2017) **9**, 38842–38853.

Doping of diamond: Importance for nanodiamond particles and nanocrystalline CVD diamond films

Haenen K.^{1,2}

ken.haenen@uhasselt.be

¹ Hasselt University

² IMEC vzw

Diamond is a material that possesses a unique combination of extreme properties [1]. With the advent of nanocrystalline diamond particles (NDP) and films (NCD) the research field has expanded quickly into novel areas where monocrystalline diamond doesn't provide a cost-effective solution. Especially the possibility to dope these materials led to versatile pathways towards advanced device concepts making use of the unique extreme and tuneable properties of diamond. While boron doped NCD films have been available for more than a decade, progress has also seen the advent of phosphorus doped NCD and doped nanoparticles [2-4].

The deposition of closed nanocrystalline diamond (NCD) thin films on non-diamond substrates requires diamond nucleation sites. An established technique for creating nucleation sites is a surface treatment with a water-based colloidal solution of ultra-dispersed nanodiamond (ND) particles [5]. In ND seeding the most important factors are the surface charge of the substrate and the zeta-potential of the used colloid. Together, they determine the nucleation density, which can lead to an extreme difference in the observed seeding density [6-10]. However, surface contamination by hydrocarbons, which is an unavoidable and quick process even in a cleanroom environment, is often not taken into consideration [11]. Here, we investigate and model the impact such surface contamination has on the ND seeding efficiency on thin Ta films, a model system for metal surfaces. We propose an analytical model that describes the dynamics of surface contamination and hydrocarbon contaminant interaction with the surface, and the resulting ND seeding density [12].

To conclude, an insight into possible applications will be given, such as ultra-thin NCD membranes serving as X-ray beam monitors, highly sensitive pressure sensors, or thin nanocrystalline films acting as hosts for germanium vacancy (GeV) colour centres [13-15].

References

1. R.J. Nemanich, K. Haenen, *et al.*, MRS Bulletin **39**/6 (2014), 490-494.
2. W. Janssen, K. Haenen, *et al.*, Physica Status Solidi RRL **8**/8 (2014), 705-709.
3. S. Heyer, K. Haenen, *et al.*, ACS Nano **8**/6 (2014), 5757-5764.
4. S. Temgoua, K. Haenen, *et al.*, submitted (2021).
5. O.A. Williams, K. Haenen, *et al.* Chemical Physics Letters **445**/4-6 (2007), 255-258.
6. O.A. Williams, *et al.*, ACS Nano **4**/8, (2010), 4824-4830.
7. P. Pobedinskas, K. Haenen, *et al.*, Applied Physics Letters **102**/20 (2013), 201609.
8. J. Hees, *et al.*, Nanotechnology **24**/2 (2013), 025601.
9. G. Degutis, *et al.*, Chemical Physics Letters **640**, (2015), 50-54.
10. S. Mandal, *et al.*, ACS Applied Materials & Interfaces **11**/43 (2019), 40826-40834.
11. T. Fujimoto, *et al.*, R. Kohli, K. Mittal (Eds.), Developments in Surface Contamination and Cleaning, William Andrew Publishing (2008), 329-474.
12. P. Pobedinskas, K. Haenen, *et al.*, Applied Surface Science **538** (2021), 148016.
13. K. Kummer, K. Haenen, *et al.*, Review of Scientific Instruments **84**/3 (2013), 035105.
14. S. Drijkoningen, K. Haenen, *et al.*, Scientific Reports **6** (2016), 35667.
15. R. Mary Joy, K. Haenen, *et al.*, submitted (2021).

The Hidden Life of Cosmic Fullerenes

Cami J.^{1,2,3}

jcami@uwo.ca

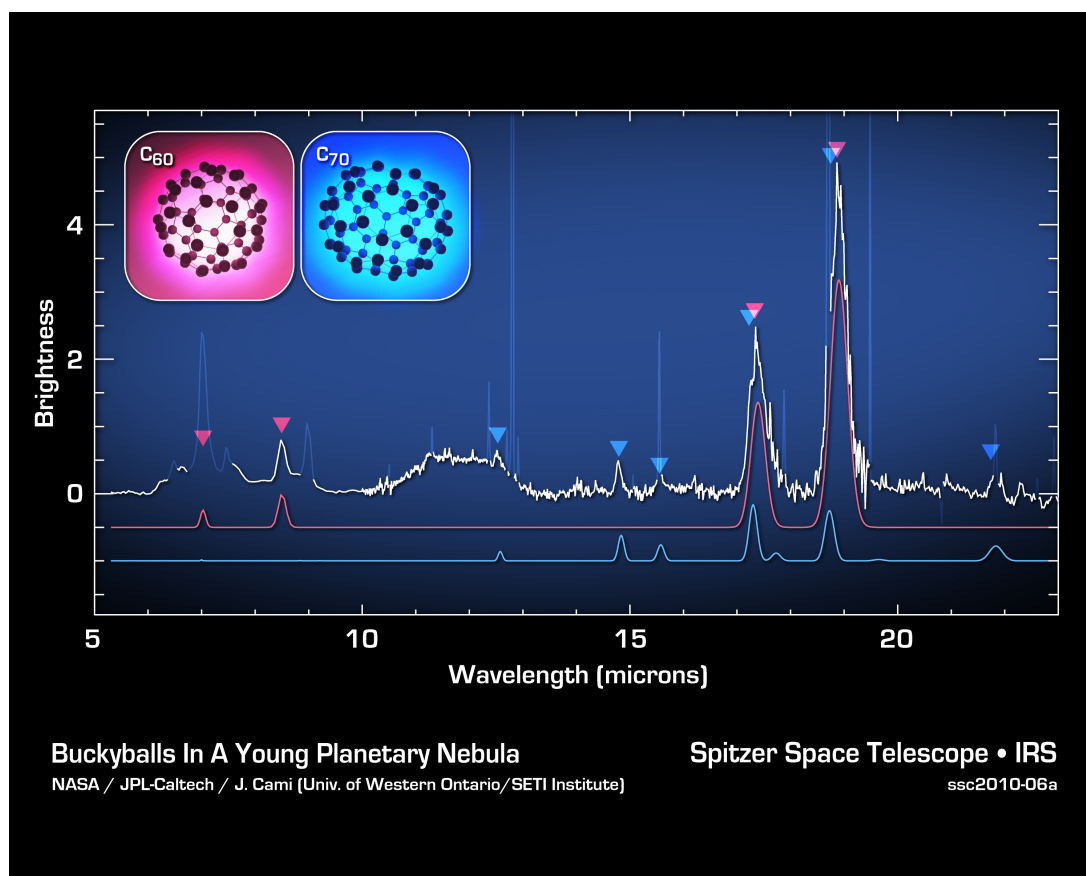
¹ Institute for Earth & Space Exploration, Western University, London N6A 3K7, Canada

² Department of Physics & Astronomy, Western University, London N6A 3K7, Canada

³ SETI Institute, 189 Bernardo Avenue, Suite 100, Mountain View, CA 94043, USA

In recent years, the fullerene species C_{60} (and to a lesser extent C_{70}) has been detected in a variety of astrophysical environments -- from the circumstellar carbon-rich surroundings of evolved stars to interstellar reflection nebulae and young stellar objects. Understanding how these species form, evolve and respond to their environment yields important insights into astrochemistry and the characteristics of large aromatics in space, thought to be the main reservoir of organic material in space.

In this talk, I will present an overview of what we have learned about cosmic fullerenes from astronomical observations, theoretical calculations and recent laboratory experiments, and show how fullerenes have significantly changed our understanding of interstellar chemistry. I will discuss the conditions that appear to be conducive to the formation and/or detection of fullerenes, and highlight some of the difficulties we still face in understanding the formation of fullerenes especially in planetary nebulae.



The infrared spectrum of the planetary nebula Tc 1, recorded by the Spitzer Space Telescope, revealing the clear and unambiguous vibrational modes of C_{60} (red) and C_{70} (blue).

Multifunctionalized carbon nanotubes for applications in diagnosis and therapy

Menard-Moyon C.¹

c.menard@ibmc-cnrs.unistra.fr

¹ CNRS, Immunology, Immunopathology and Therapeutic Chemistry, UPR 3572, University of Strasbourg, 67000 Strasbourg, France

Due to their outstanding physicochemical properties, the application of carbon nanotubes (CNTs) in nanomedicine has been extensively explored. Thanks to their high aspect ratio and tubular shape, they have the capacity to easily cross biological barriers and to be internalized in cells. Functionalization is a key step to increase the dispersibility and biocompatibility of CNTs, to conjugate bioactive molecules and also to impart multimodality.

In this talk, I will describe the synthesis and biological evaluation of CNTs filled with radioactivable metals and functionalized with a targeting antibody for anticancer therapy. I will detail the surface functionalization and characterization of CNTs filled with radioactivable metals [1]. I will also present *in vitro* studies and *in vivo* experiments to evaluate the biodistribution, therapeutic effect, and immunological profile of the conjugates [2,3]. Our results show that the encapsulation of radioisotopes within CNTs and subsequent surface functionalization with targeting ligands is a promising strategy for the selective delivery of radioactivity for therapy and/or diagnosis.

One of the fundamental characteristics of cancer is the deregulation of cell proliferation mechanisms, associated with gene amplification, overexpression or hyperactivation of various cell cycle regulators. In particular, the hyperactivation of cyclin-dependent kinases (CDKs) contributes to cell proliferation in several human cancers. Therefore, given their role in the coordination of cell division, and their prognostic value, these enzymes constitute pharmacological targets of choice for the development of anticancer therapies. In this context, I will present the conjugation of an environmentally-sensitive fluorescent peptide biosensor on the nanotube surface for fluorescence-based detection and quantification of CDK1 activity *in vitro*, in living cells, and *in vivo*. [4] Since alterations in CDK/cyclin activity have been reported in a wide variety of cancers and associated with negative prognosis, this technology should provide a direct means of probing hyperactivation of CDKs, and of guiding therapeutic intervention/decision, thereby contributing to cancer diagnostics, assisting therapeutic programs, and monitoring response to therapeutics.

References

1. Spinato C. *et al.* *Nanoscale*. 2016;8:12626.
2. Perez Ruiz de Garibay A. *et al.* *Sci Rep*. 2017;7:42605.
3. Wang J. T.-W. *et al.* *ACS Nano*. 2020;14:129.
4. Mihaela Tîlmaciu C. *et al.* *Small* 2021;17:2007177.

Day 1: Graphene & Related Materials.

Structural peculiarities of lysozyme-graphene oxide adsorption complexes

Bunyaev V.A.¹, Shnitko A.V.¹, Chernysheva M.G.¹, Ksenofontov A.L.², Badun G.A.¹

chernysheva@radio.chem.msu.ru

¹ M.V. Lomonosov Moscow State University, Moscow, Russia

² Belozersky Research Institute of Physico-Chemical Biology, Lomonosov Moscow State University

Graphene oxide (GO) is an excellent adsorbent for different compounds, including enzymes. Lysozyme is an enzyme that catalyzes the hydrolysis of peptidoglycan, which is the major component of gram-positive bacterial cell wall. It is used in many studies as the model protein and perspective antimicrobial drug. For the development of biochemical applications of GO-lysozyme composites, it is necessary to know the quantitative parameters of adsorption, and whether its enzymatic activity is preserved. We propose to use tritium labeled lysozyme and tritium probe method for quantitative determination of content and structural peculiarities of lysozyme in the adsorption complex with GO. Complex investigation including application of tritium labeled lysozyme for determination of direct amount of protein at GO surface following by tritium bombardment of lysozyme-GO adsorption complexes to reveal structural peculiarities of lysozyme in the complex from the label distribution in the amino acid residues. Besides that, enzymatic activity of lysozyme in the complex with graphene oxide was measured by means of turbidimetry in the relationship to *Micrococcus luteus*.

In present work we used single-layer graphene oxide (SLGO) produced by CheapTubes as a sorbent for lysozyme. SLGO was dispersed in water and mixed with [³H]lysozyme solution to final SLGO concentration 0.4 g/L. The experiment was carried out in protein initial concentration range from 0.17 to 1.2 g/L. Samples were incubated at room temperature for 20-24 h following by centrifugation. Then the radioactivity values of supernatant and precipitate were measured. The first value was used to calculate an equilibrium concentration, and the other one was used for adsorption calculation. It was found that surface concentration of lysozyme was linear increase with concentration growth, but the values were not so high that are presented in the Ref [1].

To determine peculiarities of lysozyme adsorption layer on the SLGO surface, we subjected SLGO-lysozyme composites to bombardment by tritium atoms generated on hot W-wire. Then acid hydrolysis of the protein was performed and specific radioactivity of amino acids was determined. The results were compared with corresponding tritium distribution for lysozyme deposited as monolayer on the glass walls of the reaction vessel. It was found that some amino acid residues, in particular phenylalanine, are not exposed to tritium labeling when protein is adsorbed on SLGO, while it is labeled with high efficiency when protein is displaced on the glass surface. Since lysozyme structure is known from protein data bank, it is possible to predict molecules orientation in the adsorption layer. Such peculiarities will be discussed in the presentation.

References

1. Bai, Z. Ming, Y. Cao, S. Feng, H. Yang, L. Chen, S.-T. Yang, *Colloids Surf. B: Biointerfaces*, (2017), **154**, 96.

Nitrogen-doped graphene with high specific surface area

Chichkan A.S.^{1,2}, Chesnokov V.V.¹

AlexCsh@yandex.ru

¹ Borekov Institute of Catalysis SB RAS, Novosibirsk, Russia

² Novosibirsk State Technical University, Novosibirsk, Russia

Graphene possesses unique electrical conductivity and mechanical properties. The development of such materials and methods for their preparation is very important because of the great potential of their use in electrochemical processes and catalysis [1, 2]. The application of graphene can be extended by modifying it with nitrogen atoms. Compared to carbon atoms, nitrogen atoms embedded in the carbon network of graphene are able to form stronger bonds with the atoms of the supported metals (Pd, Pt, Ni). This feature of N-graphene opens up possibilities for the synthesis of highly dispersed, up to atomic, metal particles [3, 4].

The purpose of this work is to develop a method for the synthesis of nitrogen-doped graphene with a high specific surface area. As a substrate onto which graphene was deposited, magnesium oxide was used; a 40% NH₃-1% C₂H₂-C₂H₄ gas mixture was chosen as the source of catalytic carbon.

The results of studying the effect of the carbonization reaction time on the amount of nitrogen-modified carbon deposited on magnesium oxide, the specific surface area, and the total pore volume at 650 °C and 700 are presented in Table 1

Tabl. 1 Characteristics of N-graphene.

N-Graphene sample	Temperature, °C	Reaction time, min	Content of carbon modified by nitrogen, wt %	Ssp, m ² g ⁻¹
01 21	650	60	5,0	1400
02 21	650	90	6,2	1300
03 21	700	60	13	900
04 21	700	90	20	650

For the first time, N-graphene with a specific surface area of 1400 m² g⁻¹ and a thickness of 2-4 monolayers has been obtained [5]. The maximum content of atomic nitrogen in N-graphene was 5 wt %. An increase in the treatment temperature of magnesium oxide in a 40% NH₃-1% C₂H₂-C₂H₄ mixture from 650 to 700°C leads to a decrease in both the specific surface area of N-graphene and the nitrogen content in it.

References

1. Ning, Z. Fan, G. Wang, J. Gao, W. Qian, and F. Wei // Chem. Commun. (2011) **47**, 5976-5978.
2. A. Bulushev, M. Zacharska, E.V. Shlyakhova, A.L. Chuvilin, Y. Guo, S. Beloshapkin, A.V. Okotrub, and L.G. Bulusheva // ACS Catal. (2016) **6**, 681-691.
3. V. Chesnokov, V.V. Kriventsov, S.E. Malykhin, A.S. Chichkan, and O.Yu. Podyacheva // J. Struct. Chem. (2018) **59**, 876-882.
4. V. Chesnokov, V.V. Kriventsov, S.E. Malykhin, D.A. Svintsitskiy, O.Y. Podyacheva, A.S. Lisitsyn, and R.M. Richards // Diamond Relat. Mater. (2018) **89**, 67-73.
5. V. Chesnokov, A.S. Chichkan, D.A. Svintsitskiy, E.Y. Gerasimov, V.N. Parmon // Doklady Physical Chemistry (2020) **495**, 159-165.

Synergetic effect in graphene/silver nanowire composite suspensions electrical conductivity

Danilov E.A.¹, Veretennikov M.R.^{1,2}, Darkhanov E.V.^{1,3}

EgADanilov@rosatom.ru

¹ JSC "Scientific Research Institute of Graphite-Based Structural Materials "NIIgrafit" (NIIgraphit), Moscow, Russia

² MPEI, Moscow, Russia

³ Mendeleev University of Chemical Technology of Russia, Moscow, Russia

One of the promising ways for obtaining thin electrically conductive patterns for modern electronics, including flexible devices, is inkjet printing technology; therefore it is necessary to improve properties of conductive inks, such as high stability, low electric resistance, small particle size, and, in some cases, optical properties.

Silver nanoparticles are great of interest as one of the ink components due to their low resistance and well-established approaches for synthesis. Graphene has also attracted a lot of attention due to its high conductivity as well as chemical stability.

The aim of the present study was to find the influence of the shape and concentration of silver nanoparticles in hybrid graphene-silver suspensions, on electrical conductivity.

Silver nanowires (AgNWs) were synthesized via a modification of polyol method [1], commercial spherical silver nanoparticles (20-30 nm) (AgNPs) were manufactured by exploding wire method. Few-layered graphene suspensions were produced using ultrasonic direct liquid phase exfoliation routine as described in [2].

Model ink suspensions were prepared by mixing graphene and silver particles suspensions in water-ethanol solution (1:1 vol.) and stabilized with polyvinylpyrrolidone. Total concentration of conductive particles was ca. 6 mg/ml for all suspensions. Electrical conductivity was measured via WTW Cond 3110 (DC).

As can be clearly seen from fig. 1, graphene-AgNWs closely follow the rule of mixtures, whereas graphene-AgNWs system has much higher electrical conductivity (3 times higher as per rule of mixtures at 66 % graphene volume content).

Possible reasons for such behavior, as well as electrical and optical properties of the films prepared from such hybrid inks will be discussed in the full report.

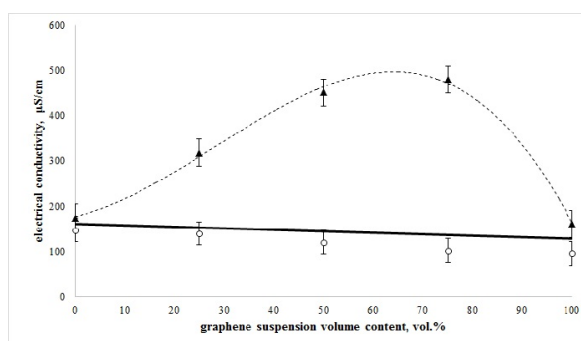


Figure 1 - Electrical conductivity of graphene-silver hybrid suspensions (▲ - graphene-AgNWs, ○ - graphene-AgNPs, solid line - rule of mixtures)

References

1. Sun, and Y. Xia, *Adv. Mater.* (2002) **14**(11), 833–837.
2. M. Samoilov, E.A. Danilov, A.V. Nikolaeva, G.A. Yerpuleva, N.N. Trofimova, S.S. Abramchuk, and K.V. Ponkratov, *Carbon* (2015) **84**, 38–46.

Investigation of alcohols transport through graphene oxide membranes.

*Gurianov K.E.*¹, *Eliseev A.A.*¹, *Petukhov D.I.*¹

GurianovKE@yandex.ru

¹Department of Material Science, Moscow State University, Moscow, Russia

Today membrane technologies are widely used in various fields of human activity. Their main advantages are simple exploitation and low energy consumption. Among the huge number of compounds used for the preparation of membranes, the approach uses two-dimensional materials, such as transition metals chalcogenides, MXenes, metall-organic framework, and graphene oxide, looks very promising. In spite of being discovered in 1850s interest in graphene oxide especially as membrane material constantly increases. The possibility of direct modification and control of its properties allows researchers to use graphene oxide based membranes in such processes as gas separation, gas dehumidification, osmosis, and pervaporation [1-2].

As a material graphene oxide represents itself graphite sheets with different quantity of hydroxyl and carboxyl groups on its surface (C:O ratio is 1,5 – 2,5). A numerous quantity of hydrophilic groups results in high water molecules permeability through membranes. That allows using of them for purification and separation of water mixtures, for example the separation of water and alcohol (C1-C4) dissolved in it.

Graphene oxide was obtained by modified Hummers' method with lateral size is about 800 nm and C:O ratio ~1.7:1. Membranes for mixture separation were formed on anodic alumina substrate by spin-coating method.

In recent work was shown, that interlayer d-spacing and permeability of graphene oxide membranes rapidly increases at growing humidity [3]. These membranes are effective at pervaporation processes, and we are interested in the determination of alcohol transport mechanism within interlayer space of these membranes. SAXS experiment showed, that upon humidity increasing d-spacing is growing up. It means, that the higher alcohol pressure is, the higher permeance of GO membranes is (Fig. 1).

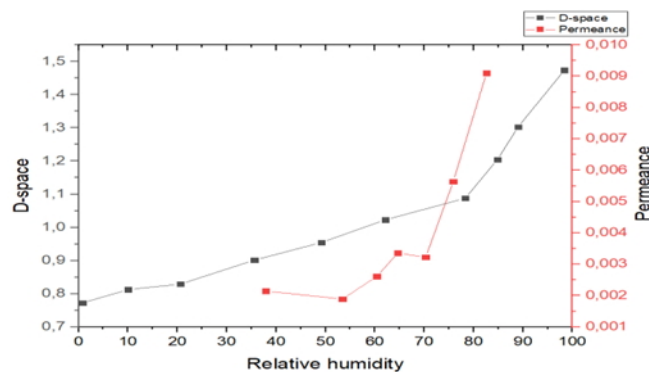


Fig.1. Dependence of interlayer d-spacing and ethanol vapor permeance to relative humidity.

References

1. Bo Guo, Quan-Ian Xiao, Shi-hao Wang, and Han Zhang. *Laser and Photonics Review* (2019), **13**, 1800327.
2. Grzegorz Romaniak, Konrad Dybowski, Agata Jeziorna, Piotr Kula, and Tomasz Kazmierczak. *J. Mater. Sci.* (2020), **55**, 9775-9786.
3. A. Eliseev, A. A. Poyarkov, E. A. Chernova, Ar. A. Eliseev, A. P. Chumakov, O. V. Konovalov, and D. I. Petukhov. *2D Materials*. (2019), **6**, 035039.

Thermal conductivity and heat capacity of nanofluid based on water modified by hybrid material of composition detonation nanodiamonds-carbon nanotubes

Vozniakovskii A.A.¹, Voznyakovskii A.P.², Kidalov S.V.¹, Ovchinnikov E.V.³, Kalashnikova E.I.⁴

kalashnikatja@bk.ru

¹ Ioffe Institute, Saint Petersburg, Russia

² Institute of Synthetic Rubber, Saint-Petersburg, Russian Federation

³ Yanka Kupala State University of Grodno, Grodno, Belarus

⁴ State Institute of Technology, Saint Petersburg, Russia

Carbon nanomaterials such as carbon nanotubes (CNT) and detonation nanodiamonds (DND) are actively used by researchers to create effective coolants, so-called. Nanofluids (NF). However, these nanocarbons have their drawbacks. Thus, it is rather difficult to obtain a stable aqueous suspension of CNT without the use of pavement or chemical surface modification. On the other hand, DND easily forms a stable suspension in water. However, to obtain a significant increase in thermal conductivity, it is necessary to use significantly larger volumes of material in comparison with nanotubes. The aim of this work was to synthesize a DND-CNT hybrid material using the CCVD method and to study its effect on the thermophysical properties of water.

For the synthesis of nanofluids, powders of carbon nanomaterials (DND; SWCNT; powder mixture of DND and SWCNT in a ratio of 7 to 3 and DND-CNT hybrid material) were added to a beaker with water with constant stirring. The beaker was then placed in an ultrasonic bath where the sample was sonicated for 30 minutes with a pause of 5 minutes after every 10 minutes of ultrasonic treatment to prevent overheating of the sample. The concentration of carbon materials was 0.2 wt. %.

As shown in Figure 1, using a hybrid material made it possible to increase thermal conductivity by 94% compared to the original water. Simultaneously, the use of DND and SWCNT made it possible to increase the increase in thermal conductivity only by 12 and 37% compared to the initial water. Simultaneously, the use of DND and SWCNT made it possible to increase the increase in thermal conductivity only by 2 and 5% compared to the initial water. It should be noted that the mechanical mixture of DND and CNT did not form a stable suspension. Moreover, we had to use a surfactant to stabilize the nanotubes. The DND-CNT hybrid material nanofluid's dynamic viscosity was 0.471 mPa*sec., comparable to the initial water's dynamic viscosity at the same temperature (0.467 mPa*sec.).

The reported study was funded by RFBR and BRFR №20-58-00056.

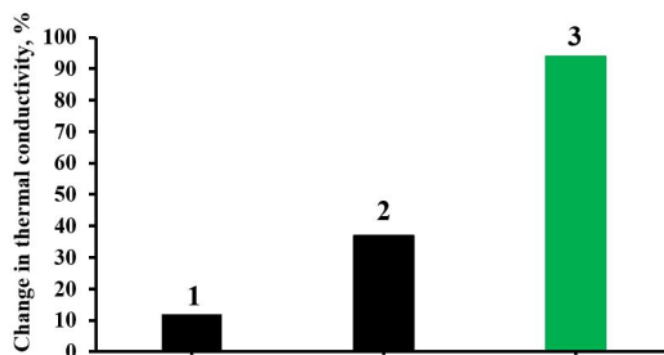


Fig. 1. - Change in thermal conductivity (%) of aqueous suspensions of DND (1), CNT (2) and DND-CNT hybrid material (3) in comparison with the initial water.

Hybrid structures based on oxygen-free graphene and aluminum phthalocyanine chloride

*Klimenko I.V.*¹, *Lobanov A.V.*^{1,2}, *Trusova E.A.*³

inna@deom.chph.ras.ru

¹ Emanuel Institute of Biochemical Physics of Russian Academy of Sciences, Moscow, Russia

² Semenov Federal Research Center for Chemical Physics Russian Academy of Sciences, Moscow, Russia

³ Baikov Institute of Metallurgy and Materials Science of Russian Academy of Sciences, Moscow, Russia

The physicochemical properties of new hybrid structures based on oxygen-free graphene and tetrapyrrole compounds have attracted significant attention because these systems can be used in various sciences and technologies as optical chemosensors, semiconductors, electrocatalysts, and photocatalysts in various chemical reactions, electroluminescent materials, photosensitizers in the photodynamic therapy of cancer, etc. However, the synthesis of such popular hybrid materials is a task of increased complexity for many reasons: environmental, economic, technical, etc. One of them is the problem of obtaining and using oxygen-free graphene, which has a clear advantage over oxidized and reduced oxidized graphene in its electronic properties.

The macroheterocyclic compound of aluminum phthalocyanine chloride (AlClPc) is a photosensitizer characterized by high photoactivity and photostability, big quantum yield of singlet oxygen ($\Phi_{\Delta}=9.1$) and rather high selective penetration into tumour tissue. However, AlClPc has some disadvantages including a tendency to aggregate in aqueous media that considerably reduces its photodynamic activity. One of the most promising method to improve these limitations is using graphene as a part of hybrid systems in conjunction with AlClPc [1].

In this work, we present an original method for the synthesis of hybrid systems based on oxygen-free graphene and AlClPc in liquid media. The sonochemical method was used to obtain a graphene suspension: the ultrasonic exfoliation of the graphene sheets from the surface of synthetic graphite in N,N-dimethylformamide (DMF) or in its mixture with aqua was carried out. The photophysical properties of these hybrid systems have been studied using optical spectroscopy. The obtained results confirm a successful synthesis. It has been proved that graphene contributes to the stabilization of aluminum phthalocyanine in the presence of aqua as a monomer which, unlike the phthalocyanine aggregates, has photochemical and luminescent properties.

The work was carried out according to the state assignment of IBCP RAS (theme No. 01201253304) and government assignment no. 075-00328-21-00. E.A. Trusova thanks RFBR (grant no. 19-03-00554_a) for financial support of the research.

References

1. I.V. Klimenko, A.V. Lobanov, E.A. Trusova, A.N. Shchegolikhin, Russ. J. of Phys. Chem. B. (2018) **13**(6), 964.

Effect of iron and nickel metal films on graphitization of the diamond surface during high-temperature annealing

*Okotrub A.V.*¹, *Gorodetskii D.V.*¹, *Palyanov Y.N.*², *Chuvilin A.L.*³, *Bulusheva L.G.*¹

spectrum@niic.nsc.ru

¹ Nikolaev Institute of Inorganic Chemistry, SB RAS, 630090 Novosibirsk, Russia

² Sobolev Institute of Geology and Mineralogy SB RAS, 630090 Novosibirsk, Russia

³ CIC nanoGUNE Consolider, E-20018 San Sebastian, Spain

Diamond crystals with a facet size exceeding the size of the focus of the X-ray beam incident on the sample were synthesized by the HPHT method were heated to a temperature of 850°C and 1250°C for 15 minutes. Annealing of samples of single crystals was carried out in a high-vacuum chamber of the Russian-German laboratory at the BESSY II synchrotron source. XPS spectroscopy was used to study the structure of carbon layers on diamond faces of different symmetries and with thin layers of iron and nickel deposited on a diamond. A higher rate of graphitization of the (111) face in comparison with (001) is shown. From the data of the angular dependence of NEXAFS, the directionality of the sp² carbon layers relative to the diamond surface is determined. The data obtained indicate a catalytic effect of the metal (iron and nickel) on the process of the formation of graphene structures. Transmission electron microscopy data demonstrate the characteristic size and misorientation of individual graphene layers for different symmetry of diamond faces.

Acknowledgement. This work was supported by the Russian Foundation for Basic Research, grant 19-03-00425.

Formation of fractal filaments under the influence of thermocapillary waves at the hydrocarbon-nanofluid interface.

Safargaliev R.F.^{1,2}, *Pakharukov Yu. V.*^{1,2}, *Shabiev F. K.*^{1,2}, *Ezdin B. S.*³, *Zarvin A. E.*³, *Kalyada V. V.*³

ruslan.safargaliev@mail.ru

¹ Tyumen State University, Tyumen, Russian Federation

² Tyumen Industrial University, Tyumen, Russian Federation

³ Novosibirsk State University, Novosibirsk, Russian Federation

Today, it has become clear that new properties are determined by the structure of the material and its dimensionality. Nanoscale objects with unique physical properties are an example of this [1]. In this connection, the media with easily changeable internal order parameters, in which the processes of self-organization of structural rearrangements are vividly realized, are of particular interest. Such a sequence (structure-properties) is most evident in nanofluids, where the interaction of associates leads to the formation of a fractal structure with unique physical properties [2]. Initially, the fractal filaments were obtained after energetic impact on the metal surface in the process of dense plasma dispersion. The critical condition for the appearance of the filaments, is an external electric field, which induces induced dipole moment on the fractal clusters. In [3] the universal character of the formation of fractal filaments was noted. An important condition was the presence of atoms, not molecules, in the evaporation of matter. In the present work, both of these conditions were excluded. Two types of nanoparticles were chosen as the object of study: graphene nanoparticles and core-shell particles. Liquid paraffin was poured into the prepared nanofluid. Previously we showed [4] that the selected nanoparticles effectively interact with hydrocarbons, forming a stable structured film at the interface. The whole system was placed in a glass cylindrical container, which was further cooled. Thus, Stefan problem conditions for paraffin crystallization from the outer boundary of the cylinder to the center were fulfilled. In the non-stationary problem, the heat removal rate was chosen so that the motion of the crystallization front would stop before reaching the center. Thus, there was liquid paraffin in the center of the cylinder. Parallel to crystallization, the growth of the nanoparticle fractal was observed deep in the cylinder. As a result of increasing pressure, the fluid was squeezed out to the surface in a thin layer, creating capillary waves from the center to the outer surface. Carbon nanoparticles pushed out by capillary waves formed macroscopic fractal threads along the perimeter (Fig. 1).

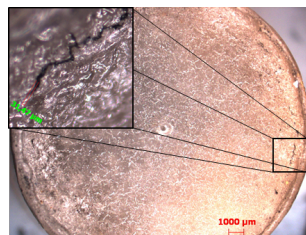


Fig.1. Fractal filaments of carbon nanoparticles on the surface of paraffin

References

1. G. Rothschild, *Fractals in Chemistry* New York: John Willey&Sons: 1998, p. 235.
2. Syzrantsev V.V., Zavyalov A.P., Bardakhanov S.P., The role of associated liquid layer at nanoparticles and its influence of nanofluids viscosity // *Int. J. of Heat and Mass Transfer.* 72. (2014). P. 501-506
3. Smirnov B M "Properties of a fractal aggregate" *Sov. Phys. Usp.* 32 181-182 (1989)
4. Pakharukov Yu.V., Shabiev F.K., Mavrinskii V.V., et al. *JETP Let.* 2019. V.109. P.615-619.

Sensor set based on spray coated carbon nanomaterials for selective detection of ammonia and hydrogen sulfide

*Struchkov N.S.*¹, *Petukhov V.A.*¹, *Romashkin A.V.*¹, *Rabchinskii M.K.*²

struchkov.nikolaj@gmail.com

¹ National Research University of Electronic Technology, Moscow, Russia

² Ioffe Institute, St. Petersburg, Russia

Discrimination of inorganic gases and volatile organic compounds in complex gas mixtures is a hardly feasible task for conventional gas analyzers based on chemical sensors. An eNose is a novel solution for a gas mixtures analysis comprising an array of sensors with varied specificity and a pattern-recognition system. High discrimination accuracy by eNose requires both a high number of sensors and highly varied selectivity. Since the conventional metal oxide sensors have poor scalability and limited selectivity, new materials should be implemented. Carbon nanomaterials are a promising platform meeting the e-nose requirements due to diversity in methods for chemical modification, which provide specific interaction with the required substances and the easiness of the deposition of carbon nanomaterials on a single chip.

The aim of the work was to discriminate ammonia and hydrogen sulfide, which are both strong reducing agents. We made a set of sensors, which are spray-coated thin films of carboxylated carbon nanotubes (CNT), reduced graphene oxide (rGO), and a novel carbonylated graphene derivative (C-ny) [1]. Despite both graphene-based materials are p-type semiconductors, the sensors demonstrated specific responses: C-ny has the negative resistive response to ammonia, while for rGO it is observed towards hydrogen sulfide. This finding does not conform to a common model based on the donation of electron from the reducing gas to p-type semiconductor and, thus, requires further in-depth study.

The presented work was financially supported by the Russian Scientific Foundation (Project No. 19-72-10052).

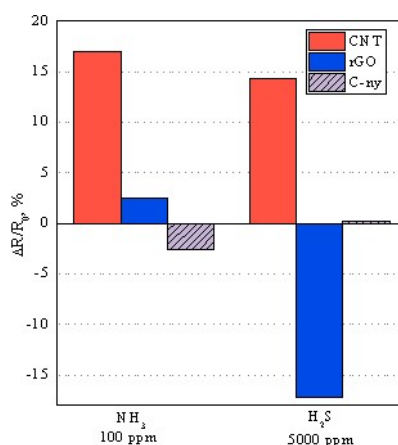


Fig.1. Chemiresistive response of CNT, rGO, and C-ny layers towards the 100 ppm of ammonia (NH₃) and 5000 ppm of hydrogen sulfide (H₂S) at 30% humidity.

References

1. K. Rabchinskii, A.S. Varezchnikov, V.V. Sysoev, M.A. Solomatin, S.A. Ryzhkov, M.V. Baidakova, D.Yu. Stolyarova, V.V. Shnitov, S.S. Pavlov, D.A. Kirilenko, A.V. Shvidchenko, E.Yu. Lobanova, M.V. Gudkov, D.A. Smirnov, V.A. Kislenko, S.V. Pavlov, S.A. Kislenko, N.S. Struchkov, I.I. Bobrinetskiy, A.V. Emelianov, P. Liang, Z. Liu, P.N. Brunkova, Carbon (2021), 172, 236.

Superlattice and nonlinear screening problem in graphene

*Baryshnikov K.A.*¹, *Dmitriev A.P.*¹, *Vasilyev Yu.B.*¹

barysh.1989@gmail.com

¹ Ioffe Institute, Saint-Petersburg, Russia

Superlattice structures in two-dimensional graphene sheets are of a keen interest since the very start of graphene era. Recent studies were concentrated on some unexpected properties of moire structures in graphene, such as cloning of Dirac fermions and Hofstadter butterfly effects [1] and unconventional superconductivity at some “magic” angles of moire superlattices in graphene [2]. Nevertheless, there is an alternative technique of superlattice structures fabrication in graphene grown on a SiH substrate using ultraviolet radiation and a special polymer coating [3]. It is crucial for terahertz detection and emission opportunities to verify if this method could produce a good periodic potential with the lattice period of the order of 100 nm. In this work, we present our calculation results for this problem.

The ultraviolet radiation technique produces electron-depleted regions in graphene grown with some initial electronic doping. Thus, making a periodic mask for ultraviolet radiation it is possible to create a periodic structure of high doped regions and low doped ones as it is shown in Fig.1. The problem is to take into account the electron redistribution between these regions and to calculate the resulting potential in a self-consistent way. We show that this problem has a substantially nonlinear character, and to obtain the screened distribution and potential for electrons one should solve some nontrivial and nonlinear integro-differential equation. We give the solution for this equation in a linear approximation regime and study the first nonlinear correction to it. The results show that at some parameters of the superlattice and Fermi level position the superlattice structure with the 100 nm period could be obtained.

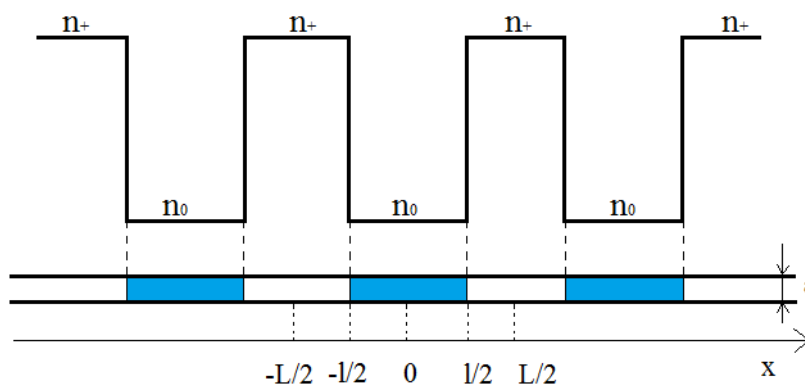


Fig.1. Graphene one-dimensional superlattice due to some effective periodic doping.

References

1. A. Ponomarenko, et. al. *Nature* (2013), **497**(7451), 594-597.
2. Cao, et. al. *Nature* (2018), **556**(7699), 43-50.
3. Yu. B. Vasilyev, et. al. *Appl. Phys. Lett.* (2018), **112**, 041111.

New way of synthesis of few-layer graphene (FLG) by the self-propagating high-temperature synthesis (SHS) method from biopolymers.

Vozniakovskii A.P.¹, Vozniakovskii A.A.², Kidalov S.V.²

Kidalov@mail.ioffe.ru

¹ Institute for Synthetic Rubber, Saint-Petersburg, Russia

² Ioffe Institute, Saint-Petersburg, Russia

We want to report on a new method for synthesizing large volumes of FLG based on the SHS method. We suggested that polysaccharides, in particular starch, could be an acceptable source of native cycles for the SHS process. The carbonization of biopolymers under the conditions of the SHS process was chosen as the basic method of synthesis. Chemical reactions, under the conditions of the SHS process, proceed according to a specific mechanism of nonsothermal branched-chain processes, which are characterized by the joint action of two fundamentally different process accelerating factors - avalanche reproduction of active intermediate particles and selfheating.

The method of obtaining SHS nanocarbon included the pyrolysis of carbohydrate in a mixture with an oxidizing agent. We used starch as carbohydrate and ammonium nitrate as an oxidizing agent. The carbohydrate and oxidizer were taken in a 1:1 ratio by mass, respectively. Pyrolysis was carried out in the mode of SHS, heating the mixture in a vessel at a speed of 20-30 °C/min to 150 °C and keeping at this temperature for 15-20 min with the discharge of excess gases into atmosphere (Figure 1).

The resulting FLG were studied by SEM, TEM, X-ray diffraction, Raman spectroscopy as well as FTIR spectrometry. The ASAP 2020 analyzer was used to determine the specific surface area of the powder of FLG.

We demonstrate that FLG itself have not more than 1-5 graphene layers.

The work is supported by the grant of the Russian Foundation for Basic Research 18-29-24129MK

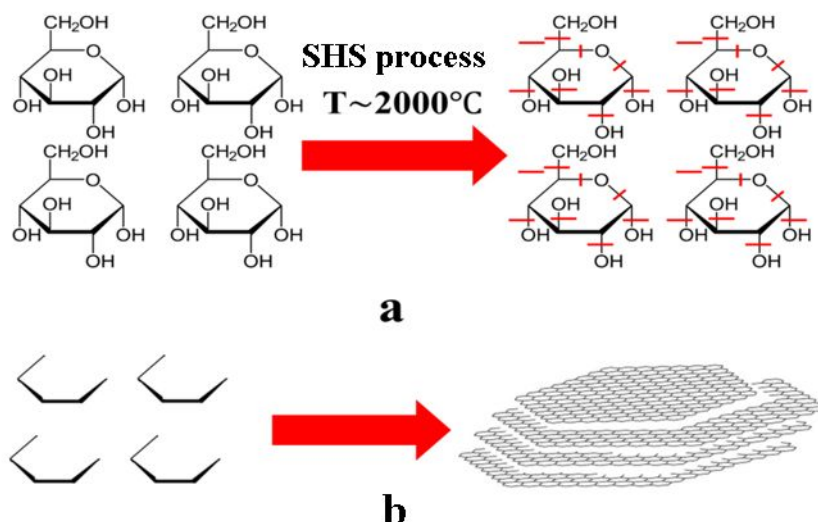


Figure 1. Simplified model for the synthesis of few-layer graphene nanostructures using the SHS method (for example, glucose). a - breaking the the weakest bonds, b - self-organization of carbon primitives with unsaturated bonds in to few-layer graphene.

AFM investigation of polygonal wrinkles on thin UV-irradiated graphene oxide films for biosensor applications

*Komarov I.A.*¹, *Rabchinskii M.K.*², *Struchkov N.S.*¹

master_kom@mail.ru

¹ Center for Probe Microscopy and Nanotechnology, National Research University of Electronic Technology, Zelenograd 124498, Russia.

² Laboratory of Physics of Cluster Structures, Ioffe Institute, Saint-Petersburg, 194021, Russia.

In this work, we for the first time demonstrate the formation of polygonal wrinkles, predominantly having a round shape, on the surface of the monolayer graphene oxide (GO) platelets carboxylated via UV irradiation in the inert atmosphere [1].

Commonly, wrinkles in graphene, GO and their derivatives have spontaneous shapes and do not arrange in ordered forms, such as squares, penta- or hexagonal structures [2]. However, in our work, we show that UV irradiation initiates the formation of wrinkles on the mono- and few-layered GO flakes. Oppositely to the reported structures, upon the provided treatment wrinkles are round-shaped, forming circle or oval structures. We assume that the formation of such ordered wrinkles is due to the interaction of the graphene layer with the gaseous products, releasing upon the UV irradiation. Considering such wrinkles contain many structural defects and functional groups, they are regarded as the active sites for coupling of chemical- or biosensing agents (like aptamers or antibodies). Thus, the found wrinkled films can be a platform for chemical or biosensors, drug delivery, or biocompatible/biotolerant coatings. The presented work was financially supported by the Russian Foundation for Basic Research (Project No. 18-29-19172).

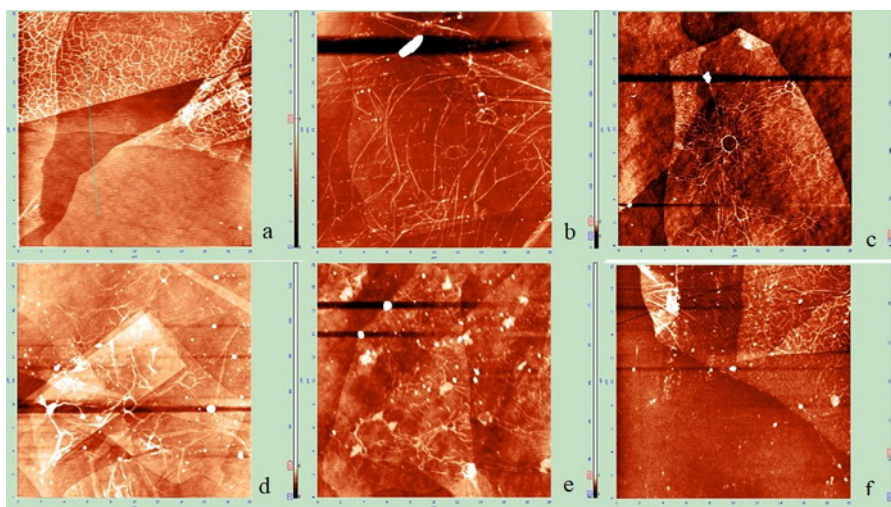


Figure 1 AFM images (topography) of structures without UV treatment and irradiated with 30 seconds, 1, 5, 10 and 20 minutes (a - f respectively).

References

1. K. Rabchinskii, V. V. Shnitov, A. T. Dideikin et al. 2016. *Journal of Physical Chemistry C*, **120**, 28261-28269.
2. Zhang, M. Arroyo. 2014. *Journal of the Mechanics and Physics of Solids*, **72**, 61-74.

Polarization-resolved terahertz spectroscopy of graphene-based films

*Kvitsinskiy A.*¹, *Rybin M.*², *Zaitsev A.*¹, *Bogdanov K.*¹, *Zykov D.*¹, *Obratsova E.*^{2,3}

anatolykvitsinskiy@gmail.com

¹ ITMO University, 49 Kronverkskiy Prospekt, Building A, Saint Petersburg, 197101, Russian Federation

² Prokhorov General Physics Institute of the Russian Academy of Sciences, 38 Vavilova Street, Moscow, 119991, Russian Federation

³ Moscow Institute of Physics and Technology, 4 Nauchny Pereulok, Dolgoprudny, Moscow Region, 141701, Russian Federation

In recent years, there has been a real breakthrough in the study of all possible carbon allotropes. The latest nanotechnology allows us to engineer materials at the atomic level and create dynamically-controlled nanostructures for their real integration into all areas of our life. And therefore, advanced science is less and less within the rigid boundaries of the classical fields, and more and more becomes truly interdisciplinary. One of these topical complex areas is terahertz (THz) photonics of low-dimensional nanostructures. In connection with the development of sources and receivers of THz radiation, it became possible to develop compact systems for data transmission and telecommunications for the next generation of communication networks. But the problem of efficient manipulation of the THz electromagnetic waves in open space remains unresolved. A promising method for solving this problem is the use of graphene as an active medium for THz wave control devices [1]. But despite the great progress achieved in the study of graphene-based structures, the question of the influence of the graphene layer number on its properties has not yet been resolved.

The goal of our work was an experimental study of multilayer graphene (MLG)-based thin films with different numbers of graphene layers using the THz time-domain spectroscopic polarimetry (TDSP) method in a frequency range 0.2–0.8 THz (~1.50–0.37 mm).

For our study, we selected three samples of MLG thin films with different number of graphene layers. The films were synthesized by the modified chemical vapor deposition method on the nickel foil as described in Ref. [2]. Then the films were transferred onto the borosilicate glass substrates with a thickness of ~150 μm. To study the structural properties of the samples, we performed the Raman spectroscopy using an excitation wavelength of 488 nm. To study the electrical properties of the samples using the THz-TDSP method [3], a custom-made system based on a THz time-domain spectrometer and three wire grid polarizers was used. All measurements were done under a controlled room temperature of 291 K, and a relative humidity of 40%.

The obtained results of the Raman spectroscopy clearly show that with an increase in the number of graphene layers, an enhancement of the G-band and suppression of the 2D-band occur, which indicates a transformation from two-dimensional carbon-based structures to quasi-bulk ones. For the analysis of the obtained THz waveforms transmitted through the samples we used the basic Tinkham thin-film calculations and modernized data processing techniques [4]. Thus, we managed to obtain the complex relative permittivity and the electrical conductance of the MLG based on THz polarimetric measurements. The results show that the real part of the graphene conductance nonlinearly depends on the number of layers and reaches value of 0.06 S for ~76 layers. These results show that by using MLG it is possible to create devices that can be used in the advanced areas of THz technologies.

The reported study was funded by the Russian Foundation for Basic Research (RFBR), project No. 20-32-90203.

References

1. P. Han *et al.*, *Adv. Opt. Mater.* (2020) **8**(3), 1900533.
2. M. G. Rybin *et al.*, *Phys. Status Solidi B* (2018) **255**(1), 1700414.
3. A. Kvitsinskiy *et al.*, *SN Appl. Sci.* (2019) **1**(12), 1714.
4. A. D. Zaitsev *et al.*, *Appl. Sci.* (2020) **10**(8), 2724.

Light-responsive membranes based on graphene oxide modified by azo-group molecules

Sadilov I.S.¹, Petukhov D.I.¹, Eliseev A.A.¹

ilsadilov@gmail.com

¹ Lomonosov Moscow State University, Moscow, Russia

Progress in membrane technologies allows to create membranes, which can change transport properties under the external stimuli such as temperature, electric, magnetic or electromagnetic fields. On the other side, the interest in two dimensional nanosheet based membranes has grown up. Membranes based on graphene oxide (GO), transition metal dichalcogenides, and MXene have been studied. Two-dimensional materials are characterized labyrinth mechanism of mass transport, in which molecules are transported through interlayer space or through the defects in nanosheets [1]. However, only a few works devoted to switchable membranes based on two-dimensional materials have been published [2]. Thus the specific goal of the current study is preparation membranes based on graphene oxide modified by azo-group molecules, which can change their transport properties under light irradiations due to cis-trans isomerization of azo-group.

Graphene oxide was obtained by modified Hummer's method the ratio of graphite and KMnO_4 was 1:20. The lateral size is about 800 nm, C/O ratio is 1,7. 10 mg of GO was modified by 10 mmol NaNO_2 and 10 mmol aniline in 6 M hydrochloric acid. The selective layer of modified graphene oxide was formed on anodic alumina support by spin-coating technique. For formed membrane water vapor permeance was measured. The permeance increase under UV irradiation and decrease under IR irradiation (Fig.1). The changing of water vapor permeance under UV light may be explained by the transition to a cis isomer of immobilized azobenzene on graphene oxide, leading to changing interlayer distance. This property of mass transport changing under external stimuli may be found application in the separation of mixtures with various content.

This work was supported by Russian Science Foundation grant № 20-79-10205

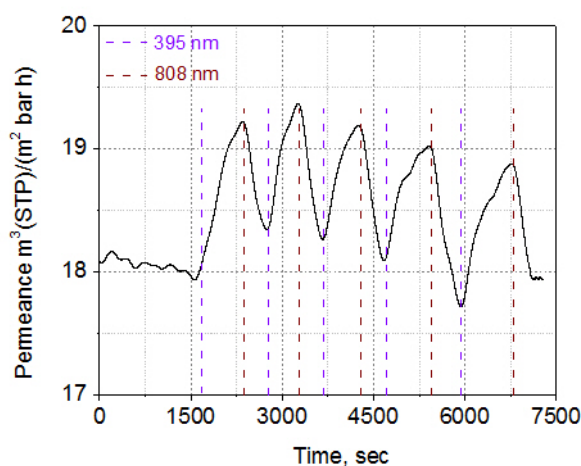


Fig.1. Water vapor permeance of modified graphene oxide. Violet dash is turn on UV irradiation with length wave 395 nm. Red dash is turn on IR irradiation with length wave 808 nm.

References

1. Liu M., Gurr P. A., Fu Q., Webley P. A., Qiao G. G. J. *Mater. Chem. A* (2018), **6**, 23169-23196.
2. Wang Y., Zhang Z., Li T., Ma P., Zhang H., Chen M., Du M., Dong W. *ACS Applied Materials & Interfaces* (2019) **11** (47), 44886-44893

Mechanical and thermophysical properties of polymer composites with few-layer graphene obtained by laser stereolithography 3D printing

*Smirnova V.E.*¹, *Vozniakovskii A.A.*², *Voznyakovskii A.P.*³, *Kalashnikova E.I.*¹, *Kidalov S.V.*²

vsmirnova13@mail.ru

¹ Saint-Petersburg State Institute of Technology, Saint-Petersburg, Russia

² Ioffe Institute RAS, Saint-Petersburg, Russia

³ Institute of Synthetic Rubber, Saint-Petersburg, Russian Federation

The advent of 3D printing has enabled the rapid prototyping of complex structures with relatively shorter production times and lower material wastage. Metals, plastics, epoxy resins, and ceramics are used as materials for 3D printing, but now they are being replaced with composites and polymers to save weight. The production of polymer composite materials with the required characteristics is achieved by selecting the initial matrix polymer and modifying it in order to directly regulate the structure and properties. One way to improve the mechanical properties of products would be to increase the stiffness and strength of the material through the addition of reinforcement particles. Examples of such particles include few-layer graphene nanoparticles (FLG). FLG has unique electrical, thermal, high strength characteristics and mechanical properties. Here, we report the successful 3D printing of FLG-polymer composites using the laser stereolithography (SLA) 3D printing.

The synthesis of FLG was carried out by the method of self-propagating high-temperature synthesis (SHS) from cellulose (analytical-grade). The FLG concentration was 0.025, 0.05, 0.075, 0.5, 1.0, 2.0, 4.0 wt. %. It was dispersed in photopolymer resin and sonicated in an ultrasonic bath for 30 min at 50°C. FLG dispersed homogenously into the resin forming a black mixture. The hardness and thermal conductivity test specimens were fabricated by a 405 nm SLA (Photon S, ANYCUBIC, China). Hardness of the samples was investigated by Brinell and thermal conductivity with the laser-flash method. The measurement results are shown in figure 1.

It was shown FLG-polymer composites structures fabricated this way could effectively increase the hardness. Addition of up to 0.05 wt. % of FLG leads to an increase in hardness, and a further increase in the proportion of FLG does not cause an increase in hardness due to a violation of the distribution of particles by volume with the formation of agglomerates. However, it should be noted that the addition of FLG did not lead to a noticeable change in thermal conductivity compared to the initial polymer.

The reported study was funded by RFBR and BRFR project number 20-53-04026.

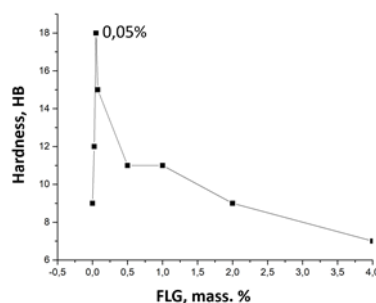


Figure 1. The dependence of the hardness of the composite on the concentration of FLG.

Features of the effect of graphene nanoplates on the properties of grease lubricants

*Rukhov Ar.V.*¹, *Bakunin E.S.*¹, *Dyachkova T.P.*¹, *Rukhov An.V.*¹, *Istomin A.M.*¹, *Obraztsova E.Y.*¹, *Kornev A.Y.*², *Burakova E.A.*¹, *Smirnova A. I.*³, *Usol'tseva N.V.*³

rukhov.av@gmail.com

¹ Tambov State Technical University, Tambov, Russia

² All-Russian Research Institute for the Use of Machinery and Petroleum Products in Agriculture, Tambov, Russia

³ Ivanovo State University, Nanomaterials Research Institute, Ivanovo, Russia

The number of machines and mechanisms used in industrial production is constantly increasing. This requires the use of a wide range of process fluids (lubricants, cooling, kinematic), including grease lubricants. An urgent task is to create new economical and environmentally friendly lubricants with high tribological characteristics. In particular, it is possible to convert used engine oils into greases. However, conventional techniques produce very low-quality, low-viscosity greases. By introducing thickeners (calcium salts of higher carboxylic acids) into them, solidols are obtained, which are widely used in technology.

According to [1], graphene nanoplates (GNP) have unique tribological, structuring, and adsorption properties; therefore, it is advisable to add them to the composition of lubricating compositions. In the present study, GNPs obtained by the method of electrochemical exfoliation [2] were introduced at the stage of obtaining a soap thickener in the amount of 15, 75, 150 and 750 ppm. The thickener was obtained by mixing calcium hydroxide with sunflower oil for 1-3 hours at a temperature of 95 ° C.

Для экспериментальных образцов смазочных композиций определялись остаточное содержание воды, доля загустителя, температура каплепадения, пенетрация и предельная величина износа с использованием машины трения. Для сравнения использован образец промышленно производимого продукта.

For experimental samples of lubricating compositions, the residual water content, the proportion of the thickener, the dropping point, the penetration and the limit value of wear using a friction machine were determined. A sample of a commercially produced product was used for comparison.

It was found that with an increase in the GNP content, the water content monotonically increases (from 0.6 to 2.3 wt. %), while the concentration of the thickener remains almost constant (about 18.5 wt. %). This also increases the penetration from 31 to 44 mm. The dropping point changes from 79 to 88 ° C at a GNP concentration of 150 ppm, and then monotonically drops to 81 ° C. The minimum wear mark is also observed at a GNP concentration of 150 ppm and is 0.215 mm, which is 25.1% lower than that of the control industrial sample. It was shown that the addition of 150 ppm GNP improves the performance of greases based on secondary motor oils containing calcium soaps. Due to the increase in the dropping point during the introduction with the introduction of GNP, it is possible to expand the temperature range of the lubricant application.

This work was supported by the Russian Foundation for Basic Research (grant no. 18-29-19150_mk).

References

1. Y. Obraztsova, M.N. Barshutina, E.S. Bakunin, A.V. Rukhov, A.A. Shipovskaya, A.V. Shuklinov, *Mendeleev communications* (2020) **30**, 2.
2. E.S. Bakunin, E.Y. Obraztsova, A.V. Rukhov, *Inorganic Materials: Applied Research* (2019) **10**, 2.

Low-threshold field electronic emission from two-dimensional carbon structures

*Vozniakovskii A.A.*¹, *Voznyakovskii A.P.*², *Fursei G. N.*³, *Polyakov M. A.*³, *Zakirov I. I.*³,
*Neverovskaya A. Yu.*²

alexey_inform@mail.ru

¹ Ioffe Institute, Saint-Petersburg, Russia

² Lebedev Research Institute for Synthetic Rubber, Saint-Petersburg, Russia

³ Research Center for Electrophysical Surface Problems, Bonch-Bruевич St. Petersburg State University of Telecommunications, St. Petersburg, Russia

Field emission from metals makes it possible to create non-incandescent cathodes for problems in vacuum nanoelectronics. Earlier it was found that field electron emission from carbon materials, incl. A graphene-like structure (GPA) is excited in electric fields 2-3 orders of magnitude lower than for traditional field emission from metals and semiconductors. This effect is called low-threshold emission (LP). It was shown that the effect of NP of electron emission is most clearly manifested in the HPS [1]. However, despite all the promising nature of HPS, their application in practice has not yet occurred, which is due to the imperfection of the methods for the synthesis of both graphene itself and HPS, which is due to the imperfection of the methods of their synthesis.

This paper presents the results of a study of the possibility of obtaining low-threshold field electron emission from low-layer graphene (FLG) synthesized by the method of self-propagating high-temperature synthesis (SHS) from starch (SC). Figure 1 shows the emission image of the SC cathode surface (a) and the current-voltage characteristic plotted in Fowler-Nordheim coordinates in stationary fields (b), respectively. As can be seen from Figure 1a, the emission distribution over the cathode surface is uniform. The emission surface does not contain any pronounced local centers. As can be seen from Fig. 1b, the linear form of the I - V characteristic indicates that the dependence of the current on the voltage is exponential. It should be specially noted that despite the fact that this dependence has an external resemblance to the Fowler-Nordheim pattern, it is not.

The threshold value of the electric fields at which the field emission occurs in the case of SC is about $1 \text{ V} / \mu\text{m}$ (in this case, the field at which the steady-state emission current equal to $I = 1 \text{ nA}$ was taken as the threshold field). For comparison, the threshold fields for metals and semiconductors are $10^3 \text{ V} / \mu\text{m}$. The obtained research results show that the SHS technology makes it possible to create efficient low-threshold field sources of electrons in a high-performance way.

The reported study was funded by RFBR and BRFR, project №20-58-00056.

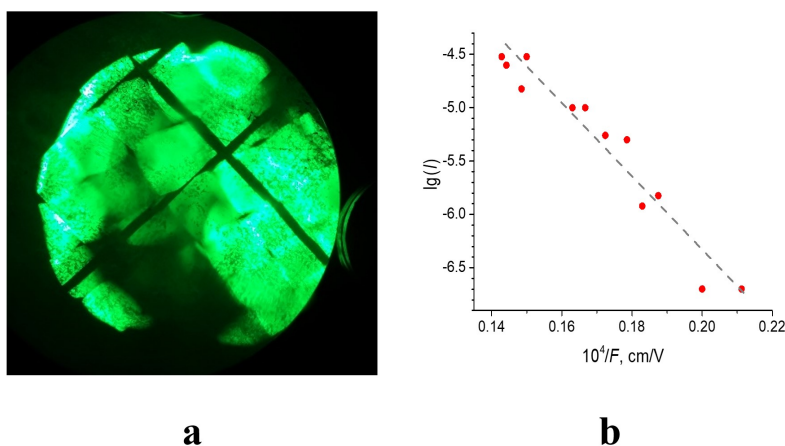


Fig. 1. An emission image of an SC emitter; B - current-voltage characteristics in stationary conditions.

Determination of Stone-Wales Structural defects in 1D and 2D nanocarbons

*Voznyakovskii A.P.*¹, *Neverovskaya A.Yu.*¹, *Vozniakovskii A.A.*², *Kidalov S.V.*²

voznap@mail.ru

¹ Lebedev Research Institute for Synthetic Rubber, Saint-Petersburg, Russia

² Ioffe Institute, Saint-Petersburg, Russia

A Stone-Wales (SW) defect is a dipole of 5-7 ring pair in hexagonal structures of nanocarbons with sp^2 hybridization of carbon atoms. SW is one of the most important defective structural in nanocarbons that will affect the mechanical, chemical, and electronic properties of nanocarbons. Stone-Wales defect is a crystallographic defect in carbon nanotubes, graphene and other crystals with a hexagonal crystal lattice appear when one of the C-C bonds is rotated through an angle of 90° , as a result of which four hexagons of carbon atoms are converted into two heptagons and two pentagons. As a result of this rearrangement, active dienophilic vacancies are formed in the structure of nanotubes and graphene. In the practice of organic chemistry, active dienophilic vacancies are used to obtain cyclic compounds by the reaction of the so-called "diene synthesis" - the reaction of [4 + 2] - cycloaddition (Diels-Alder reaction) [1]. The formation of cyclic compounds according to the diene synthesis scheme is a thermodynamically favorable reaction; therefore, the reaction proceeds irreversibly and, accordingly, quantitatively. This nature of the reaction makes it possible to use it for the quantitative determination of possible Stone-Wells defects in nanocarbons, the surface of which is formed by carbon atoms with sp^2 hybridization. For the study, we used graphene oxide (GO), and single-wall carbon nanotube (SWCNT). For comparison, there were studied few-layer graphene (FLG) obtained us by carbonization of biopolymer (starch) under the conditions of the SHS process.

To carry out the diene synthesis reaction, a mixture of α -methylstyrene and o-xylene taken in equal amounts was added to a suspension of nanocarbon in toluene. The progress of the reaction was judged by the decrease/constancy of the α -methylstyrene's concentration in the reaction mixture with respect to the non-reactive o-xylene. The concentration change was monitored by the well-known method of gas-liquid chromatography.

The specific surface of nanocarbons needed for the calculation of the surface SW concentration was calculated from BET data.

Table 1. Parameters of nanocarbon

Nanocarbon	Specific area m^2/g	C_{SW} $\times 10^5 (mol/m^2)$
GO	580	3.6
SWCNT	300	1.1
FLG	660	0

Let us elucidate that the obtained value corresponds to the number of moles of α -methylstyrene irreversibly reacted with the surface of nanocarbon by the reaction of diene synthesis, which quantitatively corresponds to the concentration of dienophilic vacancies - Stone-Wells defects.

The difference in defects of GO and FLG we attribute both to different mechanisms of their production (up-bottom/bottom-up) and to different sources of their production. As for our best knowledge, the quantitative data on SW concentrations per surface unit of nanocarbons were available for the first time.

The reported study was funded by RFBR and BRFR, project №20-58-00056

References

1. Nikolaou, K. C.; Snyder, S. A.; Montagnon, T.; Vassilikogiannakis, G. *Angewandte Chemie International Edition*. (2002) **41**, 1668.

Role of heteroatoms and defects on the obtained electrochemical characteristics of carbon materials

*Evlashin S.A.*¹

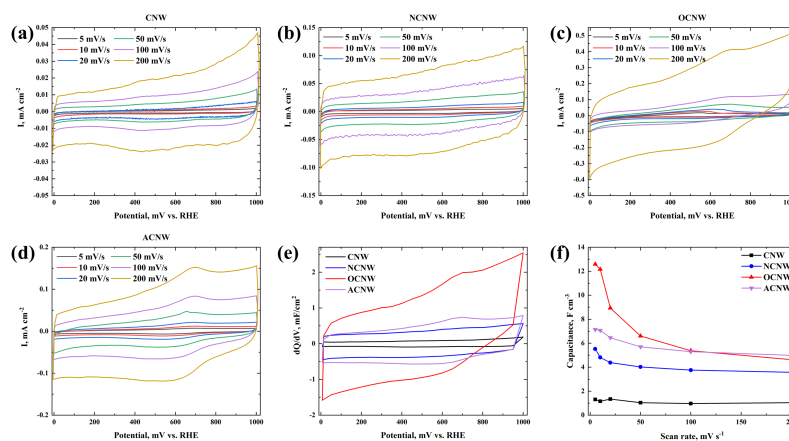
s.evlashin@skoltech.ru

¹ Skolkovo Institute of Science and Technology, Moscow, Russia

Many scientific groups are analyzing and creating new materials to improve the characteristics of energy sources. Metal oxides are used to increase the specific features of supercapacitors. However, the usage of metal oxides leads to additional steps in the production line and increasing the mass of whole devices. An alternative approach is to use the heteroatoms, which can be easily incorporated into the carbon structures. For instance, the introduction of heteroatoms such as N or O enhances the specific capacitance of these materials. However, the mechanisms that lead to the increase in the specific capacitance are not well-studied yet.

In this work, we demonstrate an effective method for modification of the surface of carbon nanowalls (CNWs) using DC plasma in atmospheres of O₂, N₂, and their mixture. Processing in the plasma leads to the incorporation of ~4 at. % nitrogen and ~10 at. % oxygen atoms. Electrochemical measurements reveal that CNWs functionalized with oxygen groups are characterized by higher capacitance. The specific capacitance for samples with oxygen reaches 8.9 F cm⁻³ at a scan rate of 20 mV s⁻¹. In contrast, the nitrogen-doped samples demonstrate a specific capacitance of 4.4 F cm⁻³ at the same scan rate.

Contrary to common belief, nitrogen appears to not be the most important element for the formation of high capacitance. According to our research, oxygen contributes the most to the pseudocapacitance. We relate this effect not only to functional groups but also to the size of the nanocrystalline domains. We can conclude that partial oxidation of the carbon lattice can lead to an increase in the capacitance of the structures, while the preservation of the crystalline structure quality, namely, the large size of the crystalline domains, is also important.



Cyclic voltammetry data, differential and integral capacitances for pristine and plasma-treated CNWs recorded at scan rates of 5, 10, 20, 50, 100, and 200 mV s⁻¹ in 1 M H₂SO₄ electrolyte; every 5th cycle is presented. a)-d) CV curves of samples before and after modification in N, O, and mixture plasma, e) differential capacitance of the samples, and f) specific integral capacitance.

References

1. Evlashin S. A. et al. N-doped carbon nanowalls for power sources //Scientific reports. – 2019. – T. 9. – №. 1. – C. 1-7.
2. Evlashin S. A. et al. Role of nitrogen and oxygen in capacitance formation of carbon nanowalls //The Journal of Physical Chemistry Letters. – 2020. – T. 11. – №. 12. – C. 4859-4865.

Thermal properties of water-based nanofluids modified with few-layer graphene

*Kalashnikova E.I.*¹, *Vozniakovskii A.A.*², *Voznyakovskii A.P.*³, *Kidalov S.V.*², *Ovchinnikov E.V.*⁴

kalashnikatja@bk.ru

¹ State Institute of Technology, Saint Petersburg, Russia

² Ioffe Institute, Saint Petersburg, Russia

³ Institute of Synthetic Rubber, Saint-Petersburg, Russian Federation

⁴ Yanka Kupala State University of Grodno, Grodno, Belarus

Coolants are still actively used as heat carriers in cooling systems for various devices, from internal combustion engines to cooling systems for computer electronic systems. Water received such spread as a coolant due to its characteristics: thermal conductivity of water at 20 °C - 0.6 W/(m*K); specific heat - 4180 J/(kg*°C), and dynamic viscosity - 1004 mPa*sec). However, with the development of industry, the volumes of heat that must be removed using coolants are constantly increasing. As a result, it becomes impossible to effectively remove heat using water without increasing the volume of water used. In addition, due to the conditionally low thermal conductivity of water, an increase in the area of the radiators is required for effective heat dissipation, and this is not always possible. As a result, many scientific groups are working on the creation of new coolants based on water, in order to improve its thermophysical properties.

In this work, to improve the thermophysical characteristics of water, we used few-layer graphene (FLG) synthesized by the method of self-propagating high-temperature synthesis (SHS) from cellulose as a modifying additive. To obtain a stable suspension of FLG in water, we used ultrasonic treatment for 30 minutes without using a surfactant. The concentration of FLG in the suspension was 0.1%, 0.2%, 0.5%.

As can be seen, the use of FLG as an additive made it possible to achieve an increase in thermal conductivity up to 57% in comparison with water at a concentration of 0.2 mass. %. At 0.5 mass. % thermal conductivity dropped due to the uneven distribution of FLG in water. It should be noted that the obtained nanofluids have almost identical dynamic viscosity as the initial water.

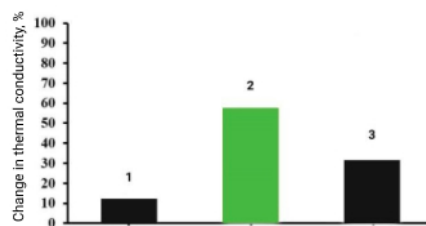


Fig. 1. - Change in thermal conductivity for stable water-based nanofluids with 0.1% (1), 0.2% (2), 0.5% (3) FLG concentration compared to the original filtered water

References

The reported study was funded by RFBR and BRFR, project number 20-58-00056 Bel_a.

Spin-coating deposition of graphene oxide from mixed water-organic solutions

*Komarov I.A.*¹, *Danilova E.A.*¹, *Denisenko E.I.*¹, *Peretiaygin V.G.*¹, *Rabchinskii M.K.*²

master_kom@mail.ru

¹ Department of Composite Construction for Space Rockets, Bauman Moscow State Technical University, Moscow, 105005, Russia

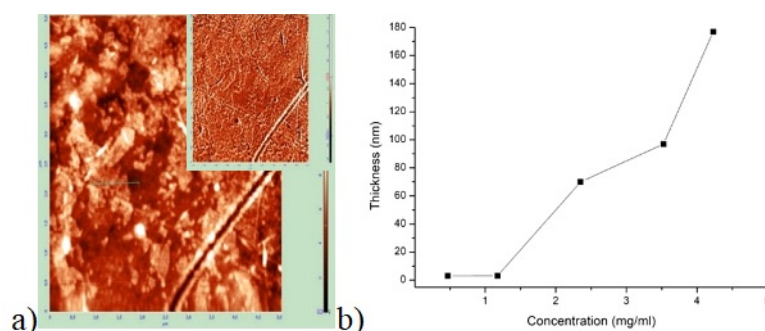
² Laboratory of Physics of Cluster Structures, Ioffe Institute, Saint-Petersburg, 194021, Russia

The development of flexible electronic devices is one of the largest trends in the application of carbon nanomaterials [1]. But one of the limitations for the advances in flexible devices is the formation of a high-quality thin conductive layer, especially within the frame of large-scale production. Among possible technologies for this purpose, spin-coating is regarded as the most facile and prospective method [2]. However, several issues must be overcome to reach utmost uniformity of the films deposited via spin-coating and the right choice of solvent is one of them.

In this work, we investigate the influence of the addition of organic solvent on the deposition of graphene oxide (GO) suspension by spin-coating. Since most part of the commercially available GO is presented in the form of water suspensions, it is necessary to improve the wettability of different substrates, including such polymer substrates as polyethylene terephthalate or polyethylene naphthalene. For this purpose, we used a mixture of the GO water suspension with *n*-methylpyrrolidone or dimethylacetamide in different proportions.

We made suspensions with a concentration of GO ranging from 4.23 mg/ml to 0.47 mg/ml, which are all found to be stable. The deposition was performed by spin-coating on the polymer substrate 150 nm of thickness. Atomic force microscopy (AFM) and Raman spectroscopy confirmed the formation of GO films after deposition for all suspensions. We found that the formation of the uniform films is possible only for the case of GO suspension with a concentration of 2.35 mg/ml. In the case of lower concentrations, we found only separate GO flakes whereas in the case of higher GO concentrations we observed high film nonuniformity indicated even with the naked eye. Thus, we found out the facile composition of water-organic solutions and GO concentration for the deposition of GO film with high uniformity via the spin-coating method.

This work is presented work was financially supported by the Russian Foundation for Basic Research (Project No. 20-04-60458).



AFM images of 3nm island-type graphene oxide film (~ 3 nm thickness) (a) and dependence of film thickness on GO concentration in mixed solution.

References

1. Wang M. Hu, H. Wang, Z. Chen, Y. Feng, J. Wang, W. Ling, Y. Huang, *Advanced Science* (2020) **7**, 2001116.
2. Nguyen A.N., Solard J, Nong H.T.T., Osman C.B., Gomez A., Valérie Bockelée V., Tencé-Girault S., Schoenstein F., Simón-Sorbed M., Carrillo A.E. and Mercone S. 2020. *Materials* **13** 1342

Nanoscale structures formed on SiC substrates for field emission devices

*Niftalieva V.V.*¹, *Kessler I.O.*¹, *Morozova J.V.*¹, *Rezvan A.A.*¹, *Klimin V.S.*¹

Niftalieva@sfedu.ru

¹ Department of Nanotechnology and Microsystems, Southern Federal University, Taganrog 347922, Russia

Currently, one of the promising self-organizing materials, which is of great importance in micro- and nanoelectronics, is graphene and its derivatives. Its main advantages are high carrier mobility and resistance to ionizing effects [1]. The main method for producing graphene films on the SiC surface is the thermal decomposition of the SiC surface [2]. The advantage of this method is the low cost and the possibility of obtaining homogeneous large-area nanocarbon films based on both conductive and semi-insulating substrates [3]. However, this method has a significant drawback - it requires annealing at very high temperatures, which can lead to the formation of high mechanical stresses in the structure. In this regard, it is important to study the use of a combination of focused ion and plasma-chemical etching to produce graphene films on SiC [4].

At the initial stage, experimental studies on the formation of nanoscale structures were carried out by the method of focused ion beams. For this purpose, a scanning electron microscope with an ion column NovaNanoLab 600 (FEI company, the Netherlands) was used. With its help, templates were formed for the subsequent etching of structures with a focused ion beam, which represented the shape of a torus with an external diameter of 2 microns and an internal diameter of 600 to 800 nm. The ion beam current was 30 pA. The accelerating voltage was 30 keV. The exposure time at the point of 1 ms. The structures were then etched onto a silicon carbide substrate.

In this experiment, studies were conducted for the formation of carbon nanostructures on the surface of silicon carbide. Experiments were performed to obtain graphene on the surface of silicon carbide by plasma etching with fluoride plasma. This technology can be used for the formation of modern vacuum microelectronic devices, as well as for the development of pressure and gas sensors.

This work was supported by the Russian Foundation for Basic Research Project № 18-29-11019 mk. The results were obtained using the equipment of the Research and Education Center "Nanotechnologies" of Southern Federal University.

References

1. V S Klimin, A A Rezvan, O A Ageev Research of using plasma methods for formation field emitters based on carbon nanoscale structures // J. of Phys: C.S, 2018. V.1124. - P. 071020.
2. Li J, Yan X, Gou G, Wang Z, Chen J 2014 Phys. Chem. 161850
3. Chen J, Li J, Yang J, Yan X, Tay B-K, Xue Q 2011 Appl. Phys. Lett. 99173104
4. Klimin V S, Solodovnik M S, Lisitsyn S A, Rezvan A A, Balakirev S V 2018 J. Phys.: Conf. Ser. 1124041024

Influence of defects in graphene on the non-adiabatic electron transfer kinetics

Pavlov S.V.^{1,2}, *Kislenko V.A.*^{1,2}, *Fedorov M.V.*¹, *Kislenko S.A.*^{2,3}

sergey.v.pavlov@phystech.edu

¹ Skolkovo Institute of Science and Technology, Nobel Str. 3, Moscow, 143026, Russian Federation

² Joint Institute for High Temperatures, Izhorskaya 13/2, Moscow, 125412, Russian Federation

³ Moscow Institute of Physics and Technology, Institutskiy per. 9, Dolgoprudny, 141700, Russian Federation

The relevance of this work is based on the fact that the search for cheap and stable catalysts for various redox systems is a significant challenge today. One of the promising directions toward new efficient electrocatalysts is the usage of carbon nanomaterials. Various defects in such materials can create local electronic states with energies close to the Fermi level, accelerating electron transport across the interface. In this work, we study these effects within the framework of modern quantum chemistry theory. Based on the Marcus and Landau-Zener theories and Density Functional Theory (DFT) calculations, we have obtained the rate constant of heterogeneous electron transfer (HET) with a 3D spatial resolution over the graphene surfaces containing different types of linear [1] and point defects [2, 3].

Fast approaches for HET estimation from periodic plane-wave DFT calculations using Tersoff-Hamann and Chen approximations of electronic coupling matrix elements were developed [3]. These approaches allow decreasing the computational cost of HET calculations by orders of magnitude. It was shown that defects could lead to catalysis of the HET strongly depending on the standard potentials of particular redox pair. The most significant effect was found for single vacancies; their presence enhances the electron transfer by order of magnitude at the standard potential from -1V to 0V vs. standard hydrogen electrode (SHE). We have shown the nonuniform electrochemical activity of graphene induced by the defects. The electron transfer rate is increased mostly above the defects. Different defects show the largest catalytic effect for different redox couples, which may be useful for applications in selective electrocatalysis and electrochemical sensors. The proposed methods could also be applied to the electrode design for electrochemical energy conversion systems.

References

1. S.V. Pavlov, R.R. Nazmutdinov, M.V. Fedorov, and S.A. Kislenko *J. Phys. Chem. C* (2019) **123**, 6627.
2. V.A. Kislenko, S.V. Pavlov and S.A. Kislenko *Electrochimica Acta* (2020) **341**, 136011.
3. S.V. Pavlov, V.A. Kislenko and S.A. Kislenko *J. Phys. Chem. C* (2020) **124**(33), 18147.

Hardness and thermal conductivity of a composite based on aluminum modified with a hybrid material detonation nanodiamond/few-layer graphene

*Podlozhnyuk N.D.*¹, *Vozniakovskii A.A.*², *Kidalov S.V.*², *Voznyakovskii A.P.*³

nikigod.1@gmail.com

¹ Saint Petersburg State Technological Institute, Saint-Peterburg, Russia

² Ioffe institute, Saint-Peterburg, Russia

³ Institute of Synthetic Rubber, Saint-Petersburg, Russian Federation

Carbon nanomaterials such as few-layer graphene (FLG) and detonation nanodiamonds (DND) have excellent physical properties such as high hardness, tensile strength, thermal conductivity from 2000 (DND) to 5000 W/(m*K) (FLG). In theory, these properties make them excellent additives in composites based on polymer and metal matrix [1,2]. However, in practice, both FLG and DNDs used as individual additives do not improve the properties of the matrix as much as expected due to the phenomenon of aggregation, in which the properties of the material are no longer determined by individual particles, but by their agglomerates. We tried to solve the problem of aggregation by synthesizing FLG-DND hybrid material (FLG-DND ratio was 1:1). The synthesis of the hybrid material was carried out using the Self-propagating high-temperature synthesis (SHS) method. The initial mixture included starch, DND, and NH_4NO_3 , which was placed in a steel glass and heated. As a result, after washing and drying, we obtained a hybrid material with a yield of 48.2%. The SEM image of the FLG-DND hybrid material is shown in Figure 1a. As seen in Figure 1a, DND aggregates are located on the surface of FLG sheets. According to the XRD results (figure 1b.), there is an X-ray amorphous halo in the range from 17 to 27 ° (2θ) at the site of the graphite peak, which indicates the presence of graphene in the material [3]. There is also a DND peak at an angle of $2\theta = 44$ °.

Using up to 0.25% of DND-FLG hybrid material, we were able to increase the hardness of the composition of aluminum / hybrid material by 111% compared to the original aluminum, while maintaining a density similar to pure aluminum. In this case, the thermal conductivity of the final composite decreased by 14% compared to the original aluminum.

This work was supported by Russian Foundation for Basic Research grant 20-58-00056 bel_a.

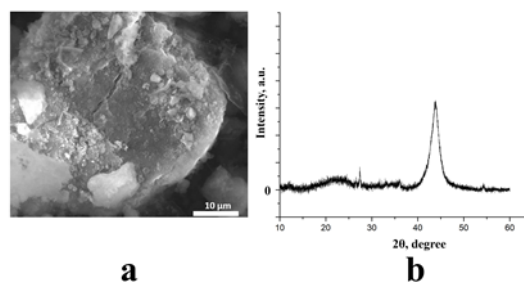


Fig.1. SEM image of a DND-FLG hybrid material and x-ray spectra of a DND-FLG hybrid material

References

1. Vorozhtsov, V. Kolarik, V. Promakhov, I. Zhukov, A. Vorozhtsov, V. Kuchenreuther-Hummel. JOM. 2016. V. 68. Is. 5. P. 1312 – 1316.
2. Chu, X. Wang, Y. Li, D. Huang, Z. Geng, X. Zhao, H. Liu, H. Zhang. Materials & Design. 2018. V. 140. P. 85 – 94.
3. Yolshina, R. Muradymov, I. Korsun, G. Yakovlev, S. Smirnov, Journal of Alloys and Compounds. 2016. V. 663. P. 449 – 459.

On the relationship between chemistry, optical properties and electronic structure of graphene derivatives: revisiting the puzzling complexity

*Rabchinskii M.K.*¹, *Stolyarova D. Yu.*², *Shnitov V.V.*¹, *Baidakova M.V.*¹, *Pavlov S.I.*¹, *Kirilenko D.A.*¹, *Brzhezinskaya M.*³, *Brunkov P.N.*¹

Rabchinskii@mail.ioffe.ru

¹ Ioffe Institute, St. Petersburg, Russia

² NRC "Kurchatov Institute", Moscow, Russian Federation

³ Helmholtz-Zentrum Berlin für Materialien und Energie, Berlin, Germany

Despite the almost two decades of extensive research, the interplay between chemistry and physics of graphene-derived materials still remains puzzling. Extensive studies are being carried out to reveal the effect of the modifying organic groups, point defects, and the extent of the sp^2 -domains on the graphene band structure, its electrophysical characteristics, optical properties.

Here, based on our recent advances graphene derivatization [1,2], we present a thorough examination of the role of organic groups and the π -conjugation length in the optical absorption of graphene derivatives. The analysis of the UV-Vis spectra of the pristine (rGO), carboxylated (C-xy), and carbonylated (C-ny) graphenes has pointed out that absorption band at $\lambda=300$ nm (A2) is not governed by the presence of chromophore carbonyl (C=O) and carboxyl (COOH) groups (Fig. 1). Theoretical calculations have supported the experimental data, indicating no effect of C=O/COOH groups on the UV-Vis spectra. These results show the fallacy of the common model of the optical absorption in GO, asserting the A2 band to arise from the $n\text{-}\pi^*$ transitions in oxygenic groups.

In turn, the decisive role of the π -conjugation extent on the UV-Vis spectra of the graphene derivatives has been shown. The analysis of a set of GO samples with the controllably altered mean extent of the π -conjugated network has revealed the appearance and evolution of a set of absorption bands in the near UV region. Collectively, experimental and theoretical studies have shown that the revealed absorption bands originate from the interband $\pi - \pi^*$ optical transitions and π^* plasmonic states, both depending on the conjugation of the π bonds.

Given the prime importance of UV-Vis spectroscopy in the express characterization of graphene derivatives, the obtained results allow to make an advance in their practical applications as well as widen our understanding of the interplay between the physics of graphene and its chemistry.

The work was supported by the Russian Foundation for Basic Researches (gr. No 18-29-19172).

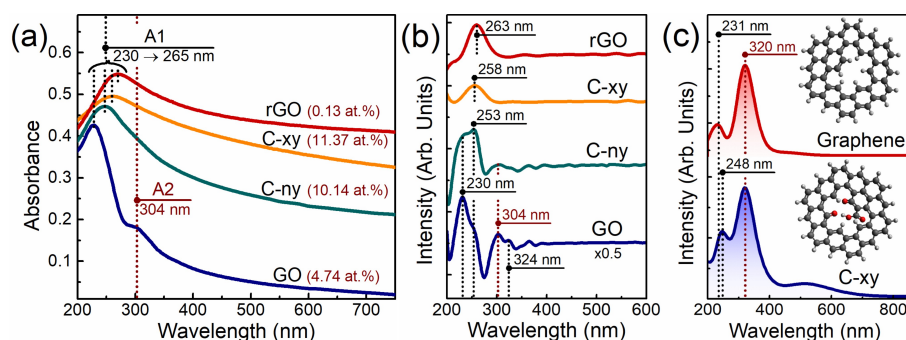


Fig. 1. (a) UV-Vis spectra and (b) their 2nd derivatives of GO, rGO, C-ny and C-xy graphenes. (c) Calculated absorption spectra of the pristine and carboxylated graphene clusters. Inset - models of the clusters

References

1. M.K. Rabchinskii et al. *Nanoscale Perforation of Graphene Oxide during Photoreduction Process in the Argon Atmosphere*. **J. Phys. Chem. C**, 2016, 120, 28261-28269
2. M.K. Rabchinskii et al. *Hole-matrixed carbonylated graphene: synthesis, properties, and highly-selective ammonia gas sensing*, **Carbon**, 2021, 172, 236-247

Creation of optically addressable spin-triplet defects in hexagonal Boron Nitride by electron irradiation

Murzakhanov F.F.¹, Yavkin B.V.¹, Mamin G.V.¹, Orlinskii S.B.¹, Mumdzhi I.E.¹, Smirnov A.N.², Davydov V.Y.², Soltamov V.A.²

victrosoltamov@gmail.com

¹ Kazan Federal University, Kazan, Russia

² Ioffe Institute, Saint Petersburg, Russia

Optically addressable high spin states ($S > 1/2$) of defects in semiconductors are one of the building blocks in the solid-state quantum technologies [1]. Widely studied in 3D crystals, defects possessing optically addressable high spin states have recently been found in 2D material formed by atomic planes of sp^2 -hybridized atoms, interconnected through van der Waals forces, namely hexagonal Boron Nitride (hBN) [2,3]. One defect in the form of negatively charged boron vacancy (V_B^-) is of particular interest since its spin-triplet ground state can be addressed and readout by means of optically detected magnetic resonance at room temperature [3]. This unique property of V_B^- combined with the inherent two-dimensionality of hBN provides sub-nanoscale closeness of the optically active paramagnetic probe to target samples for high-resolution quantum-sensing. The latter is of special importance since hBN is the most relevant encapsulation material for 2D atomically thin heterostructures built up utilizing the atomic-scale "Lego constructor" concept [4].

To further study and explore the optical and spin properties of V_B^- defects, methods of its creation in a reliable way have to be developed. Up to date, several types of irradiation techniques have been approved for the creation of V_B^- centers in hBN lattice. Namely, they are neutron irradiation [3], irradiation with a focused beam of different ions [3], and irradiation with the femtosecond laser pulses [5].

Here we demonstrate an efficient creation of V_B^- defects by means of high-energy electron irradiation. This type of irradiation technique allows to avoid clustering of defects and is widely used for the creation of a homogeneous distribution of point defects in solids. By means of micro-photoluminescence and electron paramagnetic resonance techniques, we demonstrate electron irradiation to be a robust way to create the boron vacancies in the negative charge state.

This work has been supported by the RSF grant No 20-72-10068.

References

1. Awschalom, R. Hanson, J. Wrachtrup, and B.B. Zhou, *Nat. Photonics* (2018) **12**, 516. (2018).
2. Exarhos, A. L., Hopper, D. A., Patel, R. N., Doherty, M. W. & Bassett, L. C., *Nat. Commun.* (2019) **10**, 222.
3. Gottscholl, M. Kianinia, V. Soltamov, S. Orlinskii, G. Mamin, C. Bradac, C. Kasper, K. Krambrock, A. Sperlich, M. Toth, I. Aharonovich, and V. Dyakonov, *Nat. Mater.* (2020) **19**, 540.
4. Geim, A. K. & Grigorieva, I. V., *Nature* (2013) **499**, 419.
5. Gao, S. Pandey, M. Kianinia, J. Ahn, P. Ju, I. Aharonovich, N. Shivaram, and T. Li, *ACS Photonics* (2021), Article ASAP, DOI: 10.1021/acsp Photonics.0c01847.

Spin probing of graphene oxide by 4-aminoTEMPO

*Yankova T.S.*¹, *Chumakova N.A.*^{2,1}, *Vorobiev A.Kh.*¹

ya.tatiana@gmail.com

¹ M.V. Lomonosov Moscow State University, Chemistry Department, Moscow, Russia

² N.N. Semenov Federal Research Center for Chemical Physics, Russian Academy of Science, Moscow, Russia

Graphene oxide (GO) attracts the attention of researchers since it is a precursor of various graphene-based materials, in particular, graphene oxide membranes. Many details of the internal structure of the material are still unclear. Electron paramagnetic resonance (EPR) is a powerful tool to study the molecular organization of different media, which could provide new insights into the properties of GO.

The present report is devoted to the study of GO by a site-specific spin probe. Nitroxide radical 4-aminoTEMPO was chosen as a spin probe capable of localizing acidic groups of GO. The spin probe was introduced into GO powder and GO membrane from acetonitrile according to the procedure described in [1]. It was found that the nitroxide cannot be further removed by washing with acetonitrile or water as opposed to TEMPO and TEMPOL radicals. We believe that this is due to the ion-pair binding between carboxylic groups of GO and amino groups of 4-aminoTEMPO.

Temperature dependence and angular dependence of EPR spectra were used for the determination of rotational mobility and orientational alignment of the paramagnetic molecules in the GO powder and GO membrane, correspondingly.

The orientation distribution function of the radicals has been determined through numerical simulation of the EPR spectra angular dependence, according to the method [2]. The value of the order parameter P20 was found to be 30% lower than the value of P20 for TEMPOL in the same graphite oxide membrane. As 4-aminoTEMPO reflects mostly the orientational distribution of the carboxylic groups contrary to TEMPOL, which characterizes the average orientation of the graphene planes, the data obtained experimentally confirm the assumption that the carboxylic groups are located on the edges of GO flakes.

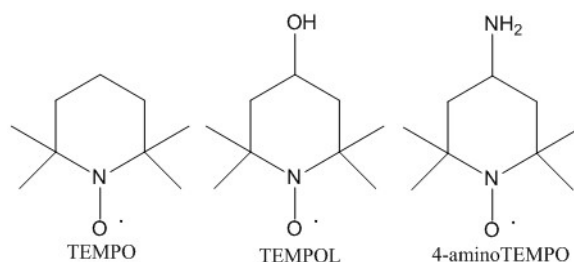


Fig. 1. Structures of the spin probes.

References

1. Chumakova N. A., Rebrikova A. T., Talyzin A. V., Paramonov N. A., Vorobiev A. Kh, Korobov M. V. *J. Phys. Chem. C.* (2018) **122**, 22750.
2. Vorobiev A. Kh., Bogdanov A. V., Yankova T. S., Chumakova N. A., *J. Phys. Chem. B* (2019) **123**, 5875.

This work was supported by the RFBR grant 18-29-19120 mk.

Highly ordered and polycrystalline graphene/Co interfaces intercalated by oxygen

*Bokai K.A.*¹, *Marchenko D.*², *Mikhailovskii V.Yu.*¹, *Vilkov O.Yu.*¹, *Usachov D.Yu.*¹

bokai.kirill@gmail.com

¹ St. Petersburg State University, 7/9 Universitetskaya nab., 199034 St. Petersburg, Russia

² Helmholtz-Zentrum Berlin für Materialien und Energie, Albert-Einstein-Str. 15, 12489 Berlin, Germany

The non-magnetic nature of graphene led to an intense search for magnetic systems, which can be combined with graphene and used for magnetic graphene-based devices. A natural and straightforward choice is to investigate the properties of magnetic contacts made of the widely used Ni or Co, which basically explains the relentless attention to epitaxial graphene/ferromagnet interfaces. The properties of such interfaces, however, are rather delicate to control, as they are sensitive to the microscopic structure and physicochemical state, that would be certainly influenced by ambient conditions at some point. In that regard, the interplay of molecular oxygen with a graphene/ferromagnet interface and its impact on the structure and properties of the latter is of remarkable importance. Within the community, huge attention is paid to the graphene/Ni(111) case, while the Co(0001) substrate remains overlooked.

Here, we present an accurate and comprehensive experimental work aimed to study the intercalation and interaction of oxygen with two technologically interesting systems: polycrystalline (highly disordered) and monocrystalline (highly ordered) graphene prepared on the Co(0001) surface. We have found that in contrast to the ordered graphene/Co(0001) interface, oxygen intercalation under polycrystalline graphene takes place fairly easily and full intercalation is quickly completed. Besides, both oxygen-intercalated systems demonstrate hole-doping effects, which makes them both interesting for electronic applications as well.

A systematic approach has allowed us to identify the key aspects of the oxygen intercalation process in both systems. For the polycrystalline graphene/Co interface, the intercalation starts around Co carbide regions that are not covered with graphene. They play a major role in the intercalation process by providing pathways for oxygen penetration to the interface and become oxidized rapidly. At the same time oxygen intercalation breaks polycrystalline graphene layer apart, which we explain by shrinkage of graphene to its equilibrium lattice parameter. The cracks appear along the grain boundaries in polycrystalline graphene, enabling a direct visualization of its domain structure. A patterned distribution of graphene domains has been revealed by this approach. On the other hand, neither regions of carbidized Co nor cracks formation upon oxygen intercalation have been observed in the ordered graphene/Co systems. These facts may conclusively explain the significantly slower rate of intercalation as compared to the polycrystalline samples.

It is known that being placed on a substrate graphene affect the chemical reactions that occur at the interface and protect surfaces from undesirable influence. In the studied systems, we have found that graphene layers prevent the oxidation of Co underneath until the prolonged thermal oxygen exposures, where the integrity of graphene layers starts to be violated by etching.

This work was supported by RFBR Grants No. 18-29-19178 and No. 19-32-90013.

Interfacial phenomena in electrical transport in graphene/molecular ions hybrid nanostructures

Butko A.V.¹, Butko V.Y.¹, Lebedev S.P.¹, I.A. Eliseyev¹, Davydov V.Y.¹, Lebedev A.A.¹, Kumzerov Y.A.¹

russprot@yahoo.com

¹Ioffe Institute, St.Petersburg, Russia

Hybrid nanostructures with large interface between different nanostructural component play increasing role in modern technology. Therefore, the electrical transport in these systems that can be strongly affected by interfacial conditions is an important object of investigations. In this work we focus our studies on interfacial phenomena in electrical transport in graphene interfaced with molecular ions in solution gated graphene field effect transistors (GFETs). These systems provide a model object for investigation of carrier mobility dependence on interfacial conditions in hybrid nanostructures and are also important for chemical and biological sensor applications.

Most of the developed GFET biological sensors use graphene that has been modified. The fabrication of these sensors is a significant achievement, but in most of these and other graphene based transistor sensors, graphene is modified via covalent bonds, chemical groups, or other methods. These types of sensors require specific methods of modification for each type of molecule that needs to be detected. Other important drawbacks are the serious reduction in sensitivity of the sensors due to a decrease in charge carrier mobility and conductance of graphene caused by the bonding (e.g., covalent) of molecules to the graphene surface. We should emphasize that graphene modification is only one of the possible ways to achieve selectivity of sensors. There are many other devices and techniques (selective membranes, filters, and others) that can be used in combination with unmodified graphene to achieve specific detection if that is the goal. Therefore, sensor applications of graphene field effect transistors (GFETs) without aforementioned modifications in which graphene is exposed directly to the environment has sparked growing interest [1]. However, practically all findings in this field were obtained for gating solutions consisting of small ions, and there are few studies of interfacial phenomena in this configuration for gating solutions consisting of large molecules despite its importance for biomedical sensors. Therefore, we focus on GFETs based on unmodified graphene gated by aqueous solutions containing lysine amino acids. We observed that an increase in the ionic concentration of lysine in these solutions leads to a suppression of unipolar electron conductance of graphene in GFETs. This dependence is opposite to the dependence typically observed in gating solutions containing smaller atomic ions. We attribute the observed suppression to electric field screening of the graphene surface from water molecules by lysine ions which are larger and have lower charge density compared to atomic ions. This novel phenomenon leads to an overall decrease of surface charge density in molecular layers formed at the graphene interface and can be applied in GFET sensors with unmodified graphene that detect the presence and concentration of large molecules in the gating solutions. We also report on dependence of charge carrier mobility in these nanostructures on interfacial conditions. The authors gratefully acknowledge that the present research is supported by the Russian Science Foundation (project 21-72-20038).

References

1. P.K. Ang, W. Chen, A.T. Wee, K.P. Loh, J. Am. Chem. Soc. (2008) **130** 14392.
2. A.V. Butko, V.Y. Butko, S.P. Lebedev, A.A. Lebedev, V.Y. Davydov, I.A. Eliseyev, Y.A. Kumzerov. Journal of Applied Physics (2020) **128**. 215302.

Processes of low-temperature functional restructuring and gas evolution of the GO from room temperature to 90 °C

*Gudkov M.V.*¹, *Rabchinskii M.K.*², *Melnikov V.P.*¹

gudkovmv@gmail.com

¹ FRCCP RAS, Moscow, Russia

² Ioffe Institute, Saint Petersburg, Russia

Graphene oxide (GO) is finding a wider and wider application in the technique. Issues of long-term stability of composition and properties of this material are very relevant. It was noted that the storage of graphite oxide at room temperature, as well as under light, is accompanied by a change in color. The ongoing processes are not clear and are difficult to control. In the literature, these changes are associated with the course of clustering processes leading to the formation of polyconjugated areas and areas enriched with oxygen-containing groups. These processes are slow and difficult to instrumentally investigate.

In this study, we report a half year experiment results with quantitative kinetic data on release CO₂ and CO gases from GO at moderate temperatures (23±2, 50, 70 and 90 °C) far from the temperature of the intensive decomposition and restructuring of the functional groups. It was shown that even at room temperature GO emits CO, CO₂ and H₂O. The emission rates were measured and activation energies of the formation of CO₂ and CO were determined. The activation energies of the formation of CO₂ and CO are almost the same. The ratio of the quantities of CO/CO₂ at room temperature is close to unity, which indicates the coordinated nature of the formation of these gases. The presented data indicate that changes in the GO functional group distribution are already proceeds at room temperature. The migration ability of oxygen-containing groups leads to clustering and separation of polyconjugated regions and regions with an increased oxygen concentration that made decay easier. A change in the CO/CO₂ ratio with increasing temperature may indicate differences in disintegrating structures formed during clustering. It may be due to a change in the relative migration rates of various functional groups. To the best of our knowledge, this is the first report on experimental quantitative data of low temperature decomposition of GO.

The research was carried out with financial support of the Program of Fundamental Researches of the Russian Academy of Sciences (project № 0082-2019-0008).

Application for gas sensing graphene

*Morozova J.V.*¹, *Rezvan A.A.*¹, *Klimin V.S.*¹

ulamrzv@gmail.com

¹ Department of Nanotechnology and Microsystems, Southern Federal University, Taganrog 347922, Russia

This paper presents a study of an ionization sensor of gases with a sensitive element based on a graphene-like film. The study used a combination of plasma-chemical etching techniques and focused ion beams. The results show that the breakdown voltage value for all detected gases is two orders of magnitude lower than that of their analogues.

When creating a sensitive element of an ionization sensor of gases, silicon carbide is used as the substrate material. The SiC substrates were previously chemically cleaned. The method of focused ion beams was used to form the pointed structures. The resulting nanoscale structure was placed in the reactor of a plasma-chemical etching plant, where the remaining gallium ions were removed in several stages after treatment with focused ion beams, and then a graphene film was formed on the surface of the structures in a fluoride plasma atmosphere by removing silicon atoms from the silicon carbide lattice. At the second stage, a layer of dielectric was applied to the attachment points of the upper contact by plasma-chemical deposition, and silicon oxide was used as the dielectric. The upper contact was formed in parallel with the sensor element and was also made of silicon carbide. Contacts were welded to the finished sensor and connected to the signal processing system [1, 2].

As a result of experimental studies, structures with a depth of 900 nm, a height of 860 nm, and a minimum structure size of 280 nm were formed. The manufactured model of the sensing element of the ionization gas sensor has the ability to select gases in gas mixtures, and also gives a breakdown voltage for all detected gases two orders of magnitude less than that of analogues. The advantages of the device are relatively small weight and size parameters, low cost and environmental friendliness of production, achieved due to modern modified nanoscale materials [3].

This work was supported by the Russian Foundation for Basic Research Project № 18-29-11019 mk. The results were obtained using the equipment of the Research and Education Center "Nanotechnologies" of Southern Federal University

References

1. Nakamura S, Senoh M, Nagahama S, Iwase N, Yamada T, Matsushita T, Kiyoku H and Sugimoto Y 1996 Japan. J. Appl. Phys. 35 L74
2. Foxon C T and Joyce B A 1977 Surf. Sci. 64 293
3. V S Klimin, A A Rezvan, O A Ageev Research of using plasma methods for formation field emitters based on carbon nanoscale structures // J. of Phys: C.S.,2018. V.1124. – P. 071020.

Methodology and results of studying the states of hydrogen in graphene structures

*Nechaev Yu.S.*¹, *Cheretaeva A.O.*², *Kostikova E.K.*³, *Shyrygina N.A.*¹, *Denisov E.A.*⁴

yuri1939@inbox.ru

¹ Kurdjumov Centre of Metals Science and Physics, Bardin Central Research Institute for Ferrous Metallurgy, Moscow, Russia

² Research Institute of Progressive Technologies, Togliatti State University, Togliatti, Russia

³ Institute of Applied Mathematical Research, Karelian Research Centre RAS, Petrozavodsk, Russia

⁴ St. Petersburg State University, St. Petersburg, Russia

In this work, the methodology [1, 2] was applied to study the states of hydrogen in graphene structures by processing and analyzing the thermal desorption spectra from [3].

The methodology [1] is based on the use of Gaussian peak approximation of thermal desorption spectra within the first- or second-order reaction model, along with final verification through numerical simulation [2].

Results of such processing of the spectrum from [3] are presented in Fig. 1. The values of the desorption activation energy ($Q = 224 \pm 25$ kJ/mol(H)) and the pre-exponential factor ($K \approx 1 \cdot 10^{15}$ s⁻¹) of the rate constant, obtained for peak # 4 in Fig. 1 in the approximation of the first-order reaction, are consistent with results [4] of analysis of the known data on “desorption” of hydrogen atoms from graphane ($Q \approx 240$ kJ/mol(H), $K \approx 10^{15}$ - 10^{13} s⁻¹).

Acknowledgements

This work was financially supported by the RFBR (Project # 18-29-19149 mk).

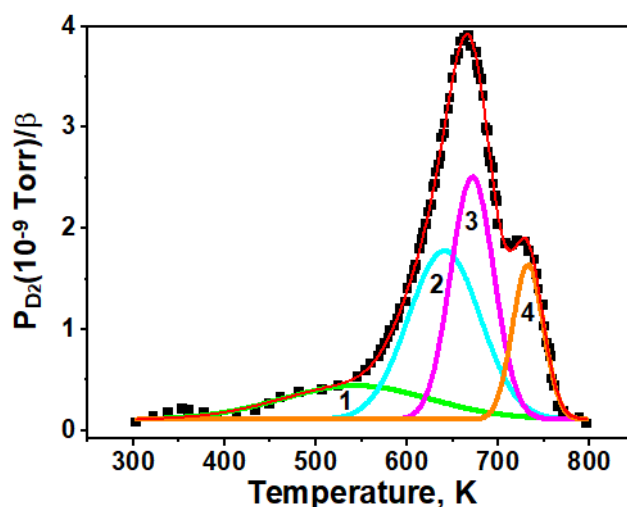


Fig.1. Approximation by four Gaussians of the thermal desorption spectrum from [3] (the heating rate $\beta = 3$ K/s) for deuterium in hydrogenated epitaxial (on Pt substrate) single layer graphene with a diamond-like structure (due to sp^3 hybridization).

References

1. Yu.S. Nechaev, N.M. Alexandrova, A.O. Cheretaeva, V.L. Kuznetsov, A. Öchsner, E.K. Kostikova, and Yu.V. Zaika, *Int. J. Hydrogen Energy* (2020) **45**, 25030.
2. Yu.V. Zaika, E.K. Kostikova, and Yu.S. Nechaev, *Techn. Phys.* (2021) **91**, 210.
3. S. Rajasekaran, F. Abild-Pedersen, H. Ogasawara, A. Nilsson, and S. Kaya, *Phys. Rev. Lett.* (2013) **111**, 085503.
4. Yu.S. Nechaev and T.N. Veziroglu, *Int. J. Phys. Sci.* (2015) **10**, 54.

Graphene-like carbon functionalization

Novikau U.¹, Razanau I.¹, Lomonosov V.¹, Filipovich S.¹

phaust@list.ru

¹ Scientific-Practical Materials Research Centre of National Academy of Sciences of Belarus, Minsk, Belarus

The application of graphene and graphene-like carbons (GLC) often requires surface chemistry optimization. For example, oxidation with subsequent partial reduction allows obtaining graphene-based electrodes for sodium-ion batteries with increased interplanar distance [1], amination of graphene honeycombs significantly improves their electric capacitance in supercapacitors [2], and so on.

We use a two-stage exfoliation technique to synthesize GLC [3]. In the first stage, the alkali metal ammine complex intercalates natural graphite from the solution of alkali metal in liquid ammonia. In the second stage, the hydrolysis or pyrolysis of the graphite intercalation compound leads to its exfoliation and GLC synthesis. The modification of the reaction mixture during the intercalation stage allows achieving graphene covalent functionalization through reactions analogous to the Birch reduction [4]. This report describes a range of GLC functionalization procedures, including amination, hydrogenation, and covalent grafting of short aliphatic chains.

We have shown that amination is the basic functionalization process during the GLC synthesis by our method. The alkali metal content in the ammonia-based reaction mixture determines the amount of the grafted nitrogen-containing groups. Hence, the functionalization proceeds through the carbon anion-radicals formed during the reduction of graphene planes by the solvated electrons in the alkali metal solution. The subsequent hydrolysis leads to additional hydroxylation and hydrogenation of the GLC.

When we add quaternary ammonium halide to the reaction mixture, an exchange reaction occurs with the alkali metal ammine complex intercalate in graphite ($[A(NH_3)_x]C_y$). As the result of the reaction, alkali metal halide (AX) and tertiary amine (NR_3) form. The remaining radical can graft to the graphene plane $[A(NH_3)_x]C_y + R_4X \rightarrow AX + C_yR + NR_3 + xNH_3$. The experiments have shown that among tetramethylammonium (TMA), tetraethylammonium (TEA), and tetrabutylammonium (TBA) halides, TEA salts are the most efficient for aliphatic fragment grafting. In the case of ammonium halide addition to the reaction mixture, graphene hydrogenation occurs via a similar route. Hydrocarbon halides such as methyl iodide and 4-bromotoluene showed a lower efficiency in grafting hydrocarbon groups to graphene planes in an analogous procedure.

In conclusion, processing natural graphite with alkali metal ammonia solution is not only an efficient way to synthesize graphite intercalation compound for subsequent exfoliation into the GLC but also an efficient reaction medium for graphene plane covalent functionalization that allows tuning GLC surface chemistry for particular applications.

References

1. Y. Wen, K. He, Y. Zhu, F. Han, Y. Xu, I. Matsuda, Y. Ishii, J. Cumings, and C. Wang, *Nature Comm.* (2014) **5**, 4033.
2. C.-M. Chen, Q. Zhang, X.-C. Zhao, B. Zhang, Q.-Q. Kong, M.-G. Yang, Q.-H. Yang, M.-Z. Wang, Y.-G. Yang, R. Schlögl, and D. S. Su, *J. Mater. Chem.* (2012) **22**, 14076.
3. U. Novikau, I. Razanau, and S. Filipovich, *MRS Advances* (2016) **1**, 1395.
4. Z. Yang, Y. Sun, L. B. Alemany, T. N. Narayanan, and W. E. Billups, *J. Am. Chem. Soc.* (2012) **134**, 18689.

Aminated graphene: From synthesis to applications

Rabchinskii M.K.¹, Ryzhkov S.A.¹, Saveliev S.D.¹, Antonov G.A.¹, Baidakova M.V.¹, Stolyarova D.Yu.², Vdovichenko A.Yu.², Pavlov S.I.¹, Kirilenko D.A.¹, Brunkov P.N.¹

Sergei.Ryzhkov@mail.ioffe.ru

¹ Ioffe Institute, St.Petersburg, Russia

² NRC "Kurchatov Institute", Moscow, Russian Federation

The synthesis of chemically modified graphenes (CMGs), which contains a given type of covalently-bonded organic groups is currently one of the central aims in the study of graphene materials. This is due to the diverse field of advantageous applications of CMGs, in particular, in gas analytical systems and chemoresistive biosensors. At the same time, despite the vast number of works devoted to the synthesis of CMGs being published every year, the question of the synthesis and characterization of these nanocarbon materials is still open.

Hereby we present a facile method for the synthesis of the aminated graphene by simultaneous reduction and amination of GO during its two-stage liquid-phase treatment with hydrobromic acid and an ammonia solution in isopropyl alcohol [1]. Using spectroscopic techniques, it was found out that the developed method allows to introduce of up to 4-5 at.% of the primary amines and rise the C/O ratio from 2.1 to 17. Further studies by the transmission electron microscopy and Raman spectroscopy demonstrated that the performed amination had resulted in a corrugation and strong bending of graphene layers, resulting in the formation of graphene mesoporous structures with a high specific area. Lyophilisation of organic suspensions of the aminated graphene allowed us to manufacture aerogels with a specific surface area of up to 350 m²/g. Electrical studies using dielectric spectroscopy and low-temperature resistance measurements revealed the complex mechanism of conductivity in the aminated graphene. Ballistic transport of electrons is indicated within a single flake whereas the hopping charge transport arises in the areas of the overlapping platelets of the aminated graphene. Finally, the chemical reactivity of the introduced amine groups was verified by applying a number of test experiments, in particular, the covalent binding of the obtained material with benzoic acid 3-chloride and the oxidation reaction of a copper chloride solution.

As a net result, the synthesized aminated graphene is regarded as a universal platform for the further formation of graphene-based composite structures by covalent bonding with various nanocarbon particles and biomolecules. Particularly, thanks to the presence of active amine groups in combination with the high electrical conductivity, aminated graphene is a promising transducer for the electrochemical biosensor

The presented work was carried out with the financial support of the Russian Foundation for Basic Research (Grant No. 18-29-19172).

References

1. M. K. Rabchinskii, S. A. Ryzhkov, D. A. Kirilenko, N. V. Ulin, M. V. Baidakova, V. V. Shnitov, S. I. Pavlov, R. G. Chumakov, D. Yu. Stolyarova, N. A. Besedina, A. V. Shvidchenko, D. V. Potorochin, F. Roth, D. A. Smirnov, M. V. Gudkov, M. Brzhezinskaya, O. I. Lebedev, V. P. Melnikov, P. N. Brunkov, *From graphene oxide towards aminated graphene: facile synthesis, its structure and electronic properties*, **Scientific Reports**, 2020, 10, 6902

On the synthesis of carboxylated graphene derivative and its application as a transducer in aptasensors

Rabchinskii M.K.¹, Saveliev S.D.¹, Ryzhkov S.A.¹, Stolyarova D.Yu.², Antonov G.A.¹, Pavlov S.I.¹, Kirilenko D.A.¹, Malkov M. N.³, Komarov I.A.⁴, Brunkov P.N.¹

Sviatoslav.Saveliev@mail.ioffe.ru

¹ Ioffe Institute, St. Petersburg, Russia

² NRC "Kurchatov Institute", Moscow, Russian Federation

³ Lomonosov Moscow State University, Moscow, Russian Federation

⁴ National Research University of Electronic Technology, Zelenograd, Russia

Rapid developments in the manufacturing of graphene-based devices have facilitated advances in the synthesis and application of chemically modified graphenes (CMGs) covered with a certain type of organic group, altering graphene chemical reactivity or physics in the desired way. Particularly, carboxyl-enriched CMGs, carboxylated (C-xy) graphenes, have attracted great attention due to the chemical reactivity of carboxyl groups, allowing to use them as anchoring points for various biomolecules, such as DNA strands and antibodies for biosensing applications.

In this work, we present a facile wet chemistry method for the synthesis of the carboxylated (X-xy) graphene in the form of organic suspensions [1]. As-synthesized C-xy graphene contains up to 8 at.% of carboxyl (COOH) groups with the substantial reduction of basal-plane hydroxyls and epoxides, which leads to partial restoration of the π -conjugated system. Besides the rise in the number of COOH the applied carboxylation also is found out to lead to a perforation of graphene layer with the formation of nanoscale holes of 50-100 nm in diameter. Owing to its holey structure and incomplete recuperation of the π -conjugated system the synthesized C-xy graphene demonstrates semiconducting nature with the resistance estimated to be 100-300 k Ω and Mott variable hopping mechanism (VRH) of charge transport indicated by the low-temperature resistance measurements. Despite such low conductivity is far from desired for optoelectronic applications, along with VRH charge transport it is advantageous for sensing applications due to enhancement of the chemiresistive response.

The chemical reactivity of carboxyl groups on the C-xy graphene has been tested by the covalent immobilization of the HO1 aptamer, which has a specific affinity to the HBsAg protein, a marker for the hepatitis B infection. The successful immobilization has been verified by the shift of the absorption maximum in the UV-Vis spectrum and directly by the appearance of the phosphorous and nitrogen signals in the X-ray photoelectron spectra due to the presence of these elements in the aptamers (Fig. 1). The subsequent tests of the biosensor prototype based on the spray-coated C-xy graphene layer with the immobilized aptamers have shown the operability of such a device with the manifestation of a chemiresistive response towards the drop-casting of alcohol solutions containing HBsAg proteins.

As a net result, a facile method for the synthesis of C-xy graphene derivative is developed and the relevance of this graphene derivative for the biosensing applications by its grafting with aptamers is demonstrated.

The presented work was carried out with the financial support of the Russian Foundation for Basic Research (Grant No. 18-29-19172).

References

1. S. A. Ryzhkov, M. K. Rabchinskii, V. V. Shnitov, M. V. Baidakova, S. I. Pavlov, D. A. Kirilenko, P. N. Brunkov. *On the synthesis of the carboxylated graphene via graphene oxide liquid-phase modification with alkaline solutions*. **J. Phys. Conf. Ser.**, 2020, 1695, 012008

Specific surface area studying of reduced graphene oxide - detonation nanodiamond compounds

*Trofimuk A.D.*¹, *Vul S.P.*¹, *Tomkovich M.V.*¹, *Kukushkina Yu.A.*¹, *Shvidchenko A.V.*¹, *Dideikin A.T.*¹

trofimuk.ad@mail.ioffe.ru

¹ Ioffe Institute, Saint-Petersburg, Russia

The most important direction in the development of carbon nanostructure technology is the creation of electrodes for energy storage for renewable energy (including supercapacitors and lithium-ion batteries). The use of graphene varieties in such electrodes is attractive due to their chemical inertness, high specific surface area (SSA), and electrical conductivity. However, there is an effect of sticking graphene plates together (restacking). It leads to a dramatically decrease in the available SSA and that's why a large number of studies are devoted to prevent restacking during the formation of three-dimensional structures [1]. Deagglomerated detonation nanodiamond (DND) is a promising candidate for the role of a spacer for graphene nanoplates. The hardness of DND crystallites makes it possible to use the final material where frequent and / or prolonged mechanical stress is required, and its size - 4-5 nm - should theoretically both prevent restacking and ensure the preservation of a high SSA of the final material.

In this work, a suspension of graphene oxide (GO) ($\zeta < 0$) obtained by the modified Hammers method was mixed with a suspension of DND ($\zeta > 0$). The isoelectric point corresponds to the mass ratio of DND / GO = 3.5. In three out of four samples, significantly more diamond was added; the deviation from the isoelectric point was compensated by the addition of an appropriate amount of another type of DND ($\zeta < 0$). The resulting suspensions were dried at 80°C and then treated at 700°C in H₂ stream for 3 h. The resulting powders were analyzed by gas adsorption (N₂). The results are shown in Table 1.

Table 1 - Results of BET analysis.

Sample	DND / GO mass ratio, unitless	BET SSA, m ² ·g ⁻¹	BET pore size, nm
DND Z+	---	251	16,11
DND and GO 3.5	3,5	386	1,97
DND and GO 13	13	272	7,48
DND and GO 29	29	290	5,97
DND and GO 61	61	274	9.01

It can be seen from the results that the SSA significantly increases with the addition of DND to the GO in the DND / GO mass ratio = 3.5. However, with further addition of diamond, the SSA decreases and becomes comparable to the specific surface area of DNDs, which indirectly indicates a decrease in the contribution of reduced graphene oxide plates to the surface properties.

Apparently, the best way of further work will be the use of compositions with a ratio of DND and GO masses close to the isoelectric point. In addition, the mutual compensation of the charges of the GO ($\zeta < 0$) and DND ($\zeta > 0$) cause the tendency to the formation of self-assembled structures.

The work was supported by Russian Foundation for Basic Research (grant № 18-29-19159).

References

1. Gorgolis, G., Galiotis, C. 2D Mater. (2017) 4, 032001

Computer simulation of the three-dimensional structure of fluorinated graphene crystals

*Belenkov M. E.*¹, *Chernov V. M.*¹

me.belenkov@gmail.com

¹Chelyabinsk State University, Chelyabinsk, Russia

Functionalization of graphene with non-carbon atoms and molecular groups allows changing its properties for practical applications. The most promising is fluorographene, since it has high thermal stability. It is theoretically predicted that the existence of many fluorographene polymorphs is possible, differing from each other in the order of adsorption of fluorine atoms to the graphene surface, as well as in properties [1]. Fluorographene polymorphs can be obtained not only by functionalization of hexagonal graphene, but also by fluorination of various graphene polymorphs, such as 4-8, 3-12, 4-6-12, or 5-7 [2-4].

Theoretical calculations of these fluorographene compounds were performed earlier for isolated monolayers. However, the properties of layered nanostructures strongly depend on the substrate or crystal with which they interact. Therefore, in this paper, calculations of the three-dimensional structure and properties of crystals of polymorphic fluorographene varieties formed on the basis of graphene layers L_6 , L_{4-8} , L_{3-12} , L_{4-6-12} and L_{5-7} , were performed. Computer simulation of the three-dimensional structure of crystals was carried out by the method of atom-atomic potential. Calculations of energy characteristics and electronic properties were carried out by the method of density functional theory in the generalized gradient approximation. In total, 15 different crystals of functionalized graphene were investigated. Figure 1 shows an example for a CF- L_6 T5 type fluorographene layer. It was found that the sublimation energy of fluorographene crystals in comparison with monolayers changes insignificantly - by 0.04-0.08 eV. Apparently, this occurs due to the additional energy of interlayer bonds in crystals. The band gap in crystals varies in the range from 2.51 to 4.60 eV, which is significantly less (by 0.20 - 0.62 eV) compared to isolated monolayers. Polymorphic varieties of fluorographene can be used in nanoelectronics.

The reported study was funded by Russian Foundation for Basic Research (RFBR), project number 20-32-90002.

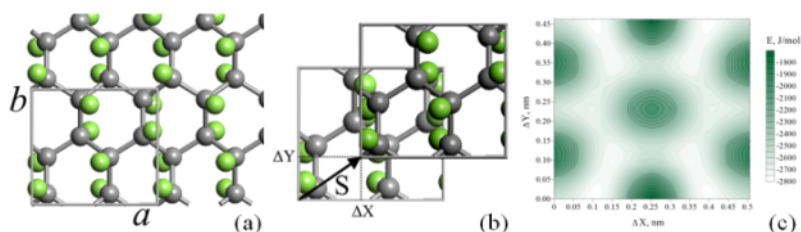


Fig.1. The structure of a CF- L_6 T5 type fluorographene layer (a), a scheme for setting the relative shift of adjacent layers in three-dimensional crystals (b) and a graph of the energy of interlayer bonds versus the shift vector (c).

References

1. E. Belenkov, V.M. Chernov, and E.A. Belenkov, *J. Phys. Conf. Ser.* (2018) **1124**, 022010.
2. E. Belenkov, V.M. Chernov, and E.A. Belenkov, *IOP Conf. Ser.: Mater. Sci. Eng.* (2019) **537**, 022058.
3. E. Belenkov, and V.M. Chernov, *Letters on Materials* (2020) **10**, 254
4. E. Belenkov, and V.M. Chernov, *Physical and chemical aspects of the study of clusters, nanostructures and nanomaterials* (2020) **12**, 326

The first free-standing transparent fluorinated graphene film

Colin M.¹, Chen X.², Guerin K.¹, Dubois M.¹

marie.colin@uca.fr

¹ ICCF, 24 Avenue Blaise Pascal, 63170 Aubiere, FRANCE

² UNSW, 2/89 Dangar Street, Randwick NSW 2031, AUSTRALIA

Graphene oxide (GO), synthesized by oxidation and exfoliation of graphite through Hummer's method, possesses many different oxygen-containing functional groups such as epoxy, hydroxy and carboxylic acid. Contrary to graphene, GO are known as a polar, hydrophilic adsorbent compound with large surface area, thus, GO can be used for solid phase extraction of metal ions adsorption. [1] GO films made of stacked/overlapping GO sheets can be prepared by flow-directed assembly, e.g., vacuum filtration of the GO dispersion on substrates, followed by separation after drying.

The fluorination of GO films at low temperature (70°C) under F₂ gas in a closed reactor allowed transparent fluorinated graphene oxide (FGO) films to be prepared, which maintained its initial film-like form. During fluorination process, most of oxygen atoms were replaced by fluorine atoms to form covalent carbon-fluorine bonds. The amount of fluorine depends on the reaction temperature, the amount of reactive molecular fluorine and the reaction time. The C-F bonding was studied by infra-red spectroscopy, ¹⁹F, ¹³C and cross-polarization ¹⁹F→¹³C nuclear magnetic resonance. Besides these techniques, C-F bonding, F/C, F/O and O/C atomic ratios were estimated by X-ray photoelectron spectroscopy too. The changes of surface chemistry and surface energy during fluorination were also investigated through contact angle and tribological measurements. Both the morphology and the roughness were studied by scanning and transmission electron microscopies as well as atomic force microscopy. Potential application of FGO films as free-standing cathode material for primary lithium batteries will be discussed according to their deep physical-chemical characterization in particular the singular C-F bonding with weakened covalence and high fluorine content.

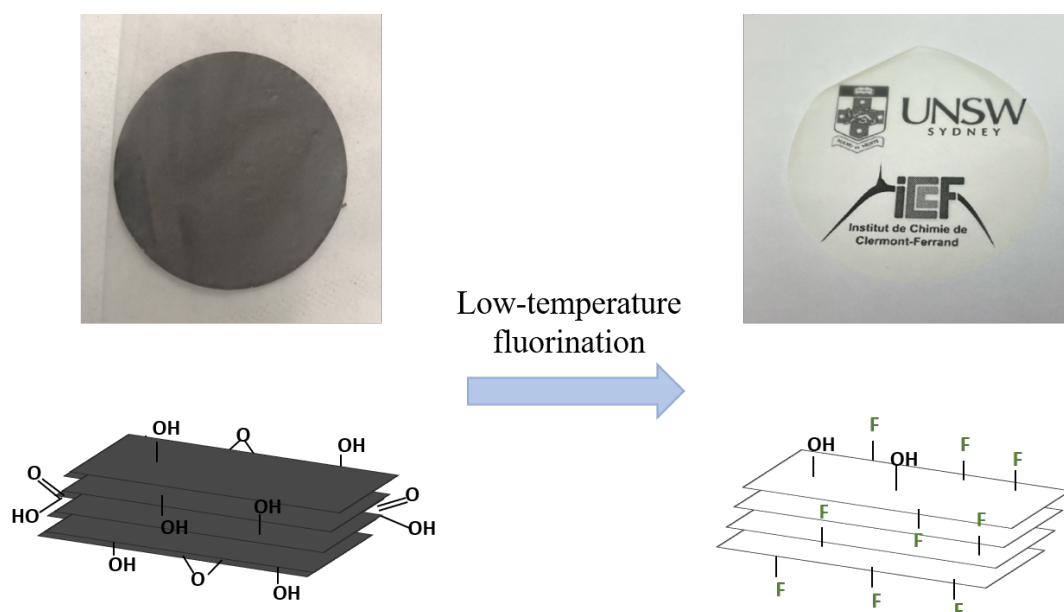


Figure 1 : Modifications of graphene oxide films after fluorination

References

1. R. Sitko, B. Zawisza, E. Malicka, Graphene and Derivatives: Sample Handling. In *Reference Module in Chemistry, Molecular Sciences and Chemical Engineering*, Elsevier, 2018, p340-343.

Sorption of polar liquids by GO powders and membranes

Kaplin A.V.¹, Rebrikova A.T.¹, Avramenko N.V.¹, Eremina E.A.¹, Gudilin E.A.¹, Korobov M.V.¹
mkorobov49@gmail.com

¹ M.V. Lomonosov Moscow State University, Chemistry Department, Leninskiye Gory 1/3, Moscow, 119991, Russia

Graphite oxide membranes (GOM) attracted recently wide attention. These mechanically strong and relatively cheap devices were successfully used for cleaning of water, separation of gas mixtures etc. From a scientific perspective, a challenging problem is mechanism of transmembrane diffusion. The interaction of polar substances with GO powders and GOM leads to swelling of GO materials. Swelling is a combination of two processes, namely, of sorption of liquids into the interplane space of GO and of simultaneous increase of interplane distances. The latter process is well documented by X-ray diffraction (XRD)¹ while quantitative data on sorption of polar liquids are limited. Almost no data are available for sorption into membranes.

In this experimental study we were focused on sorption of a series of polar liquids into Brodie and Hummers GO, BGO and HGO respectively. In particular, we were interested in comparison of sorption in powders and membranes, prepared from the same carefully characterized materials. The initial characterization of the materials were performed using XRD, XPS, IR. Sorptions were measured using DSC and isopiestic method. Basic results of the study may be summarized as follows:

1) Equilibrium sorption into GO obtained by direct contact with the adsorbed liquid is the same for membranes and powders. These data were obtained by DSC and are in accord with the XRD data² on interplane distances obtained under similar conditions.

2) Sorption of the same liquid through the vapor phase is restricted by the kinetic factors. Sorption is significantly higher for powders compared to membranes as was evidenced by measurements of sorption performed by isopiestic method under strictly identical conditions.

3) Swollen structures formed by BGO powders may be considered as solid solvates of BGO. These structures experienced phase transitions (incongruent melting). Two types of such transitions were observed in the systems of B-GO with n-alcohols. Search for the same phenomena was performed for the swollen B-GO membranes.

4) Values of sorption are reproducible and insensitive to the minor changes in the syntactic procedure for GO powders. However, sorption into BGO and HGO differ significantly.

This work was supported by the RFBR grants 18-29-19120 mk and 19-08-00498. XPS measurements were performed in the shared scientific center "Nanochemistry and Chemistry of the Atmosphere" of the Department of Chemistry, MSU.

References

1. A.V. Talyzin, G. Mercier, A. Klechikov et al. Carbon 2017, 115, 430 - 440
2. A. Iakunkov, J. Sun, A. Rebrikova et al. J. Mater. Chem. A, 2019, 7, 11331-11337

Structure of graphene oxide aerogels

*Kulvelis Yu.V.*¹, *Rabchinskii M.K.*², *Baidakova M.V.*², *Pavlov S.I.*², *Gudkov M.V.*³

kulvelis_yv@pnpi.nrcki.ru

¹ Petersburg Nuclear Physics Institute named by B.P. Konstantinov, NRC "Kurchatov Institute", Gatchina, Russia

² Ioffe Institute, St. Petersburg, Russia

³ N.N. Semenov Federal Research Center for Chemical Physics, Russian Academy of Sciences, Moscow, Russia

Graphene oxide (GO) and its derivatives were used to prepare aerogels by freeze-drying from aqueous suspensions. Reduced GO (rGO) aerogel was obtained by additional annealing at 400°C. The samples were studied by small-angle X-ray scattering and X-ray diffraction (SAXS and XRD) techniques, complemented by small-angle neutron scattering (SANS) and scanning electron microscopy (SEM) to find the fine structure of GO aerogel prior to and after annealing.

Fig. 1 shows typical Porod-law scattering ($I(q) \sim q^{-4}$) in the SAXS range and the presence of the 00.2 diffraction maximum at $q = 7 \text{ nm}^{-1}$ in XRD for initial GO aerogel. These results point out that walls of aerogel have lamellar structure presented by stacks of smooth GO layers with a thickness 120 nm (~ 11 -12 GO layers). In turn, annealing results in the reduction of the walls' thickness due to diminishing of the interlayer distance and corrugation of the GO layers indicated by the shift of the 0.02 maximum (XRD data) and the changes in the slope in the SAXS at $q < 0.15 \text{ nm}^{-1}$ ($I(q) \sim q^{-2.8}$). Scanning electron microscopy revealed the porous structure of aerogels with the system of penetrating channels (5-10 μm). The studied aerogels have excellent specific surface areas (300-350 m^2/g) and a surface conductivity (200-230 S/m), making them prospective to use in sensor technologies as transducers with increased susceptibility, as well as in electrochemical energy storage systems.

The properties of aerogels may be further improved in the case of aminated GO aerogel and GO-nanodiamond compositional aerogel, depending on the composition and conditions of preparation.

The work was supported by the Russian Foundation for Basic Researches (gr. No 18-29-19172).

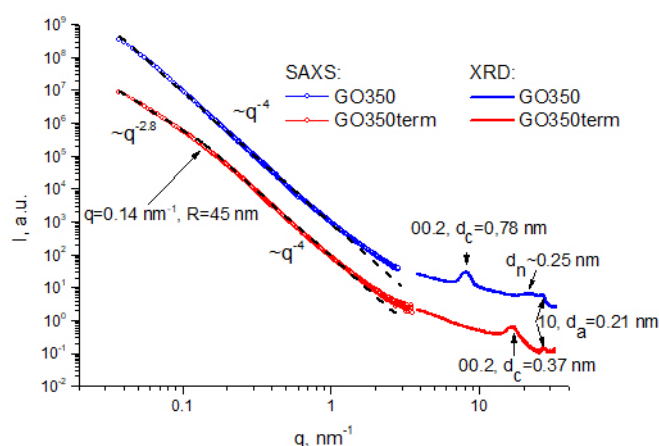


Fig.1. SAXS and XRD on initial GO aerogel (sample GO350) and annealed (GO350term).

Mechanisms of graphene oxide reduction under ultrafast laser irradiation: insights from reactive molecular dynamics

Potapov D.O.^{1,2}, Evlashin S.A.³, Orekhov N.D.^{1,2}

potapov.do@phystech.edu

¹ Moscow Institute of Physics and Technology, Dolgoprudny, Russia

² Joint Institute for High Temperatures of Russian Academy of Sciences, Moscow, Russia

³ Skolkovo Institute of Science and Technology, Moscow, Russia

At temperatures exceeding $T=800\text{--}1000$ K and in the presence of oxygen pure carbon undergoes rapid combustion. Nevertheless, recent experimental results on nanosecond laser irradiation of GO demonstrate that after heating up to $3000\text{--}3300$ K this material transforms into graphene with high local order [1]. To shed light on the mechanisms behind this surprising effect we perform molecular-dynamics modeling of GO reduction under high temperature conditions. Calculations were performed using LAMMPS program package [2] with reactive interatomic potential ReaxFF and its CHO-2017 set of parameters [3].

Our results demonstrate that ultrafast heating produced by nanosecond laser combined with a fast cooling (the result of an extraordinary heat conductivity of graphene) leads to a fascinating regime of almost oxygen-free GO reduction in the air at $T=2500\text{--}3300$ K. While on the edges of GO at such temperatures we observe combustion process that captures atmospheric oxygen into CO and CO₂ molecules, central regions of GO undergoes rapid reduction and annealing with only little signs of oxidation. As a result, after a small loss of mass (primarily from its edges), GO transforms into graphene with a high local ordering.

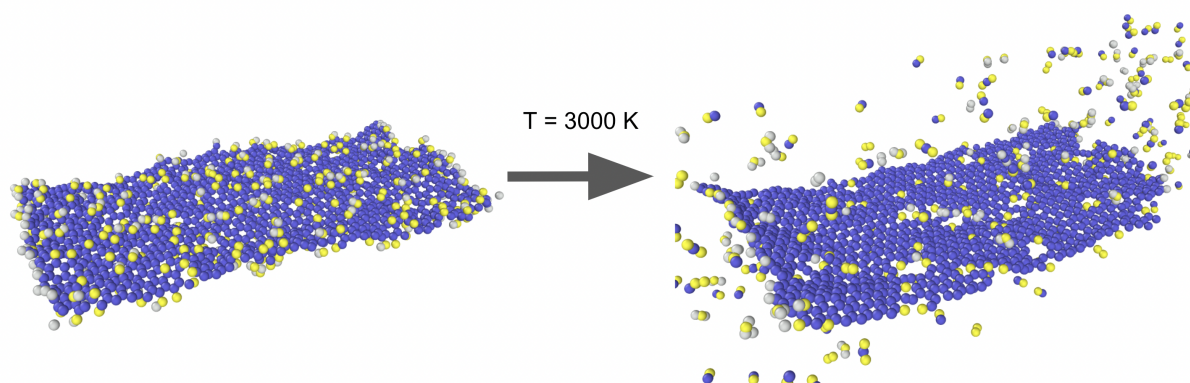


Fig.1. Snapshots of computational cell before (left) and after (right) high temperature treatment of graphene oxide sheet.

References

1. S.A. Evlashin, S.E. Svyakhovskiy, F.S. Fedorov, Y.A. Mankelevich, P.V. Dyakonov, N.V. Minaev, S.A. Dagesyan, K.I. Maslakov, R.A. Khmel'nitskiy, N.V. Suetin, I.S. Akhatov, and A.G. Nasibulin, *Adv. Mater. Interfaces* (2018) **5**, 1800737.
2. S. Plimpton, *J. Comput. Phys.* (1995) **117**, 1.
3. C. Ashraf, and A.C. Van Duin, *J. Phys. Chem. A* (2017) **121**, 1051.

Graphene chemical derivatives as gas sensing layers: From the synthesis to the theory behind

*Rabchinskii M.K.*¹, *Varezchnikov A.S.*², *Sysoev V.V.*², *Stolyarova D. Yu.*³, *Shnitov V.V.*¹, *Baidakova M.V.*¹, *Pavlov S.I.*¹, *Kirilenko D.A.*¹, *Struckov N.S.*⁴, *Solomatina M.A.*², *Brunkov P.N.*¹

Rabchinskii@mail.ioffe.ru

¹ Ioffe Institute, Saint Petersburg, Russia

² Yuri Gagarin State Technical University of Saratov, Saratov, Russia

³ NRC "Kurchatov Institute", Moscow, Russian Federation

⁴ National Research University of Electronic Technology, Zelenograd, Moscow, Russia

The synthesis and study of chemically modified graphenes (CMGs) for sensing applications are at the forefront of graphene studies nowadays. Such an excitement arises from the excellent sensing performance of graphene oxide (GO) and reduced GO (rGO) towards numerous gases and volatile organic compounds (VOCs), including NO₂, NH₃, CO, etc. at room temperature. Nevertheless, further advances in the selectivity of CMG-based gas sensors are to be approached for practical applications and to give a hint about the mechanisms involved in their chemiresistive response.

Here, the synthesis of holey carbonylated (C-ny) and carboxylated (C-xy) graphene derivatives and their application for gas sensing are demonstrated. The applied liquid-phase carbonylation and carboxylation methods have resulted in the rise in the concentration of carbonyl (C=O) and carboxyl (COOH) groups up to 9 at.% in C-ny and C-xy graphenes, respectively, with substantial elimination of other oxygen functionalities [1,2]. Such a chemical modification is accompanied by the perforation of the graphene network with the appearance of matrices of nanoscale holes, leading to corrugation of the layer and its sectioning into localized domains of the π -conjugated graphene network. Combined with the predominant presence of C=O or COOH groups, granting the specificity in gas molecules adsorption, these features result in the enhanced gas sensing properties of C-ny and C-xy graphenes at room temperature with a selective response to NH₃. Opposite chemiresistive response towards ammonia when compared to other analytes, such as ethanol, methanol, acetone, and CO₂, is demonstrated for the C-ny and C-xy graphenes both in humid or dry air background. Moreover, a selective discrimination of all of the studied analytes is further approached by employing a vector signal generated by C-ny or C-xy multielectrode chip and its processing in terms of linear discriminant analysis (LDA) (Fig. 1). Comparing the experimental results with the calculations performed in the framework of density functional theory, we have clarified the effect of partial charge transfer caused by water and ammonia adsorption on the chemiresistive response.

The work was financially supported by the Russian Scientific Foundation (gr. № 19-72-10052).

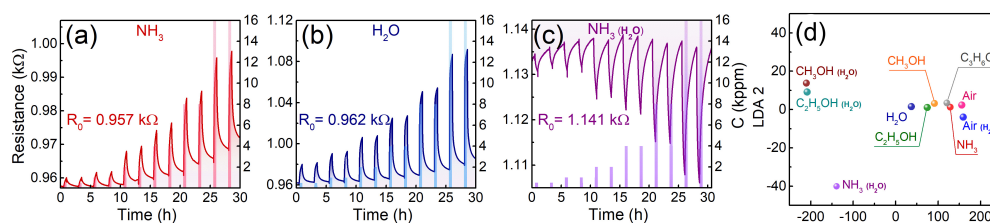


Fig. 1. Chemiresistive response of C-xy graphene towards (a) NH₃, (b) H₂O, and (c) NH₃ in humid air. (d) The results of the recognition of the studied analyte VOCs using LDA

References

1. M.K. Rabchinskii et al. *Nanoscale Perforation of Graphene Oxide during Photoreduction Process in the Argon Atmosphere*. **J. Phys. Chem. C**, 2016, 120, 28261-28269
2. M.K. Rabchinskii et al. *Hole-matrixed carbonylated graphene: synthesis, properties, and highly-selective ammonia gas sensing*, **Carbon**, 2021, 172, 236-247

Long-lived luminescence and transient absorption of graphene oxide quantum dots, prepared by laser ablation

*Seliverstova E.*¹, *Ibrayev N.*¹, *Menshova E.*¹

genia_sv@mail.ru

¹ Institute of Molecular Nanophotonics, Buketov Karaganda University, Karaganda, Kazakhstan

Graphene and carbon quantum possess high solubility in water, chemical inertness and resistance to photobleaching and they are very promising objects for photocatalysis, photovoltaics, biophysics and etc.

The long-lived luminescence and transient absorption of graphene oxide quantum dots (GO QDs) obtained by laser ablation is presented in this work.

Quantum dots were obtained by ablation of graphene oxide (Cheaptubes) dispersion by Nd:YAG laser with $\lambda_{\text{gen}} = 532$ nm. Data obtained from dynamic light scattering (Zetasizer S90, Malvern) and SEM (Mira 3LMU, Tescan) showed that the size of GO sheets was varied in the range of 300-800 nm before ablation. After ablation, the size of GO sheets was decreased to 75 ± 20 nm.

The absorption spectrum (Cary 300, Agilent) of GO QDs exhibits the bands with maxima at 240 and 380 nm. The intensity and position of the fluorescence spectrum (Eclipse, Agilent) depends on the excitation wavelength. The maximum fluorescence intensity (at 410 nm) was observed at $\lambda_{\text{exc}} = 300$ nm. To study long-lived luminescence and transient absorption, the GO QDs solution was degassed. The transient absorption spectrum (LP-980K, Edinburgh Instr.) of GO QDs exhibits a spectra with a maxima at 400 and 500 nm with the lifetimes of 42.1 and 160 ns for $\lambda_{\text{reg}} = 400$ nm, and 31 and 130 ns for 500 nm. In the spectra of long-lived luminescence a band with a maximum at ~ 520 nm and shoulders at 410 was registered (Figure). The decay kinetics can be described by a two-exponential law with the short-lived component equal to 1.2 and 0.74 ms and long-lived component equal to 4.4 and 1.75 ms for 410 and 520 nm, respectively.

This work was carried out as part of the research project AP08052672, funded by the Ministry of Education and Science of the Republic of Kazakhstan.

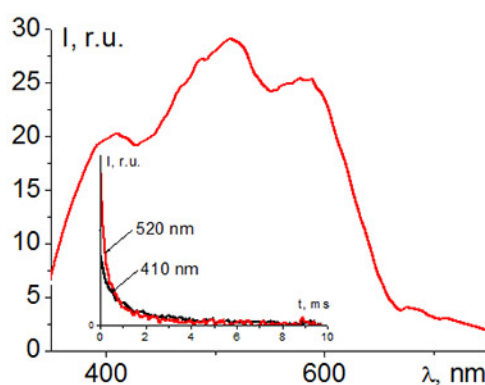


Fig. Spectrum and kinetics (in the inset) of long-lived luminescence of GO QDs

Influence of different types of low-layer graphite fragments on tribological and rheological properties of plastic lubricants

Stolbov D.N.^{1,2}, Smirnova A.I.¹, Savilov S.V.², Shilov M.A.^{3,4}, Burkov A.A.⁴, Parfenov A.S.⁵, Usoltseva N.V.¹

nv_usoltseva@mail.ru

¹ Nanomaterials Research Institute, Ivanovo State University, Ivanovo, Russia

² Moscow State University named after M.V. Lomonosov, Moscow, Russia

³ Ivanovo State Energy University named after V.I. Lenin, Ivanovo, Russia

⁴ Vyatka State University, Kirov, Russia

⁵ Ivanovo State Medical Academy, Ivanovo, Russia

The dispersions of low-layer graphite fragments (LGF) and their nitrogen-doped analogues (N-LGF) in three commercially available plastic lubricants (**PL**) and a model grease - Medical Vaseline (**VM**) were studied by tribological and rheological methods. The presence of nitrogen atoms in the structure of N-MGF increases its hydrophilicity in comparison with MGF changing the properties of the material.

The synthesis of LGF and N-LGF was carried out by chemical vapor deposition on an MgO template. Hexane and acetonitrile were used as precursors for LGF and N-LGF, correspondingly. The obtained carbon nanostructures were characterized by X-ray photoelectron spectroscopy and transmission electron microscopy. The content of carbon nanostructures in dispersions was ranged from 0.1 to 1.5 wt.%. Tribological studies were carried out on an MTU-01 friction machine (the "ring-disk friction pair" made of hardened steel grade ShKh-15, load range 0-250 N). Rheological properties were studied on a multifunctional Rheologica StressTest rheometer in rotational and oscillatory modes.

In tribological experiments with **PL**, the introduction of both LGF and N-LGF resulted in different values of friction coefficients (up to the opposite effect). This could be due to the presence of various components contained in the formulation of the base lubricant.

When **VM** was used as a lubricant, both additives reduce the friction coefficient of their dispersions in comparison with base **VM**. The more significant reduction was noticed when the N-LGF additive was applied (by 42%), in comparison with LGF (by 27%).

The common feature for all investigated dispersions based on studied **PL** is a decrease in *dynamic viscosity* (*destructive rheological tests*) over the entire range of shear stresses irrespective to the nanocarbon additive. In contrast, their introduction into **VM** increases the shear stress values.

Nondestructive rheological tests have shown that the presence of N-LGF in **VM** or **PL** leads to an increase in the value of the elastic component of the complex shear modulus and a decrease in the viscous component in the entire frequency range (0.1-12 Hz). The maximum increase in the value of G' was observed for the dispersions with 0.25 wt. % of additives. This fact was confirmed by a decrease in the loss angle δ within the entire range from 0 to 90° depending on the frequency, which meant a decrease in viscous and, accordingly, an increase in elastic contributions to the characteristics of the tested samples. The results were processed using the Gaussian numerical smoothing method. The compliance of the studied systems was calculated. Dispersions with N-LGF showed a decrease in the compliance value in the entire frequency range. The dispersions with LGF showed the opposite character in terms of all above mentioned.

This work was supported by the RFBR (project no. 18-29-19150_mk and 20-33-90043_asp) and the Ministry of Education and Science of the Russian Federation (project no. FZZM-2020-0006).

Photovoltaic 2D graphene structures for safe explosion

*Voznyakovskiy A.P.*¹, *Ilyushin M.A.*², *Shugalei I.V.*², *Vedernikov Y.N.*³, *Smirnov A.V.*³,
*Vozniakovskii A.A.*⁴

voznap@mail.ru

¹ Lebedev Research Institute for Synthetic Rubber, Saint-Petersburg, Russia

² Saint-Petersburg State Institute of Technology, Saint-Petersburg, Russia

³ Research and production enterprise Krasnoznamens Saint-Petersburg, Russia

⁴ Ioffe Institute Saint-Petersburg, Russia

The high-energy impulse effect of the products of the explosive decomposition of energy-saturated substances (EW) on various objects and materials is widely used in industrial practice. An essential requirement for energetic condensed substances (explosives) is to ensure the maximum safety of their use. To achieve increased safety parameters, two approaches are used: the exclusion of the use of initiating explosive systems from the charge assembly and the exclusion of the electric method of initiating an explosion. Thus, the fulfillment of these two complementary requirements can be ensured by the use of laser initiation of energy-saturated substances, promoted by the inclusion of graphene additives in the charge composition [1]. However, for the real use of graphene in the practice of blasting, it is necessary to ensure the possibility of its large-scale production. We have developed a high-performance technique for producing 2D nanocarbons by carbonization of biopolymers under the conditions of a self-propagating high-temperature synthesis (SHS process). However, the applied technique makes it possible to obtain mainly samples of multilayer graphene (FLG) [2].

The purpose of the present work was to test the possibility of initiating explosive decomposition of the complex energy saturated substance/FLG under the influence of a flow of photons of a laser diode (976 nm long, 10 W power, 105 μm diameter) - the production of a laser detonator. We used the well-known pentaamine- (5-nitro-2H-tetrazolato-N2) cobalt (III) perchlorate (NCP) complex [3]. For the experiments, we prepared an energy composite NCP / FLG (97/3%).

As our experiments have shown, laser initiation in all cases (10 repetitions) has resulted in the explosive decomposition of the resulting energy composite laser beam with an enzyme of ~170 times less than for the NCP complex, which indicates the validity of our assumption about the possibility of using FLG particles in energy composites designed to create laser capsules for detonators of low-layer graphene particles obtained by our original method.

It should be noted that the mechanism of initiation of explosive decomposition of explosives is still debatable. When formulating a certain phenomenological model of laser initiation of energy complexes including graphene, one can rely on the well-known phenomenon of graphene photovoltaics [4]. The ability of graphene FLG to generate electron fluxes makes it possible to compare the mechanism of initiation of the explosive decomposition of the NCP complex modified by FLG with the mechanism of electrical breakdown.

The reported study was funded by RFBR and BRFB, project №20-58-00056.

References

1. Qi-Long Yan, Michael Gozin, Feng-Qi Zhao, Adva Cohen, Si-Ping Pang *Nanoscale*, 2016, **8**, 4799.
2. Vozniakovskii, A.A., Voznyakovskii, A.P., Kidalov, S.V., V.K. Osipov. *J Struct Chem* 2020 **61** 826.
3. Ilyushin, M. A., I. V. Tselinsky, and I. V. Shugalei. *Central European Journal of Energetic Materials* 2012. **9** 293 *Nano Energy* 2018 **47** 51
4. Done Wook Chang, Hvon-Jung Choi, Alan Filer, Jong-Beom Baek *J. Mater. Chem. A*, 2014 **2** 12136.

Structure and properties of pseudo-graphene

*Abramenko N.D.*¹, *Rozhkov M.A.*¹, *Kolesnikova A.L.*^{1,2}, *Romanov A.E.*^{1,3}

ndabramenko@itmo.ru

¹ ITMO University, Kronverksky pr. 49, 197101, St. Petersburg, Russia

² Institute for Problems in Mechanical Engineering, RAS, Bolshoj pr. 61, Vas. Ostrov, 199178, St. Petersburg, Russia

³ Ioffe Physical-Technical Institute, RAS, Polytechnicheskaya 26, 194021, St. Petersburg, Russia

Carbon can form allotropes - solids built of the same chemical element, but different in structure. The existence of allotropes is caused by the behaviour of electrons on the outer shell, which is responsible for the mutual interactions of carbon atoms.

If one takes an isolated layer of graphite, then graphene forms - a two-dimensional carbon crystal with a hexagonal lattice. The physical and mechanical properties of graphene can be controlled by external influences: mechanical, electrical, and magnetic and by changing the local crystalline perfection of graphene.

Numerous works consider two-dimensional carbon crystals other than graphene. These crystals are called *graphene allotropes* or *pseudo-graphenes*. However, a uniform nomenclature for such materials is not yet suggested and their properties are not investigated in deep details. In this report we analyse the current state of research of pseudo-graphenes.

First, we propose a classification of two-dimension carbon structures based on graphene, as well as its naming method for the discovered materials. Second, we discuss analytical and numerical approaches proposed and used in theoretical studies of pseudo-graphenes.

As a result, a table of pseudo-graphenes with their properties and new proposed nomenclature is compiled. The examples of crystal lattice structure of pseudo-graphenes are given in Fig.1.

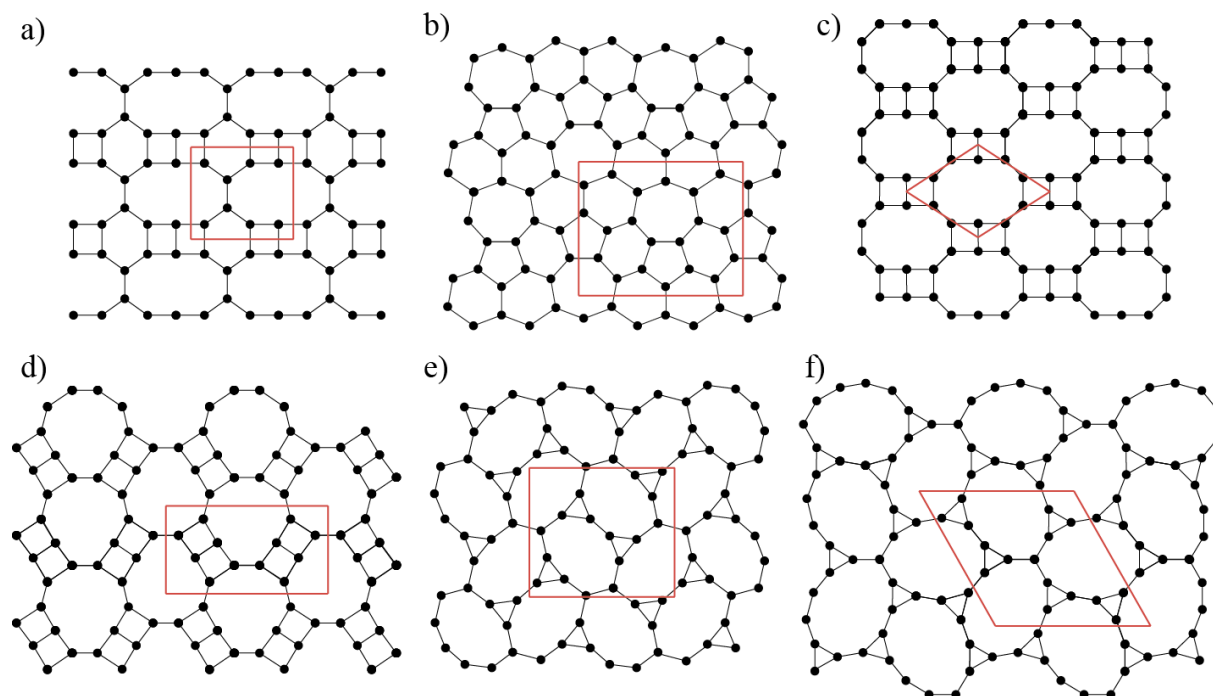


Fig.1. Pseudo-graphenes: a) S-graphene, b) Phagraphene, c) C4-10-I, d) C4-10-II, e) C3-9-R, f) C3-11. Red rectangles and rhombs mark the borders of the primitive cells in pseudo-graphene crystal lattice.

Composite materials based on reduced graphene oxide and their magnetic properties

Bugrov A.N.^{1,2}, *Smyslov R.Y.*¹, *Ionov A.N.*³, *Runov V.V.*⁴, *Volkov M.P.*³, *Nikolaeva M.N.*¹, *Dideikin A.T.*³, *Ivan'kova E.M.*¹

alexander.n.bugrov@gmail.com

¹ Institute of Macromolecular Compounds, Russian Academy of Sciences, St. Petersburg, Russia

² Saint Petersburg Electrotechnical University (ETU "LETI"), St. Petersburg, Russia

³ Ioffe Institute, St. Petersburg, Russia

⁴ Petersburg Nuclear Physics Institute, National Research Center Kurchatov Institute, Gatchina, Russia

The absence of intrinsic magnetic moments makes it challenging to use graphene in spintronics, the effects of which are based on the use of spin-polarized transport. Considerable efforts have been directed towards enhancing the magnetic response of two-dimensional carbon structures due to defects that could induce localized magnetic moments in the diamagnetic primary π -electron system. According to the literature, in reduced graphene oxide (RGO), anomalous electrical and magnetic effects can occur due to a change in the conducting π - π^* states in the interlayer space [1]. Theoretical calculations previously predicted the magnetic moments, but their origin and relationship with oxygen-containing groups in the layers of graphite oxide and RGO are still questionable. In experimental works, it is noted that the most nontrivial electrical and magnetic properties are manifested in more defective samples with a significant deviation from stoichiometry. Moreover, they are enhanced by introducing graphene and its derivatives into polymer matrices [2].

In this regard, in the process of in situ radical copolymerization, we synthesized a series of composite materials based on graphene oxide reduced in different media, which was fixed in the matrices of the vinyl series due to covalent bonds. The graphite oxide films obtained using the modified Hummers method were reduced at different temperature conditions in argon, hydrogen, and air by adjusting the number of oxygen-containing groups on the surface of graphene galleries. The remaining hydroxyl and carboxyl groups were used to functionalize the surface of RGO flakes with $\text{CH}_2=\text{CH}$ - bonds to twist its layers relative to each other during copolymerization with styrene and methyl methacrylate. Besides, defects in the basal planes of multilayer RGO were also formed upon photoreduction using UV radiation.

The structure of the composites synthesized in this work was comprehensively studied by such methods as X-ray diffraction, IR, NMR, dielectric and Raman spectroscopy, SEM, AFM, thermogravimetry, and differential scanning calorimetry. Experiments on the small-angle scattering of polarized neutrons revealed the presence of magnetic nuclear interference scattering in external magnetic fields H about 1 T, which unequivocally indicates magnetized regions of 1000 Å in the composites under investigation. Using a vibrating magnetometer, one has found that composite magnetization loops of composites exhibit type II superconductivity up to room temperature, probably due to mechanical stresses created in the RGO layers during copolymerization. In addition, it has been shown that the photoreduction process leads to the formation of many submicron holes distributed inside RGO flakes, which can create edge defects, causing magnetic ordering due to superconductivity rather than ferromagnetic ordering.

This work was financially supported by RFBR grant № 20-02-00918 A.

References

1. A. Diamantopoulou, S. Glenis, G. Zolnierkiwicz, N. Guskos, V. Likodimos, *Journal of Applied Physics* (2017) **121**, 043906
2. A.N. Ionov, M.P. Volkov, M.N. Nikolaeva, R.Y. Smyslov, A.N. Bugrov, *Nanomaterials*. (2021) **11**, 403

Graphene oxide membranes: tuning the microstructure for gas dehumidification

*Chernova E.A.*¹, *Petukhov D.I.*¹, *Kapitanova O.O.*¹, *Brotsman V.A.*¹, *Boytsova O.V.*^{1,2}, *Valeev R.G.*³, *Chumakov A.P.*⁴, *Eliseev Ar. A.*¹, *Eliseev A. A.*¹

chernova.msu@gmail.com

¹ Lomonosov Moscow State University, Moscow, Russia

² Kurnakov Institute of General and Inorganic Chemistry Russian Academy of Sciences, Moscow, Russia

³ Udmurt Federal Research Center of the Ural Branch of Russian Academy of Sciences

⁴ Deutsches Elektronen-Synchrotron

Graphene oxide (GO), structurally represented by graphene nanosheets modified with oxygen-containing groups, is a bright star among 2D materials owing to its highly tunable d-spacing, feasibility of adjusting carbon-to-oxygen (C:O) ratio coupled with diversity of surface modification. The presence of polar oxygen groups endows GO with high permeance towards water molecules making graphene oxide an advanced membrane material suitable for the variety of separation processes including dehumidification and nanofiltration. Today, despite an increasing number of studies devoted to structural and functional features of GO membranes, there is still a gap concerning two key points. The first one is a need for an in-depth understanding of the influence of C:O ratio on the transport properties of GO-based membranes both towards water vapors and permanent gases as the variation of oxygen-containing groups contributes to changes of GO interlayer spacing. It should be noted that this type of study especially requires accurate observance of GO membranes chemical composition and structural characteristics. The second problem arises when GO membranes operate in pressure-driven nanofiltration and dehumidification processes: under elevated pressures, GO interlayer galleries become compacted accompanied with water molecules ousting from GO d-spacing which inevitably leads to significant drop of GO-based membranes water permeance.

To address the first issue, we have prepared composite GO-based membranes with variable C:O ratio of GO nanosheets from 2.2 to 1.7 by simple adjusting of the graphite:oxidizer ratio during the synthesis by improved Hummers' method. GO-based composite membranes were prepared by the formation of thin GO selective layers using spin-coating of GO suspensions on the surface of porous anodic alumina (AAO) supports. In accordance with measurement of permeation and sorption characteristics of the membranes, it was revealed, that with an increase in C:O ratio, only a slight decrease of GO permeance towards permanent gases is observed, accompanied by rise in water vapor permeance up to over $60 \text{ m}^3 \cdot \text{m}^{-2} \cdot \text{atm}^{-1} \cdot \text{h}^{-1}$. It was also elucidated, that the water vapor transport is mainly governed by water diffusivity not by H_2O sorption capacity of graphene oxide.

To improve water vapors stability, the microstructure of GO-based selective layers was modified using two different types of intercalants: flat-shaped graphene oxide nanoribbons and ball-shaped fullerenols with variable OH content. The pressure stability of the membranes was tested under stepwise pressure increase-decrease cycles with long-lasting exposure under transmembrane pressure of 0.1 MPa. It has been shown that graphene oxide nanoribbons create flexible pressure-resistant nanochannels between GO nanosheets but still leading to an irreversible decline in water permeance up to ~35%. On the other hand, ball-shaped fullerenols endowed GO-selective layers with prominent pressure stability leading to decline of only 10% of water permeance under transmembrane pressure of 0.1 MPa and nearly complete permeance restoration after pressure release.

Acknowledgements:

The work is supported by the Russian Fund for Basic Research project 18-29-19105.

Spin probe method for investigation of graphite oxide materials - possibilities and perspectives

Chumakova N.A.^{1,2}, *Rebrikova A.T.*², *Vorobiev A.Kh.*², *Korobov M.V.*²

harmonic2011@yandex.ru

¹ N.N. Semenov Federal Research Center for Chemical Physics

² M.V. Lomonosov Moscow State University, Chemistry Department

The main factors determining the permeation properties of the GO membranes are the state and mobility of sorbed liquids within the interplane space of swollen graphite oxide. The influence of the orientational ordering of the graphene planes on membrane permeability is also very likely. Experimental data on the mechanism of transmembrane diffusion are limited. Electron paramagnetic resonance spectroscopy (EPR) is widely used for the study of the structure and dynamics of various materials - polymers, glasses, liquid crystals, biological tissues, etc. The present report is devoted to the potential of the spin probe technique for the investigation of graphite oxide materials.

It was shown that the rotational mobility of the radicals adsorbed on the inner surface of GO depends on the inter-plane distance. This dependence permits investigation of the phase transformation in the systems "BGO - acetonitrile" and "BGO - methanol". EPR spectra of the spin probes demonstrate that this transformation proceeds within a temperature range of $\sim 30^\circ$. We believe that this range reflects partial inhomogeneity within the material.

The rotational mobility of the probes located in the intercalated liquids (water, acetonitrile, and methanol) just a little slowed down compared to rotation in the bulk liquids. This observation indicates the high mobility of the intercalated liquids. It was observed that the spin probe method is more sensitive to a small amount of unfrozen liquid intercalated into GO than NMR spectroscopy.

The spin probe method is a unique technique for quantifying layer ordering in graphite oxide membranes. As an illustration, the Figure shows the orientation distribution functions of two nitroxide radicals inside the HGO membrane. It is seen that the paramagnetic molecules including aromatic fragments are more sensitive for orientational ordering of the membrane.

Quantitative determination of the alignment of the material is a promising technique for the control of membrane quality. It seems to be interesting to consider the correlation between the membrane alignment and its permeability for various liquids and gases.

This work was supported by the RFBR grant 18-29-19120 mk.

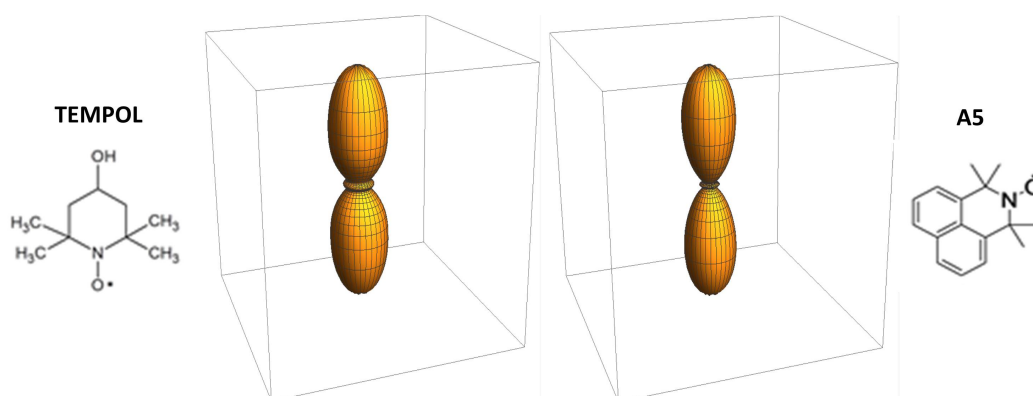


Figure 1. Orientation distribution functions of the nitroxide radicals inside the HGO membrane.

An approach to the preparation of aerogels with ultra-high molecular weight polymers using the rGO template on the example of UHMWPE

*Gudkov M.V.*¹, *Brevnov P.N.*¹, *Shiyanova K.A.*¹, *Krashennnikov V.G.*¹, *Anosov A.A.*¹, *Potorochin D.V.*^{2,3,4}, *Rabchinskii M.K.*⁵, *Ryabkov Ye.D.*⁶, *Baidakova M.V.*⁵, *Gorenberg A.Ya.*¹, *Novokshonova L.A.*¹, *Melnikov V.P.*¹

gudkovmv@gmail.com

¹ FRCCP RAS, Moscow, Russia

² ITMO University, Saint Petersburg, Russia

³ DESY, Hamburg, Germany

⁴ TU Bergakademie Freiberg, Freiberg, Germany

⁵ Ioffe Institute, Saint Petersburg, Russia

⁶ Institute of fine chemical technology named after M.V. Lomonosov, RTU MIREA, Moscow, Russia

In this study, we propose a previously unknown template-directed polymerization strategy for producing graphene/polymer composite aerogels with elevated mechanical properties, the preservation of the nanoscale pore structure, the extraordinary crystallite structure and tunable electrical properties. We develop the novel approach of ethylene polymerization on the surface of reduced graphene oxide (rGO) sheets pre-structured as an aerogel template with the formation of ultra-high molecular weight polyethylene (UHMWPE). It is shown that the in-situ polymerization of ethylene on the surface of rGO sheets uniformly throughout the volume of aerogel. At less than 20 wt.% content of UHMWPE, the composite materials demonstrate completely reversible deformation and well conductivity. Ultra-high polymer content (more than 80 wt.%) results in materials with a pronounced plasticity, improved hydrophobic properties and increased the elastic modulus compared with the pure rGO aerogel. The polymer content variation allows to tune the electro conductive properties of the aerogel in a wide range. The structural features of UHMWPE grown on rGO sheets were studied using XRD analysis. Such an approach will make it possible to create composite materials with ultra-high molecular weight polymers with highly developed nanostructural morphology and advanced properties controlled by the thickness of the polymer layer on the surface of rGO template particles. These composites can be used in reconstructive surgery to replace unloaded bone parts, electroactive materials for supercapacitors and li-ion batteries, as well as heat insulating elements operating at very low temperatures in the space and aviation industries or in the far north conditions.

The research was carried out with financial support of the Program of Fundamental Researches of the Russian Academy of Sciences (project № 0082-2019-0008).

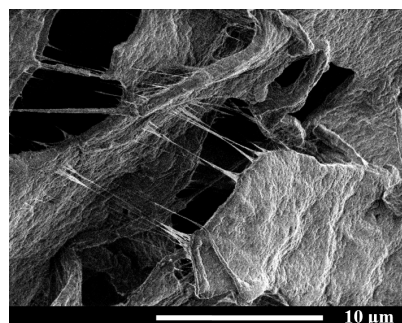


Fig.1. SEM image of the composite aerogel with 93 wt.% of the UHMWPE.

Graphene-like carbon additive to negative electrodes of lead-acid battery

Novikau U.¹, Razanau I.¹, Filipovich S.¹, Lomonosov V.¹

phaust@list.ru

¹ Scientific-Practical Materials Research Centre of National Academy of Sciences of Belarus, Minsk, Belarus

Nanostructured carbon additives to negative active material (NAM) can significantly improve the characteristics of lead-acid batteries. Such additives can act as a capacity buffer, improving the battery's charge acceptance, especially under the high-rate partial state-of-charge (HRPSoC) cycling conditions. It can also facilitate electrochemical reactions inside the electrode mass and prevent lead sulfate recrystallization leading to large crystal formation and battery degradation [1]. In the present report, we describe the study of graphene-like carbon (GLC) as the additive to NAM of lead-acid battery.

We used an original two-stage method of GLC synthesis through graphite exfoliation comprising intercalation of natural graphite with sodium ammine complex from the solution of sodium in liquid ammonia [2] with subsequent intercalate flame pyrolysis. Intercalate synthesis in a strongly reducing medium prevents graphene structure degradation characteristic of oxidation-based synthesis methods. The synthesis method is also characterized by high productivity and significantly improved ecology friendliness.

Negative electrodes of the test lead-acid cells were prepared using a typical procedure [3]. The GLC was added to the initial mixture of lead, BaSO₄, and lignosulfonate from 0 to 1 mass %. We used positive electrodes from commercially available lead-acid batteries for the prepared elementary cells. Part of the cells included absorbent glass mats (AGM) as the separators.

The cells with the GLC additive showed an approximately two-fold increase in the lifetime under the conditions of full-discharge cycling without AGM. With AGM, the GLC-containing cells lost 20% of their initial capacity after up to a 1.5-times-longer cycling compared to the GLC-free cells. The optimal content of GLC was 0.25%. The initial capacity of the GLC-containing cells was 11-26% higher under the same quantity of lead per electrode.

Under the conditions of HRPSoC without AGM, the GLC-containing cell showed approximately the same lifetime as the GLC-free cell. However, the latter demonstrated higher voltage at the end of the charging step of the HRPSoC cycle, pointing at the more intensive water electrolysis. Under the conditions of HRPSoC with AGM, the GLC-containing cells showed an increase in the lifetime up to 3 times compared to the GLC-free cell.

In conclusion, the synthesized GLC showed itself as a perspective additive to NAM of lead-acid batteries, considerably improving their operation under HRPSoC and full-discharge conditions and somewhat increasing their capacity. The structure and chemical composition of the GLC allows the improvement to be achieved under the additive content of only 0.25 %.

References

1. T. Mosley, D.A.J. Rand, A. Davidson, and B. Monahov, J. Energy Storage (2018) **19**, 272.
2. U. Novikau, I. Razanau, S. Filipovich, MRS Advances (2016) **1**, 1395.
3. D. Pavlov, Lead-Acid Batteries: Science and Technology (Elsevier B.V., 2017), p. 324.

Guiding the chemistry of GO via the use of $\text{KMnO}_4/\text{K}_2\text{Cr}_2\text{O}_7$ oxidizing agents

Rabchinskii M.K.¹, Ryzhkov S.A.¹, Gudkov M.V.², Baidakova M.V.¹, Pavlov S.I.¹, Kirilenko D.A.¹, Shiyanova K.A.², Antonov G.A.¹, Brunkov P.N.¹

Sergei.Ryzhkov@mail.ioffe.ru

¹ Ioffe Institute, St.Petersburg, Russia

² N.N. Semenov Federal Research Center for Chemical Physics, Russian Academy of Sciences, Moscow, Russia

Synthesis of graphene derivatives with the desired composition of organic groups, primarily the oxygenic ones, has attracted much attention in recent years owing to the intriguing opportunity to tailor the physical properties of the material. Large efforts are being made to develop advantageous methods for the synthesis of graphene oxide (GO) with the requested ratio of different oxygenic moieties for further sensing, catalysis, and electrochemical applications.

Hereby, we present an advanced method to manage graphene oxide (GO) chemistry via its synthesis using $\text{KMnO}_4/\text{K}_2\text{Cr}_2\text{O}_7$ oxidizing agents at different ratios [1]. The linear two-fold reduction in the number of the hydroxyls and epoxides with the simultaneous three-fold rise in the content of carbonyls and carboxyls is demonstrated upon the transition from the KMnO_4 to $\text{K}_2\text{Cr}_2\text{O}_7$ as a predominant oxidizing agent in the mixture. The alteration of the GO chemistry is suggested to arise from the transition from the diffusion oxidation mechanism in the case of KMnO_4 predominance to the edge-promoted graphite oxidation in the abundance of the $\text{K}_2\text{Cr}_2\text{O}_7$. Furthermore, the oxidation of GO with high $\text{K}_2\text{Cr}_2\text{O}_7$ ratios in the reaction mixture has been found out to result in a structural disorder of graphene layers, expressed by the formation of the in-plane nanoscale defects, namely vacancies and sub-nanometer holes terminated with carbonyl and carboxyl groups. The presence of these defects is inevitably accompanied by the out-of-plane sheet structural variations, which have been identified via X-ray diffraction and transmission electron microscopy techniques.

Given these results, a facile method for the synthesis of GOs with the desired chemistry is developed, allowing to make an advance in the application of GO in biosensing and gas sensing.

The work was supported by the Russian Foundation for Basic Researches (gr. № 20-04-60458).

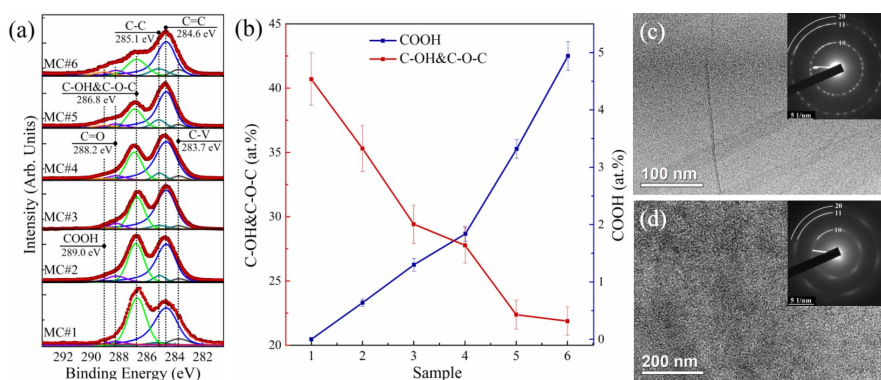


Fig.1. (a) C 1s X-ray photoelectron spectra and (b) number of carboxyls (COOH), hydroxyls (C-OH), and epoxides (C-O-C) in the GOs synthesized with different $\text{KMnO}_4/\text{K}_2\text{Cr}_2\text{O}_7$ ratios. TEM images of the GOs synthesized using only (c) KMnO_4 and (d) $\text{K}_2\text{Cr}_2\text{O}_7$, demonstrating the difference in the nanostructure.

References

1. A. Shiyanova, M. V. Gudkov, M. K. Rabchinskii, et al. *Graphene oxide chemistry management via the use of $\text{KMnO}_4/\text{K}_2\text{Cr}_2\text{O}_7$ oxidizing agents*. **Nanomaterials**, 2021, 11, 915

Unveiling graphene N-doping upon Hummers oxidation and its effect on electrical properties

Rabchinskii M.K.¹, Saveliev S.D.¹, Ryzhkov S.A.¹, Gudkov M.V.², Baidakova M.V.¹, Pavlov S.I.¹, Kirilenko D.A.¹, Stolyarova D.Yu.³, Brzhezinskaya M.⁴, Brunkov P.N.¹

Sviatoslav.Saveliev@mail.ioffe.ru

¹ Ioffe Institute, St. Petersburg, Russia

² N.N. Semenov Federal Research Center for Chemical Physics, Russian Academy of Sciences, Moscow, Russia

³ NRC "Kurchatov Institute", Moscow, Russian Federation

⁴ Helmholtz-Zentrum Berlin für Materialien und Energie, Berlin, Germany

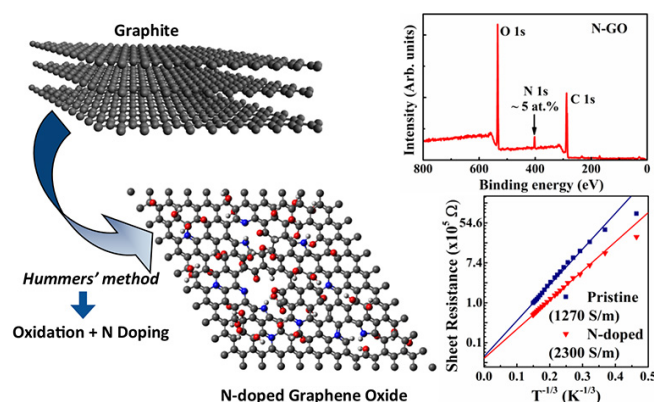
Graphene nitrogen doping (N-doping) has been proposed as a facile and advanced approach to tailor graphene physics due to its relative simplicity and substantial effect of the introduced nitrogen on the electrophysical properties of the graphene layer. Yet the problem of the synthesis of N-doped graphenes with both the utmost concentration of the embedded nitrogen and rational design of the introduced species (N-species) to maximize their impact on the graphenes' physics is still to be solved.

Here we for the first time demonstrate efficient nitrogen doping of graphene oxide (GO) with nitrogen concentration of up to almost 5 at.% and desired type of the nitrogen species via modified Hummers' method [1]. The mechanism of the observed doping has been proposed, allowing one to tune the concentration of the incorporated nitrogen. Applying core-level spectroscopy techniques we have found out that the embedded nitrogen is predominantly presented in the form of graphitic-N, highly desirable for the modulation of graphene electrophysical properties. In turn, the thermal reduction of the synthesized N-doped GO has resulted in the conversion of graphitic-N into the pyridinic-N and pyrrolic-N, which are advantageous for the application of the material for catalysis of oxygen reduction reactions (ORR).

Further comprehensive electrical studies combined with the transmission electron microscopy (TEM) and density functional theory (DFT) modeling have demonstrated the performed N-doping to result in doubling of the material conductivity due to the provided n-doping and corresponding increase of the DOS near the Fermi level. The conductivity mechanism has been determined to correspond to the Mott-VRH mechanism with a localization length of about 2.63 nm.

Thus, a simple method to synthesize N-doped graphene with specific N-species has been developed, which leads to new perspective applications for graphene, particularly in gas sensing.

The work was financially supported by the Russian Scientific Foundation (gr. № 19-72-10052)



References

1. M. K. Rabchinskii, S. A. Ryzhkov, M. V. Gudkov, et al. *Unveiling a facile approach for large-scale synthesis of N-doped graphene with tuned electrical properties*, **2D Materials**, 2020, **7**, 045001

Valence Band Electron Structure of Graphene Derivatives: Study by XPS measurements and DFT modeling

*Shnitov V.V.*¹, *Rabchinskii M.K.*¹, *Pavlov S.V.*², *Baidakova M.V.*¹, *Stolyarova D.Yu.*³, *Gudkov M.V.*⁴, *Brzhezinskaya M.*⁵, *Smirnov D.A.*⁶

v.shnitov@mail.ioffe.ru

¹ Ioffe Institute, St.Petersburg, Russia

² Skolkovo Institute of Science and Technology, Skolkovo Innovation Center, Moscow, Russia

³ NRC Kurchatov Institute, Moscow, Russia

⁴ N.N. Semenov Federal Research Center for Chemical Physics, Moscow, Russia

⁵ Helmholtz-Zentrum Berlin für Materialien und Energie GmbH, Berlin, Germany

⁶ Institut für Festkörper und Materialphysik, Technische Universität Dresden, Dresden, Germany

The synthesis and study of various graphene derivatives (GDs) are at the forefront of graphene studies nowadays [1,2]. Owing to the presence of certain types and amounts of basal and edge functional groups GDs exhibit new electronic properties and can be easily grafted with various moieties. All this makes them very promising candidates for using in such highly demanded areas of practical application as development of advanced photovoltaic and optoelectronic devices, gas and bio sensing applications.

In this report, we present a detailed study, both experimental and computational, of the valence band (VB) electron structure of carbonylated (Cny) and carboxylated (Cxy) GDs prepared in accordance with the chemical methods described in our previous works [1,2]. The experimental part of the study was performed at Russian-German beamline of synchrotron BESSY-II and included measurements of VB (at $\hbar\omega=130$ eV) and respective survey and C1s and O1s core level (at $\hbar\omega=736$ eV) X-ray photoemission spectra (XPS) of Cny, Cxy and some other GDs which were carried out before and after high vacuum annealing of respective samples. The computational modeling of the VB structure of Cny and Cxy graphenes was performed using the DFT method realized in the form of so-called Vienna Ab initio Simulation Package (VASP) codes and consisted in calculation of the energy and spatial dependent densities of edge-group-related electron states of these GDs.

The comparative analysis of all VB spectra allowed us to reliably separate the their edge-groups-related and graphene-related features. Computational simulation of corresponding GDs structures made it possible to establish the true physical nature of the all edge-groups-related VB features i.e. to determine the localization and symmetry of electron states contributing into each of these features, to visualize the distribution of electron density associated with these states and identify the type of covalent bonding (o, π or n) in formation of which these states are involved.

Thus, the very fruitful combination of XPS measuring and computational modeling of VB electron structure of different GDs reveal itself as very powerful approach providing the great number of highly informative data on VB structure of these species. The data obtained in such a way can significantly clarify the understanding of the specificity of their electronic properties and thereby promote the emergence of new technical and bio applications of such type of graphene related materials.

The presented work was financially supported by the Russian Foundation for Basic Research (grant no. 20-04-60458). The XPS experiments were carried out on the equipment of the Russian-German beamline of electron storage ring BESSY-II (Helmholtz-Zentrum Berlin).

References

1. Rabchinskii M.K., et. al. *Graphene oxide conversion into controllably carboxylated graphene layers via photoreduction process in the inert atmosphere*. **Fullerenes, Nanotubes and Carbon Nanostructures**, 2020, 28, 221-225.
2. Rabchinskii M.K., et. al. *Carbonylated graphene: synthesis, characterization, and application for highly-selective ammonia gas sensing*, 2021, **Carbon**, v.172 ,236-247.

Day 2: Carbon Nanostructures. Carbon Nanotubes.

Complexes "boron+vacancy" on the hydrogenated C(100)-(2×1) diamond surface

*Digurova A.I.*¹, *Lvova N.A.*^{1,2}

ryazanova@phystech.edu

¹ Moscow Institute of Physics and Technology, Dolgoprudny, Moscow Region, Russia

² Technological Institute for Superhard and Novel Carbon Materials, Troitsk, Moscow, Russia

The combination of such unique properties as high hardness, thermal conductivity, wear resistance, transparency makes diamond a promising material for many areas of high technology. "Boron+vacancy" complexes are currently considered as alternatives to NV defects. Since the optical activity of "impurity+vacancy" centers is directly related to the distance between the defect and the surface, the use of complexes located in the near-surface layers is very promising for achieving the highest resolution in measurements at the nanoscale. However, mainly experimental and theoretical [1,2] studies have been focused on defects in the bulk of the diamond. The aim of this work was to determine the structure and properties of diamond "boron+vacancy" surface defects using semi-empirical quantum chemical methods.

Modeling of the reconstructed hydrogenated diamond surface C(100)-(2×1) was carried out on the $C_{244}H_{116}$ cluster using the semiempirical PM3 method implemented in the MOPAC software package [3]. In this work, we investigated the effect of surface passivation on the structural, electronic, and energy properties of the complexes. The influence of the charge state (negative, neutral, positive) on the properties of complex BV defects has been studied. It was found that the presence of hydrogen on the surface significantly affects the position of defects on the energy scale. It was found that, in all charge states of a defect on a clean surface, the structure "vacancy in the third layer + boron in the fourth layer" is the most stable. It is shown that the main stabilizing factor is the local graphitization of the surface in the immediate environment of the considered defects. The structure in which both the intrinsic and impurity defect included in the complex are located in the upper carbon bilayer is the most stable on the hydrogenated C(100)-(2×1) diamond surface.

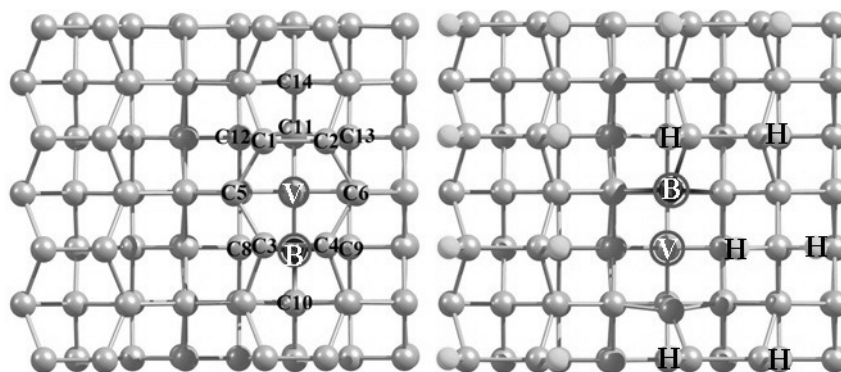


Fig.1. The most stable "boron+vacancy" complexes: clean surface (left); hydrogenated surface (right).

References

1. Kunisaki, M. Muruganathan, H. Mizuta and T. Kodera, *Jpn. J. Appl. Phys.* (2017) **56**, 04CK02.
2. P. Goss, P.R. Briddon, M.J. Rayson, S.J. Sque, and R. Jones, *Phys. Rev. B.* (2005) **72**, 035214.
3. MOPAC2016, [HTTP://OpenMOPAC.net/](http://OpenMOPAC.net/), Version 16.158W, J.J.P. Stewart, Stewart Computational Chemistry, Colorado Springs, CO, USA.

Synthesis and chemical activation of porous nitrogen-doped carbon materials for sodium-ion batteries

*Fedoseeva Y.V.*¹, *Shlyakhiva E.V.*¹, *Vorfolomeeva A.A.*¹, *Stolyarova S.G.*¹, *Grebenkina M.A.*¹, *Okotrub A.V.*¹, *Bulusheva L.G.*¹

fedoseeva@niic.nsc.ru

¹ Nikolaev Institute of Inorganic Chemistry SB RAS, Novosibirsk, Russia

According to the principle of operation and energy characteristics, the sodium-ion battery (SIB) is close to the lithium-ion battery (LIB), while sodium is many times cheaper and abundant than lithium. Although graphite is used as the negative electrode in conventional LIBs, attempts to use it in SIBs have been hampered by the inability of Na to intercalate into the graphitic structure. The development of new carbon anode materials for SIBs is a great challenge for modern electrochemistry. Porous nitrogen-doped carbon materials (PNCMs) are a three-dimensional carbon framework consisting of disordered nitrogen-doped graphitic-like layers. PNCMs have been synthesized as a result of chemical vapor deposition of acetonitrile at 750 °C following thermal decomposition of calcium salts (tartrate, adipate or glutarate). Hydrochloric acid treatment resulted in the removal of calcium oxide nanoparticles and the formation of mesopores, which replicate these particles. PNCMs have a high specific surface area, hierarchical porous structure and good electrical conductivity, which is appreciated for electrochemical applications.

In the present work, hydrothermal treatments in water or ammonia solution, potassium hydroxide melt treatment, annealing at 1000 °C were used for etching and chemical modification of PNCMs. The morphology, composition, and structure of the samples have been studied by electron microscopes, X-ray diffraction, Raman scattering, infrared spectroscopy, nitrogen gas adsorption method, X-ray photoelectron spectroscopy (XPS), near-edge X-ray spectroscopy fine structure (NEXAFS) spectroscopy. The effect of vacuum thermal deposition of sodium on the brominated products was investigated by *in situ* XPS and NEXAFS methods. PNCMs have been tested as electrode materials in sodium half-cell using sodium foil as an opposite electrode and 1M solution of NaClO₄ in EC/DC as electrolyte.

Electrochemical testing of PNCMs revealed the adsorption mechanism of sodium storage at defects and pore volume of carbon material, while intercalation of Na into graphitic structure does not occur. All treatments with a solution and KOH resulted in the partial etching of carbon outer surface, which increases in its specific surface area and volume of micropores and small mesopores. However, ammonia solution treatment increased in the concentration of nitrogen doping, while the activation of KOH removed it. The applied modification of PNCMs resulted in an increase in their sodium-ion storage capacity by 100 mAh g⁻¹. Annealing of PNCMs at 1000 °C decreased the number of defects, which reduced their electrochemical performance in SIBs. The activation method developed in this work is hopeful to open up a new route of designing porous nitrogen-doped carbon materials for electrochemical applications.

The work was financially supported by the Russian Science Foundation (Grant 19-73-10068).

The mechanical properties of diamond nanopolycrystals by machine learning interatomic potentials

*Jalolov F.N.*¹, *Kvashnin A.G.*¹

faridun.jalolov@skoltech.ru

¹ Skolkovo Institute of Science and Technology, Moscow, Russia

The cubic diamond (further just diamond) provides an impressive combination of chemical, physical and mechanical properties and can be used in a variety of applications. Due to the strong covalent bonding the diamond is the hardest known material, with the Vickers hardness in the range of 90-120 GPa [1,2]. Most promising are mechanical applications in the mining (cutting and rock-breaking tools), processing (polishing, grinding, metalworking, etc.), defense (armor, hard protective coatings) and space (hard protective coatings) industries due to their unique mechanical properties (hardness, crack resistance, etc.).

Recently it has become very important to study polycrystalline with high mechanical properties. In recent years, nanopolycrystals have become a rapidly developing multidisciplinary research field. Polycrystals are composed of many small grains that have the same arrangement but are inconsistent in orientation. The nanopolycrystalline material contains a large number of grain boundaries or other interfaces, and has extremely high interfacial strengthening ability, thus exhibiting distinctive mechanical properties. It is represented by the Hall-Petch Equation [3]. From this equation it follows that with a decrease in the characteristic size of the structure, an increase in hardness should be expected.

$$\sigma_y = \sigma_0 + k d^{-1/2}$$

where σ_y is the yield strength, σ_0 is the lattice resistance, k is the material correlation coefficient, and d is the average grain size.

In this project was done comparative study of mechanical properties of diamond single crystals and nanopolycrystals with different grain sizes by using molecular dynamic simulations with Tersoff [4] and machine learning interatomic potentials [5]. Were investigated elastic constants and elastic moduli of diamond nanopolycrystals. Finally, was done comparative analysis and discussed possible applications.

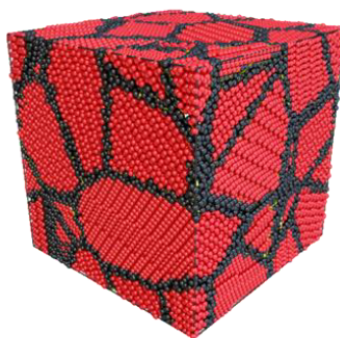


Fig.1. An example of an NPD structure used in the simulations.

References

1. Andrievski, J. Refrac, *Metals Hard. Mater.* **2001**, 19, 447.
2. Li, J. Hao, H. Liu, *J. Phys. Rev. Lett.* **2015**, 115, 1055.
3. A. Meyers, A. Mishra, D.J. Benso., *Prog. Mater. Sci.* **2006**, 51, 427.
4. Tersoff, *Phys. Rev.* **1989**, 39, 5566.
5. V. Shapeev, *Multiscale Model. Simul.* **2016**, 14, 1153.

Synthesis of hydrophobic carbon sponges from MOF type HKUST and melamine-formaldehyde sponges for the absorption of oil dispersed in water.

*Oliva Gonzalez C.M.*¹, *Kharisov B.I.*¹, *Serrano Quezada T.E.*¹, *Kharissova O.V.*¹, *Gonzalez Lucy T.*², *Longoria Rodriguez F.E.*³

bkhariss@mail.ru

¹ Universidad Autonoma de Nuevo Leon, Pedro de Alba S/N, Ciudad Universitaria, San Nicolas de los Garza 66455, Mexico

² Tecnologico de Monterrey, Escuela de Ingenieria y Ciencias, 64890 Monterrey, Nuevo Leon, Mexico.

³ Centro de Investigacion en Materiales Avanzados, S.C., Unidad Monterrey, Mexico.

Currently, numerous investigations have focused on generating highly hydrophobic materials (1,2), low cost and high absorption capacity to eliminate oil dispersed in water from accidents caused during the transport of oil by sea (3,4), for this reason in this work the production of a series of carbon sponges with hydrophobic characteristics decorated with spherical metal nanoparticles on its surface is presented. The carbon sponges were synthesized using commercial melamine-formaldehyde sponges coated with HKUST type MOF (as can be seen in figure 1a-d), using trimesic acid as a binder and nickel, cobalt as a cations and the combination of the two mentioned cations, subsequently the coated sponges were subjected to a pyrolysis treatment in a nitrogen atmosphere at 300, 500 and 700°C. Hydrophobicity tests were performed by measuring the contact angle of the synthesized sponges and their oil absorption capacity was measured using the standardized method of ASTM F726-99, additionally, the synthesized materials were characterized with scanning electron microscopy (SEM), Spectroscopy Fourier transform infrared (FT-IR) and X-ray powder diffraction (XRD), the results obtained show that the carbon sponges obtained are promising candidates to be applied in the remediation of oil dispersed in water because they have hydrophobic and good absorption capacities.

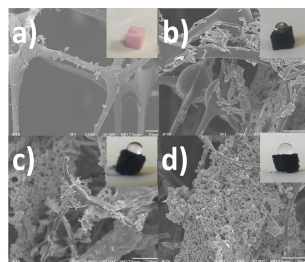


Fig. 1. SEM micrographs and photographs of sponges coated with BTC-Ni/Co: a) the coated sponge without pyrolysis, b) pyrolyzed at 300°C, c) pyrolyzed at 500°C and d) pyrolyzed at 700°C under a nitrogen atmosphere.

References

1. Wu MB, Huang S, Liu TY, Wu J, Agarwal S, Greiner A, et al. Compressible Carbon Sponges from Delignified Wood for Fast Cleanup and Enhanced Recovery of Crude Oil Spills by Joule Heat and Photothermal Effect. *Adv Funct Mater.* 2021;31(3):1-8.
2. Lei Z, Zheng P, Niu L, Yang Y, Shen J, Zhang W, et al. Ultralight, robustly compressible and super-hydrophobic biomass-decorated carbonaceous melamine sponge for oil/water separation with high oil retention. *Appl Surf Sci.* 2019;489:922-9.
3. Shen K, Chen X, Chen J, Li Y. Development of MOF-Derived Carbon-Based Nanomaterials for Efficient Catalysis. *ACS Catal.* 2016;6(9):5887-903.
4. Stolz A, Le Floch S, Reinert L, Ramos SMM, Tuaille-Combes J, Soneda Y, et al. Melamine-derived carbon sponges for oil-water separation. *Carbon*, 2016;107:198-208.

Vibrational spectroscopy of carbon nanoparticles interactions with biomacromolecules

*Laptinskiy K.A.*¹, *Burikov S.A.*², *Dolenko T.A.*²

laptinskiy@physics.msu.ru

¹ D.V. Skobeltsyn Institute of Nuclear Physics, M. V. Lomonosov Moscow State University, Moscow, Russia

² Physical Department, M. V. Lomonosov Moscow State University, Moscow, Russia

In modern medicine, nanotechnology is playing an increasing role. One of the most important directions in this area is the creation of theranostic nanoagents. Various carbon allotropes, such as nanodiamonds, carbon dots, etc. Despite the significant progress achieved in the study of the properties of these nanoparticles, questions about the mechanisms of interaction of carbon nanoparticles (CNPs) with molecules of the environment, in particular, biological, still remain open.

Various methods, including spectroscopic ones, are used to study the interactions between CNPs and surrounding molecules. However, today traditional research methods face a number of problems. For example, the presence of autofluorescence of biological tissue complicates the transition from model media (aqueous suspensions) to real biological tissues when conducting studies using fluorescence spectroscopy and spontaneous Raman spectroscopy. Therefore, there is a need to use new spectroscopic methods.

In this work, along with the indicated spectroscopic methods, the method of coherent anti-Stokes Raman scattering (CARS) was used. CARS signals are much more intense than spontaneous Raman signals, and the transition to the anti-Stokes region of the spectrum makes it possible to largely exclude the factor of autofluorescence. Therefore, the use of CARS provides fundamentally new information on the mechanisms of interactions of nanoparticles with surrounding biomacromolecules and the effect of these interactions on the properties of nanoparticles and the biological environment.

This work presents the results of a comprehensive study of the interactions of CNPs (nanodiamonds, carbon dots) with biomacromolecules (DNA chains, lysozyme) by vibrational spectroscopy methods (Raman light scattering, coherent anti-Stokes Raman scattering, IR absorption). The mechanisms of adsorption of proteins and DNA oligonucleotides on the surface of CNPs of a certain functionalization have been established, conformational changes in biomolecules as a result of their interaction with nanoparticles have been studied, and the relationship between these changes and the retention of the bioactivity of molecules has been shown.

This work was supported by the Russian Science Foundation (project No. 20-72-00144).

Magnetic properties of birch biocarbon

Popov V.V.¹, Spitsyn A.A.², Ponomarev D.A.², Orlova T.S.¹

13745pop@mail.ru

¹ Ioffe Institute, St. Petersburg, Russia

² St. Petersburg State Forest Technical University, St. Petersburg, Russia

Carbon structures obtained by the pyrolytic method from various organic substances can have both para- and ferromagnetic properties. Moreover, the composition and morphology of the initial materials determine the magnitude and nature of the magnetization of the resulting structures. In this paper, the magnetic properties of biocarbon samples obtained by pyrolysis from natural wood (birch) and composites based on a mixture of ground carbon with a binder are investigated. Such biocarbon is an amorphous material that preserves the highly porous structure of the original wood. The samples were first carbonized at a temperature of 700 °C, and then activated with steam at a temperature of 970 °C. The magnetic moment was measured in magnetic fields up to $H=140$ kOe and in the temperature range $T=2-300$ K using a system PPMS QD with a vibrating sample magnetometer.

The dependences of the magnetization M on the magnetic field for all the studied samples are shown in Fig.1. As seen (curve 1), the magnetization of natural wood carbonized at a temperature of 700 °C has a weak ferromagnetic behavior in low fields, but with increase in the field it changes sign and dependence $M(H)$ becomes linear, diamagnetic. After the sample is activated (arrow), the ferromagnetic contribution disappears (curve 2). In composites, the ferromagnetic contribution increases strongly: curve 3 for the composites carbonized at $T=700$ °C, curve 4 - after subsequent activation by steam at $T=970$ °C.

At low temperatures ($T<50$ K), the magnetic moment increases in all samples, which is due to the contribution of paramagnetic (PM) centers. The analysis of magnetization field dependences using the Brillouin function allowed us to determine the quantum number J of the total angular momentum of the PM centers, and its spin S : $J=S=1/2$.

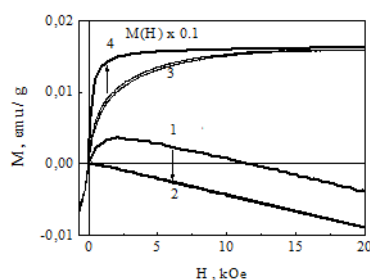


Figure 1. Field dependences of experimental magnetization M at 300 K.

References

1. T.L. Makarova, Semiconductors (2004) **38**, 615.

Evaluation of the in-plane electronic conjugation in carbon nanobelts

Tomilin O.B.¹, Rodionova E.V.¹, Rodin E.A.¹, Soldatova V.I.¹

evg.rodin54@gmail.com

¹ National Research Mordovia State University, Saransk, Russia

Carbon nanobelts (CNB) are a group of compounds consisting of benzene rings condensed or connected by a simple (or multiple) bond, located on a cylindrical surface. The first successful synthesis of carbon nanobelts was carried out about 10 years ago, and at present the structural variety of the CNBs is constantly expanding. In this work, we investigated model molecules similar to cyclacenes, cyclofenacenes, para-phenylenes and cyclacenes, and cyclofenacenes in the form of Möbius belts with different diameters (Fig. 1). The simulation of the CNBs electronic structure was carried out in a constant electric field of strength $E = 0.0 - 2.1 \text{ V/\AA}$ with a step of 0.3 V/\AA . The field strength vector was directed along the cylindrical axis of the nanobelts. The electronic structure of the CNBs was calculated by the DFT/B3LYP/6-31G method.

Evaluation of the CNBs emission properties was carried out within the framework of the concept emission molecular orbitals [1, 2]. Comparing the electronic and emission properties of CNBs of various types, one can note:

1. The demonstration of emission properties is determined by the level of realization of in-plane electronic conjugation in the nanostructure.
2. The emission properties of the cyclafenacene type nanobelts are higher than the emission properties of cyclacene CNBs. However, the demonstration of field emission is expected only in very small diameter cyclafenacene CNBs. This fact can be explained by the higher efficiency of in-plane electronic conjugation in cylindrical nanostructures with a large curvature of the surface.
3. In the family of CNBs with the Möbius strip topology, the efficiency of in-plane electronic conjugation is lower than in cyclacenes and cyclafenacenes. This is due to the fact that in in-plane Möbius CNBs, electronic conjugation is realized only on a part of the cylindrical surface of the nanobelts and is interrupted by the twisting region.
4. In-plane electronic conjugation in p-phenylene CNBs is demonstrated to a lesser extent compared to cyclofenacene nanobelts, since in p-phenylene CNBs the number of carbon atoms per nanobelt of a certain diameter is less than the corresponding value for cyclofenacene CNBs.

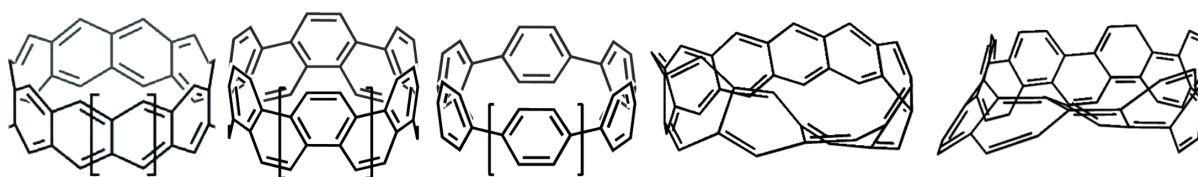


Fig.1. Example of model molecules.

References

1. O. B. Tomilin, E. V. Rodionova, E. A. Rodin, Russian Journal of Physical Chemistry A (2020) **94**, 1242.
2. O. B. Tomilin, E. V. Rodionova, E. A. Rodin, V. I. Soldatova, T. S. Koscheeva, Fuller. Nanotub. Carbon Nanostructures (2019) **28**, 129.

Optical properties of N- and S-doped carbon quantum dots

*Ibrayev N. Kh.*¹, *Amanzholova G.*¹, *Dzhanabekova R.Kh.*¹

niazibrayev@mail.ru

¹ Institute of Molecular Nanophotonics, Buketov Karaganda University, Karaganda, Kazakhstan

The spectral and luminescent properties of carbon quantum dots (CQDs) obtained via microwave synthesis using citric acid and L-cysteine. The resulting product was purified by centrifugation and dialysis (3.5 kDa MWCO dialysis membrane). Three solutions were prepared for the study: the initial product (after centrifugation), dialysate and retentate.

CQDs were characterized by electron microscopy, dynamic light scattering and FTIR spectroscopy. According to microscopic data, the average size of carbon dots was varied within 10–60 nm for the initial product. In the dialysate, particles with the sizes in the range of 3–6 nm were registered. FTIR spectra confirm the presence of -CN, -NH, -SH, C=O, -COO and -OH groups.

The band with a maximum at 350 nm and the shoulder at 230–240 nm exhibits in the absorption spectra for all studied solutions. CQD's fluorescence was registered under the excitation with the wavelength ranges of 350–560 nm. The maximum intensity was recorded under excitation at 350 nm. An increase in the excitation wavelength led to a bathochromic shift of the fluorescence band (up to 600 nm). The fluorescence behavior of all three solutions of CQDs is similar. Fluorescence excitation spectra are in good correlation with absorption spectra.

The quantum yields of CQDs were estimated by the absolute method and were equal to 0.47, 0.60, and 0.03 for the initial solution, dialysate and retentate, respectively. The fluorescence lifetimes measured by the time-correlated photon counting method were equal to 7.8 ns, 7.3 ns, 5.9 ns for the above-mentioned series of solutions.

Pulsed photoexcitation of CQDs solutions revealed delayed fluorescence, the spectrum of which almost completely coincides with the fluorescence band. The lifetime of delayed fluorescence was equal to 15 ms. The excitation spectrum of delayed fluorescence repeats the excitation spectrum of fluorescence.

Phosphorescence of CQDs with the maxima at 530 nm and lifetime of 18.6 ms was registered in PVA films. The intensity of phosphorescence was increased under the decreasing film temperature. The phosphorescence lifetime was equal to 32 ms at T=106 K.

This research is funded by the Science Committee of the Ministry of Education and Science of the Republic of Kazakhstan (Grant No. AP09259913).

Effect of metal dopant in structure and supercapacitor property of templated-assisted porous nitrogen carbon

*Shlyakhova E.V.*¹, *Nishchakova A.D.*¹, *Grebenkina M.A.*^{1,2}, *Okotrub A.V.*¹, *Bulusheva L.G.*¹, *Fedoseeva Y.V.*¹

shlyakhovaev@niic.sbras.ru

¹ Nikolaev Institute of Inorganic Chemistry of SB RAS, Novosibirsk, Russia

² Novosibirsk State University, Novosibirsk, Russia

The electrochemical properties of porous carbon materials largely depend on pore structure of the carbon as well as on any heteroatom modifiers built into a porous structure.

Porous nitrogen-containing carbon materials were obtained at 750°C using calcium tartrate doped with iron, copper, and manganese, with a dopant concentration of up to 2 wt% as a precursor the template and acetonitrile vapor for the production of carbon. A complex of methods, including electron microscopy, Raman scattering, nitrogen adsorption and spectral method, studied the morphology and chemical state of carbon materials comprehensively. Understanding the role of the transition metal in the structure of nitrogen-containing porous carbon was obtained because of a comparative study of materials obtained using undoped and metal-doped tartrate.

Porous carbon materials produced using metal-doped calcium tartrate exhibit higher values of gravimetric capacitance than the carbon by non-doped salt. This capacitance behavior indicates that the carbon samples have a developed pore structure, which provides a large-area contact of the electrode with an electrolyte, facilitating the accumulation of ionic particles.

This work was supported by the Russian Science Foundation (project No. 19-73-10068).

Brominated porous carbon materials for sodium-ion batteries

Stolyarova S.G.¹, Fedoseeva Y. V.¹, Vorfolomeeva A.A.¹, Grebenkina M.A.¹, Okotrub A.V.¹, Bulusheva L.G.¹

stolyarova@niic.nsc.ru

¹ Nikolaev Institute of Inorganic Chemistry SB RAS, Novosibirsk, Russia

Sodium-ion batteries (SIB) are considered as a future alternative for lithium-ion power supplies due to the lower cost of sodium compounds, higher energy density and greater storage safety in comparison with lithium [1]. However, sodium is more difficult to intercalate into graphite than lithium therefore, standard graphitic anode materials for lithium-ion batteries are not suitable for use in SIB (Fig.1). Theoretical calculations proved that different defects (vacancies, atom-dopants) in graphene planes and large interplanar distance promotes sodium intercalation. The presence of pores is another factor that increases the capacity of carbon materials due to the formation of pathways for the diffusion of alkali metal ions and their adsorption and accumulation. Therefore, new specific materials with a large interplanar spacing, the presence of pores and defects for sodium intercalation and adsorption are needed for SIB.

In our work we used two different types of carbon materials - carbon nanohorns (CNHs) and nitrogen-doped porous carbon materials (N-PC). CNHs were obtained by the arc-discharge method, and thermal oxidation in air at 500 ° C were used for CNHs to create vacancy defects and open pores. N-PC were synthesized by acetonitrile vapor deposition on the products of thermolysis of calcium tartrate, adipate and glutarate. Carbon materials were brominated using molecular bromine at room temperature, which is capable of intercalating ordered graphite fragments with an increase in interplanar spacing or interacting with the formation of C-Br bonds. All samples were characterized by X-ray diffraction (XRD), X-ray photoelectron spectroscopy (XPS), scanning electron microscopy (SEM), and Raman spectroscopy. The interaction with sodium was studied by cycling materials in sodium-ion half-cells in the voltage range 0.01-2.5 V in a galvanostatic mode. The study of CNHs showed that the combination of thermal oxidation for opening pores and bromination leads to an increase in the sodium storage capacity by more than 2 times up to 120 and 60 mAhg⁻¹ at current densities of 0.1 and 2 Ag⁻¹. Comparison of different PC showed that bromination leads to an increase in capacity at all current densities, and the brominated N-PC sample produced from the calcium tartrate demonstrated the best performance of 245 mAhg⁻¹ at 0.1 Ag⁻¹.

The work was conducted with financial support from the Russian Science Foundation (Grant 19-73-10068).

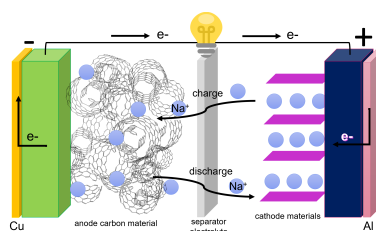


Fig. 1. Scheme of sodium-ion battery

References

1. A.A. Fedosova, S.G. Stolyarova, Y. V. Shubin, A.A. Makarova, A. V. Gusel'nikov, A. V. Okotrub, L.G. Bulusheva, Sodium storage properties of thin phosphorus-doped graphene layers developed on the surface of nanodiamonds under hot pressing conditions, FULLER NANOTUB CAR N. (2020) **28**, 335.

Ab initio calculations of layered compounds consisting of sp^3 or $sp+sp^2$ hybridized carbon atoms

*Belenkov E.A.*¹, *Greshnyakov V.A.*¹, *Mavrinskii V.V.*²

belenkov@csu.ru

¹Chelyabinsk State University, Chelyabinsk, Russia

²Nosov Magnitogorsk State Technical University, Magnitogorsk, Russia

There are three crystalline allotropic varieties of carbon - carbyne, graphite and diamond, which consist of carbon atoms in two-, three- and four-coordinated states in the corresponding crystal structure [1]. The valence electron orbitals of the carbon atoms in these compounds are sp -, sp^2 -, or sp^3 -hybridized. There are various carbon nanostructures - fullerenes, nanotubes, graphene layers, in most of which carbon atoms are sp^2 -hybridized. Therefore, they can be considered as polymorphic varieties of the graphite allotrope [2]. It is necessary to investigate the possibility of the existence of diamond-like and carbyne-like carbon nanostructures. In this work, we calculated the structure and electronic properties of carbon bilayers consisting of sp^3 -hybridized atoms and hybrid monolayers of $sp+sp^2$ -hybridized atoms.

The calculations were performed by the method of density functional theory in the generalized gradient approximation. The primary structure of diamond-like bilayers was constructed as a result of cross-linking pairs of graphene layers for five polymorphic varieties according to the technique proposed in [3]. Graphyne $sp+sp^2$ layers were built on the basis of 5-7 graphene by replacing carbon-carbon bonds with fragments of carbyne chains [4]. As a result of calculations of diamond-like bilayers, the possibility of stable existence of five structural varieties of these compounds was established (Fig. 1.a). The most stable is the DL_6 diamond-like layer. Diamond-like layers are semiconductors with a band gap ranging from 1.36 to 2.38 eV. Out of 43 theoretically constructed graphyne layers, only 21 layers were found to have a stable structure (Fig. 1.b, c). The band gap at the Fermi energy level for most graphyne layers is zero, and their properties should be metallic. The remaining seven layers have band gaps, the width of which varies from 0.05 to 0.20 eV. New sp^3 and $sp+sp^2$ carbon compounds with a layered structure can find practical applications in electronics and as molecular sieves.

The research was funded by RFBR and Chelyabinsk Region, project number 20-43-740015.

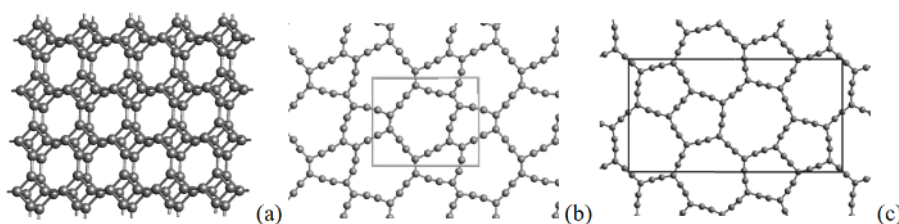


Fig.1. Structure of carbon layers: (a) diamond-like DL_6 bilayer from sp^3 atoms; $\beta 2-L_{5-7a}$ (b) and $\alpha-L_{5-7b}$ (c) graphyne layers from $sp+sp^2$ atoms.

References

1. A. Belenkov, and V.A. Greshnyakov, Phys. Solid State (2017) **59**, 1926.
2. A. Belenkov, and V.A. Greshnyakov, Phys. Solid State (2013) **55**, 1754.
3. A. Greshnyakov, and E.A. Belenkov, J. Struct. Chem. (2020) **61**, 835.
4. Belenkov, M. Brzhezinskaya, and V. Mavrinskii, Graphynes: advanced carbon materials with layered structure. Handbook of graphene. Volume 3, Wiley, (2019) chapter 4, 113-151.

Features of carbon nanostructures modification by stearic acid

*Dyachkova T.P.*¹, *Burakova E.A.*¹, *Kupreenko S.Y.*², *Pasko A.A.*¹, *Parfenov A.S.*³, *Savilov S.V.*², *Smitnova A.I.*³, *Tkachev A.G.*¹, *Usol'tseva N.V.*³

dyachkova_tp@mail.ru

¹ Tambov State Technical University, Tambov, Russia

² Department of Chemistry, Lomonosov Moscow State University, Moscow, Russia

³ Ivanovo State University, Nanomaterials Research Institute, Ivanovo, Russia

Carbon nanostructures, characterized by unique physical and mechanical characteristics, are a promising component of compositions with improved tribotechnical parameters. Various functionalization methods are used to enhance the interaction of carbon nanotubes (CNT) and graphene nano-flakes (GNF) with solvents, polymers and oils. As a result of the formation of functional groups or modifying layers on the surface of CNT and GNF, it is possible to more evenly disperse carbon nanomaterials and reduce the rate of their consumption to achieve the necessary effects.

In the present study, GNF and CNT with conical and cylindrical graphene layers were functionalized by interaction with stearic acid vapor under reduced pressure. The effect of preliminary preparation of carbon nanomaterials by means of oxidation and doping with nitrogen [1], temperature conditions and the duration of interaction of carbon nanomaterials with stearic acid on the change in the surface composition was evaluated.

Functionalized carbon nanostructures samples were studied by electron microscopy, XPS, FTIR and Raman spectroscopy, TG / DSC analysis. The sedimentation stability of toluene and oil suspensions of the raw and functionalized CNT and the dispersed phase particles sizes in them were determined by visual assessment, analysis of micrographs, and also on the basis of optical density data.

It was found that the presence of hydroxyl groups on the surface of carbon nanotubes promotes effective interaction with stearic acid, as a result of which covalent bonds are formed. According to the data of X-ray photoelectron spectroscopy, the samples contain alkyl and carboxyl groups. At the same time, in SEM images, there is no amorphous layer on the surface of functionalized CNTs and GNFs.

Carbon nanostructures functionalized by stearic acid are uniformly dispersed in toluene. A decrease in the carbon nanotubes agglomerates average size by an order of magnitude or more is observed in comparison with suspensions containing raw CNTs. Compositions based on industrial mineral oil with 0.1-0.2% content of functionalized CNTs demonstrate sedimentation stability.

Thus, functionalization with stearic acid improves the compatibility of carbon nanostructures with non-polar matrices and makes it possible to obtain concentrated stable suspensions based on them.

This work was supported by the Russian Foundation for Basic Research (grant no. 18-29-19150_mk).

References

1. S.A. Chernyak, A.M. Podgornova, E.A. Arkhipova, R.O. Novotortsev, T.B. Egorova, A.S. Ivanov, K.I. Maslakov, S.V. Savilov, V.V. Lunin, *Applied Surface Science* (2018) **439**, 371.

Gold decorated MOF-derived CuO, ZnO and NiO for CO₂ photoreduction.

*Cedeno M.E.*¹, *Mendez-Rojas M.A.*², *Kharisov B.I.*¹

bkhariss@mail.ru

¹ Universidad Autonoma de Nuevo Leon, Pedro de Alba S/N, Ciudad Universitaria, San Nicolas de los Garza 66455, Mexico

² Universidad de las Americas Puebla, ExHda. Sta. Catarina Martir s/n, San Andres Cholula, 72820 Puebla, Mexico

Climate change and energy shortage are among the main challenges for our society in this century. CO₂ emissions are known as the major contributor to the greenhouse effect, which is strongly related to climate change [1]. Currently, the principal actions to tackle this problem are focused on carbon taxes and a progressive switching to renewable energies. However, another alternative is the conversion of CO₂, as solar fuel, into useful molecules by artificial photosynthesis. This technique may employ suitable semiconductors, water, and solar energy to yield high-valued chemical compounds [2]. Though several semiconductors have been evaluated for this application, metal organic-framework (MOF)-derived materials composites are foreseen as one of the most promising candidates in this field. MOF-derived materials exhibit outstanding properties such as great surface area, porosity, good conductivity, and chemical stability [3]. Moreover, they can be coupled with plasmonic nanoparticles, such as gold nanoparticles, to further increase their photocatalytic properties [4].

Herein, we present the synthesis of three metal oxides embedded in carbon matrixes obtained from the thermal decomposition of three different MOFs (Ni-BTC, Zn-BTC and Cu-BTC), and its decoration with gold nanoparticles. Furthermore, their photocatalytic CO₂ photoreduction performance was evaluated. The materials were characterized before and after the calcination process by XRD, SEM, DRS, BET and FTIR. After decoration with gold nanoparticles, the carbon matrixes were characterized by SEM and DRS. The CO₂ photoreduction activity was evaluated in a photocatalytic reactor and the resulting products were identified and quantified by HPLC. The results indicate that the presence of gold nanoparticles increases the rate of solar fuels transformation into derived-chemicals due to their plasmonic properties. The combination of a sacrificial electron agent as TEOA and gold nanoparticles provides a continuous supply of free electrons making a great contribution to the photoreduction system. This work presents a novel and promising composite in the field of CO₂ photoreduction.

References

- [1] R. Vooradi, M. O. Bertran, R. Frauzem, S. B. Anne, and R. Gani, "Sustainable chemical processing and energy-carbon dioxide management: Review of challenges and opportunities," *Chem. Eng. Res. Des.*, vol. 131, pp. 440-464, 2018.
- [2] S. C. Peter, "Reduction of CO₂ to Chemicals and Fuels: A Solution to Global Warming and Energy Crisis," *ACS Energy Lett.*, vol. 3, no. 7, pp. 1557-1561, 2018.
- [3] W. Zhan, L. Sun, and X. Han, "Recent Progress on Engineering Highly Efficient Porous Semiconductor Photocatalysts Derived from Metal-Organic Frameworks," *Nano-Micro Lett.*, vol. 11, no. 1, pp. 1-28, 2019.
- [4] S. Gautam et al., "Metal oxides and metal-organic frameworks for the photocatalytic degradation: A review," *J. Environ. Chem. Eng.*, vol. 8, no. 3, p. 103726, 2020.

Morphology of graphene obtained in DMF and DMF-aqua media

*Klimenko I.V.*¹, *Trusova E.A.*², *Afzal A.M.*^{2,3}, *Jurina L.V.*¹, *Shchegolikhin A.N.*¹

inna@deom.chph.ras.ru

¹ Emanuel Institute of Biochemical Physics of Russian Academy of Sciences, Moscow, Russia

² Baikov Institute of Metallurgy and Materials Science of Russian Academy of Sciences, Moscow, Russia

³ Peoples' Friendship University of Russia, Moscow, Russia

New materials based on nanocarbon (nanotubes, fullerenes, graphene) due to their outstanding physicochemical properties are of great interest when producing organic electronic devices for photovoltaics and biocompatible composite materials for biological and biomedical applications. Also, there is a growing research interest in new ways of introducing graphene into multicomponent supramolecular systems based on phthalocyanines or chlorines, used as photosensitizers in such areas of medicine as photodynamic therapy and diagnostics. However, the production of pure oxygen-free graphene, which has unique electronic, mechanical, optical and thermal properties, is a fundamental problem. Nowadays, different organic, aqueous and aqueous-organic media are used for stabilization of the graphene sheets and preventing their agglomeration. In addition, when creating materials for biomedical applications related to vector drug delivery, it is very important to use graphene with controlled layering and sheet sizes.

In this study, we performed a qualitative and quantitative comparison of the graphene suspensions obtained by the sonochemical method in N,N-dimethylformamide (DMF) and its aqua solution. The task was to determine the shape and size of graphene particles, as well as the modality of their size distribution in two liquid media differing in the presence of aqua. Based on a comprehensive analysis of the data obtained using TEM, dynamic light scattering (DLS), FTIR, Raman and optical spectroscopy, the presence of graphene in the resulting suspensions was confirmed. Electron diffraction also confirmed the multilayering of graphene particles. According to TEM, the linear dimensions of flat or curved graphene sheets are of several hundred nanometers with a thickness of 7-9 nm. Using the DLS, it was shown that there are bi- or three-modal particle size distributions depending on the nature of the liquid phase (respectively, for DMF and its mixture with aqua). It was also shown that the presence of aqua in a graphene suspension leads to the predominant formation of graphene particles with larger linear dimensions than in pure DMF. It was found that the optical properties of graphene suspension depend on the composition of liquid phase and are apparently determined by the nature of the interaction of graphene sheets with DMF and aqua molecules as well as the nature of the formed complex.

The work has been carried out according to government assignment no. 075-00328-21-00 and within the state assignment of IBCP RAS (theme No. 01201253304). Trusova E.A. Afzal A.M. thank Russian Foundation for Basic Research (grant no. 19-03-00554_a) for financial support of the research.

Heavy metal nanosensor based on fluorescent carbon dots

*Laptinskiy K.A.*¹, *Burikov S.A.*², *Chugreeva G.N.*², *Tomskaya A.E.*³, *Dolenko T.A.*²

laptinskiy@physics.msu.ru

¹ D.V. Skobeltsyn Institute of Nuclear Physics, M. V. Lomonosov Moscow State University, Moscow, Russia

² Physical Department, M. V. Lomonosov Moscow State University, Moscow, Russia

³ North-Eastern Federal University, Yakutsk, 677007, Russia

At present time, a topical problem is the diagnosis of heavy metal ions in aqueous technological environments, in beverages, in organisms. To solve this problem, it is necessary to be able to identify and control the content of heavy metals in water. Carbon dots (CDs) have good prospects for use as optical nanosensors in problems of metal ions diagnostics in multicomponent media. This is due to their intense, time-stable and photobleaching-resistant photoluminescence, which is sensitive to changes in the parameters of the medium as like temperature, pH, the presence of certain types of ions and macromolecules, and their concentration.

In this study, the mechanisms of interaction of CDs obtained by the hydrothermal synthesis method with the ions Cr^{3+} , Fe^{3+} , Cu^{2+} , Zn^{2+} , Ag^+ , Pb^{2+} were investigated. Two types of CDs were used as objects of study: 1) synthesized from trans-aconitic acid and ammonia aqueous solution, the maximum fluorescence emission of which is in the region of 415 nm (CDs-V) and 2) synthesized from citric acid and ethylenediamine, the maximum fluorescence emission of which is in the region of 450 nm (CDs-B). Mixtures of aqueous suspension of CDs and solutions of inorganic salts were prepared in the range of salt concentration variation from 0 to 0.3 mM. An comparative analysis of the obtained fluorescence spectra of the prepared mixtures was carried out (Fig.1), and a conclusion about the mechanisms of interaction of CDs with the studied ions was made.

This study has been performed at the expense of the grant of RFBR (project № 20-32-70150).

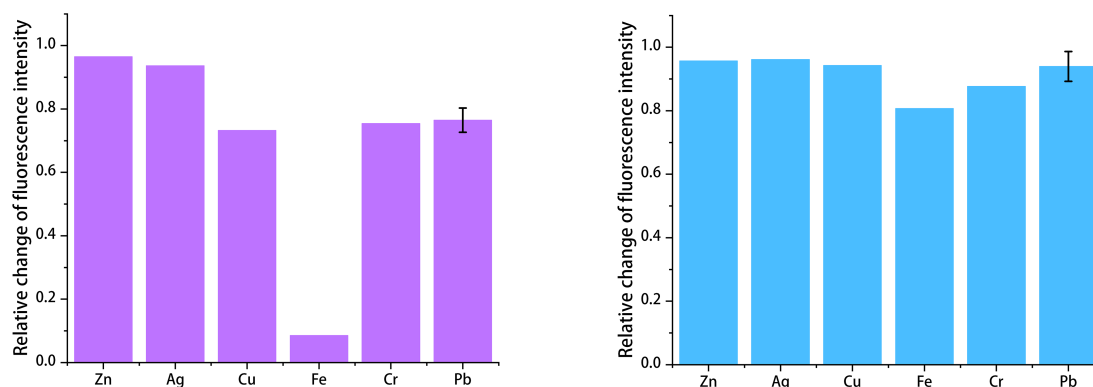


Fig. 1. Relative change in the fluorescence intensity of CDs in the presence of heavy metal ions (CDs-V - left, CDs-B - right).

Properties of carbon dot luminophores studied by polarized luminescence experiments

*Nelson D. K.*¹, *Starukhin A. N.*¹, *Fedorov D. L.*¹, *Kurdyukov D. A.*¹, *Eurov D. A.*¹, *Stovpiaga E. Yu.*¹, *Golubev V. G.*¹

d.nelson@mail.ioffe.ru

¹ Ioffe Institute, St. Petersburg, Russia

Carbon dots are a new type of man-made luminophores with unique properties. The dots are quasi-spherical nanoparticles (up to 10 nm in size) consisting of layers of graphite or turbostratic carbon [1]. The surface of a carbon dot contains various functional groups that significantly affect the optical properties, chemical activity, and other properties of the dots. Carbon dots are easily synthesized, inexpensive, low-toxic and chemically inert, which distinguishes them favorably from semiconductor quantum dots. From the point of view of various applications, carbon dots are of particular interest for biology and medicine. Although the structure of carbon dots has been studied in sufficient detail, the question of the origin of the luminescence of the dots remains open [2]. The answer to this question would facilitate the targeted synthesis of luminescent carbon dots with the desired characteristics. In this regard, an in-depth study of the luminescent properties of carbon dots is important.

The present work is devoted to the study of polarized luminescence of solutions of carbon dots in glycerol-water mixtures of different viscosities and temperatures. It is shown that the excitation of solutions by linearly polarized light induces linear polarization of the solution emission. It has been found that a decrease in the viscosity and an increase in the temperature of the solutions lead to depolarization of the emission. The depolarization of emission is explained by the rotational diffusion of luminous entities in colloidal solutions (Levshin-Perrin model [3]). A comparison of the experimental data with the theory of the phenomenon shows that the rotational motion of luminous entities in solutions is characterized by two rotational correlation times corresponding to the rotation of the carbon dot as a whole and the limited rotational motion of its luminous fragment ("luminophore") [4]. It is established that the maximum angle at which the luminophore can rotate depends on the wavelength of the emission. The effective volumes of the carbon dot as a whole (10.5 nm³) and of its luminous fragment, which is 3% of the dot volume, are determined. It is suggested that the luminescence of the carbon dots under study comes from the oxidized outer graphene layers ("graphene oxide") of the carbon dots with possible inclusions of fragments of polyaromatic or heterocyclic compounds.

References

1. M. Carbonaro, R. Corpino, M. Salis, F. Mocci, S. V. Thakkar, C. Olla, P. C. Ricci, C – J. Carbon Research (2019) **5**, 60.
2. Sciortino, A. Cannizzo, F. Messina, C – J. Carbon Research (2018) **4**, 67.
3. R. Lakowicz, Principles of Fluorescence Spectroscopy (Springer, Boston, MA, 2006).
4. A. Starukhin, D. Nelson, D. Eurov, D. Kurdyukov and V. Golubev, Phys. Chem. Chem. Phys. (2020) **22**, 8401.

Structural characterization and magnetic behavior of nickel nanoparticles encapsulated in monolithic wood-derived porous carbon

Orlova T.S.¹, Spitsyn A.A.², Ponomarev D.A.², Kirilenko D.A.¹, Popov V.V.¹

orlova.t@mail.ioffe.ru

¹ Ioffe Institute, St. Petersburg, Russia

² St. Petersburg State Forest Technical University, St. Petersburg, Russia

Encapsulated magnetic nanoparticles are very promising for different application such as magnetic data storage, magnetic carriers in biomedicine, magnetic separation, catalysis, magnetic sensors, electromagnetic wave shielding and others [1,2].

Magnetic monolithic composites C/Ni nanoparticles (NiNPs) consisting of highly porous carbon matrix and well separated Ni nanoparticles covered by graphite-like shells (Fig.1) were prepared by a new environmentally friendly and simple method. The method is based on sintering/carbonization of the pressed mixture of wood-derived carbon powder with addition of nickel nitrate and wood decomposition product (tar) as a binder. Two sets of the C/NiNPs composites with maximum carbonization temperature $T_{carb}=700$ и 970 °C were prepared. The specific structural features were studied by X-ray diffraction (XRD) and transmission electron microscopy (TEM). Magnetic properties of the both sets of the C/NiNPs composites were systematically investigated.

The composites with maximum $T_{carb}=700$ °C has uniformly distributed NiNPs with the average size $D_{av}\sim 9$ nm (Fig.1c) and demonstrate superparamagnetic (SP) behavior. The SP behavior of NiNPs is well described by the Langevin function with parameters which are in good agreement with microstructural parameters. The increase in T_{carb} to 970 °C results in increase of the particle size to $D_{av}\sim 18$ nm and in change of NiNPs magnetic character for the ferromagnetic behavior. The macroscopic magnetization 3.5 emu/g (38 emu/g(Ni)) was achieved for the nanocomposites with small amount of nickel (8.8 wt.%) in the low magnetic fields 2-4 kOe at room temperature, that makes them ideal candidates for applications involving magnetic separation (heterogeneous catalysis, adsorption of contaminants in aqueous media, etc.). The obtained maximum magnetization 38 emu/g(Ni) of carbon-encapsulated NiNPs somewhat exceeds that of similar core-shell Ni nanoparticles obtained by other methods.

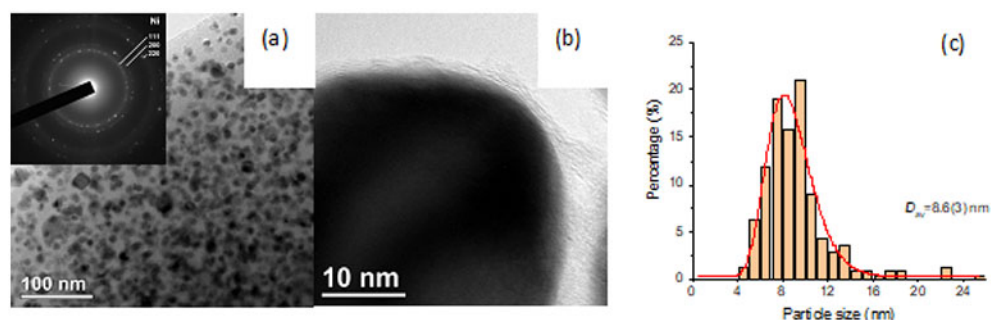


Fig. 1. Typical TEM image of C/NiNPs composite ($T_{carb}=700$ °C) with electron diffraction (a). A nickel particle covered by graphite-like shell (b). Distribution of the Ni nanoparticles on size (c).

References

1. H. Lu, E. L. Salabas, F. Schüth, *Angew Chem. Int. Ed.* (2007) **46** (8), 1222.
2. Ch. Wang, V. Murugadoss, J. Kong, Zh. He, X. Mai, Q. Shao, Y. Chen, L. Guo, Ch. Liu, S. Angaiah, Zh. Guo, *Carbon* (2018) **140**, 696.

Magnetic properties of polymerized exfoliated graphite

Popov V.V.¹, Berezkin V.I.², Tomkovich M.V.¹

13745pop@mail.ru

¹ Ioffe Institute, St. Petersburg, Russia

² Research Center for Ecological Safety, Russian Academy of Sciences, Saint Petersburg, Russia

The initial exfoliated graphite (EG) is a material that was obtained by rapidly heating finely ground graphite intercalated with inorganic acids (sulfuric or nitric) with the separation of the carbon layers in the graphite. With compression of initial EG, a chemical solid-phase reaction of polymerization of EG particles into a low-porous carbon monolith is carried out. The lower is the pressure, the lower are the density, and the degree of orientation of the carbon layers in the sheet.

The investigated material in the form of monolithic plates was obtained at room temperature by pressing the initial EG in air with an external pressure of 0.7 GPa. The content of possible impurities remaining after the intercalation process and subsequent purification of the obtained EG was analyzed in the source material by X-ray spectral microanalysis in a Quanta 200 scanning electron microscope equipped with an EDAX X-ray microanalyzer. Measurements of the magnetic moment by the vibration method were performed on the PPMS QD measuring unit in the temperature range of $T=3-400\text{K}$ and in magnetic fields up to 5 T.

Figure 1 shows the experimental dependences of the magnetization value M on the magnetic field H , at different temperatures T . The observed dependences of $M(H)$ can generally be represented as the sum of the components: M_D - dia-, M_{FM} - ferro-, and M_{PM} - paramagnetic. It can be seen that dependences of $M(H)$ at low temperatures $T=3\text{K}$ and 50K (curves 1 and 2 in Fig.1) have a form typical of paramagnetic behavior with saturation in strong magnetic fields. To determine the type and concentration of paramagnetic magnetic centers, the experimental $M_{PM}(H)$ curve is compared with the Brillouin function: the dependences extracted from the experiment correspond to the value of the quantum number $J=S=2$ (J is equal to the spin number S for carbon) and are close to the value $J=5/2$ determined for graphene in [1].

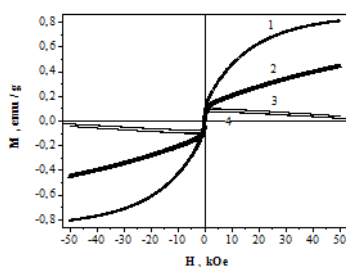


Figure 1. Magnetic response of polymerized exfoliated graphite. T, K: 1 - 3; 2 - 50; 3 - 300; 4 - 400.

References

1. M. Sepioni, R. R. Nair, S. Rablen, J. Narayanan, F. Tuna, R. Winpenney, A. K. Geim, and I.V. Grigorieva, Phys.Rev.Lett. (2010) **105**, 207205.

Influence of the p-electrons concentration in carbon nanobelts on their emission properties

Tomilin O.B.¹, Rodionova E.V.¹, Rodin E.A.¹, Adilov V.F.¹

evg.rodin54@gmail.com

¹ National Research Mordovia State University, Saransk, Russia

In this work, we investigated the effect of the p-electrons concentration in carbon nanobelts (CNB) on the their emission properties demonstration. Variation of the p-electrons concentration was achieved by introducing a "pyridine" nitrogen atom into the CNB (isoelectronic structure with CNB) and a "pyrrole" nitrogen atom (increasing of the p-electrons number). In fig.1 it is shown the elementary repeating fragments of researched CNBs.

The electronic structure of model molecules were examined at the density functional theory (B3LYP/6-31G) by using the FireFly software package. The simulation of the constant uniform electric field effect on the electronic structure of carbon nanobelts at a field strength of 0.0 to 2.1 V/Å with a step of 0,3 B/Å.

The nanostructures emission properties description was based on the mechanism of field emission from carbon nanotubes [1].

The results obtained show:

1. "Pyridine" nitrogen does not change the number of p-electrons in relation to the CNB, but creates a Coulomb "locking" layer for emission due to the electron lone pair located on the cylindrical surface [2].
2. "Pyrrole" nitrogen changes the number of p-electrons in the conjugated system in relation to the CNB. Increase in the concentration of p-electrons improve on the emission properties.
3. The location of "pyridine" and "pyrrole" nitrogen in the nanobelts can generate anisotropy of the electrons field emission, depending on the direction of the electric field strength.

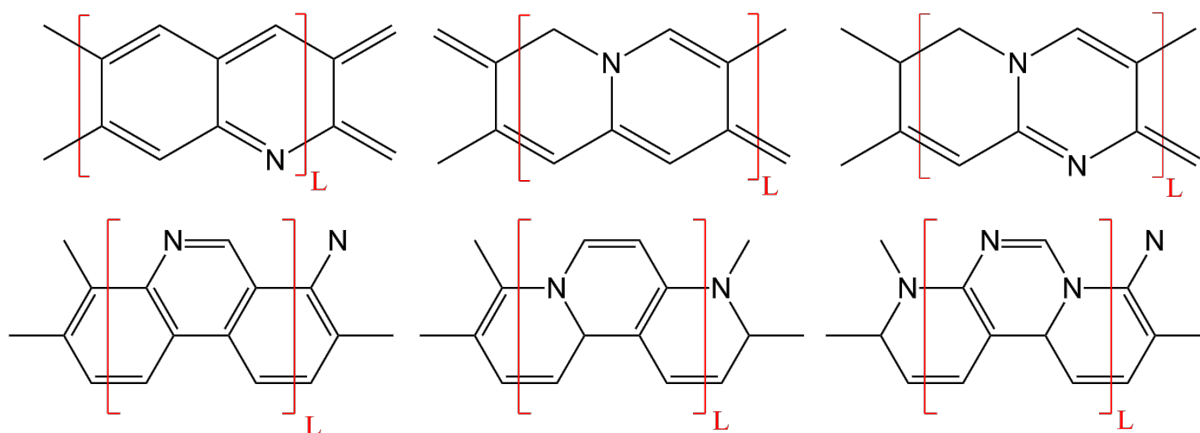


Fig.1. Elementary repeating fragments of the CNBs.

References

1. O. B. Tomilin, E. V. Rodionova, E. A. Rodin, Russian Journal of Physical Chemistry A (2020) **94**, 1242.
2. O. B. Tomilin, E. V. Rodionova, E. A. Rodin, V. I. Soldatova, T.S. Koscheeva, Fullerenes, Nanotubes and Carbon Nanostructures (2020) **28-2**, 129.

Difference between oxygen-containing groups on sp^2 and sp^3 carbons: deprotonation

Vervald A.M.¹, Kozhushnyi K.A.¹, Dolenko T.A.¹

alexey.vervald@physics.msu.ru

¹ Faculty of Physics, Lomonosov Moscow State University, Moscow, Russia

The surface properties of carbon nanoparticles (CNPs) largely determine how nanoparticles interact with their environment. The colloidal stability of nanoparticles, their biocompatibility, adsorption properties, as well as surface photoluminescence depend on the composition of surface groups. Like that, the oxidized surface provides high biocompatibility, dispersibility, and intense photoluminescence for carbon dots and nanodiamonds. However, the question arises: are the same oxygen-containing functional groups on carbon in sp^3 and sp^2 hybridization on the surfaces of nanodiamonds and carbon dots truly the same or differ in their properties?

In this study, quantum mechanical calculations were used to compare the properties of carboxyl and hydroxyl groups on sp^2 - and sp^3 -hybridized surface regions of carbon nanoparticles. It was found that with a change in the hybridization of the base, the binding strength of hydrogen to the group – the length of the O-H bond – changes. Based on the known relationship between the bond lengths of O-H groups and pK_a for simple organic molecules, the pH ranges of deprotonation of -OH and -COOH groups on the CNP surfaces were calculated. It turned out that the deprotonation of the carboxyl group occurs in the pH range from 3 to 5 and only weakly depends on the hybridization of the base, while the deprotonation of the hydroxyl group depends strongly: for the sp^2 base it occurs in the pH range from 8 to 11, for sp^3 from 15 to 19 (Fig. 1). The group deprotonation was confirmed experimentally by a change in the zeta potential value with a change in pH for deprotonation nanodiamonds with a high content of sp^2 -hybridized carbon on the surface.

This study has been performed at the expense of the grant of RFBR (project № 20-32-70150).

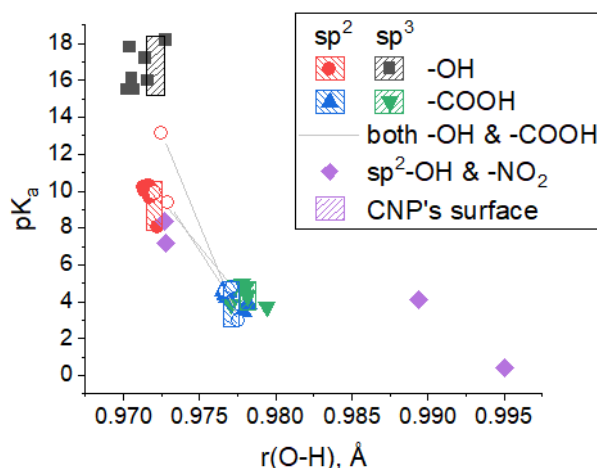


Figure 1. Correspondence of the calculated O-H bond lengths of the hydroxyl and carboxyl groups to their pK_a values for nanoparticles (lattice) and simple molecules (dots).

High-temperature synthesis of linear carbon chains confined in carbon nanotubes

Arutyunyan N.R.^{1,2}, *Obraztsova E.D.*^{1,2}

natalia.arutyunyan@gmail.com

¹ Prokhorov General Physics Institute of the Russian Academy of Sciences, Moscow, Russia.

² Moscow Institute of Physics and Technology (National Research University), Moscow, Russia.

Linear carbon chain (LCC) or carbyne, is a linear *sp* hybridized carbon allotrope with double (cumulene) or alternating triple and single bonds (polyyne) between carbon atoms. Carbyne is very sensitive to the surrounding media due to the high reactivity and therefore unstable at ambient conditions. The synthesis of polyynic chains in liquid media [1] allowed to form molecules up to few tens of atoms. Recently, it has been demonstrated that LCC formation is possible inside double-wall carbon nanotubes (DWCNT) with small inner diameters [2]. Due to the spatial confinement and protection from the gas molecules the authors succeeded to form extremely long LCC (more than 6000 atoms).

In this work the results of the LCC formation inside DWCNT and (6,5) nanotubes are presented. The nanotubes were heated up to 1450 C in argon atmosphere, and carbon chains were self-organized inside nanotubes from the free C atoms or defects. The influence of the temperature, the duration of the treatment, the diameter of nanotubes were analyzed.

The presence of LCC in the material has been confirmed by Raman spectroscopy (Fig.1). The fingerprint vibration of LCC has a frequency of $\sim 1850\text{ cm}^{-1}$, while the Raman bands of carbon nanotubes are situated at $100\text{-}350\text{ cm}^{-1}$ (radial breathing mode RBM), 1350 and 1590 cm^{-1} (D and G peaks). It has been revealed that LCC are formed only in small nanotubes, as the band 1850 cm^{-1} is observed only simultaneously with high-frequency RBM ($>250\text{ cm}^{-1}$) that corresponds to nanotubes with diameters less than 1 nm.

Acknowledgements The research was supported by RFBR grant N 20-32-70013.

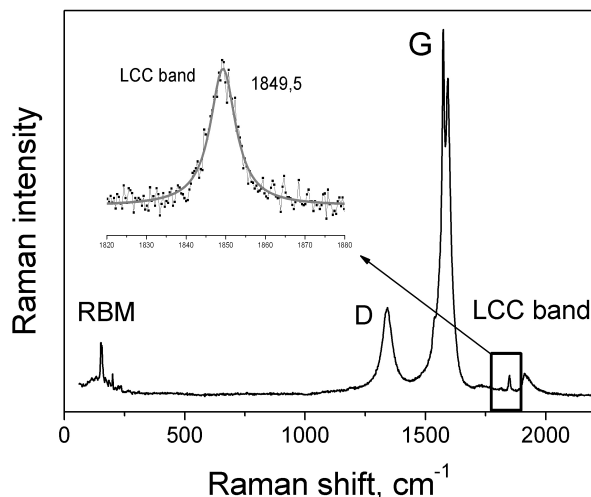


Fig.1. Raman spectrum of LCC@DWCNT with excitation 532 nm. The band at 1850 cm^{-1} is the fingerprint of carbyne.

References

1. F. Cataldo, Carbon (2004) **42** 129.
2. L. Shi, Ph. Rohringer, K. Suenaga, Y. Niimi, J. Kotakoski, J.C. Meyer, H. Peterlik, M. Wanko, S. Cahangirov, A. Rubio, Z.J. Lapin, L. Novotny, P. Ayala, and T. Pichler, Nature Materials (2016) **15**, 634.

Modeling the structure and interlayer interactions of twisted bilayer graphene

*Belenkov M.E.*¹, *Brzhezinskaya M.*², *Greshnyakov V.A.*¹, *Belenkov E.A.*¹

me.belenkov@gmail.com

¹ Chelyabinsk State University, Chelyabinsk, Russia

² Helmholtz-Zentrum Berlin für Materialien und Energie, Berlin, Germany

Bilayer graphene changes its properties depending on the angle of rotation of adjacent graphene layers [1-3]. When the graphene layers are turned in the bigraphene layers, Moire structures are formed, which can have a periodic structure at strictly defined so-called magic turning angles. How the binding energy of layers in bigraphene changes and whether the magic angles of rotation correspond to local energy minima is still poorly understood.

Therefore, in this work, at the first stage, the analysis of the angles of mutual rotation of the layers was performed at which the structure of the bigraphene layer is periodic.

At the second stage, the energies of interlayer bonds were calculated depending on the angles of layer rotation in bilayer graphene. Calculations were carried out by the atom-atom potential method. To describe the van der Waals interactions between carbon atoms in adjacent layers, the Buckingham potential was used. In the simulation, the total binding energy between all the atoms of one layer and the atoms of the other layer was calculated, and then the specific binding energy per atom was found. The layers had a rounded shape of the finite size. The diameter of the layers was chosen in such a way that an increase in the layer size did not lead to a change in the specific binding energy by more than 0.01 %. The number of atoms in the layers under this condition was at least 10,000. Calculations were performed for different angles of rotation of layers in bigraphene in the range from 0 to 60 degrees with a step of 0.1. With a relative twist of the layers, the packing of the bilayers changed from AA to AB at rotation angles of 0 and 60°, respectively. As a result of calculations it was established that in the twist angle range from 0 to 4° there is a rapid decrease in bond energy. Then, in the range from 4 to 56°, the energy changes insignificantly. In the next range of angles from 56 to 60 degrees, the binding energy decreases rapidly again, reaching a minimum at the angle of rotation of 60°, which corresponds to AB packing. Local minima of the energy of interlayer bonds are observed in the second interval of rotation angles. At the same time, the height of potential barriers between local minima is small, which casts doubt on the possibility of stable existence of any structure with a twist angle different from 60°.

In addition, the angles at which local minima of the energy of interlayer bonds are observed weakly correlate with magic angles leading to the formation of periodic moire structures.

References

1. E. Suarez Morell, J. D. Correa, P. Vargas, M. Pacheco, and Z. Barticevic, Phys. Rev. B (2010) **82**, 121407.
2. Y. Cao, V. Fatemi, S. Fang, K. Watanabe, T. Taniguchi, E. Kaxiras, and P. Jarillo-Herrero, Nature (2018) **556**, 43.
3. Y. Cao, V. Fatemi, A. Demir, S. Fang, S. L. Tomarken, J. Y. Luo, J. D. Sanchez-Yamagishi, K. Watanabe, T. Taniguchi, E. Kaxiras, R. C. Ashoori, and P. Jarillo-Herrero, Nature (2018) **556**, 80.

Tribological properties of carbon-containing composite materials prepared by high-pressure high-temperature synthesis

Chernogorova O.P.¹, Ekimov E.A.², Drozdova E.I.¹, Lukina I.N.¹, Prokopenko D.A.¹

tchern@imet.ac.ru

¹ Baikov Institute of Metallurgy and Materials Science, RAS, Moscow 119334, Russia

² Vereshchagin Institute of High Pressure Physics, RAS, Moscow 142190, Russia

The bulk composite materials (CM) reinforced with fullerene-derived particles of diamond-like carbon (10 wt. % in a Co matrix) or diamond (70 wt. % with a Ti-Cu binder) were prepared by high-pressure high-temperature synthesis (5-8 GPa, 800-1400°C) and studied for tribological properties. The methods of optical microscopy, electron microscopy, dynamic indentation, tribological tests, and wear-resistance measurements were used to establish the correlations between the structure and properties of the CM and the reinforcing phase and to determine the limits of the applicability of the CM as tribo- and electrical materials [1].

It has been shown that ultra low (0.08 - 0.03) coefficient of friction is achieved by the cobalt-based CM reinforced with superhard ($H_{\text{IT}} = 35 - 45$ GPa) diamond-like phase particles obtained from the ball-milled fullerenes as well as by the CM with diamond regardless of binder type and particle size. The abrasive wear resistance (weight loss per a path of 9 m) of the CM increases with increasing content and hardness of the reinforcing diamond-like particles reaching the characteristics of the CM with diamonds.

The condition for obtaining super wear-resistant CM from mixtures of metals with ball-milled fullerenes is a relatively low synthesis temperature ($\sim 800^\circ\text{C}$), which ensures the collapse of fullerene molecules, but limits the graphitization of the diamond-like structure. Under conditions of dry friction, such CM are applicable for short-term heating up to 1000°C , and can be permanently used at temperatures up to 300°C .

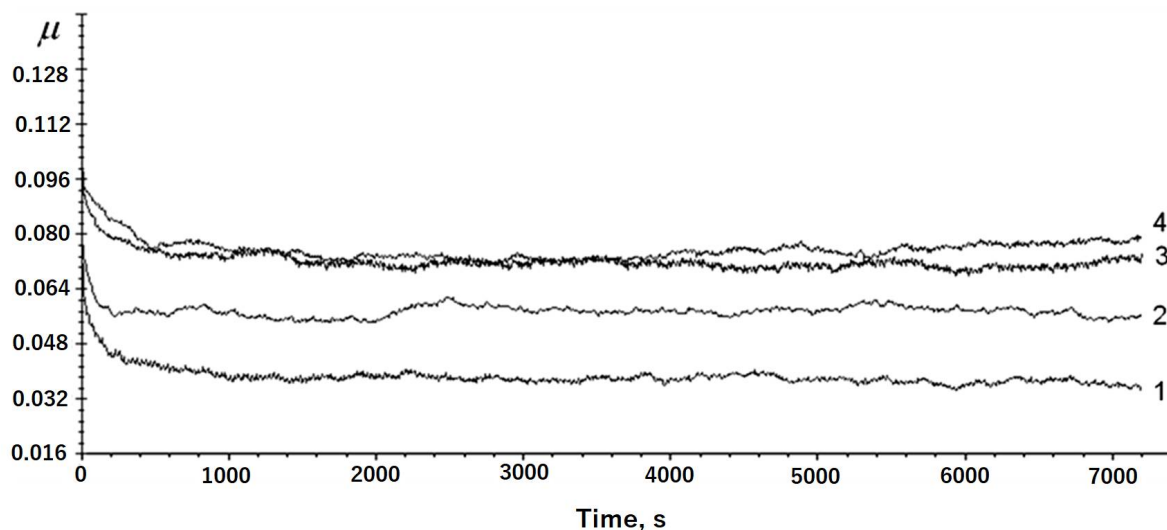


Fig. 1. Friction coefficients of the CM reinforced with diamond of 40-50 microns (1), and 80-100 microns (3) in size and the CM reinforced with diamond-like phase particles obtained from $C_{60/70}$ (2) and C_{60} (4) fullerenes ball-milled for 1 h and 4 h, respectively.

References

1. V.V. Izmailov, I. N. Ushakova, E. I. Drozdova, O. P. Chernogorova, and E. A. Ekimov, J. Frict. Wear (2016) **37**, 253.

Structural transformations of graphite during dispersion

Fazlitdinova A.G.¹, Tyumentsev V.A.¹

fazlitdinovaag@mail.ru

¹Chelyabinsk State University, Chelyabinsk, Russian Federation

The features of graphitization of carbon materials, as well as the structural destruction of graphite in the process of neutron irradiation or mechanical dispersion, have been studied in numerous works. In particular, it was shown that an increase in the size of the coherent scattering regions L_{002} and a decrease in the interlayer distance d_{002} develop monotonically in the course of graphitization. At the same time, it has been shown in a number of works that as the temperature of carbon material processing or graphite dispersion increases, plateaus are observed on the dependences of the change in d_{002} at values of ~ 3.36 , ~ 3.37 , ~ 3.40 , ~ 3.425 , ~ 3.44 and $3.55 / 3.68$ Å [1, 2]. The authors believe that the stepwise change in d_{002} may be due to the formation of metastable carbon phases differing in the value of the interlayer distance. The change in the structure of graphite dispersed in a planetary mill Fritsch Pulverisette 6 in an air atmosphere has been studied in this work. As the graphite is dispersed, as shown in Fig., an increase in the asymmetry and integral width of the (002) peak is observed. This effect may be due to the formation of metastable states, the parameter d_{002} of which differs from graphite. In this regard, we decomposed the (002) asymmetric peak of samples into the minimum number of components described by the Voigt function. It was shown that the 002 peak of graphite after long-term dispersion can be represented in the form of two or three components, which correspond to d_{002} given in the table (determination coefficient $R^2 \sim$ from 0.955 to 0.998).

Duration of dispersion, min.	d_{002} values calculated from the decomposition components of asymmetric peak, Å		
15-90	3.37	3.40	-
105-450	3.37	3.40	3.44
480-660	3.37	3.425	3.44
720-960	3.37	3.425	3.55/3.60
1200-1320	3.40	3.425	3.55/3.60
1380-2700	3.40	3.44	3.55/3.60

The obtained dependence of the component composition on the duration of dispersion suggests that the process of the transition of graphite into a disordered carbon material, apparently, develops through a number of metastable states.

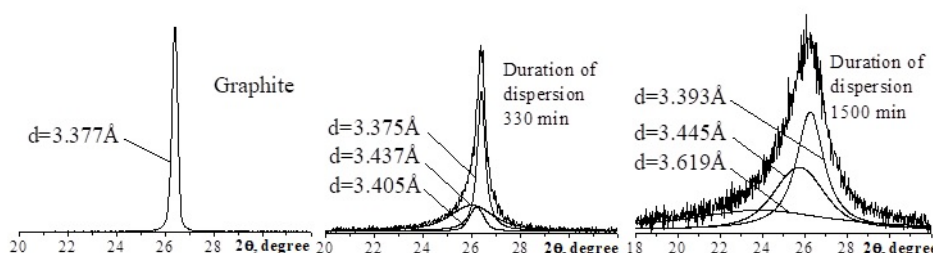


Fig. Profiles of (002) diffraction peaks graphite samples and the results of dividing asymmetric peaks into components

References

1. Lachter J., Bragg R.M., Phys. Rev. B. (1986) 33(12), 8903.
2. Aladekomo J.B., Bragg R.H. Carbon (1990) 28(6), 897.

Electrical conductivity of carbon films obtained by thermal sputtering of shungite

Moshnikov I.A.¹, Kovalevski V.V.¹, Markovskii Yu.A.¹

igorm@krc.karelia.ru

¹Institute Geology KRC RAS, Petrozavodsk, Russia

Thin carbon films are of interest at present due to their high temperature resistance, good electrical conductivity, low density, and excellent resistance to aggressive environments [1]. There are many methods and precursors that can be used to produce thin carbon films with different structures and properties. One such raw material may be shungite, a fullerene-like carbonaceous substance [2]. Shungite belongs to the non-graphitized variety of carbon and is characterized by the turbostratic structure of carbon layers. In addition, shungite exhibits some fullerene-like carbon features both at the level of structure and physical properties [2].

Electromagnetic properties are the most informative and relevant characteristics of carbon materials needed for modern technologies. These properties of carbonaceous materials are closely related to their band and atomic structure and are directly determined by the degree of graphitization, the size of the crystallites, the length and imperfection of the graphene layers, and so on. Previously, it was shown on powder samples that for shungites, a typical dependence of electrical conductivity on temperature is observed, which is characteristic of a crystalline semiconductor when the charge carriers are polarons [3]. The purpose of this work was to determine the dependence of the electrical conductivity on the temperature of carbon films obtained by thermal sputtering shungite.

The films were prepared from various types of shungite by thermal sputtering. Graphite films were obtained for comparison by the same way. The structural state of the films was evaluated by Raman spectroscopy using a Nicolet Almega XR X-ray Raman spectrometer with a green laser (532 nm, Nd-YAG). The studies revealed a difference in the intensities and positions of the G and D peaks of the spectra for various films. To analyze the differences between the films, element mapping was performed using a VEGA 11 LSH scanning electron microscope from Tescan with an INCA Energy (EDS) energy spectrometer from Oxford Instruments. For the studied films, the absence of isolated non-carbon inclusions with a homogeneous distribution of a small amount of silicon and aluminum, and the trace contents of iron, nickel and copper were found.

The electrical conductivity of the obtained films was measured by a two-contact method at a frequency of 1 kHz in the temperature range from the liquid nitrogen to room temperature. The measurements showed differences in the type of dependence of electrical conductivity on temperature for shungites of different type. For graphite films and shungite films from the Shunga locality, a monotonous increase in electrical conductivity with increasing temperature occurs, that is typical for semiconductors. For films obtained from other shungites, the dependence had the form of a V-shaped curve with a minimum at a temperature in the region of 180-200 K.

References

1. Diaf H., Pereira A., Melinon P., Blanchard N., Bourquard F., Garrelie F., Donnet C., Vondrack M. *Physical review materials* (2020) 4(6), doi.org/10.1103/PhysRevMaterials.4.066002
2. Kovalevski V.V., Prikhodko A.V., Buseck P.R. *Carbon* (2005) 43(2), 401
3. Moshnikov I.A., Kovalevski V.V. *Nanosystems-Physics Chemistry Mathematics* (2016) 7(1), 214

Characterization of new functional materials based on graphitized bath sponge scaffold

*Petrova O.V.*¹, *Sivkov V.N.*¹, *Nekipelov S.V.*¹, *Molodtsov S.*², *Ehrlich H.*³

teiou@mail.ru

¹ Institute of Physics and Mathematics Komi SC UrD RAS, Syktyvkar, Russia

² European XFEL GmbH, Schenefeld, Germany

³ Institute of Electronics and Sensor Materials, TU Bergakademie Freiberg, Freiberg, Germany

In the last decade the usage of renewable, naturally prefabricated non-toxic and biodegradable organic source as a base for novel carbon material with controlled microstructure and morphology has gain significant attention in modern material science.

Bath sponges as renewable sources of naturally prefabricated 3D materials are of great interest to the scientific community owing to their unique mechanical properties and interesting biological functionality [2,3]. In addition, the bath sponge carbon scaffold can withstand the high temperature up to 1200C in nitrogen environment without loss of their hierarchical 3D structure. The functionalization of the carbonized spongin scaffolds and synthesis of 3D carbonized-spongin Cu/Cu₂O composite can be carried out by electroplating method.

In current work the idea of fabricating unique nanostructured 3D (carbonized spongin)/(Cu and Cu₂O) composite catalyst from marine sponge scaffolds is put into practice [1]. The investigation of the structural and chemical changes of spongin scaffolds during its carbonization at temperatures before and above the onset of thermal degradation (in the range between 400C and 1200C) and the identification of corresponding copper phases at the carbonized spongin scaffolds surface of 3D carbonized-spongin Cu/Cu₂O composite were carried out by SEM, TEM, XPS, NEXAFS and Raman spectroscopy. Pristine, carbonized and metalized spongin scaffold sample preparation and its preliminary study were carried out by Prof. Ehrlich research group (Institute of Electronic and Sensor Materials (IESM), TU Bergakademie Freiberg). The NEXAFS and XPS studies were carried out at the Russian-German beamline (RGLB) of BESSY II synchrotron radiation source.

This work was supported by the Bilateral Program of the Russian-German Laboratory at BESSY II, RFBR and the Komi Republic No 20-42-110002 and grant of the President of Russian Federation No MK-3796.2021.1.2.

References

1. H. Ehrlich (Ed.), *Extreme Biomimetics*. Springer International Publishing, 2017, pp. 276.
2. T. Szatkowski, K. Koczyński, M. Motylenko, H. Borrmann, B. Mania, M. Graś, G. Lota, V.V. Bazhenov, D. Rafaja, F. Roth, J. Weise, E. Langer, M. Wysokowski, S. Żółtowska-Aksamitowska, I. Petrenko, S.L. Molodtsov, J. Hubáľková, C.G. Aneziris, Y. Joseph, A.L. Stelling, T. Jesionowski, H. Ehrlich, *Nano Research* (2018) **11(8)** 4199.
3. Petrenko, A.P. Summers, P. Simon, S. Żółtowska-Aksamitowska, M. Motylenko, C. Schimp, D. Rafaja, F. Roth, K. Kummer, E. Brendler, O.S. Pokrovsky, R. Galli, M. Wysokowski, H. Meissner, E. Niederschlag, Y. Joseph, S. Molodtsov, A. Ereskovsky, V. Sivkov, S. Nekipelov, O. Petrova, O. Volkova, M. Bertau, M. Kraft, A. Rogalev, M. Kopani, T. Jesionowski, H. Ehrlich, *Science Advances* (2019) **5(10)** 2805.

Emission properties of $C_x(BN)_y$ nanobelts

Tomilin O.B.¹, Rodionova E.V.¹, Rodin E.A.¹, Myakishev A.Y.¹

rodionova_j87@mail.ru

¹ National Research Mordovia State University, Saransk, Russia

Acene-type carbon nanobelts (NB) are new promising nanostructures that can be successfully synthesized. We research the emission properties of $C_x(BN)_y$ nanobelts with heteroatoms isoelectronic to carbon nanobelts. In fig. 1 the repeating elementary fragments of the considered NBs are shown.

The dangling bonds of the atoms were saturated with hydrogen atoms. The diameter of the nanobelts are corresponded to the diameter of nanotubes with chirality indices $(n,0)$, where $n = 6, 8, 9, 10, 12$. The nanobelts electronic structure was modeled in a constant electric field. The strength of constant electric field was changed from 0.0 to 2.1 V/Å with a step of 0.1 V/Å. The field strength vector was considered in opposite directions (A and B) along the NB axis. The calculation of the electronic structure of the NB was carried out by the method DFT/B3LYP/6-31G (Firefly program package).

The emission properties of nanobelts were considered within the mechanism of field emission from carbon nanotubes [1]. The research results show the introduction of heteroatoms into the carbon NBs causes the polarization of the nanobelts, which leads to the appearance of effective positive and negative charges on the opposite edges of the NB. The separation of charges at the edges of the NBs provides a hindering effect (“locking”) and facilitating effect (“unlocking”) for the escape of electrons occupying emission molecular orbitals from the inner region of the NB. This factor can explain the significant anisotropy of the considered nanobelts emission properties relative to the direction of the applied constant electric field.

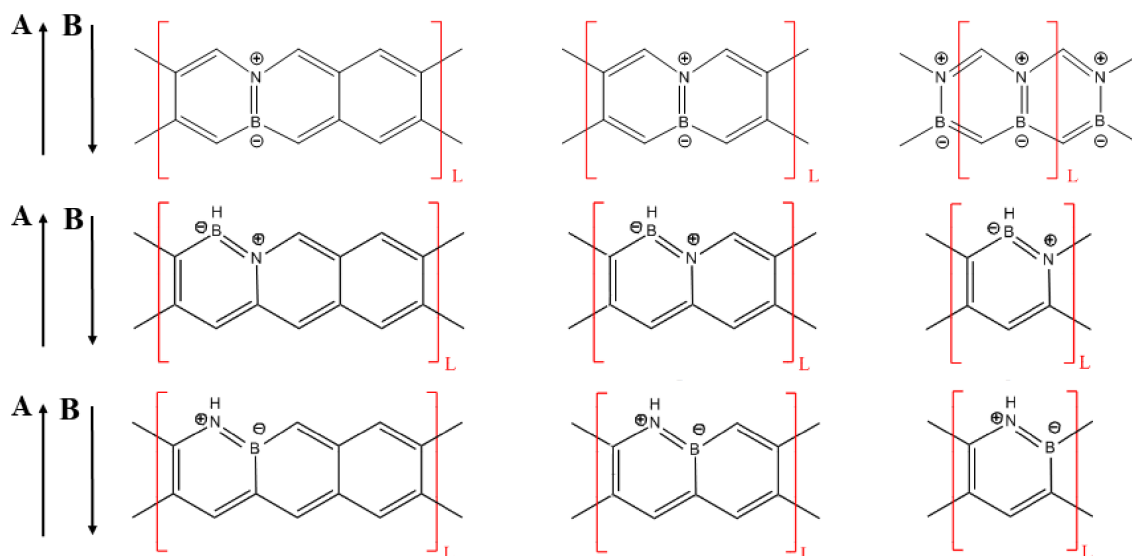


Fig.1. The repeating elementary fragments of the considered NBs and the direction of the constant electric field strength vector (A, B).

References

1. O. B. Tomilin, E. V. Rodionova, E. A. Rodin, Russian Journal of Physical Chemistry A (2020) **94**, 1242.

The evaporation study of 1-Ethyl-3-methylimidazolium chloride

*Semavin K.D.*¹, *Chilingorov N.S.*¹, *Skokan E.V.*¹

kirillsemavin55@gmail.com

¹ Moscow State University, Chemistry Department, Moscow, 119991, Moscow, Russia

The ionic liquids (ILs) have a great potential for their use in various fields of chemistry. These compounds were applied as lubricants, solvent and heat-transfer agents [1-3]. Moreover, ILs based on the imidazolium cation with chlorine were applied such as solvents of cellulose for synthesis a carbon nanostructure materials [4]. Also, some authors reported about using these ILs as a electrolyte in supercapacitors based on carbon nanostructure [5]. So, synergy of ILs and carbon nanostructures is hot topic in nowadays.

Unfortunately, not all thermodynamic parameters of ILs are determined. For example, evaporation data of 1-ethyl-3-methylimidazolium chloride is not imperfect. The data of vapor pressure of 1-ethyl-3-methylimidazolium chloride is not available in the literature. In this study we have investigated this compound and have determined the vapor pressure by Knudsen effusion mass spectrometry. In this temperature the sample are decomposed, but the calculation of vapor pressure are possible. We have refined the data of thermal stability of this liquid; vapor pressure was determined under decomposition conditions for the first time.

References

1. Kamimuraa, T. Kubob, I. Minamib and S. Mori, *J. Tribol int.* (2007) 40, 620.
2. Zhang, Z. Xue, Y. Xue, Z. Huang, Z. Li and J. Hao, *J. RSC Adv.* (2016) 6, 6358.
3. Wang, Z. Wu, Y. Zhang, B. Li and B. Sundén, *J. Appl. Therm. Eng.* (2018) 142, 457.
4. Mugadza, P. Ndungu, A. Stark and V. Nyamori, *J. Mater. Chem. Phys.* (2019), 234, 201.
5. Bettini, M. Galluzzi, A. Podestà P. Milani and P. Piseri, *J. Carbon.* (2013), 59, 212.

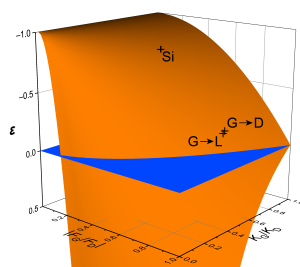
Deductive molecular mechanics of carbon materials

*Tchougreff A.L.*¹

tchougreff@phyche.ac.ru

¹ A.N. Frumkin Institute of Physical Chemistry and Electrochemistry RAS, Moscow, Russia

Recently we propose a new efficient and chemically transparent model for describing covalent materials dubbed as deductive molecular mechanics (DMM) [1-4]. It has been widely numerically tested until it has been realized that it allows not only for numerical, but also for analytical treatment of simple molecules [5] and not that simple crystals [6]. In the present communication we present our recent results concerning relative stability of diamond and graphite as readdressed from a the DMM perspective [7-9]. Unlike most theoretical studies done numerically, we use an analytic model to get an insight into fundamental reasons for quasi-degeneracy of these allotropes with very different bonding patterns. We derive the relative energies of the allotropes and prove several general statements. Our analysis yields a quasi-degenerate electronic ground state for graphite and diamond at 0 K. Numerical estimates based on it are in a astonishingly good agreement with experimental data and recent results of numeric modeling, although obtained with a drastically smaller numerical effort. An extension of the proposed treatment to the allotropes of silicon proves to be very successful as well. Following similar lines we extended the proposed treatment to the four-coordinated allotropes of carbon and developed the software package ADAMAS which is capable to calculate energies of allotropes and their elastic properties (elasticity modules). Similarly, to the case of diamond and graphene some general statements could be *proven* within the DMM setting. Specifically it is shown that among the four coordinated allotropes the *cubic diamond* structure represents the true minimum. In the cases of allotropes which contain some C-C bonds stronger than those in diamond the energy gain is compensated by the mandatory presence of weaker bonds in the same allotrope finally leading to the overall increase of the energy relative to the diamond.



General view of the relative energetics of the diamond and graphene allotropes of carbon in which the orange surface shows the ratio of the stabilization energies of the two allotropes relative to the degeneracy point shifted by unity: $\varepsilon = (F_G^2/K_G):(F_D^2/K_D) - 1$. The axes are the ratios $|F_G/F_D|$ and K_G/K_D , the relative forces and rigidities for diamond and graphene at the degeneracy point.

References

1. Tokmachev A.M., Tchougréeff A.L. J. Comp. Chem. 2005. V. 26. P. 491-505.
2. Tchougréeff A.L. J. Mol. Struct. THEOCHEM. 2003. V. 630. P. 243-263.
3. Tokmachev A.M., Tchougréeff A.L. Int. J. Quant. Chem. 2002. V. 88. P. 403-413;
4. Tchougréeff A.L., Tokmachev A.M. Int. J. Quant. Chem. 2004. V. 96. P. 175-184.
5. Tchougréeff A. L., Dronskowski R. Mol. Phys. 2016. V. 114. P. 1423-1444.
6. A.L. Tchougréeff. Theor. Chem. Acc., 137 (2018) 138
7. Popov I.V., Görne A.L., Tchougréeff A.L., Dronskowski R. Phys. Chem. Chem. Phys. 2019. V. 21. P. 10961-10969.
8. Popov I. V., Slavin V. V., Tchougréeff A.L., Dronskowski R. *ibid.* 2019. V. 21. P. 18138-18148.
9. И.В. Попов, А.Л. Чугреев, Р. Дронсковски. Физ. Низк. Темп. 46 (2020) № 7, 781-798.

Chiral carbon dots synthesized via room temperature surface modification and one-pot carbonization

Das A.¹, Arefina I.A.¹, Danilov D.V.², Koroleva A.V.², Zhizhin E.V.², Parfenov P.S.¹, Kuznetsova V.A.¹, Ismagilov A.O.³, Litvin A.P.^{3,1}, Fedorov A.V.¹, Ushakova E.V.¹, Rogach A.L.^{4,5}

el.ushakova@gmail.com

¹ Center of Information Optical Technologies, ITMO University, Saint Petersburg, Russia

² Saint Petersburg State University, Saint Petersburg, Russia

³ Laboratory of Quantum Processes and Measurements, ITMO University, Saint Petersburg, Russia

⁴ Department of Materials Science and Engineering, and Centre for Functional Photonics (CFP), City University of Hong Kong, Kowloon, Hong Kong SAR, P. R. China

⁵ Shenzhen Research Institute, City University of Hong Kong, Shenzhen, P. R. China

Since the chirality is one of the phenomena often occurring in nature, optically active chiral compounds are important for applications in the fields of biology, pharmacology, and medicine. With this in mind, chiral carbon dots (CDs), which are eco-friendly and easy-to-obtain light-emissive nanoparticles, offer great potential for sensing, bioimaging, enantioselective synthesis, and development of emitters of circularly polarized light. Herein, chiral CDs have been produced via two synthetic approaches using a chiral amino acid precursor L/D-cysteine: (i) surface modification treatment of achiral CDs at room temperature and (ii) one-pot carbonization in the presence of chiral precursor (Figure 1). The chiral signal in the absorption spectra of synthesized CDs originates not only from the chiral precursor but from the optical transitions attributed to the core and surface states of CDs. The use of chiral amino acid molecules in the CD synthesis through carbonization results in a substantial (up to 8 times) increase in their emission quantum yield. Moreover, the synthesized CDs show two-photon absorption which is an attractive feature for their potential bioimaging and sensing applications [1].

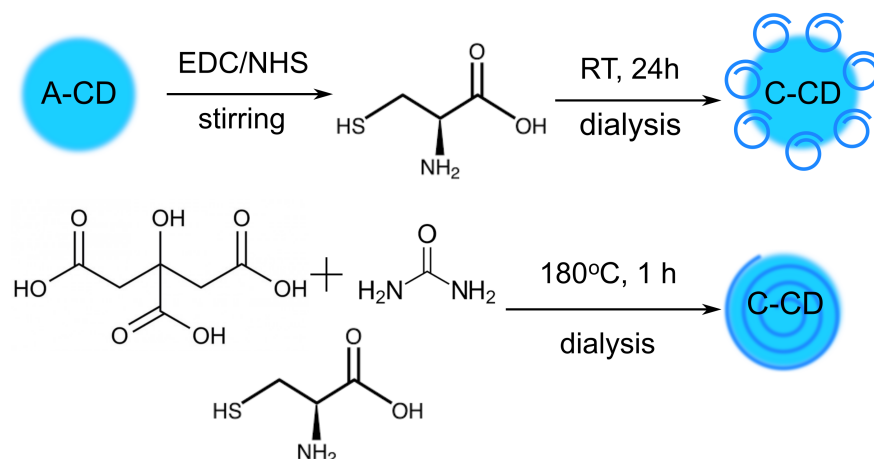


Fig.1. Synthesis of chiral carbon dots (C-CD) by: surface modification treatment of achiral CDs (A-CD) via EDC/NHS bonding with L/D-cysteine at room temperature (upper panel), one-pot carbonization of citric acid, urea, and L/D-cysteine (lower panel)

References

1. A. Das, I.A. Arefina, D.V. Danilov, A.V. Koroleva, E.V. Zhizhin, P.S. Parfenov, V.A. Kuznetsova, A.O. Ismagilov, A.P. Litvin, A.V. Fedorov, E.V. Ushakova, A.L. Rogach, *Nanoscale* (2021), DOI: 10.1039/D1NR01693H

Distribution of nitrogen-vacancy NV⁻ centers in cubic diamond crystals revealed by ODMR and PL tomography

Yakovleva V. V.¹, Breev I. D.¹, Titkov S. V.², Anisimov A. N.¹, Baranov P. G.¹

valya_yakovleva_1999@mail.ru

¹ Ioffe Institute, Saint-Petersburg, Russia

² Institute of Geology of Ore Deposits, Petrography, Mineralogy, and Geochemistry, Moscow, Russia

Nitrogen-vacancy NV⁻ centers, which are of considerable interest for quantum electronics, are usually artificially produced in the diamond structure by irradiation and subsequent annealing. In this work, these centers were revealed in natural diamonds of cubic habit (type IaA + Ib according to physical classification) from an industrial placer deposit of the Anabar River (NE Siberian platform) using the method of optically detected magnetic resonance (ODMR).

The NV⁻ center is one of the most studied defects in the structure of diamonds using modern spectroscopic methods. Great interest in this center is associated with the possibility of controlling its spin states, which makes it possible to use it in spintronics to create quantum sensors for magnetic, electric, and temperature fields, and as qubits for quantum computers. The NV⁻ center in the diamond structure is composed by a nitrogen atom replacing carbon and a vacancy located in the neighbour structural position (center W15 according to the notation adopted in the EPR spectroscopy of diamonds). It has a negative charge. The center manifests itself in the photoluminescence (PL) spectra (zero-phonon line at 637 nm, phonon band at 690 nm) and in absorption spectra in the visible region. Irradiation with light with a wavelength of 530-570 nm causes an optically induced alignment of spin levels with $S = 1$ with a predominant population of the sublevel with $M_s = 0$, which makes it possible to study it using the method of optically detected magnetic resonance (ODMR) at room temperature.

The studies were carried out using an ODMR spectrometer, equipped with a confocal optical scheme and piezoscanner. This spectrometer allows the ODMR and PL signals to be registered in the region of $\sim 1 \mu\text{m}^3$ at room temperature and the distribution of the PL and ODMR centers to be studied in the sample volume with a submicron spatial resolution. In the present study, PL was excited by a laser with a wavelength of 532 nm and was recorded near the zero-phonon line at 637 nm and the phonon sidebands of the NV⁻ centers. We studied plane-parallel plates manufactured from diamond crystals weighing 0.92-1.38 ct. The ODMR and PL spectra were recorded along a profile passing through the center of the crystal. The ODMR and PL signals were scanned along this profile in the central and peripheral regions of the crystal, and the distribution maps of the NV⁻ centers were obtained.

Localization of the NV⁻ centers in the dislocations slip planes $\{111\}$, separated by distances of about 5 μm , was established by means of scanning the ODMR and PL signals with a submicron resolution. In various crystals, one or two intersecting systems of such slip planes have been revealed. The largest amounts of these defects were found in the peripheral zones of crystals containing increased amounts of single isomorphous nitrogen atoms in the structure. The data obtained indicate the formation of the NV⁻ centers in natural diamonds under post-crystallization plastic deformation, i.e., by a mechanism that differs from the widely used method of their artificial production.

This work was supported by the Russian Foundation for Basic Research Project No.19-52-12058.

Novel methods of carbon nanotubes suspensions stabilizing

*Gerasimova A.V.*¹, *Dyachkova T.P.*¹, *Memetov N.R.*¹, *Chapaksov N.A.*¹, *Melezhik A.V.*¹, *Smirnova A.I.*², *Parfenov A.S.*², *Usol'tseva N.V.*²

dyachkova_tp@mail.ru

¹ Tambov State Technical University, Tambov, Russia

² Ivanovo State University, Nanomaterials Research Institute, Ivanovo, Russia

Due to their unique properties, carbon nanotubes (CNTs) can be used in polymer composites with improved characteristics. In order for the effect of the use of CNTs to be maximum, their uniform distribution in the polymer matrix is necessary. This problem requires a solution, because CNTs are prone to microscale aggregation due to van der Waals forces. One of the possible ways is to use masterbatches based on stable CNT suspensions in liquid media. For stabilization, carbon nanotubes are subjected to covalent functionalization or non-covalent modification with surfactants. The advantages of the second method are the absence of aggressive chemical action and the preservation of the π -electron structure of nanotubes. Numerous surfactants currently used make it possible to stabilize CNT suspensions with a low concentration (up to 2.5 g/L).

It was shown that phenol-formaldehyde resin (PFR) and aminocumulene (AK) [1] can be used as stabilizers of CNTs in aqueous media. Phenol-formaldehyde resin exhibits its effect in weakly basic media and makes it possible to obtain stable suspensions containing 11 g/L of CNTs. Aminocumulene is a mixture of oligomeric compounds with $=C-NH_2$ groups. It stabilizes suspensions in acetic acid solutions containing up to 20 g/L of CNTs.

It has been shown by the method of dynamic light scattering that the effective sizes of particles of the dispersed phase in stable suspensions with the use of AK and PFR are noticeably reduced. The methods of XRD, FTIR, Raman mapping and thermogravimetric analysis have been used to prove the interaction of oxidized CNTs with AA and PPS through the formation of hydrogen and covalent bonds.

The obtained stable suspensions of carbon nanotubes retain their aggregate stability for at least one month. The efficiency of using CNTs modified with aminocumulene and phenol-formaldehyde resin for introduction into various polymer matrices in order to obtain composites with high mechanical strength and electrophysical properties is shown.

This work was supported by the Russian Foundation for Basic Research (grant no. 18-29-19150_mk).

References

1. A.V. Gerasimova, O.V. Alekhina, L. García-Cruz, Jesús Iniesta, A.V. Melezhik, A.G. Tkachev, C - the journal of carbon research (2019) **54**, 1.

Thermogravimetry study of selected surfactants annealing from single-wall carbon nanotube films

Gnedova E. A.¹, Tomskaya A. E.^{1,2}, Arutyunyan N. R.^{3,2}, Obraztsova E. D.^{1,2}

gnedova.ea@phystech.edu

¹ Moscow Institute of Physics and Technology (National Research University), Moscow, Russia.

² Prokhorov General Physics Institute of the Russian Academy of Sciences, Moscow, Russia.

³ Moscow Institute of Physics and Technology (National Research University), Moscow, Russia

Dehydration of single-wall carbon nanotube (SWNT) aqueous suspension is one of the efficient ways to form homogeneous SWNT film. Various surfactants are commonly used for making a stable suspension of SWNTs in water. They permit to separate, to purify, or to isolate various fractions of SWNTs. However, for the further applications it is necessary to remove the surfactants, since the electrical and optical properties of SWNT films may be affected [1]. Treatment with organic solvents [2] and evaporation by vacuum annealing [3] have been proposed as methods for removing surfactants.

The aim of this work is to study the thermal stability of the most commonly used surfactants (sodium dodecyl sulfate (SDS), sodium dodecylbenzenesulfonate (SDBS), sodium cholate (SC), sodium taurodeoxycholate hydrate (TDOC), sodium deoxycholate (DOC), Pluronic F127), in air and Ar atmosphere.

Thermogravimetry studies have revealed that some surfactants couldn't be removed completely by annealing, their residual mass at 700 °C was in the range 9-60% (Table. 1). However, F127 was successfully annealed at air atmosphere ($T_{\text{onset}} = 202$ °C), which was lower than the oxidation temperature of the SWCNTs. This means that the hydrocarbon surfactant F127 can be oxidized completely and removed from the SWNT films by heating without damage of nanotubes.

Table 1. Temperatures of annealing and residual masses (700 °C) in Ar and air atmosphere, the heating rate is 10 K/min (Ar) and 5 K/min (air)

surfactants and SWNTs	Phase transition T in Ar, °C	Residual mass at 700 °C in the Ar, %	Phase transition T in air, °C	Residual mass at 700 °C in the air, %
SDS	228	38,2	207	23,1
DOC	416	26,9	305	19,9
SDBS	143	38,2	161	62,4
CMC	262	38,6	262	24,9
SC	394	22,2	310	9,1
TDOC	379	22,4	335	18,1
F127	366	2,3	202	0
TuBall	no decomposition	100	571	20,9
CoMoCAT (6.5)	weak decomposition	94	435	5,9

Acknowledgements The research was supported by Russian Science Foundation (project N 20-42-08004).

References

1. J. Yun, J. M. Kim, H. Ra, S. J. Byun, H. Kim, G. S. Park, S. H. Park and S. W. Rhee, *Organic Electronics* (2013) **14**, 2962.
2. E. Rossi, K. J. Soule, E. Cleveland, S. W. Schmucker, C. D. Cress, N. D. Cox, A. Merrill and B. J. Landi, *Journal Of Colloid And Interface Science* (2017) **495**, 140.
3. A. Kane, A. C. Ford, A. Nissen, K. L. Krafcik and F. Leonard, *Acs Nano*(2014) **8**, 2477.

Bend sensor based on biocompatible composite nanomaterials

*Ichkitidze L.*¹, *Gerasimenko A.Y.*², *Telyshev D.V.*², *Kitsyuk E.P.*³

ichkitidze@bms.zone

¹ Institute for Bionic Technologies and Engineering of I.M. Sechenov First Moscow State Medical University, Moscow, Russia

² I.M. Sechenov First Moscow State Medical University, Moscow, Russia

³ Scientific-Manufacturing Complex "Technological Centre", Zelenograd, Moscow, Russia

Composite nanomaterials, which include carbon nanotubes (CNTs), upon deformation acquire the properties of a tensoresistive effect. In the present work, changes in the resistance ($R/R-1$) from the bending angle θ of a film of a biocompatible composite nanomaterial are considered. Here R is resistance in the absence of deformation, R is resistance in the presence of deformation.

Films with dimensions of $0.05-0.5 \mu\text{m} \times 2 \text{ mm} \times 25 \text{ mm}$ made of bovine serum albumin (BSA) or microcrystalline cellulose (MCC) containing multi-walled CNTs (MWCNTs) served as a strain-sensitive element. In this case, layers of paper or textiles (calico) with a thickness of up to $50 \mu\text{m}$ were used as a flexible substrate.

Aqueous dispersions of composite nanomaterials consisted of BSA or MCC matrices and a filler, MWCNT. The components in the composition of the dispersions had the following ratios: 20 wt.% BSA/0.5 wt.% MWCNT; 3 wt.% MCC/0.2 wt.% MWCNT. In tab. 1 shows the typical parameters of nanomaterial films studied as a prototype of a bending strain sensor, where d is the film thickness, ρ is the film specific resistivity, $S_\theta = (R/R-1) / \Delta\theta$ - is the bending sensitivity, $\Delta\theta = \pm 90^\circ$ - is bending angle changes.

Tab. 1 Typical approximate parameters of a prototype strain sensor

Composite nanomaterials	d , μm	ρ , $\text{m}\Omega \cdot \text{m}$	S_θ , $\%/\text{deg}$
BSA/WCNT	0.5	60	0.2
	0.2	80	0.5
MCC/MWCNT	0.4	20	1.3
	0.1	40	1.7

From Tab. 1, a correlation follows: high bending strain sensitivities are realized on thinner films with relatively high resistivity. Note that the obtained values of the bending sensitivities $S_\theta \sim (1.3 \div 1.7) \%/ \text{deg}$ are high and acceptable for medical applications.

We believe that it is possible to select the required parameters of the strain sensor, taking into account the characteristics of the skin of a particular person. Also, the considered composite nanomaterials, due to their high degree of biocompatibility, electrical conductivity and the possibility of applying to the skin surface, are promising for the rapidly developing areas of elastomers and "Skin electronics".

This work is supported by the Ministry of Science and Higher Education of the Russian Federation (project No. 075-03-2020-216 of December 27, 2019).

Electronic structure of a metal-decorated carbon nanotube (8,0): first-principles modelling

*Ivanov P.D.*¹, *Sozykin S.A.*¹

ivanov-pavel98@mail.ru

¹ South Ural State University, Chelyabinsk, Russia

The control over the conductivity of single-walled carbon nanotubes (SWCNTs) could lead to the creation of novel nanoelectronic devices based on SWCNTs. The nanotubes' electronic properties can be changed by heteroatoms decoration [1]. In this study, we modelled the adsorption of six different metal atoms (Al, Ni, Ti, Cr, Ru, Pt) on the SWNT surface.

Calculations were performed using density functional theory with the generalized gradient approximation (Becke-Lee-Yang-Parr parameterization) for the exchange-correlation functional. The SIESTA (Spanish Initiative for Electronic Simulations with Thousands of Atoms) and the VASP (Vienna Ab initio Simulation Package) packages were utilized [2, 3]. For structure visualization in SIESTA, we used the GUI4dft [4].

We considered SWCNT (8,0) with a diameter of 6.3 Å. The unit cell contained 96 carbon atoms, which corresponds to the translational length of ~11.4 Å. The values of pristine tube bandgaps were 0.64 and 0.58 eV for the SIESTA and VASP calculations, respectively, which suggests the semiconducting nature of SWCNT (8,0).

Metal atoms were placed in the following starting positions: above a centre of a carbon hexagon, above a carbon atom, and above a centre of a C-C bond. The initial geometries were optimized in the SIESTA package using the conjugate gradient method. The resulting configurations with the lowest total energy were further optimized in the VASP package.

The calculated adsorption energies are in good agreement with the available data. The charge transfer between metal atoms and the tube indicates the interaction of the metal atom electron shell with the nearest carbon atoms.

The calculations of the decorated SWCNT (8,0) bandgap and density of states showed a decrease in the bandgap for all considered metal adatoms. In some cases, the nanotube remained semiconducting with slightly smaller or noticeably reduced bandgap (Ni, Pt, Ru). However, for most metals we observed the intersection of the Fermi level and the conduction band, therefore, the conducting properties of metal-decorated nanotubes could be expected.

Acknowledgments: The reported study was funded by RFBR, project number 20-42-740002.

References

1. Cho, C. Kim, H. Moon, Y. Choi, S. Park, C.-K. Lee, S. Han, *Nano Lett.* (2008), 81
2. García, N. Papior, A. Akhtar, E. Artacho, V. Blum, E. Bosoni, P. Brandimarte, M. Brandbyge, J.I. Cerdá, F. Corsetti, R. Cuadrado, V. Dikan, J. Ferrer, J. Gale, P. García-Fernández, V.M. García-Suárez, S. García, G. Huhs, S. Illera, R. Korytár, P. Koval, I. Lebedeva, L. Lin, P. López-Tarifa, S.G. Mayo, S. Mohr, P. Ordejón, A. Postnikov, Y. Pouillon, M. Pruneda, R. Robles, D. Sánchez-Portal, J.M. Soler, R. Ullah, V. Yu, Z. Wen, and J. Junquera, *J. Chem. Phys.* (2020) 152, 204108.
3. Kresse, and J. Furthmuller, *Phys. Rev. B* (1996) 54, 11169.
4. A. Sozykin, *Comput. Phys. Commun.* (2021) 262, 107843.

Single-walled carbon nanotube additive for improvement of lithium-ion storage performance of nanostructured MoS₂

*Kotsun A.A.*¹, *Stolyarova S.G.*¹, *Okotrub A.V.*¹, *Bulusheva L.G.*¹

kotsun15@gmail.com

¹ Nikolaev Institute of Inorganic Chemistry SB RAS, Novosibirsk, Russia

Currently, the anode material of commercial lithium-ion batteries (LIB) is graphite. Its theoretical capacity of 372 mAh g⁻¹ and power density do not meet the requirements of modern devices. Disulfides of transition metals (MoS₂, WS₂, ZrS₂, and SnS₂) have layered structures similar to graphite. An electrochemical accumulation of lithium ions in these compounds occurs via intercalation and conversion reactions.

Molybdenum disulfide (MoS₂) is a promising anode material for LIB due to the following reasons: large interlayer distance (0.65 nm) and high theoretical capacity of 669 mAh g⁻¹, which is approximately 2 times larger than that of graphite [1]. However, electrodes made of bulk MoS₂ degrade during the prolonged cycling because of volumetric expansion of the material when lithium ions are embedded and its low electrical conductivity. To eliminate these disadvantages conductive carbon materials additives are used [2]. In this work, we use single-walled carbon nanotubes (SWCNTs from the OCSiAl company) to increase the conductivity and stability of our material during repetitive charge/discharge of LIB.

Nanostructured hexagonal MoS₂ materials were obtained by the rapid decomposition of the ammonium thiomolybdate aerogel in an inert atmosphere at temperatures from 400 to 700°C. The structure and composition of the materials were studied by electron microscopy, X-ray diffraction, Raman spectroscopy, and elemental CHNS analysis. An aqueous suspension containing SWCNTs (0.2 wt%) and PVDF (2 wt%) was mixed with MoS₂ and the was slurry applied to a copper foil. Coin-type cells with lithium metal as a counter electrode were collected with the prepared electrodes and tested in a galvanostatic regime in a potential range of 0.1–2.5 V. Electrochemical properties of the materials were investigated by cyclic voltammetry and electrochemical impedance spectroscopy. The composite MoS₂/SWCNT electrodes were characterized by improved stability and an increased specific capacity at high current densities as compared to the electrodes composed without the SWCNT additive. The electrode with the MoS₂ synthesized at 500°C showed the best performance among the studied samples. It was able to deliver 1070 and 990 mAh⁻¹ at a current density of 1 and 2 Ag⁻¹, respectively

This work was supported by the Russian Scientific Foundation (21-53-12021).

References

1. Stephenson T. et al. Lithium ion battery applications of molybdenum disulfide (MoS₂) nanocomposites //Energy & Environmental Science. – 2014. – T. 7. – №. 1. – C. 209-231.
2. Zhang R. et al. How does Molybdenum Disulfide Store Charge: A Minireview //ChemSusChem. – 2020.

Improving the frost resistance of concrete reinforced with carbon nanotubes

Kulakov R.A.¹, Goshev A.A.¹

kulakovroman37@yandex.ru

¹ Northern Arctic Federal University (NARFU), Arkhangelsk, Russia

Concrete is one of the most popular building materials in the world. It consists of sand, cement, water and various additives. Recently, carbon nanotubes (CNTs) have been used as these additives [1-3]. The addition of CNTs to cement composites increases their strength. Thus, in [1], the influence of CNT on the strength properties of cement composites is considered. And in the article [2], the influence of CNT in the composition of a complex additive on the phase composition and hydration kinetics of cement stone is considered.

In this work, the authors investigated the effect of adding CNTs with a concentration of 0.1% on the strength properties of concrete. For this, several batches of composites were prepared. The first consisted of cement, sand and water. The second is made of cement, sand, water and CNTs with a concentration of 0.1% [3]. Uniform distribution of CNTs over the sample was achieved by mixing in a ball mill. After the samples have hardened (28 days). Some of the composites were placed in distilled and salt water. After three days, the sample was placed in a freezer.

As a result, an increase in moisture resistance and frost resistance of the obtained composite nanomaterial was revealed.

Thus, the strength of composites with tubes in comparison with pure samples increased: - for the first series of samples by 29%, - for the second series of samples by 37%, - for the third series of samples by 72 %.

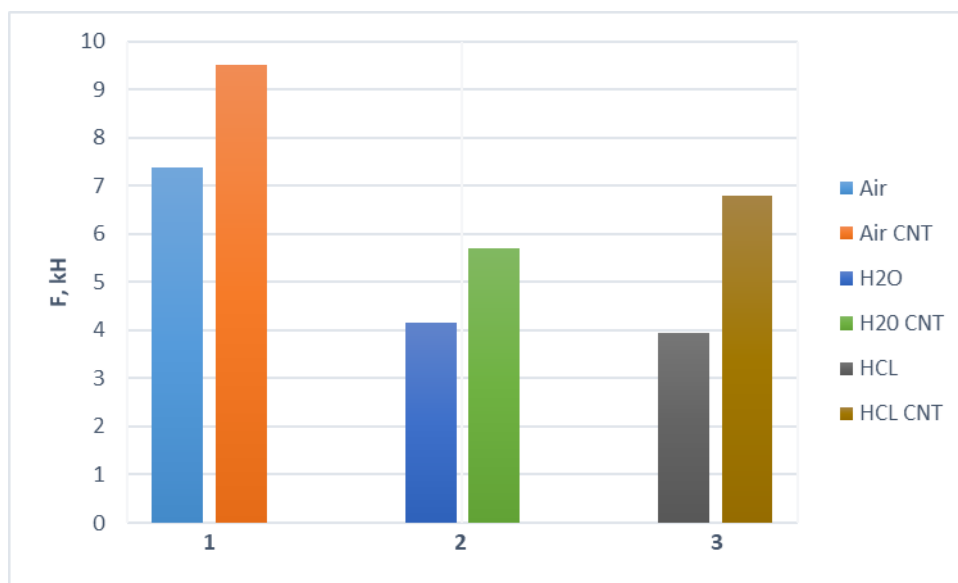


Fig.1. Increasing the strength properties of composites with CNT additives. 1- A series of samples that were in the air. 2- A series of samples that were 3 days in distilled water and 3 days at a temperature of -14 °C. 3- A series of samples that were 3 days in salt water and 3 days at a temperature of -14 °C

References

1. Makeeva T., Khavkin A., Georesursy (2007). № 1. 55-57.
2. Ibragimov R., Kiyamova L., Herald of technological university (2015). **18**. №7. 211-213.
3. Kim V., Goshev A., XX Anniversary International Conference on Science and Technology Russia-Korea-CIS. NSTU Publisher. (2020). 262. 96.

Current-voltage characteristics of a carbon nanotube (6,6): first principle calculations

*Latypov R.M.*¹, *Sozykin S.A.*¹

ruslan.xxx33@yandex.ru

¹ South Ural State University, Chelyabinsk, Russia

Carbon nanotubes are thermally and mechanically stable while carrying high current densities [1]. So, it's desirable to replace metal lines by CNT in future electronic devices [2].

Current-voltage characteristics of ideal single wall carbon nanotubes (6,6) (SWNT) have been calculated using the software package SIESTA [3], based on the density functional theory and non equilibrium Green's function method with double- ζ (DZ) basis sets [4]. Optimization of the carbon nanotube's geometry and the local density of states (LDOS) calculations were performed based on the local density approximation (LDA) and the generalized gradient approximation (GGA) with Ceperley-Alder (CA) and Becke-Lee-Yang-Parr (BLYP) pseudoatomic potentials, respectively. GUI4dft is used to analyze calculation's output [5].

Relaxed SWNT's geometries, consisting of 72 and 96 atoms, are used to construct simulation models with the central region through which current is driven in response to a voltage applied to the left and the right regions which are treated as electrodes. The structure is oriented in such a way, that the tube is parallel to the z direction. There are 8 models in total, which're called "72-72", "72-96", "96-72", "96-96", where the first number is the quantity of atoms in both electrode regions, the second one is the number of atoms in the central region, for LDA and GGA, respectively.

SWNT with (6,6) chiral indices is an armchair nanotube with the resistance 6450 ohm (theoretical calculations) [6]. The calculated values correspond to the theoretical prediction to a less 0.5 per cent of error. The most stable model is "72-96 LDA" with 0.41 per cent of error.

Next, the central region of "72-96 LDA" is rotated around the z axis to calculate angular dependence of SWNT's resistance. Obtained simulation models are called, for example, "72-96-2", where the third number is the angle (degree) of the central region rotation relatively to the electrode regions. Obtained values show, an exponential angular dependence of SWNT's resistance in range from 0 to 6 degrees exists.

LDOS was obtained for the "rotated" models in range from 0 to 18 degrees. It shows an electron's transition to junctions of the central and the electrode regions at high angles.

Acknowledgements: the reported study was funded by RFBR, project number 20-42-740002.

References

1. Q. Wei, R. Vajtai and P. M. Ajayan. *Appl. Phys. Lett.* (2001) **79(8)**, 1172.
2. A. Naeemi and J. D. Meindl. *Rev. Mater. Res.* (2009) **39**, 255.
3. S. M. José, E. Artacho, G. D. Julian, G. Alberto, J. Javier, O. Pablo and S. J. Daniel. *Phys.: Condens. Matter* (2002) **14**, 2745.
4. N. Papior, N. Lorente, T. Frederiksen, A. García, and M. Brandbyge. *Computer Physics Communications* (2017) **212**, 8.
5. A. Sozykin. *Computer Physics Communications* (2021) **262**, 107843.
6. R. Saito, G. Dresselhaus, and M.S. Dresselhaus. *Physical properties of carbon nanotubes*, Imperial College Press London, 2001.

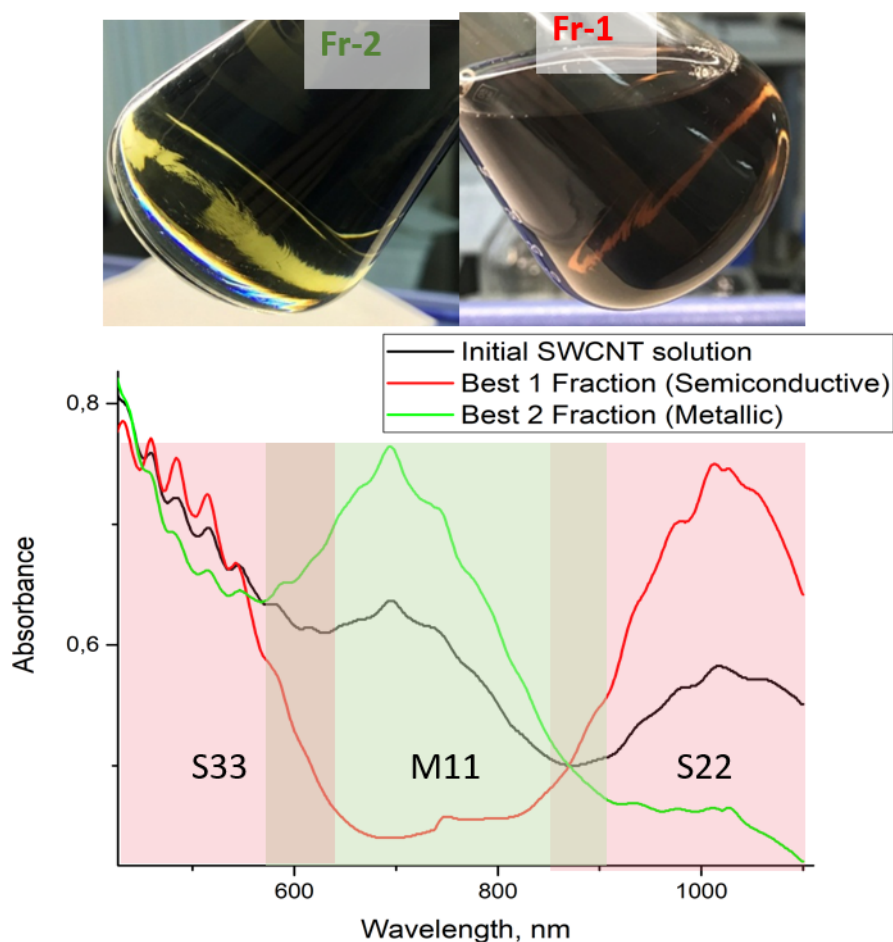
Simple and cost-efficient method for sorting single-wall carbon nanotubes with modified cotton.

Khamidullin T.L.¹, Dimiev A.M.¹, Galyaltdinov S.F.¹, Brusko V.V.¹

TiLHamidullin@kpfu.ru

¹ Kazan Federal University, Kazan, Russian Federation

We developed a new cheap and efficient method for separating single wall carbon nanotubes (SWCNT). The method is applicable for separating the most promising SWCNTs produced by OCSiAl under the Tuball brand. The presented method is based on the interaction of a SWCNT surfactant solution with chemically modified cotton wool. The modification involves partial nitration. As the result of the separation, we obtained 2 fractions, significantly enriched in metallic SWCNTs and semiconducting ones, respectively. The main advantages of the method are a high degree of separation, cost efficiency of the process, and the possibility for industrial scale-up. The as-separated SWCNTs are fully characterized by UV-Vis spectroscopy, PL spectroscopy, Raman spectroscopy, and HRTEM.



Influence of defectiveness of carbon nanotubes on their piezoelectric response

Osotova O.I.¹, Il'ina M.V.¹, Il'in O.I.¹

osotova@sfnu.ru

¹ Southern Federal University, Institute of Nanotechnologies, Electronics and Electronic Equipment Engineering, Taganrog, Russia

Previous studies have shown that the vertically aligned carbon nanotubes (CNTs) exhibit memristor effect due to the deformation process and occurrence of the internal electric field resulting from anomalous piezoelectric properties of nanotubes [1]. At the moment, an urgent task is to study the piezoelectric properties of CNTs and their influence on the memristor effect. The aim of this work is to study the influence of the defectiveness of CNTs on their piezoelectric response and memristor effect.

As the experimental samples we used two arrays of vertically aligned CNTs grown by plasma-enhanced chemical vapor deposition on a TiN sublayer. The thickness of the catalytic nickel layer was 5 nm, the growth temperature was 615 °C for the first array. For the second array, the thickness was 20 nm and the temperature was 660 °C. The choice of these growth parameters was due to a significant difference in the defectiveness of the grown CNTs. So, for the first sample, the ratio of the intensities of the D- and G- peaks (I_D / I_G) of the Raman spectra was 0.84. For the second array, I_D / I_G was 0.75. Investigations of the magnitude of the piezoelectric response of CNTs were carried out using a previously developed technique based on the method of atomic force microscopy (AFM) [2]. As a piezoelectric response, the current generated by the CNT as a result of the formation of the surface potential during its deformation by the AFM probe was detected. Then the current-voltage characteristics of deformed CNTs were measured (Fig. 1). As a result, it was found that the piezoelectric response of CNTs is 16 and 8 nA for the first and second array, respectively. This dependence is explained by a decrease in the defectiveness of CNTs, which is the main source of the piezoelectric properties of CNTs. The values of the resistance ratios of CNTs in the high- and low-resistance states were 3774 and 2 for the first and second array, respectively. Thus, it was shown that a twofold decrease in the magnitude of the piezoelectric response of CNTs led to a decrease in the memristor effect by more than 1500 times. The results obtained can be used in the development of promising nanopiezotronics elements based on oriented carbon nanotubes.

This work was supported by the Russian Foundation for Basic Research (project No. 20-37-70034).

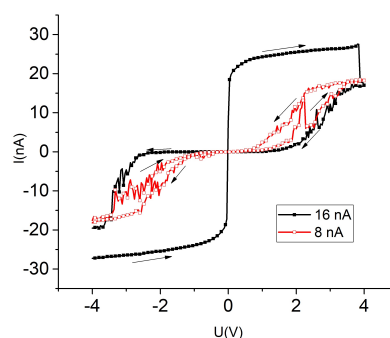


Fig. 1. Current-voltage characteristics of deformed CNTs with different piezoelectric responses

References

1. V. Il'ina, O.I. Il'in, Yu.F. Blinov et al. Carbon (2017) **123**, 514.
2. V. Il'ina, O.I. Il'in, Yu.F. Blinov, A.A. Konshin, B.G. Konoplev, O.A. Ageev Materials (2018) **11**, 638.

Experimental and theoretical study of carbon nanotube growth inside porous anodic alumina membranes

*Ryzhkov I.*¹, *Kharchenko I.*¹, *Mikhлина E.*², *Minakov A.*³, *Guzei D.*³, *Nemtsev I.*⁴, *Volochaev M.*⁴, *Korobko A.*⁵, *Kozlova S.*¹, *Simunin M.*³

rii@icm.krasn.ru

¹ Institute of Computational Modelling SB RAS, Krasnoyarsk, Russia

² Institute of Computational Modelling SB RAS, Krasnoyarsk, Russia

³ Siberian Federal University, Krasnoyarsk, Russia

⁴ Federal Research Center KSC SB RAS, Krasnoyarsk, Russia

⁵ Reshetnev Siberian State University of Science and Technology, Krasnoyarsk, Russia

Porous anodic alumina (PAA) membranes represent a widely used and extensively studied template for production of carbon nanotubes (CNT) [1]. The PAA-CNT membranes possess a number of unique properties, such as controllable nanotube geometry, size- and chemically-based selectivity as well as high water permeability [2,3]. In this work [4], we first propose a combination of gas phase and surface reaction models to quantitatively describe the growth of carbon nanotubes in PAA membranes in a commercial CVD reactor. A complimentary experimental study of CNT formation from ethanol precursor with argon as a carrier gas is performed. A new method for characterizing carbon nanotubes geometry by SEM and TEM image processing of membrane cross-sections is proposed. The simulations show that the carbon growth rate (in nm/min) averaged over the membrane remains constant during the deposition process until the pore diameter becomes relatively small, and rapidly falls to zero after that. The carbon nanotube thickness near the membrane surface is slightly higher than that in the membrane center. The carbon growth rate increases with synthesis temperature and pressure, while it decreases with the argon flow rate. The dependence of carbon growth rate on the ethanol/water flow rate reaches maximum at some intermediate value. These results are supported by the experimental data obtained from SEM/TEM image processing. It is found that the SEM data provide overestimated values of nanotube diameter and thickness in comparison with the TEM data. The obtained results provide new insights into the CNT growth kinetics in nanoporous media, and develop quantitative guidelines for synthesis of CNT-PAA membranes with precisely controlled nanopore geometry. It also validates the combined homogenous / heterogeneous reaction model by comparison with carbon deposition kinetics on a nanometer scale.

This work is supported by the Russian Foundation for Basic Research, Project 18-29-19078. The physicochemical analysis of materials was carried out in Krasnoyarsk Regional Center of Research Equipment of Federal Research Center 'Krasnoyarsk Science Center SB RAS'.

References

1. W. Lee, S.J. Park. Porous Anodic Aluminum Oxide: Anodization and Templated Synthesis of Functional Nanostructures. *Chem. Rev.* 114 (2014), 7487-7556.
2. A.O. Rashed, A. Merenda, T. Kondo, M. Lima, J. Razal, L. Kong, C. Huynh, L.F. Dumeé. Carbon nanotube membranes - Strategies and challenges towards scalable manufacturing and practical separation applications. *Sep. Purif. Techn.* 257 (2021) 117929.
3. R. Das, Md.E. Ali, S.B.A. Hamid, S. Ramakrishna, Z.Z. Chowdhury. Carbon nanotube membranes for water purification: A bright future in water desalination. *Desalination* 336 (2014) 97-109.
4. I.I. Ryzhkov, I.A. Kharchenko, E.V. Mikhлина, A.V. Minakov, D.V. Guzei, I.V. Nemtsev, M.N. Volochaev, A.V. Korobko, M.M. Simunin. Growth of carbon nanotubes inside porous anodic alumina membranes: simulation and experiment. *Int. J. Heat Mass Transfer*, 2021. Accepted, in press.

Electrochemical properties of phosphorus-filled single-walled carbon nanotubes

*Vorfolomeeva A.A.*¹, *Stolyarova S.G.*¹, *Bulusheva L.G.*¹, *Okotrub A.V.*¹

vorfolomeeva@niic.nsc.ru

¹ Nikolaev Institute of Inorganic Chemistry SB RAS, Novosibirsk, Russia

Recently phosphorus was identified as a promising anode material for lithium-ion batteries (LIBs) due to its high theoretical specific capacity of 2596 mAh/g [1]. Moreover, the low cost of commercial phosphorus compared with standard graphite (the main material currently used as the anode in LIBs) makes it attractive as a material for large-scale production of the batteries. However, poor electrical conductivity and large volume expansion of phosphorus when interacting with lithium lead to quick capacity fading during the LIB cycling [2]. Creation of phosphorus-carbon hybrids can help for solving this problem. Single-walled carbon nanotubes (SWCNTs) are one of the promising structures for this purpose. They are conductive, stable chemically and mechanically and have an inner cavity for phosphorus accommodation.

In this work, we successfully filled SWCNTs with phosphorus using the vaporization-condensation technique and H-shaped ampules. By varying synthesis parameters, such as temperature, time, and ratio of the reagents, we achieved about 8 at% of phosphorus filling according to the data of X-ray photoelectron spectroscopy and thermogravimetric analysis. Preliminary sonication of the SWCNTs allowed increasing the filling up to 15 at%. We also confirmed the presence of phosphorus using HR TEM, which showed the formation of chain structures inside the nanotubes.

Obtained samples demonstrated better electrochemical characteristics in LIBs in comparison with those for initial SWCNTs. The best characteristics were obtained for a P@SWCNT sample containing 15 at% of phosphorus. This sample was able to deliver 760 mAh/g at a current density of 0.1 A/g, which is three times larger than the capacity of the initial SWCNTs (245 mAh/g). This effect is associated with the reversible reactions of lithium ions with phosphorus with the formation of various intermediates Li_xP [3] and the intercalation of lithium between the bundled nanotubes.

References

1. S.A. Ansari, Z. Khan, M.O. Ansari, M.H. Cho, Earth-abundant stable elemental semiconductor red phosphorus-based hybrids for environmental remediation and energy storage applications, *RSC Adv.* (2016) **6**, 44616-44629.
2. J. Sun, H.W. Lee, M. Pasta, Y. Sun, W. Liu, Y. Li, H.R. Lee, N. Liu, Y. Cui, Carbothermic reduction synthesis of red phosphorus-filled 3D carbon material as a high-capacity anode for sodium ion batteries, *Energy Storage Mater.* (2016) **4**, 130-136.
3. J. Sangster, A.D. Pelton, H. Okamoto, The Li-P (lithium-phosphorus) system, *J. Phase Equilibria.* (1995) **16**, 92-93.

Ion trapping effect and enhancement of orientational order parameter in nematic liquid crystals dispersed with a dilute amount of carbon nanotube

Singh B.P.¹, Sikarwar S.², Manohar R.¹

rajiv.manohar@gmail.com

¹ Liquid crystal Research Lab, Department of Physics, University of Lucknow

² Department of Physics, Baba Saheb Bhimrao Ambedkar University Lucknow

Abstract: We have demonstrated purification of liquid crystal (LC) with the dispersion of a small amount of carbon nanotube (CNT) in LC by probing dielectric spectroscopy. CNT in LC media acts as ion-catchers; therefore, rotational viscosity decreases and as a result the dynamic response of LC-CNT blend decreases. CNT doping slightly reduce the threshold voltage by suppression of screen effect, reduced splay elastic constant and increased dielectric anisotropy. Long axis of CNT follows the nematic director field due to strong anchoring energy of hybrid system induced by p-p electron stacking between LC and CNT molecules. Which results significant increase in dielectric anisotropy, birefringence and indicating a significant increment in the orientational order parameter of LC-CNT hybrid system. The threshold limit of the CNT concentration has been also optimised after which the system has no longer faster response.

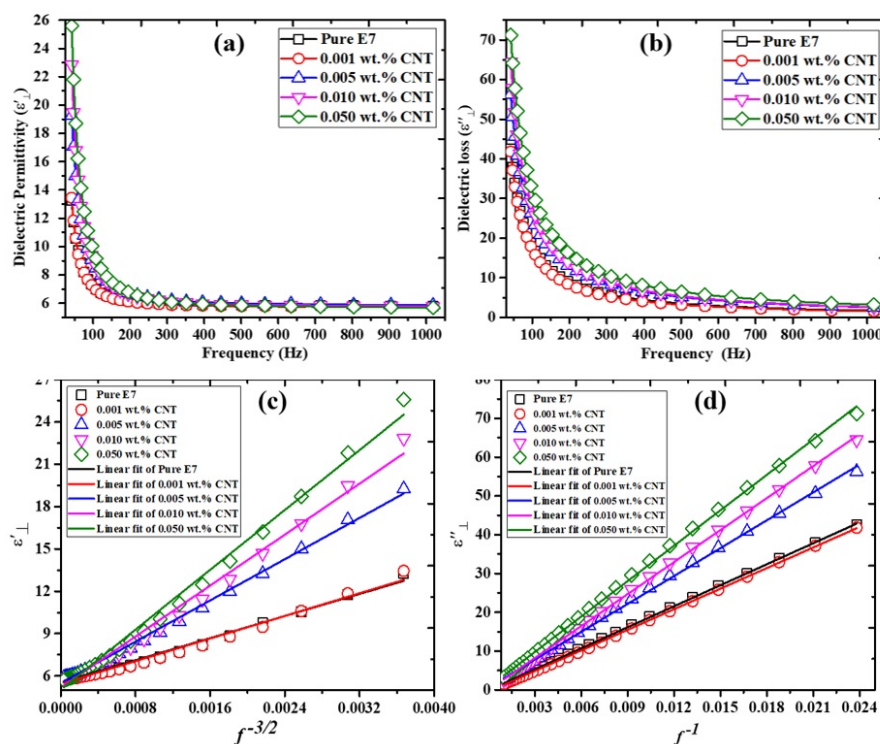


Fig. 1. (a) Real and (b) imaginary parts of the complex dielectric permittivity; (c) and (d) represent the linear fitting of the experimental data of the corresponding dielectric permittivity of the NLC at different doping concentrations of CNTs at room temperature.

References

1. E. Ouskova, O. Buchnev, V. Reshetnyak, Y. Reznikov, H. Kresse, *Liquid Crystals* 30 (2003) 1235.
2. R. Basu, G.S. Iannacchione, *Phys Rev E Stat Nonlin Soft Matter Phys* 80 (2009) 010701.
3. Neeraj, K.K. Raina, *Phase Transitions* 83 (2010) 615.

Strengthening of polymeric materials based on polypropylene by doping with carbon nanotubes.

Elbakyan L.S.¹, Zaporotskova I.V..¹, Vilkeeva D.E.¹

lusniak-e@yandex.ru

¹ Volgograd State University, Universitetsky Ave., 100, 400062 Volgograd, Russia

Today, the problem of obtaining polymeric materials with increased strength properties is extremely urgent. We have investigated the strength properties of polymeric materials based on polypropylene. A method for producing composite materials based on polypropylene doped with carbon nanotubes has been developed. Were obtained prototypes of granular polypropylene with different percentages of carbon nanotubes [1-2]. Experimental studies of the most significant strength characteristics (maximum permissible load) of the obtained composite materials have been carried out. A model of the device was developed that allows the best possible achievement of the desired result. The results obtained make it possible to predict the possibility of obtaining new polymeric materials based on polypropylene by introducing CNTs.

We have performed calculations of the DFT behavior of propylene monomer with the surface of single-walled nanotubes of different types: (6,6), (6,0) and (7,1). To confirm the possibility of creating stable composite space complexes CNT + PP, theoretical calculations of three structural units of propylene with CNTs were also carried out.

The results obtained explain the possibility of creating a composite polymer material based on propylene, reinforced with CNTs.

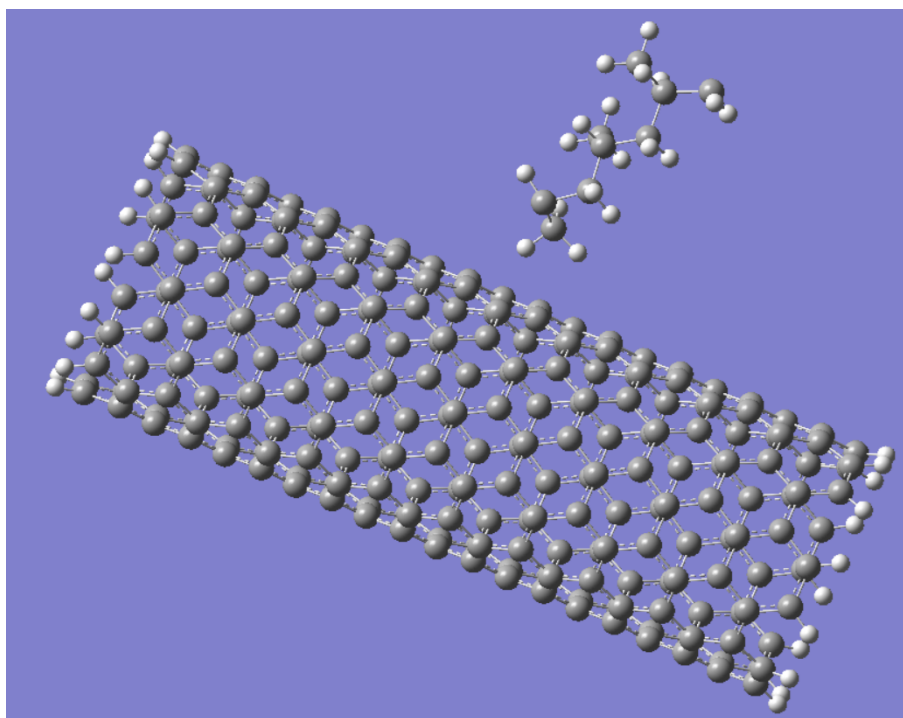


Fig.1. Interaction of three structural units of PP+CNTs.

References

1. Yeletskiy A.V. Sorption properties of carbon nanostructures 2004 Advances in physical Sciences, no. 11, Vol. 174, pp. 1191-1231.
2. Zaporotskova I.V. Carbon and non-carbon nanomaterials and composite structures based on them: structure and electronic properties. - Volgograd: VolSU Publishing House 2009, 490 p.

Simulation of supramolecular microporous structures on the basis of carbon nanotubes and toluene coordinator molecules

*Gaidamavichute V.V.*¹, *Shkolin A.V.*¹, *Fomkin A.A.*¹, *Menshchikov I.E.*¹

mgavik@yandex.ru

¹ A.N. Frumkin Institute of physical chemistry and electrochemistry of Russian academy of sciences (IPCE), Moscow, Russia

A numerical experiment on the formation of supramolecular structures based on arrays of single-walled carbon nanotubes (SWCNTs) and coordinator molecules was carried out in this work, using the method of molecular dynamics (MD), as it allows to observe the development of a model structure in time. A mechanism formation of supramolecular structures based on nanotubes and coordinator molecules has been employed as a working hypothesis for simulation model [1].

An array of three nonchiral SWCNTs with a diameter of ~ 1 nm and a length of ~ 5 nm, coordinated by toluene was chosen as the object of study. The numerical experiment was carried out in a cubic simulation cell with 10 nm edges, with maintained temperature of 298 K. Calculations were performed using the TINKER software package [2] using the OPLS-AA universal potential [3].

At the first stage three parallel SWCNTs were fixed in the central part of the simulation cell. Then, 200 toluene molecules were injected into the cell in random order. After that, the energy minimization algorithm was launched with fixed position of the nanotubes. The calculation was carried out until the value of the total energy of the simulation system stabilized. At the second stage, the condition for fixing the nanotubes was removed, allowing them to move freely along the simulation cell together with the toluene molecules. At this stage SWCNTs formed a supramolecular structure with coordinating molecules, which moved along the simulation cell. At the third stage, toluene molecules were removed from the simulation cell in small portions. Selection of molecules for removing was carried out one by one in a random manner based on the Monte Carlo method.

As a result of simulation procedure, it was found that the toluene molecules "move apart" SWCNTs and orient them parallel to each other, creating triangular-type array. The gradual removal of coordinator molecules makes it possible to preserve the coordination of the nanotubes and create porosity in the space between them. The supramolecular structure occurs to be stable even, when a small number of toluene molecules (up to 6) remain in the simulation cell. At the same time coordinator molecules are distributed between SWCNTs closer to the center of the newly formed supramolecular structure.

The authors are grateful to the developers of the Tinker software: "A Modular Software Package for Molecular Design and Simulation" for the opportunity to use it in this work.

The work was supported in frames of the state assignment No. 0081-2019-0018.

References

1. Shkolin A.V., Fomkin A.A., Yakovlev V.Y., Men'shchikov I.E.. Colloid Journal. 2018. T. 80. № 6. pp. 739-750.
2. Rackers J.A., Wang Z., Lu C., Laury M.L., Lagardère L., Schnieders M.J., Piquemal J.P., Ren P., Ponder J.W.. Journal of Chemical Theory and Computation. 2018. T. 14. № 10. pp. 5273-5289.
3. Jorgensen W.L., Maxwell D.S. Tirado-Rives J.. Journal of American Chemical Society. 1996. T. 118. № 45. pp. 11225-11236.

Electrical properties of low-doped carbon nanotubes/epoxy resin composite material hardened in an electric field

*Khantimerov S.M.*¹, *Garipov R.R.*¹, *L'vov S.G.*¹, *Suleimanov N.M.*¹

khantim@mail.ru

¹ Zavoisky Physical-Technical Institute, FRC Kazan Scientific Center of RAS, Kazan, Russia

The study of polymer-carbon nanotubes composites (CNT) has been a pressing research problem for recent times, given their many promising practical applications. For example, when inserted into the polymer matrix of CNT, the dielectric material becomes conductive - the polymer acquires a percolation conductivity, in which the transfer of charge carriers is carried out on a small number of conductive channels formed by filler particles [1].

The transition from non-conductive to conductive state is determined by the threshold of percolation, i.e. the concentration of electrically conductive particles in the dielectric matrix, at which conductivity appears. In the absence of external exposure, carbon nanotubes are oriented erratically in the polymer matrix. The application of the electric field during the preparation leads to the orientation of the CNT, which is expected to reduce the threshold of percolation and improve the electrical conductive properties of the material.

The paper studied the behavior of electrical conductivity of the CNT/epoxy resin composite in curing conditions in dc- and ac-electrical fields in the low-concentration range (≤ 0.05 wt.%) of filler. CNTs subjected to liquid phase oxidation in various compositions was used [2].

The boundary conditions of the procedure for the formation of the studied composite material in the electric field to reach the maximum values of DC- and AC-electroconductivity have been defined.

Acknowledgment

The research was carried out within the state assignment of Ministry of Science and Higher Education of the Russian Federation.

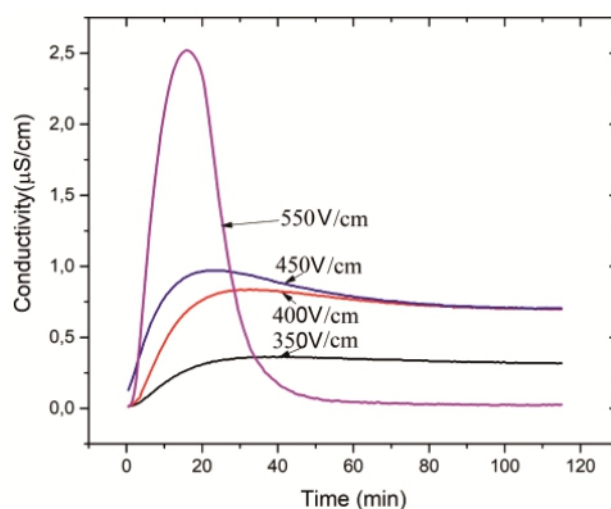


Fig.1. Dynamics of electrical conductivity of epoxy resin doped with 0.025 wt.% carbon nanotubes when it hardened in a DC field.

References

1. Sh. Sulaberidze and E. A. Skorniakova, IOP Conference Series: Materials Science and Engineering (2020) **919**, 022009.
2. R. Garipov, S. M. Khantimerov, S. G. L'vov, V. A. Shustov, N. V. Kurbatova and N. M. Suleimanov, Fullerenes, Nanotubes and Carbon Nanostructures (2021) **29**, 251-257.

Effect of the growth temperature on parameters of vertically aligned carbon nanotubes

Il'in O.I.¹, Il'ina M.V.¹, Rudyk N.N.¹, Polyvyanova O.R.¹, Fedotov A.A.¹

oiilin@sfnu.ru

¹ Southern Federal University, Institute of Nanotechnologies, Electronics, and Electronic Equipment Engineering, Taganrog, Russia

The unique properties of carbon nanotubes (CNTs) have made them a promising object for research over the past 30 years. Various methods have been investigated for the synthesis of CNTs, such as arc discharge, laser ablation and chemical vapor deposition. However, the plasma enhanced chemical vapor deposition (PECVD) has shown the most promise with the possibility of subsequent scaling for device applications. The influence of many parameters of the PECVD (growth temperature, pressure, material of the sublayer and catalyst, pressure, etc.) make it possible to control the growth kinetics, geometric dimensions and properties of CNTs. Recent research have shown unusual piezoelectric properties for CNTs [1, 2]. In this work, we study the effect of the growth temperature on parameters of vertically aligned CNTs for use in nanopiezotronic devices (nanogenerators, energy nanoharvesters), where the density and geometric dimensions of nanotubes are crucial.

CNTs were grown on Si substrates. Two types of samples were prepared with different sublayer materials (Cr and Mo) with 100 nm thick. A 5 nm thick Ni catalytic layer was formed on top. CNTs were grown by the PECVD in an atmosphere of acetylene and ammonia in the temperature range of 615-690 C°. The geometric dimensions of CNTs and their density were estimated using the method of scanning electron microscopy (SEM). The value of CNTs piezoelectric response was determined by piezoresponse force microscopy (PFM). It was found that with an increase in temperature, the CNT density decreases from 1.1 to 0.001 μm^{-2} for Mo, and from 26 to 0.1 μm^{-2} for Cr. In this case, the average diameter of CNTs grown on the Mo sublayer decreases with increasing temperature, which may be associated with the acceleration of catalyst diffusion between the grains of the sublayer material. On the Cr sublayer, the average diameter of CNTs increases with increasing temperature, which is associated with the coalescence of small catalytic centers into larger ones. Also, coalescence of catalyst centers leads to a decrease in the CNT density. An increase in the length of CNTs was observed on both sublayers, which is probably due to the better solubility of carbon in the catalytic centers with an increase in temperature and an increase in the rate of carbon diffusion through the catalyst.

Analysis of the current arising in the process of nanotubes deformation under the influence of the atomic force microscope probe made it possible to estimate the piezoelectric response value for CNTs grown on Cr and Mo sublayer (8-14 nA and 3-23 nA, respectively). As a result of the work, the regularities of the growth temperature and sublayer material influences on the density, geometric dimensions and piezoelectric response of CNTs were established.

Studies of piezoelectric properties of CNTs by the PFM method were supported by the Russian Foundation for Basic Research (project No. 20-37-70034). Studies of the influence of PECVD modes on geometric parameters and density of CNTs were supported by the Ministry of Science and Higher Education of the Russian Federation; the state task in the field of scientific activity No. 0852-2020-0015.

References

1. M. Il'ina, O. Il'in, Y. Blinov, A. Konshin, B. Konoplev, A. Ageev, *Materials* (2018) **11**, 638.
2. M. Il'ina, O. Il'in, Y. Blinov, V. Smirnov, A. Kolomiytsev, A. Fedotov, B. Konoplev, O. Ageev, *Carbon* (2017) **123**, 514.

Vertically aligned carbon nanotubes for piezoelectric nanogenerator

Il'ina M.V.¹, Osotova O.I.¹, Il'in O.I.¹

mailina@sfedu.ru

¹ Southern Federal University

The development of technologies in the field of wearable electronics and of self-powered nanosystems requires the search for suitable energy sources. One of such alternative energy sources are nanogenerators capable of converting environment mechanical energy into electrical energy using the piezoelectric effect [1, 2]. The first nanogenerator was demonstrated based on ZnO nanowires in 2006. Currently, there is a search for nanostructures capable of providing the highest sensitivity to external nanoscale deformations and maximum power. Among nanostructures, special attention is paid to aligned carbon nanotubes (CNTs), which have high mechanical parameters and exhibit anomalous piezoelectric properties [3-5]. The aim of this work is to study the effect of the mechanical pressure on the magnitude of the generated by vertically aligned CNTs current for the development of a nanogenerator.

The studies were carried out in 6 arrays of vertically aligned CNTs grown by the PECVD method at a catalytic nickel layer thickness of 5 and 20 nm on sublayers of Mo, TiN, and Cr. Deformation of the CNTs (with pressing force of 4 μN) and detection of the current arising as a result of the formation of the surface potential of CNTs during their deformation were performed using atomic force microscopy.

As a result, it was found that the largest current (up to 200 nA) is generated by arrays of separately standing vertically aligned CNTs grown on a Mo sublayer with a catalytic layer thickness of 5 nm. An increase in the thickness to 20 nm led to a significant decrease in the current to 18 nA, which weakly depends on the pressing force. A similar situation was observed for CNTs on a TiN sublayer at a catalytic layer thickness of 5 nm. However, an increase in the detected current to 80 nA was observed with an increase in the thickness of the catalytic layer to 20 nm. Carbon nanotubes grown on a Cr sublayer exhibited the lowest current (up to 18 nA). The observed dependences are associated with an increase in the length and diameter of CNTs when an increase in the thickness of the catalytic layer, as well as with a strong dependence of the CNT density in the array and the hierarchy of the array on the sublayer material. Thus, the growth of separately standing vertically aligned CNTs with a density of 1 μm^{-2} was on the Mo sublayer. On the opposite side the combined into bundles CNTs with a density of 10 μm^{-2} were grown on the Cr sublayer. The growth of vertically aligned CNTs with a high density (more than 30 μm^{-2}) was observed on the TiN sublayer. In addition, an increase in the hierarchy of the array with a large spread of CNTs in diameter (69 ± 34 nm) was observed with an increase in the thickness of the catalytic layer. It also led to an increase in the value of the detected current. The obtained results can be used to create energy efficient nanogenerators based on arrays of vertically aligned CNTs.

This work was supported by the Russian Science Foundation (project No. 20-79-00284).

References

1. Briscoe, S. Dunn *Nano Energy* (2015) **14**, 15.
2. Xu, Y.Qin, C.Xu, Y.Weil, R. Yang, Z. L. Wang *Nature Nanotech.* (2010) **5**, 366.
3. I. Kundalwal, S.A. Meguid, G.J. Weng *Carbon* (2017) **117**, 462.
4. V. Il'ina, O.I. Il'in, Yu.F. Blinov, A.A. Konshin, B.G. Konoplev, O.A. Ageev *Materials* (2018) **11**, 638.
5. M.V. Il'ina, A.A. Konshin, E.G. Solomin *Journal of Physics: Conf. Series* (2018) **1124**, 071010.

Aluminum Based Composite Materials with Carbon Nanofibers Obtained by Hot Extrusion and Rolling

Skvortsova A.N.¹, Mozhayko A.A.^{1,2}, Staritsyn M.V.¹

annaanna-1996@mail.ru

¹ NRC "Kurchatov Institute" - CRISM "Prometey", St. Petersburg, Russia

² Higher School of Applied Physics and Space Technologies, Peter the Great St. Petersburg Polytechnic University, St. Petersburg, Russia

Modern composite materials with metal matrix reinforced with carbon nanofibers (CNF) are the object of a large number of researches due to the high strength, wear resistance and thermal conductivity.

The objective of the present work is the creation of high-strength and wear-resistant bulky composite materials of *aluminum - carbon fiber* (Al-CNF) system with the use of yield strain.

Carbon nanofibers were obtained by gas-phase synthesis on a surface of aluminum powder [1, 2]. By varying the concentration of the nickel catalyst the composite powder materials were fabricated with 1 - 2 wt. % carbon. The microstructures showed that the carbon product had a fibrous structure. CNF had a diameter range from 50 to 100 nm and a length of more than 1 μm .

Composite powder materials with carbon nanofibers of 1 - 2 wt. % were used to develop bulky composite materials [3, 4]. During the experiments performed by hot extrusion and rolling the following composite mixtures were used: Al-8% Al_2O_3 ; Al-0.2% CNF and Al-0.4% CNF. Upon the extrusion of the compressed powder material 2 rods from each composition were manufactured. Mechanical tensile tests were performed as per GOST 1497. The formation of the sample neck indicated good adhesion of the composite powder of the Al-CNF system after the hot extrusion. The most perspective composite material was a sample with 0.4% CNF. The sample was obtained after hot extrusion and rolling. It was found that the sample with Al-0.4% CNF had the highest ultimate tensile strength (σ_w is 370 MPa), and the relative deformation was 7.6%. Rolling of rods after the extrusion improves the mechanical strength properties by a factor of two.

Practical use of the developed bulky composite materials has feasible application prospects for structural elements in aviation and automobile industries.

References

1. I. Rudskoy, T.S. Koltsova, O.V. Tolochko, V.G. Mikhailov, F.M. Shakhov, *Metal Science and Heat Treatment* (2014) V55. N 9-10, P. 564-558.
2. I. Nasibulina, T. Joentakanen, A.G. Nasibulin, E.I. Kauppinen, T.S. Koltsova, O.V. Tolochko, J.E.M. Malm, M.J. Karppinen, *Carbon* (2010) V. 48. N 15. P. 4559-4562.
3. Kwon, H. Kurita, M. Leparoux, A. Kawasaki, *Journal of Nanoscience and Nanotechnology* (2011) 11, P. 4119-4126.
4. D. Breki, T.S. Kol'tsova, A.N. Skvortsova, O.V. Tolochko, S.E. Aleksandrov, A.G. Kolmakov, A.A. Lisenkov, Y.A. Fadin, A.E. Gvozdev, D.A. Provotorov, *Inorganic Materials: Applied Research* (2018) 9(4), P. 639-643.

On the “intercalation” of 7 wt.% hydrogen into graphite nanofibers

*Nechaev Yu.S.*¹, *Denisov E.A.*², *Cheretaeva A.O.*³, *Gavrilov Yu.V.*⁴, *Verzhichinskaya S.V.*⁴

yuri1939@inbox.ru

¹ Kurdjumov Centre of Metals Science and Physics, Bardin Central Research Institute for Ferrous Metallurgy, Moscow, Russia

² St. Petersburg State University, St. Petersburg, Russia

³ Research Institute of Progressive Technologies, Togliatti State University, Togliatti, Russia

⁴ Department of Chemical Technology of Carbon Materials, Mendeleev University of Chemical Technology of Russia, Moscow, Russia

Processing, with the help of technique [1], of the thermal desorption and thermogravimetric data [2, 3] on hydrogen “super” storage in activated graphite nanofibers (GNFs) showed the presence of the main hydrogen desorption peak #1 (Fig. 1) with the following characteristics: 1) an anomalously high hydrogen content ~7 wt.%, i.e. the atomic (H/C) ratio ≈ 0.9 ; 2) relatively low values of the desorption activation energy ($Q = 45 \pm 5$ kJ/mol(H₂)) and the pre-exponential factor ($K \approx 0.4$ s⁻¹) of the rate constant.

The physics of such a process was revealed using the study results [4-6] for processes noted there as I and II, along with using the analysis results [4-6] of the data [7].

Acknowledgements

This work was financially supported by the RFBR (Project # 18-29-19149 mk).

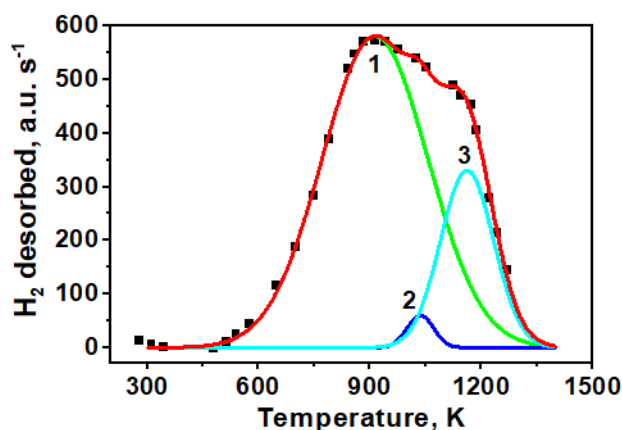


Fig.1. Approximation by 3 Gaussians (peaks #1-3) of the thermal desorption spectrum (curve “a” from Fig. 8 in [2], the heating rate $\beta = 0.17$ K/s) for a herringbone-like activated GNFs sample that had been subjected to the high-pressure H₂ adsorption-desorption treatment (300 K, 11-4 MPa, 24 h).

References

1. Yu.S. Nechaev, N.M. Alexandrova, A.O. Cheretaeva, V.L. Kuznetsov, A. Öchsner, E.K. Kostikova, and Yu.V. Zaika, *Int. J. Hydrogen Energy* (2020) **45**, 25030.
2. C. Park, P.E. Anderson, A. Chambers, C.D. Tan, R. Hidalgo, and N.M. Rodriguez, *J. Phys. Chem. B* (1999) **103**, 10572.
3. R.T.K. Baker, *Encyclopedia of Materials: Science and Technology*, Elsevier (2005) p. 932.
4. Yu.S. Nechaev and T.N. Veziroglu, *Int. J. Phys. Sci.* (2015) **10**, 54.
5. Yu.S. Nechaev, *Physics – Uspekhi* (2006) **49**, 563; *UFN* (2006) **176**, 581.
6. Yu.S. Nechaev, N.M. Alexandrova, N.A. Shurygina, and A.O. Cheretaeva, *Fullerenes, Nanotubes and Carbon Nanostructures* (2020) **28**, 233.
7. B.K. Gupta, R.S. Tiwari, and O.N. Srivastava, *J. Alloys Comp.* (2004) **381**, 301.

Ab-initio study of electronic properties of 2D and 3D regular arrays of carbon nanotubes

Polozkov R.G.^{1,2}, *Pavlov A.V.*², *Portnoi M.E.*^{1,3}, *Shelykh I.A.*^{1,4}

polozkov@itmo.ru

¹ ITMO University, Saint Petersburg, Russia

² Alferov University, (Former St Petersburg Academic University), Saint Petersburg, Russia

³ School of Physics, University of Exeter, Exeter, United Kingdom

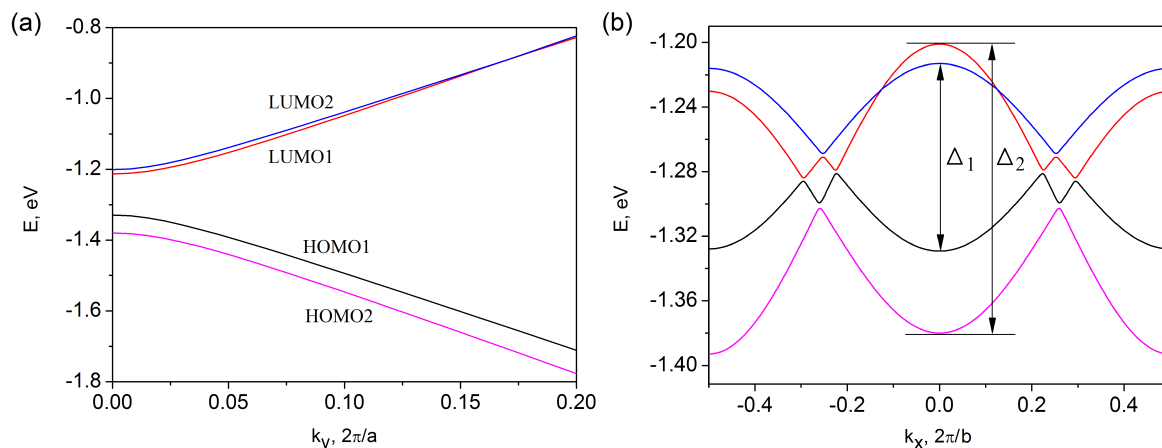
⁴ Science Institute, University of Iceland, Reykjavik, Iceland

Carbon nanotubes (CNT) [1] and more complex systems constructed on the basis of CNTs have attracted great attention due to their unique electronic and mechanical properties. For example, results of experimental studies of self-assembled horizontally aligned carbon nanotube arrays were recently published [2].

In this work the equilibrium geometry and electronic band structure of 2D and 3D regular arrays of CNT are studied with use of the density functional theory (DFT). The many-electron correlations and van der Waals corrections are taken into account. The optimal distance between nanotubes in the array corresponding to the minimum of the total energy of the system is found.

We have found that 2D and 3D regular array of CNTs separated by an optimal distance governed by van der Waals forces have a strongly anisotropic hyperbolic dispersion for its low-energy charge carriers. Thus, we have predicted a new type of hyperbolic van der Waals material with a rich energy spectrum promising interesting physical effects and optoelectronic applications.

We acknowledge support from Horizon 2020 Marie Skodowska-Curie RISE projects CoExAN (grant No 644076) and TERASSE (grant No 823878). MEP acknowledges support through the ITMO Fellowship and Professorship Program.



Electronic band structure of 2D array of (15,0) zigzag CNT separated by $d=6$ a.u. obtained within DFT calculations: (a) along the tube axis; (b) in the direction normal to the tube axis.

References

1. Iijima S, Nature (1991) **354**,
2. Zhang R, Zhang Y and Wei F, Soc. Rev. (2017) **46**, 3661.

Li-decorated carbon nanotubes: charge analysis

*Sozykin S.A.*¹, *Beskachko V.P.*¹

sozykinsa@susu.ru

¹ South Ural State University, Chelyabinsk, Russia

Despite the estimation of an atomic charge in molecular and crystal systems strongly depends on the used methodology, this value is often used to assess the charge density redistribution during the formation of a molecule or crystal from independent atoms. For example, the commonly used Mulliken method results in charge values that depend on the utilized basis set and could be non-physical.

A lithium atom adsorbed on a carbon nanotube donates almost all its valence (2s) electron to the tube. In this study, this statement was verified for 1-4 lithium atoms, adsorbed on a carbon nanotube (7,7), using various methods for charge estimation. The periodic boundary conditions were used. The length of the model was 1 nm, which resulted in lithium concentrations from 1/112 to 1/28 atomic percent.

The study was carried out within the framework of the density functional theory with the local density approximation, using the SIESTA [1] and VASP [2] packages. In SIESTA calculations, we estimated charges by Mulliken, Voronoi, and Hirshfeld methods. In the case of the VASP package, we used the DDEC6 [3], Hirshfeld, and CM5 (a development of the Hirshfeld method) [4] methods for charge analysis.

We considered 12 datasets (lithium adsorption on the outer and inner surfaces of carbon nanotube, two programs, three methods), we came to the following conclusions:

1. The Hirshfeld method in both used DFT packages gave similar results for Li charges, which were minimal among the considered methods.
2. The DDEC6 charges were the closest to the Mulliken values. However, the non-physical results were not observed (the lithium ion charge did not exceed $|e|$).
3. The intermediate results (between Hirshfeld and Mulliken charges) were obtained by the CM5 method.
4. The lithium charge close to $|e|$ was obtained only by the Mulliken and DDEC6 methods.

Acknowledgments: The reported study was funded by RFBR, project number 20-42-740002.

References

1. García, N. Papior, A. Akhtar, E. Artacho, V. Blum, E. Bosoni, P. Brandimarte, M. Brandbyge, J.I. Cerdá, F. Corsetti, R. Cuadrado, V. Dikan, J. Ferrer, J. Gale, P. García-Fernández, V.M. García-Suárez, S. García, G. Huhs, S. Illera, R. Korytár, P. Koval, I. Lebedeva, L. Lin, P. López-Tarifa, S.G. Mayo, S. Mohr, P. Ordejón, A. Postnikov, Y. Pouillon, M. Pruneda, R. Robles, D. Sánchez-Portal, J.M. Soler, R. Ullah, V. Yu, Z. Wen, and J. Junquera, *J. Chem. Phys.* (2020) **152**, 204108.
2. Kresse, and J. Furthmuller, *Phys. Rev. B* (1996) **54**, 11169.
3. T.A. Manz, and N. Gabaldon Limas, *RSC Advances* (2016) **6**, 47771.
4. T.A. Manz, and D.S. Sholl, *J. Chem. Theory Comput.* (2012) **8**, 2844.

Hybrid nanomaterial TiC/MWCNTs: synthesis, application as strengthening components in aluminum alloys

Vilkov I.V.¹, Ob'edkov A.M.¹, Ketkov S.Yu.¹, Aborkin A.V.²

mr.vilkof@yandex.ru

¹ G.A. Razuvaev Institute of Organometallic Chemistry of RAS, Nizhny Novgorod, Russia

² Vladimir State University named after Alexander and Nikolay Stoletovs, Vladimir, Russia

Multi-wall carbon nanotubes (MWCNTs) and hybrid materials based on them have great strength for which they are suitable for use as reinforcing additives in various structural materials. Primarily, these are polymer and metal-matrix composites. Due to carbon nanotubes, perspectives for the creation of structural materials with a relatively low density and high strength characteristics are opening up.

In this work, the possibility of creating a hybrid nanomaterial TiC/MWCNTs, which are MWCNTs decorated with TiC nanocoatings, is presented. Also, the influence of additions of both initial MWCNTs and TiC/MWCNTs on the strength characteristics of aluminum alloys obtained by powder metallurgy technology is shown.

Synthesis and research of MWCNTs and hybrid nanomaterial TiC/MWCNTs was carried out in the Laboratory of hybrid nanomaterials, IOMC RAS. MWCNTs were obtained by a catalytic method using ferrocene and toluene as precursors. A hybrid material TiC/MWCNT was obtained using the MOCVD technology in vacuum, Cp_2TiCl_2 served as the precursor of the nanocoating. MWCNTs and TiC/MWCNTs were investigated by different physicochemical methods. The chemical and phase compositions, morphology, structure and thermal resilience of the samples were determined.

The resulting initial MWCNTs and hybrid nanomaterials were investigated as strengthening additives in aluminum alloys prepared by powder metallurgy technology. A significant increase in tensile and compressive strength is shown.

This work was supported by the RSF (Project 18-79-10227) and partly of IOMC RAS state assignments using the equipment of the Collective Scientific Centers "Physics and Technology of Micro and Nanostructures" (IPM RAS) and Analytical Center, IOMH RAS.

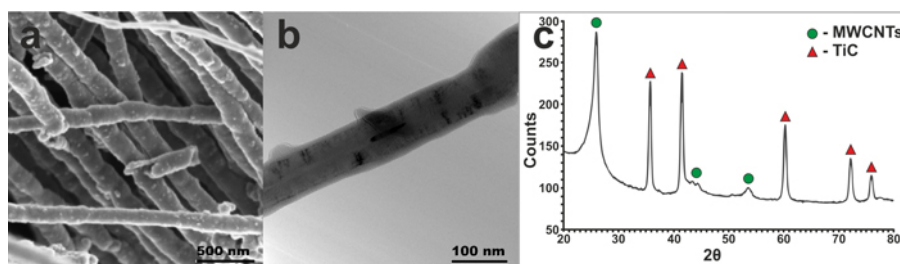


Fig. 1. SEM (a) and TEM (b) images and XRD diffractogram (c) of the hybrid TiC/MWCNTs nanomaterial

References

1. B.S. Kaverin, A.M. Obiedkov, S.Yu. Ketkov, K.V. Kremlev, N.M. Semenov, S.A.Gusev, D.A. Tatarskiy, P.A. Yunin, I.V. Vilkov, M.A. Faddeev, J. Surf. : X-Ray, Synchrotron Neutron Tech. (2018) 7, 54

Day 3: School for Young Scientists.

The use of nanodiamonds in solid composite electrolytes

Alekseev D.V.^{1,2}, *Mateyshina Yu.G.*^{1,2,3}

d.alekseev1@list.ru

¹ Institute of Solid State Chemistry and Mechanochemistry SB RAS, Novosibirsk, Russia

² Novosibirsk State University, Novosibirsk, Russia

³ Novosibirsk State Technical University, Novosibirsk, Russia

The number of energy carriers is increasing every day. These devices include batteries, fuel cells, supercapacitors, etc. All such electrochemical devices consist of two electrodes and an electrolyte, the choice of which directly affects the characteristics of the device.

There are several options for different electrolytes, such as liquid, ionic liquid, polymer and solid [1-3]. One of the most common types of electrolytes is liquid electrolytes with high conductivity and good electrode wettability. Nevertheless, such electrolytes also have a several disadvantages, such as narrow ranges of operating temperatures and electrochemical stability. These problems can be solved by the transition to solid electrolytes. The disadvantages of such electrolytes include low conductivity and poor wettability of the electrodes. The solution to the first problem is achieved by creating a nanocomposite solid electrolyte of the MX - A type (where MX is an ionic salt, A is a nanodispersed inert additive) [4]. It is assumed that in the transition to nanoscale systems, several factors appear that affect the transport properties of ionic salts. This is due to the effect of surface interaction on the bulk properties of ionic salts. In this case, the salt passes into a new state that is not characteristic of a pure substance, the properties of which are determined not only by the bulk characteristics of MX but also by the parameters of the interaction of the salt with the surface of the dispersed additive A [5].

Thus, the requirements for inert dispersed additives are a high specific surface area, thermal and chemical stability towards the electrolyte. Usually, various oxides are used as component A in solid electrolytes, for example, Al₂O₃, TiO₂, SnO₂, Fe₂O₃ [5]. In this work, we propose to use a unique carbon material - nanodiamond (produced by the FRPC "Altai", Biysk, S_s = 300 - 320 m²/g) as a dispersed additive. This material meets all the requirements for dispersed additives, at the same time being lighter and harder. Also, the functionalization of nanodiamonds can open up new unexpected properties in the composite material system.

The purpose of this work is to study the transport properties of composites (1-x) MX - x(Nanodiamonds), where x is the proportion of nanodiamonds. Based on the composites obtained, a model of a solid-state electrochemical device was constructed and its characteristics were investigated.

References

1. Hikmet, R.A.M., Organic Electrolytes and Electrodes for Batteries, in Encyclopedia of Materials: Science and Technology, K.H. Jürgen Buschow and Merton C., Eds, Amsterdam: Elsevier Science Ltd., 2001, p. 6534.
2. Van Aken, K.L., Beidaghi, M., Gogotsi, Y. Formulation of ionic-liquid electrolyte to expand the voltage window of supercapacitors, *Angew. Chem.*, 2015, vol. 54, p. 4806.
3. Abbas, Q., Mirzaeian, M., Olabi, A.G., Gibson, D., Solid State Electrolytes, Paisley: Elsevier Reference Module in Materials Science and Materials Engineering, 2020, p. 1-11.
4. Ivanov-Schitz, A.K., Murin, I.V., Solid state ionics (in Russian), St. Petersburg: S.-Peterburg. Univ, 2010. 1000 p.
5. Uvarov, N.F., Composite solid electrolytes (in Russian), Novosibirsk: Publishing House SB RAS, 2008. 258 p.

Nanostructures VS_x/reduced graphene oxide materials for energy storage applications

Kotsun A.A.¹, Stolyarova S.G.¹, Okotrub A.V.¹, Bulusheva L.G.¹

kotsun15@gmail.com

¹ Nikolaev Institute of Inorganic Chemistry SB RAS, Novosibirsk, Russia

Lithium-ion batteries (LIBs) have firmly entered the life of human society, providing sources power for various portable devices (smartphones, laptops, headphones, etc.) and more powerful devices (buses, subways, electric motors, and hybrids, etc.). However, nowadays, traditional materials for LIB electrodes are being replaced by more efficient and modern ones in order to improve the electrochemical characteristics of current storage devices.

Vanadium disulfide (VS₂) has a layered structure with a large interlayer distance (0.57 nm) and high theoretical capacity for lithium: 466 and 1397 mAh g⁻¹ in the case of Li₂VS₂ and Li₆VS₂, respectively [1]. Metallic conductivity of VS₂ and low diffusion barriers for lithium ions intercalation can also provide a high charge/discharge rate of the VS₂-based materials [2]. To increase the stability of the operation of the electrodes and to reduce their degradation during the cycling, the sulfides can be fixed on a carbon substrate, forming mechanically stable compositions VS₂/C. The use of the carbon component ensures the dispersion of VS₂ nanoparticles, fast electron transport in the electrochemical cell, and increases the stability of the nanoparticles during the charge/discharge of LIBs. Nanostructuring of VS₂ makes it possible to increase the capacity by forming a large number of boundaries, where lithium can be reversibly adsorbed.

In this work, a one-stage synthesis via rapid heating of an aerogel composed of ammonium thiovanadate and graphite oxide (GO) in an argon atmosphere at temperatures of 300–700°C is proposed. The structure and the composition of the nanostructured particles were characterized by X-ray photoelectron spectroscopy, Raman spectroscopy, and X-ray diffraction. The obtained series of VS_x/reduced GO samples were tested as electrodes in electrochemical cells using metallic lithium as a counter electrode. The best cycling capacity of 620 mAh g⁻¹ at a current density of 0.1 A g⁻¹ was shown by the material obtained at 300°C. It also stood a long-term operation at high current densities of 2 and 5 A g⁻¹ with good specific capacities of 400 and 250 mAh g⁻¹, respectively

This work was supported by the Russian Scientific Foundation (21-53-12021).

References

1. Wu D. et al. Porous bowl-shaped VS₂ nanosheets/graphene composite for high-rate lithium-ion storage //Journal of Energy Chemistry. - 2020. - N. 43. - p. 24-32.
2. Wang D. et al. Two-dimensional VS₂ monolayers as potential anode materials for lithium-ion batteries and beyond: first-principles calculations //Journal of Materials Chemistry A. - 2017. - N. 5. - I. 40. - P. 21370-21377.

Synthesis, functionalization and electrochemical properties of N-free and N-doped porous carbon materials

*Nishchakova A.D.*¹, *Fedoseeva Yu.V.*¹, *Bulusheva L.G.*¹

nishchakova@niic.nsc.ru

¹ Nikolaev Institute of Inorganic Chemistry SB RAS, Novosibirsk, Russia

Porous carbon materials (PCMs) are one of the modern branches of the carbon material's development. They consist of graphene-like layers with multiple defects, leading to bending of these layers, which determines a high specific surface area and pores of various sizes and shapes. Due to PCMs unique properties, namely chemical, thermal and mechanical stability, the presence of a developed surface and the possibility of its modification during and after synthesis (for example, the creation of additional structural defects due to post-treatment of materials and/or the change in the electronic state due to heteroatoms doping), low cost of synthesis and ease of handling, PCMs are used as carriers of catalytically active particles, as sorbents for various gases, organic liquids, and also as materials for electrodes.

In this work, a porous carbon material was synthesized at 800°C via the CVD method from ethanol vapor on template CaO particles obtained in situ by the decomposition of the L-isomer of calcium tartrate $\text{CaC}_4\text{H}_4\text{O}_6$ under reduced pressure in an argon atmosphere. To functionalize the obtained material, post-synthetic fluorination of the sample in an atmosphere of 10% BrF_3/Br_2 solution for 7 days was used, after which the fluorinated PCM was treated with gaseous ammonia for 30 minutes at the temperature of 400°C.

The samples obtained at each stage of the synthesis were studied by XPS. Despite the rather high degree of fluorination of the sample at the second stage of the synthesis (the fluorine content was ~34 at.%), after reduction of the sample in a stream of gaseous ammonia, only ~4 at.% of nitrogen was found on the surface. We measured the capacities of double-layer electrochemical capacitors with electrodes made of the studied nitrogen-containing PCM in acidic (1M H_2SO_4) and alkaline (6M KOH) media at different sweep rates of 2-1000 mV/s. The specific surface area and pore distribution of the samples were measured, which also helped to establish the relationship between the synthesis parameters, structure, and electrochemical characteristics of the investigated PCM samples.

This work is financially supported by Russian Scientific Foundation (№ 19-73-10068). The XPS studies were conducted using the equipment of the Center of Collective Use «National Center of Catalyst Research».

Influence of additives of multi-walled carbon nanotubes on the porosity and macrostresses in the composite «hydroxyapatite - MWCNTs»

*Rezvanova A.E.*¹, *Barabashko M.S.*², *Ponomarev A.N.*¹, *Tkachenko M.V.*³, *Nikolaev V.V.*⁴

nastya.rezvanova@mail.ru

¹ Institute of Strength Physics and Materials Science of SB RAS, Tomsk, Russia

² B.Verkin Institute for Low Temperature Physics and Engineering of NAS of Ukraine, Kharkiv, Ukraine

³ V.N. Karazin Kharkiv National University, Kharkiv, Ukraine

⁴ Tomsk State University, Tomsk, Russia

Calculations of thermal diffusivity and the analysis of temperature gradients in composite ceramics based on hydroxyapatite (HA) with additives of multi-walled carbon nanotubes (MWCNTs) is carried out. The concentration of nanotubes was varied in the range 0 - 0.5 wt%. HA is a bioactive matrix, while MWCNT additives can improve the mechanical properties of ceramics. In particular, the additives of MWCNTs lead to the unique electrical, thermal, and mechanical properties of composite materials [1,2].

It was found that an increase of the temperature difference between the surface and the center of the HA ceramic sample occurs during heating of the ceramic on the first stage of sintering. It is observed due to the change of thermal diffusivity of HA with increasing the temperature [3]. The surface of the samples is heated faster than the central part. Therefore, the surface of the material expands faster and experiences compressive stresses.

X-ray diffraction studies of ceramics indicate that the presence of macrostresses in the sample of HA ceramics due to its low thermal diffusivity. MWCNT additives reduce macrostresses in the composite to the better thermal diffusivity of MWCNT.

Absorption coefficient for samples of hydroxyapatite with additives of MWCNT was measured in the radiation frequency range of 0.2-1.6 THz by using a T-SPEC spectrometer. It was found a correlation between the values of absorption coefficient and porosity of samples. The HA sample without MWCNT additives has the highest absorption coefficient. An increase in the concentration of nanotubes leads to a decrease in porosity and absorption coefficient.

It was found that HA ceramics has higher macrostresses than in the case of HA ceramics with the additives of MWCNTs. HA ceramics have low thermal diffusivity and the temperature gradients occur during heterogeneous heating/cooling of different parts of ceramics at sintering. The additives of MWCNTs allow to increase the thermal diffusivity and reduce internal residual macrostresses in the HA-MWCNT ceramics and decrease the porosity values of the ceramics.

• **Acknowledgements:**

The work of A.Rezvanova and A.Ponomarev was performed according to the Government research assignment for ISPMS SB RAS, project FWRW-2021-0007.

References

1. S. Barabashko, M. Drozd, D. Szewczyk et al., *Fullerenes, Nanotubes and Carbon Nanostructures* (2021) **29**, 331.
2. N. Mazov, I. A. Ilinykh, V. L. Kuznetsov et al., *J. Alloys Compd.* (2014) **586**, 440.
3. Kijima and M. Tsutsumi, *J. Am. Ceram. Soc.* (1979) **62**, 455.

Organosilicon polymer compositions based on carbon nanotubes in tensoresistive applications

*Semenukha O.V.*¹, *Voronina S.Yu.*¹, *Simunin M.M.*^{1,2,3}

semenukha.cool@mail.ru

¹ Reshetnev Siberian State University of Science and Technology Krasnoyarsky Rabochy Av.,31 660037 Krasnoyarsk, Russia

² Krasnoyarsk Scientific Center SB RAS, Akademgorodok, 50, 660036 Krasnoyarsk, Russia

³ Siberian Federal University, Svobodny 79, 660041 Krasnoyarsk, Russia

Silicone rubbers, due to the organosilicon polymer chains, have low internal friction and are capable of stretching over large values, and their high chemical inertness and thermal stability makes these materials, in general, an interesting and promising matrix for creating tensoresistive nanocomposites [1,2]. Carbon nanotubes are a versatile additive that modifies the properties of a material while maintaining its quality. In particular, when carbon nanotubes are added to polymers, their strength increases and conductivity appears, which can be varied within wide limits.

The objects of study were samples based on ELASTOSIL RT 604 silicone rubber manufactured by WACKER (Munich, Germany) with various concentrations (1, 2, 3 and 5 wt.%) of concentrate based on TUBALL™ single-wall carbon nanotubes manufactured by OCSiAl (St. Novosibirsk, Russia), 3 wt.% Graphene, 5 wt.% Graphene / multi-walled nanotubes (038 AMG), 0.5 wt.%, 1 wt.% Taunit-M (multi-walled nanotubes) manufactured by NanoTechCenter LLC [3]. The resistance of composites with different concentrations of carbon nanotubes was measured by the strip probe method under different loads and depending on the number of loading cycles.

It was shown that for single-walled carbon nanotubes the composite has a resistivity of about 13 kΩ*m at 1 and 2 wt% and above 3 wt% about 1 kΩ*m, which indicates a change in the substructure of carbon nanotubes in the composite. Also, with an increase in concentration, the spread in the resistivity value increases, this is due to the drawbacks of the technique of homogenizing carbon nanotubes over the volume of the polymer matrix. The more carbon nanotubes need to be introduced, the more difficult it is to distribute them uniformly in the matrix. It was also found that with equal mass fractions of single-walled and multi-walled carbon nanotubes, the latter more strongly reduce the resistivity of the material. This is determined by the presence of semiconductor nanotubes in the material of single-walled carbon nanotubes. In turn, this feature gives a sharper temperature dependence of the material resistivity.

In general, the material obtained has shown itself to be an effective resistive material, whose resistance varies representatively from external influences.

This work was carried out by the team of the scientific laboratory “Smart Materials and Structures” within the state assignment of the Ministry of Science and Higher Education of the Russian Federation for the implementation of the project “Development of multifunctional smart materials and structures based on modified polymer composite materials capable to function in extreme conditions” (Project No. FEFE-2020-0015).

References

1. Cai JH, Li J, Chen XD, Wang M. (2020). Multifunctional polydimethylsiloxane foam with multi-walled carbon nanotube and thermo-expandable microsphere for temperature sensing, microwave shielding and piezoresistive sensor. *Chemical Engineering Journal*, 393:124805.
2. Chen YF, Li J, Tan YJ, Cai JH, Tang XH, Liu JH, Wang M. (2019). Achieving highly electrical conductivity and piezoresistive sensitivity in polydimethylsiloxane/multi-walled carbon nanotube composites via the incorporation of silicon dioxide micro-particles. *Composites Science and Technology*, 177:41-48.
3. Tkachev AG, Melezhik AV, Memetov NR. (2019) Method of producing graphene material. RU Patent № 2693755.

Influence of the synthesis temperature on electrochemical properties of porous nitrogen-containing carbon in sodium-ion batteries

*Vorfolomeeva A.A.*¹, *Shlyahova E.V.*¹, *Grebenkina M.A.*^{1,2}, *Fedoseeva Yu.V.*¹, *Bulusheva L.G.*¹, *Okotrub A.V.*¹

vorfolomeeva@niic.nsc.ru

¹ Nikolaev Institute of Inorganic Chemistry SB RAS, Novosibirsk, Russia

² Novosibirsk State University, Novosibirsk, Russia

Nanoporous carbon, which is a three-dimensional carbon skeleton, has good electrical conductivity, chemical inertness, physical stability, and low cost, and is a promising material for sodium-ion batteries (SIBs). The accumulation mechanism includes not only the intercalation of sodium ions into the interlayer space of carbon material but also their adsorption on defects and pores. Consequently, the capacity of the carbon material depends on the pore size as well as the nature of the defective areas. The development of efficient anode materials for SIBs requires the establishment of clear relationships between the structure and electrochemical characteristics of the material.

Herein, porous nitrogen-doped carbon materials have been synthesized via template-assisted chemical vapor deposition (CVD) technique at 650, 750 and 850 °C. The process includes the production of template nanoparticles through thermal decomposition of calcium tartrate, followed by CVD growth using acetonitrile and removal of mineral template with diluted hydrochloric acid. By varying the synthesis temperature, size of template-induced mesoporous and concentration of microporous originated from nitrogen-inserting and atomic defects can be tuned (Fig. 1). Nitrogen sorption analysis shows that porous nitrogen-doped carbon materials have template-induced mesoporous of size 3-30 nm. With decreasing the synthesis temperature, content of small mesoporous, pore-volume, and a specific surface area greatly increase.

Electrochemical testing toward sodium-ion storage and electrochemical impedance spectroscopy measurements have been performed. The sample grown at 650 °C demonstrates the highest electrochemical capacity (184 mAh/g at a current density of 0.05 A/g) due to the presence of the large number of small mesoporous and in-plane "hole" defects in graphitic shells. These defects improve sodium-ion diffusion due to the presence of interconnected open pores and adsorption sites for ion storage.

This work was supported by the Russian Science Foundation (project No. 19-73-10068).

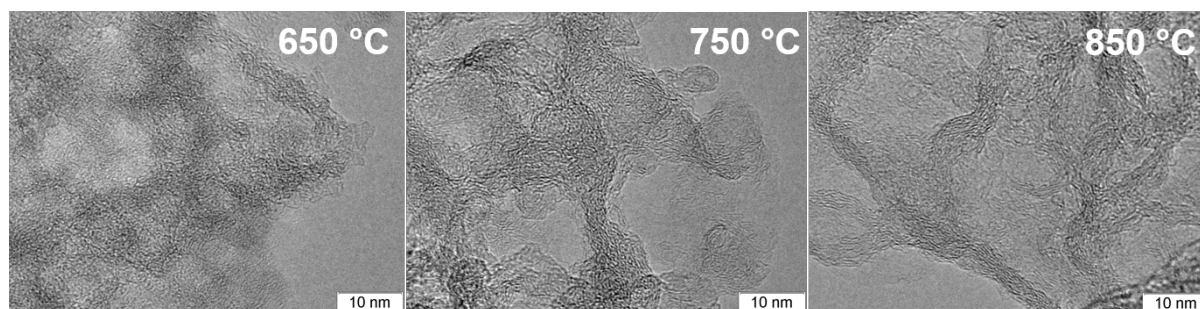


Fig.1. Demonstration of various pore sizes in porous nitrogen-doped carbon material depending on synthesis temperature using transmission electron microscopy.

Synthesis of a suspension of detonation nanodiamonds modified with nickel ions

Chizhikova A.S.^{1,2}, Yudina E.B.²

anastasia.chizhikova@mail.ru

¹ Saint-Petersburg State Institute of Technology, St.Petersburg, Russia

² Ioffe Institute, St.Petersburg, Russia

Diamond nanoparticles obtained by detonation synthesis, the so-called detonation nanodiamonds (DNDs), have attracted increasing interest of materials scientists in recent years due to possibility of various applications [1]. The presence of functional groups (carboxyl, hydroxyl) on the surface of DNDs makes it possible to change their physicochemical properties by modification the surface with metal ions [2]. The application of nickel ions for this modification is of special interest as magnetic nanoliquids [3].

The aim of this work is to synthesize a stable suspension of the carboxylated deagglomerated detonation nanodiamonds with a surface modified by Ni (II) ions via an exchange reaction between metal ions and protons of surface carboxyl groups.

The modification was carried out by mixing DNDs hydrosol with solutions of Ni(NO₃)₂·6H₂O (**1**) and Ni(CH₃COO)₂·4H₂O (**2**) in an ultrasonic bath and subsequent centrifugation.

The initial particle size of the detonation nanodiamonds was 4-5 nm. The binding of Ni ions to two carboxyl groups resulted in formation of aggregates (about 10-15 nm). ζ-potential of the obtained suspensions was -28.4±0.9 mV (concentration 0.10 wt.%) and -30.2±0.6 mV (concentration 0.57 wt.%) for samples **1** and **2**, respectively. The suspensions have sedimentation stability.

A number of bound Ni²⁺ with the maximum possible number of carboxylate ions (COO⁻) was determined by conductometric and potentiometric titration methods. The content of nickel ions, determined by conductometric titration, was equal to ~0.62·10⁻⁴-0.73·10⁻⁴ mol/g and ~1.34·10⁻⁴-1.45·10⁻⁴ mol/g for samples **1** and **2**, respectively. The content of nickel ions, determined by potentiometric titration, was equal to ~1.04·10⁻⁴ mol/g for sample **1**.

The content of nickel ions was determined by energy-dispersive X-ray analysis and was equal to ~0.54·10⁻⁴ mol/g and ~1.92·10⁻⁴ mol/g for samples **1** and **2**, respectively. IR spectra of the obtained samples coincided with IR spectrum of original nanodiamonds, no additional anions were detected.

As result, the possibility of modification the surface of detonation nanodiamonds nanoparticle with divalent nickel ions has been shown. The content of bound nickel ions to the surface of detonation nanodiamonds was 0.62·10⁻⁴-1.04·10⁻⁴ mol/g and 1.34·10⁻⁴-1.92·10⁻⁴ mol/g when using nickel nitrate and nickel acetate.

References

1. Detonation Nanodiamonds. Technology, structure, properties and applications: edited by Vul' A. Ya.; Shenderova O. A. (Ioffe Institute, St.-Petersburg, 2016), p. 384.
2. Yudina, E. B., Aleksenskii, A. E., Fomina, I. G., Shvidchenko, A. V., Danilovich, D. P., Eremenko, I. L., Vul, A. Y., Eur. J. Inorg. Chem. (2019), 1.
3. Sundar, L. S., Shusmitha, K., Singh, M. K., Sousa, A. C. M., Int. Commun. Heat&Mass Transfer (2014), 57, 1.

Phase transition in the system “BGO - CH₃CN” - dependence on characteristics of the material

Popov D.S.¹, Kaplin A.V.¹, Rebrikova A.T.¹, Eremina E.A.¹, Chumakova N.A.^{1,2}

greendmitrymos@mail.ru

¹ M.V. Lomonosov Moscow State University, Chemistry Department, Leninskiye Gory 1/3, Moscow, 119991, Russia

² N.N. Semenov Federal Research Center for Chemical Physics, Russian Academy of Science, Kosygin St. 4, Moscow, 119991, Russia

It was recently revealed that systems “BGO - polar liquid” demonstrate the reversible transition of the low-temperature phase into the high-temperature phase with the release of part of the sorbed liquid [1]. Later using the spin probe method it was shown that the phase transformation proceeds within a temperature range of $\sim 30^\circ$ [2]. Apparently this range reflects partial inhomogeneity of the material. The literature describes various types of BGO obtained by repeated sequential oxidation of graphite according to Brodie's method. The present work is devoted to study the dependence of the phase transition characteristics on the stage of oxidation and characteristics of the material.

We synthesized the graphite oxide by classical Brodie's method. Two stages of oxidation were performed. The interplane distance and the sorption of acetonitrile were determined for BGO-1 and BGO-2. For observation of the phase transition in the system “BGO - CH₃CN” the DSC and EPR methods were applied. In the latter case, the stable nitroxide radical TEMPOL was used as a spin probe and the temperature dependence of the distance between the low field and high field components of the EPR spectrum was recorded (Fig.1). A non-monotonic course of the dependence reflects a non-monotonic temperature dependence of the rotational mobility of the radicals, which is caused by a change of interplane distances of GO during the phase transition.

It was revealed that the system “BGO-1 - CH₃CN” doesn't demonstrate phase transformation. In the system “BGO-2 - CH₃CN” there is a reversible transition in the temperature ranges close to the ranges observed in [2]. Further oxidation of BGO-2 to BGO-3 is in the plan.

This work was supported by the RFBR grant 18-29-19120 mk. XPS measurements were performed in the shared scientific center “Nanochemistry and Chemistry of the Atmosphere” of the Department of Chemistry of MSU.

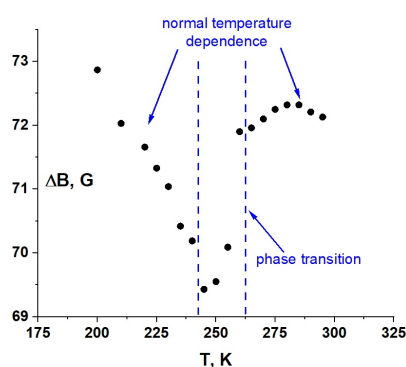


Fig.1. Temperature dependence of the distance between the low field and high field components of the EPR spectrum of TEMPOL in “BGO-2 - CH₃CN”

References

1. You, S. J.; Luzan, S. M.; Yu, J. C.; Sundqvist, B.; Talyzin, A. V. *J. Phys. Chem. Lett.* (2012) **3**, 812.
2. Chumakova N. A., Rebrikova A. T., Talyzin A. V., Paramonov N. A., Vorobiev A. Kh, Korobov M. V. *J. Phys. Chem. C.* (2018) **122**, 22750.

Adjustment of the functional composition of graphene oxide at the synthesis stage

*Shiyanova K.A.*¹, *Gudkov M.V.*¹, *Rabchinskii M.K.*², *Sokura L.A.*², *Stolyarova D.Y.*³, *Bidakova M.V.*², *Shashkin D.P.*¹, *Trofimuk A.D.*², *Smirnov D.A.*⁴, *Komarov I.A.*⁵, *Timofeeva V.A.*¹, *Melnikov V.P.*¹

shiyanovakseniya@mail.ru

¹ N.N. Semenov Federal Research Center for Chemical Physics, Russian Academy of Sciences, Moscow, Russia

² Ioffe Institute, Saint Petersburg, Russia

³ NRC Kurchatov Institute, Moscow, Russia

⁴ Institut für Festkörper und Materialphysik, Technische Universität Dresden, Dresden, Germany

⁵ Department of Composite Construction for Space Rockets, Bauman Moscow State Technical University, Moscow, Russia

In recent years, graphene has attracted much attention from both experimental and theoretical research groups due to its unique structural, mechanical, heat-conducting, and electricity-conducting properties [1,2]. It should be noted that the ideal graphene structure is not required in all potential applications. An increasing number of studies have been devoted to the synthesis and application of graphenes modified with organic groups and having a defect structure, which — in many publications — are also called ‘functionalized graphenes’ or ‘chemically modified graphenes’ (CMGs). One of the most important CMGs is graphene oxide.

In this work, we demonstrated for the first time an approach for the management of GO chemistry via the use of $\text{KMnO}_4/\text{K}_2\text{Cr}_2\text{O}_7$ oxidizing agents at different ratios [3]. The almost linear dependence of the content of the basal-plane hydroxyls/epoxides and the edge-located carbonyls/carboxyls on the KMnO_4 to $\text{K}_2\text{Cr}_2\text{O}_7$ ratio was indicated. Combined with almost two-fold change in the number of hydroxyls/epoxides and the threefold change in the number of carbonyls/carboxyls upon the transition from the KMnO_4 to $\text{K}_2\text{Cr}_2\text{O}_7$ as a predominant oxidizing agent, the proposed approach is asserted to allow the synthesis of GOs with the desired composition of oxygenic groups. The modification of the GO chemistry is suggested to arise from the difference in the mechanisms of the oxidation of graphite with $\text{K}_2\text{Cr}_2\text{O}_7$ and KMnO_4 indicated by the studies by Optical microscopy during the oxidation process. In comparison to the well-known diffusion-based mechanism of graphite oxidation by KMnO_4 , the reactions lying behind the graphite treatment with $\text{K}_2\text{Cr}_2\text{O}_7$ require further studies.

Given these results, a facile and easily-scalable method for the low-cost bulk-quantity production of GOs with the desired chemistry and optical properties is proposed, opening up new horizons for the application of graphene-based materials in a wide field of applications.

The reported study was funded by RFBR, project number 20-33-90278.

References

1. Papageorgiou, D.G.; Kinloch, I.A.; Young, R.J. Mechanical properties of graphene and graphene-based nanocomposites. *Prog. Mater. Sci.* 2017, 90, 75–127.
2. McChesney, J.L.; Bostwick, A.; Ohta, T.; Seyller, T.; Horn, K.; González, J.; Rotenberg, E. Extended van Hove singularity and superconducting instability in doped graphene. *Phys. Rev. Lett.* 2010, 104, 136803.
3. Shiyanova, K.A. et al. Graphene Oxide Chemistry Management via the Use of $\text{KMnO}_4/\text{K}_2\text{Cr}_2\text{O}_7$ Oxidizing Agents. *Nanomaterials*, 2021, 11(4), 915.

Formation and properties of structures based on Graphene Oxide and Detonation Nanodiamonds in water

Tudupova B.B.^{1,2}, *Shvidchenko A.V.*¹

biligma0201@gmail.com

¹ Ioffe Institute, St.Petersburg, Russia

² Peter the Great St.Petersburg Polytechnic University, St.Petersburg, Russia

Graphene due to its large specific surface area is an extremely popular electrode material in new generation energy storage devices like supercapacitors. But the main issue of formation of graphene-based electrodes for supercapacitors is stacking of atomically thin graphene flakes. It leads to reduction in specific surface area of electrode material. The solution may be in making composite material of graphene flakes and conductive nanoparticles that prevent stacking.

One of the possible solutions to this problem can be the creation of a composite based on graphene oxide (GO) and detonation nanodiamond (DND). Nanodiamond particles located between graphene flakes will prevent them stacking. Heat treatment of such composite will make it conductive.

Hereby we present the results of our research to form a composite material from aqueous dispersions of positive charged diamond nanoparticles and graphene oxide flakes in different DND/GO mass ratios. We used individual nanodiamond particles with a size 4-5 nm and their agglomerates with a size of about 100 nm.

A method for the formation of the GO-DND structures in water is proposed. The binding of GO flakes with DND particles was shown by method of static light scattering. Studies of pH and electrical conductivity of the resulting aqueous mixtures were carried out. Analysis of electrophoretic mobility of such structures showed the presence of an isoelectric point. The limit of DND adsorption to GO flakes was set.

Solid-state fluorinating agents for fluorination of graphene

Zhirov M.S.¹

zhirovmaxim@gmail.com

¹ Moscow State University, Chemistry Department, Moscow, Russia

Graphene features many notable physical properties, such as high electronic and heat conductivity. To form semiconductor zones tunable opening of the graphene bandgap can be achieved by chemical functionalization, e.g. by attachment of monovalent addends like hydrogen or fluorine. Thus, there is a need for such chemical functionalization techniques that would produce domains of pre-defined size and shape with appropriately altered electrophysical properties. Various gas-phase fluorination techniques expectably result in fluorination across the entire surface of graphene. To create the desired localization of fluorination patterns, one can prepare a respective distribution of defects by means of, e.g. bombardment with focused ion beams. Yet the remaining, defect-free portion of graphene surface will still be accessible to partial fluorination, though sparser. Alternatively, the regions intended to remain intact can be blocked with some protective entities to prevent access of gaseous fluorinating agents (such as XeF₂). Furthermore, during fluorination carbon materials can pass into the gas phase, and therefore it is necessary to carry out fluorination under soft conditions.

Solid state fluorination of graphene is one of the most diverse approaches to chemical functionalization [4]. Solid fluorinating agents that thermally release adsorbed atomic fluorine can be used for this purpose. The aim of the present work is to find convenient solid fluorinating agents for graphene fluorination.

Thermal behavior of two promising thermal sources of atomic fluorine – MnF₄ and PtF₄ – was studied by Knudsen Effusion Mass-Spectrometry (KEMS). Thermodynamic properties of these compounds have been determined. PtF₄ was formed *in situ* by fluorination of Pt and combined Pt-Ni plates of various designs. It has been found that fluorination of Pt involves migration of atomic fluorine on the surface, and it is possible to control the direction of F_{ads} flows by changing the design of the plate. Pt-F systems [Pt₂F₆-PtF₄] solid solution] appear to be highly effective fluorinating agents and are advantageously more stable compared to the deposited fluorides. In addition, such reagents are less hazardous and toxic compared to fluorine or xenon difluoride. Thus, the use of specifically profiled substrates for the graphene layer and/or the solid-phase fluorinating reagent offers a promising approach to create fluorinated zones of the desired shape and size.

References

1. Geim, A.K.; Novoselov, K.S. The rise of graphene. *Nature Materials* **2007**, *6*, 183-191.
2. Li, X.; Cai, W.; An, J.; Kim, S.; Nah, J.; Yang, D.; Piner, R.; Velamakanni, A.; Jung, I.; Tutuc, E.; Banerjee, S.K.; Colombo, L.; Ruoff, R.S. Large-area Synthesis of High-Quality and Uniform Graphene Films on Copper Foils. *Science* **2009**, *324*, 1312-1314. DOI: 10.1126/science.1171245
3. Cheng, S. H.; Zou, K.; Gutierrez, H. R.; Gupta, A.; Shen, N.; Eklund, P. C.; Sofo, J. O.; Zhu, J.; Okino, F. Reversible fluorination of graphene: Evidence of a two-dimensional wide bandgap semiconductor. *Rev. B* **2010**, *81*, 205435.
4. Norbert S. Chilingarov*, Eugene V. Skokan, Alexander V. Knot'ko, Andrei A. Eliseev, CHEMNANOMAT (2021), Vol. 7, Issue 4, pages 443-446.

Tritium labeled graphene oxide as a component of a nuclear battery

Bunyaev V.A.¹, Badun G.A.¹, Chernysheva M.G.¹, Verbetsky V.N.¹

vitalii1992@mail.ru

¹ M.V. Lomonosov Moscow State University, Moscow, Russia

Materials that include radionuclides are required for beta-voltaic sources of electric current. Currently, ⁶³Ni and tritium are considered as preferable radionuclides for a nuclear battery because its beta radiation energy is below the threshold of radiation damage of semiconductor converters. Moreover, tritium does not create radiation safety problems during operation.

In this work, we applied graphene oxide as a radiation-resistant material and tritium carrier. Tritium was introduced into graphene oxide by means of tritium thermal activation method. In this method tritium atoms are generated on a tungsten wire heated by an electric current up to 2000 K and labeled substance is located at a certain distance from the wire. Since the gas pressure is low and W-wire heating intervals are short, the target material does not experience significant thermal loads. So, tritium thermal activation method allows the introduction of tritium into the material that covers the semiconductor with a thin layer without degrading its properties.

The report presents the results of tritium labeling graphene oxide (Cheap Tubes) deposited on silicon substrates with titanium layer and on the glass walls of the reaction vessel. W-wire was heated to 2000 K during 20 - 60 s, then the residual gas was replaced with fresh portion of gaseous tritium. After the reaction, the graphene oxide was suspended in water, and after exposure, it was dried off under vacuum to remove tritium from the labile positions. Then graphene oxide was resuspended in 70 % nitric acid and heated to boiling point with a reverse refrigerator for 3 hours. The radioactivity of tritium was determined by liquid scintillation spectrometry by mixing an aliquot of such prepared solution with a scintillator that withstood nitric acid additives without reducing the registration efficiency.

The kinetic parameters of tritium accumulation in graphene oxide are determined. It was shown that there is the first-order reaction the with an effective constant equal to 0.0027 s⁻¹ and tritium content in graphene oxide is proportional to the available surface area. Since hydrogen substitution by tritium occurs in a thin layer of graphene oxide, the maximum specific activity was achieved when graphene oxide was distributed on the walls of the reaction vessel.

Note that 22 min reaction between the atomic tritium and graphene oxide results in the specific radioactivity of 3.0 Ci/mg that exceeds the specific content of tritium in the form of titanium hydride. However, the specific radioactivity decreased to 0.5 Ci/mg when tritium was removed from the labile positions of graphene oxide, but it was still sufficient for the operation of a beta-voltaic semiconductor battery. The preparation of a composite coating of a silicon semiconductor with titanium tritide with a protective layer of nickel and tritium labeled graphene oxide as an upper layer is discussed.

The work was supported by the Russian Foundation for Basic Research (Grant no. 19-08-00452).

Impact of C₆₀ based star macromolecules & ionic liquid as novel membrane modifiers on pervaporation performance in lactic acid dehydration

*Dubovenko R.R.*¹, *Rostovtseva V.A.*¹, *Pulyalina A.Yu.*¹, *Vinogradova L.V.*², *Polotskaya G.A.*²

st062444@student.spbu.ru

¹ Saint Petersburg State University, Institute of Chemistry, Saint Petersburg, Russia

² Institute of Macromolecular Compounds, Russian Academy of Sciences, Saint Petersburg, Russia

The individual specific problems of membrane separation of liquid mixtures require special developments of diffusion membranes with a purposefully formed structure, high selectivity, and permeability. One of the urgent problems is the dehydration of lactic acid, which is the most important raw material for the production of biodegradable polymers. The known methods of lactic acid purification are not economical and environmentally friendly; therefore, membrane separation processes are attracting great attention as effective energy-saving processes.

In this work, poly(2,6-dimethyl-1,4-phenylene oxide) (PPO) membrane was modified with 5 wt% of a composition consisting of a fullerene C₆₀ based star macromolecules (C₆₀-stars) and ionic liquid (IL) (1-butyl-3-methylimidazolium bis(trifluoromethylsulfonyl) imide) taken in equal amounts. The C₆₀-stars are star-shaped macromolecules in which six polystyrene chains and six chains of poly-2-vinylpyridine-*block*-poly-*tert*-butyl methacrylate are covalently attached to the common fullerene C₆₀ core.

Comparative studies on the structure and physical parameters of PPO, C₆₀-stars/PPO, and (C₆₀-stars:IL)/PPO membranes were carried out. The methods of X-ray diffraction, thermogravimetric analysis, differential scanning calorimetry, and flotation method for density determination were used. The membrane transport properties were studied during sorption experiments and pervaporation of a lactic acid–water mixture. It was found that a membrane modified by (C₆₀-stars:IL) composition is characterized by a high separation factor $\alpha_{\text{water/lactic acid}} = 2560$ and permeability equal to 16.2 g/m²·h. The most thermodynamically favorable interactions between various membrane components, which explain the experimental results, have been determined by the methods of quantum-chemical calculations.

Acknowledgments

The investigation was carried out with financial support of Russian Science Foundation (RSF), grant 18-79-10116. Equipment of Resource Centers of St. Petersburg State University, namely, “Chemical Analysis and Materials Research Centre”, “Cryogenic department” and “Thermogravimetric and calorimetric methods of investigation” were used for investigation.

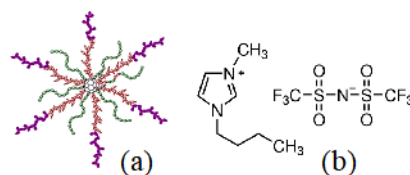


Fig.1. Star macromolecule with C₆₀ core (a) and ionic liquid (b).

3D ultrashort optical pulses in anisotropic optical medium with carbon nanotubes and an order parameter

*Kulbina A.S.*¹, *Konobeeva N.N.*¹, *Belonenko M.B.*^{1,2}

kylbinaa@mail.ru

¹ Volgograd State University, Volgograd, Russia

² Entropique Group Ltd., Dunedin, New Zealand

In this paper, we study the influence of the order parameter on the dynamics of three-dimensional ultrashort optical pulses in a nonlinear anisotropic optical medium with carbon nanotubes (CNTs). Environments with CNTs are of interest primarily for their unique nonlinear properties [1, 2], for example, they can withstand very intense electric fields. Media with a phase transition, i.e. with the order parameter, are interesting for the enormous number of practical applications [3]. Such media include all ferroelectrics and ferromagnets.

In previous studies, we took into account only one polarization (linear), when the electric field was co-directed to the axis of carbon nanotubes [4]. Here, special attention is paid to the change in the pulse shape during propagation in the anisotropic optical medium, including birefringence, as well as taking into account the effect of different orientations of the input pulse on the propagation of ultrashort pulses. Thus, in the system of equations, it is necessary to take into account two polarization directions.

We consider the dynamics of the scalar order parameter. The easiest way to obtain the equations of motion is using the phenomenological approach developed in the works of Patashinsky and Pokrovsky [3]:

$$\begin{aligned} dP/dt &= -\Gamma (\delta\Phi/\delta P), \\ \Phi &= \Phi_0 + \rho P^2 + \beta P^4 + \chi EP \end{aligned} \quad (1)$$

where Γ is the kinetic coefficient, P is the order parameter, Φ is the density of the free energy functional, which in the presence of an electric field and applied stress may be written as a Taylor expansion in terms of the order parameter P . Φ corresponds to the origin of energy for a free unpolarized and unstrained medium, and E is the applied electric field.

The dependence of the shape of three-dimensional ultrashort optical pulses on the relaxation rate of the order parameter, the equilibrium value of the order parameter, and the angle between the electric field of the pulse and the axis of nanotubes is investigated.

This work was supported by the Ministry of Science and Higher Education of the Russian Federation, RF President's Grants Council (Grant MD-3173.2021.1.2).

References

1. Yu. Astakhova, O.D. Gurin, M. Menon, and G.A. Vinogradov, *Phys. Rev. B.* (2001) **64**, 035418.
2. R. Sadykov, E.T. Muratov, I.A. Pilipenko, and A.V. Aporoski, *Physica E: Low Dimens. Syst. Nanostruct.* (2020) **120**, 114071.
3. N. Konobeeva, E.G. Fedorov, N.N. Rosanov, A.V. Zhukov, R. Bouffanais, and M.B. Belonenko, *J. Appl. Phys.* (2019) **126**(20), 203103.
4. Z. Patashinskii, V.L. Pokrovskii, *Fluctuation theory of phase transitions* (Pergamon Press, Oxford, 1979), 321 p.

Iron- and silicon-intercalated graphene on silicon carbide

Lobanova E.Yu.¹, Mikhailenko E.K.^{2,3}, Grebenyuk G.S.⁴

elobanova@itmo.ru

¹ ITMO University, St. Petersburg, Russia

² Saint Petersburg Electrotechnical University "LETI", St. Petersburg, Russia

³ Petersburg Nuclear Physics Institute named by B.P. Konstantinov of National Research Centre "Kurchatov Institute", Gatchina, Russia

⁴ Ioffe Institute, St. Petersburg, Russia

Graphene is an attractive material for various technological applications [1]. One of the most popular ways for its synthesis is the thermal decomposition of silicon carbide. This method allows to obtain high-quality large scale graphene on a dielectric substrate. However, it is accompanied by the formation of a buffer layer consisting of carbon atoms and located between graphene and the substrate [2]. The buffer layer is strongly coupled with the substrate, which causes a high rate of carrier scattering and hence negatively affects graphene transport characteristics. A promising way to reduce the interaction between the buffer layer and the substrate is the intercalation process, i.e. introduction of atoms of other substances under graphene. Intercalation can also be a tool for modifying graphene properties and synthesizing new materials. In particular, the intercalation of graphene with magnetic atoms and the creation of graphene/ferromagnet/dielectric structures is one of the possible ways to create spintronic devices based on graphene. Therefore, the present work aims to study graphene/ferromagnet/dielectric structures obtained from graphene grown on silicon carbide by its intercalation with iron and silicon atoms.

The experiments were carried out using the equipment of Russian-German laboratory at Helmholtz-Zentrum Berlin (BESSY II). Graphene-covered 4H-SiC(0001) samples were previously prepared as described in [2]. In the beginning, the samples were cleaned by annealing at 500°C. Intercalation of iron and silicon was performed using thermal deposition of thin films of these materials on the surface of samples with subsequent annealing at various temperatures. Characterization of the samples was done by photoelectron spectroscopy (PES) and low energy electron diffraction (LEED). The optimal conditions of iron and silicon intercalation are realized in the temperature range of 400-500°C. Subsequent intercalation of graphene with iron and silicon leads to the formation of Fe-Si solid solution layer covered with surface silicide Fe₃Si.

Ab initio calculations were done using density functional theory (DFT) as implemented in open-source software Quantum ESPRESSO [3]. It is shown that intercalated metal and silicon atoms are localized between the buffer layer and the substrate. Formation of a metal film under graphene is accompanied by a strong hybridization of the states of iron and carbon atoms of the buffer layer. Further introduction of silicon atoms leads to the relaxation of the buffer layer and its transformation into the second graphene layer.

References

1. K.S. Novoselov, D.V. Andreeva, W. Ren, G. Shan, *Front. Phys.* (2019) **14**, 13301.
2. V.Y. Davydov, D.Y. Usachov, S.P. Lebedev, A.N Smirnov, V.S. Levitskii, I.A. Eliseyev, P.A. Alekseev, M.S. Dunaevskiy, O.Y. Vilkov, A.G. Rybkin, A.A. Lebedev, *Semiconductors* (2017) **51(8)**, 1072.
3. P. Giannozzi, O. Andreussi, T. Brumme, O. Bunau, M.B. Nardelli, M. Calandra, R. Car, C. Cavazzoni, D. Ceresoli, M. Cococcioni, N. Colonna, *J. Phys.: Condens. Matter.* (2017) **29**, 465901.

Preparation and properties of Myramistin-hyaluronic acid coatings on the nanodiamond surface

*Sinolits A.V.*¹, *Votyakova V.S.*¹, *Petrova V.I.*¹, *Chernysheva M.G.*¹, *Badun G.A.*¹

mighty-mouser@yandex.ru

¹ M.V. Lomonosov Moscow State University, Moscow, Russia

Detonation nanodiamonds (DND) are a promising platform for drug delivery with controlled release [1]. Developed surface of nanodiamonds provides high adsorption capacity and possibility of formation of stable adsorption complexes with drugs including antibiotics. The example of such complex that was previously obtained and well described is nanodiamond-myramistin composite [2-4]. Being surface active compound myramistin can form adsorption complexes with both positively and negatively charged nanodiamonds [3].

When nanodiamond is proposed as a drug delivery platform or as a covering material for biological tissues, its biocompatibility is critically important. To provide biocompatibility to nanodiamond-antibiotic composite coating with biological material is considered as a perspective tool. Hyaluronic acid is a promising material in this capacity.

Nanodiamond produced by PlasmaChem (Germany) as a powder as well as a suspension were used to prepare nanodiamond-myramistin-hyaluronic acid complexes. To reveal a direct amount of both myramistin and hyaluronic acid in the complex, tritium labeled compounds were used. Tritium label was included either in drug or in biopolymer, so the amount of labeled compound can be determined by means of liquid scintillation spectrometry on the background of non-labeled component.

The following questions were considered: (1) how myramistin coverage influence on hyaluronic acid adsorption in wide range of biopolymer concentration; (2) how hyaluronic acid molecular weight influence on the adsorption, (3) how myramistin surface concentration influence the hyaluronic acid adsorption; and finally (4) how stable the adsorption complexes are in biological-alike media.

Zeta potential of nanodiamond play a key role in the adsorption process that is under strong influence of the presence of drug. It was found that maximum adsorption of hyaluronic acid occurs, when zeta-potential is close to 20 mV, it can be reached either by application of initially positively charged nanodiamond or by adsorption of myramistin. Adsorption of hyaluronic acid on nanodiamonds converts zeta potential of positively charged nanodiamonds and does not influence on zeta potential of negatively charged nanodiamonds, but significantly adsorbes on its surface. Peculiarities of nanodiamond-myramistin-hyaluronic acid adsorption complexes formation will be described in the presentation.

This work was supported by Russian Foundation for Basic Research (grant № 19-33-90151).

References

1. Benson, A. Amini., *Cancer Drug Resist.* (2020), **3**, 854.
2. G. Chernysheva, A.G. Popov, V.N. Tashlitsky, G.A. Badun, *Colloids Surfaces A Physicochem. Eng. Asp.* (2019) **565**, 25.
3. G. Chernysheva, N.S. Melik-Nubarov, I.D. Grozdova, I.Y. Myasnikov, V.N. Tashlitsky, G.A. Badun, *Mendeleev Commun.* (2017), **27**, 421.
4. V. Sinolits, M.G. Chernysheva, O.D. Matveeva, A.G. Popov, G.A. Badun, *Fullerenes, Nanotub. Carbon Nanostructures* (2020) **28**, 299.

Day 4: Nanodiamond Particles. Fullerenes.

Influence of modification of tetryl detonation nanodiamonds on the combustion process of model pasty rocket fuels (RF)

Naryzhny S.Yu.¹, Dolmatov V.Yu.¹, Kozlov A.S.¹, Fomenko V.V.¹, Semashkin G.V.¹, Marchukov V.A.¹, Desyatov S.V.¹

diamondcentre@mail.ru

¹ Federal State Unitary Enterprise "Special Design and Technological Bureau "Technolog", St. Petersburg, Russia

The most important problem is the disaggregation and uniform distribution of disordered aggregates of detonation nanodiamonds (DND) in the fuel composition. DND disaggregation was carried out by thermalizing a dry powder in air at a temperature of 425-430 °C for 2 hours, the sizes of aggregates decreased from 127 nm to 58 nm. Then DNDs were introduced into a concentrated solution of ammonium perchlorate (APC) and precipitated with isopropyl alcohol on the surface of APC granules.

Investigated 3 formulations - (№ 1 - basic), № 2 and № 3 additionally contained DND and DB (diamond-containing blend), respectively, 2.5% wt. based on the finished RF.

The laws of combustion of the compounds were determined:

- Recipe № 1: $U(P) = 1,43 + 3,681(P-1)^{0,480}$, $0 < P < 1100$ atm.
- Recipe № 2: $U(P) = 1,95 + 6,002(P-1)^{0,424}$, $0 < P < 1100$ atm.
- Recipe № 3: $U(P) = 2,81 + 6,192(P-1)^{0,392}$, $0 < P < 150$ atm.

Findings:

1. The use of APC granules coated with DND or DB leads to an increase in the combustion rate of the fuel composition and a decrease in the temperature of the combustion products of the composite propellant. Both factors have a beneficial effect on the operation of the rocket fuel system and increase its efficiency.
2. The advantage of DND introduced as part of the oxidizer is a high increase in the rate of fuel combustion by 26.5% and a decrease in the temperature of combustion products by 242 °C at 100 atm.
3. The use of DB, introduced in the composition of the oxidizing agent, gives an increase in the rate of 15.7% at 100 atm. This value is less than that of an oxidizing agent with DND, but the use of DB is more preferable from an economic point of view.

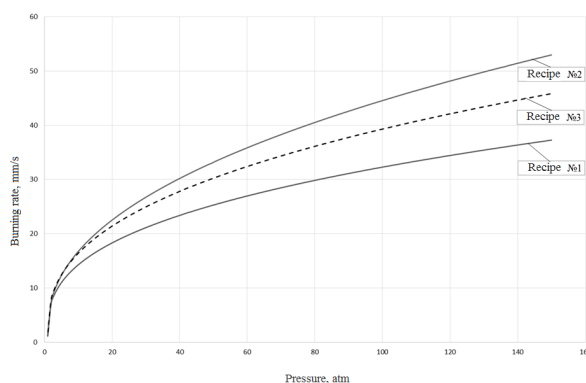


Figure 1. Dependences of the combustion rate of the compositions (U) on the pressure U(P) in the pressure range up to 150 atm.

Complexes of nanodiamonds with Gd-fullerenols for biomedicine

*Lebedev V.T.*¹, *Kulvelis Yu.V.*¹, *Peters G.S.*², *Bolshakova O.I.*¹, *Sarantseva S.V.*¹, *Popova M.V.*¹, *Vul A.Ya.*³

lebedev_vt@pnpi.nrcki.ru

¹ Petersburg Nuclear Physics Institute named by B.P.Konstantinov, NRC "Kurchatov Institute", Gatchina, Leningrad distr., Russia

² NRC "Kurchatov Institute", Moscow, Russia

³ Ioffe Institute, St.-Petersburg, Russia

Development of structures composed of nanoparticles with different type of orbital hybridization of carbon (sp^2 , sp^3) makes it possible to create new biomedical materials luminescent or magnetic and modified by lanthanides for the applications in Photodynamic Therapy or Magneto-Resonance Imaging. The results are devoted to the synthesis, physical-chemical and synchrotron studies of complexes of detonation nanodiamonds (DND, particle size 4-5 nm) and fullerlenols $Gd@C_{82}(OH)_x$ ($X \sim 30$) (Fig.1). The complexes formation, structure and self-assembly in aqueous media were studied for the systems which differ by the sign of diamond surface ζ -potential (± 30 -40 mV) [1,2]. The association of positively charged particles DND Z+ and electro-negative fullerlenols creates the complexes being stable under heating (25-70°C) while the assembly of fullerlenols with DND Z- particles is less probable. The X-ray scattering revealed a formation of diffusive borders of DND Z+ particles due to adsorbing fullerlenols. It strengthened the association of diamonds into chain-like cluster structures [1,2]. Such ordering into fractal aggregates became more stable due to additional linking of diamond particles via fullerlenols. The complexing intensified magneto-resonance properties of fullerlenols as compared to their pristine characteristics in solutions. The series of tests on biological cells have confirmed low toxicity of the examined complexes that allows to use them as prospective biomedical materials.

The work was supported by the Russian Foundation for Basic Researches (gr. No 18-29-19008).

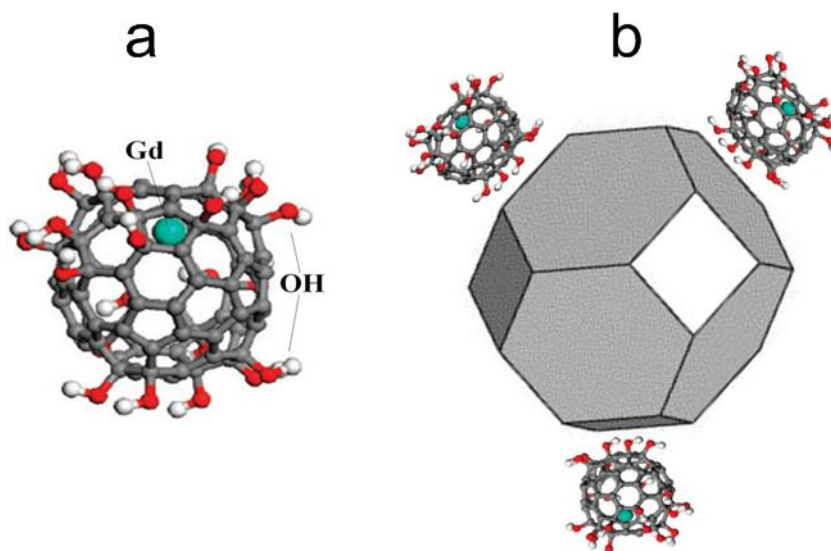


Fig.1. Fullerenol $Gd@C_{82}(OH)_x$ ($X \sim 30$) and diamond DND Z+ interacting with fullerlenols (a,b).

References

1. A.Ya. Vul, E.D. Eidelman, A.E. Aleksenskiy et al., Carbon (2017) **114**, 242.
2. V.T. Lebedev, Yu.V. Kulvelis, V.V. Runov, J. of Surface Invest.: X-ray Synch. and Neut. Techn. (2020) **14**, 134.

On mechanism of diamond growth: role of atomic carbon

*Leshchev D.V.*¹, *Gorbachev Y.E.*²

dimvovich@narod.ru

¹ Center for Advanced Studies of Peter the Great Saint-Petersburg Polytechnic University, Saint-Petersburg, Russia

² Coddan Technologies LLC, Saint-Petersburg, Russia

Chemical vapor deposition (CVD) of diamonds is not only a well-developed technique with many existing and potential commercial applications [1,2], but also a convenient system for investigation the process of diamond deposition [3]. The CVD technology involves the use of a low-pressure reactor into which molecular hydrogen with small admixture of hydrocarbon (generally methane) is injected. The mixture composition, as well as gas and substrate temperatures and pressure, determine the ultimate structure and quality of the growing diamond [4,5].

A significant progress has been achieved both in synthesis of the diamonds and in modeling of the gas-dynamic processes within the direct simulation Monte Carlo (DSMC) method [3,6] and continuum approach [7,8]. However, a mismatch between the computational results and the experiment has been observed [8].

Usually, it is assumed that the main species contributing diamond growth is a methyl radical. Based on a quantum chemistry modelling we have shown that an atomic carbon can effectively deposit directly on a surface. Proposed model, that includes both C and CH₃ deposition, has been confirmed by gas dynamic simulations which agree with the experimental data. Thus, we can conclude that the methyl plays a role of diamond phase (sp³-hybridization) formation holder and atomic carbon contributes to the growth of diamond compatible, or even greater than methyl.

Acknowledgements. This work was partially supported by the Russian Foundation for Basic Research (project № 19-08-00533) and by the Ministry of Science and Education of Russian Federation (project № 0784-2020-0025).

References

1. May, Philos. Trans.R. Soc. (2000) **A 358**, 473.
2. K.Rebrov, Physics-Uspekhi (2017) **60:2**, 179.
3. A.Emelyanov, M.Y.Plotnikov, I.B.Yudin, Journal of Physics: Conference Series (2018) **1105**, 012120.
4. K.Rebrov, M.N.Andreev, T.T.Bieiadovskii, K.V.Kubrak, Surface and Coatings Technology (2017) **325**, 210.
5. Rebrov, M.Plotnikov, Y.Mankelevich, I.Yudin, Physics of Fluids (2018) **30**, 016106.
6. Y.Plotnikov, E.V.Shkarupa, Journal of Physics: Conference Series (2018) **1105**, 012110.
7. Gorbachev, Yu E., et al. Journal of Physics: Conference Series (2019) **1382**, 012152.
8. E. Gorbachev, D.V.Leshchev, FNCN (2020) **28.4**, 277.

Nanodiamonds as a component for composite solid electrolytes

Mateyshina Yu.G.^{1,2,3}, *Alekseev D.V.*^{2,1}, *Uvarov N.F.*^{1,2,3}

yuliam@solid.nsc.ru

¹ Institute of Solid State Chemistry and Mechanochemistry SB RAS, Novosibirsk, Russia

² Novosibirsk State University, Novosibirsk, Russia

³ Novosibirsk State Technical University, Novosibirsk, Russia

Solid-state electrochemical devices are more resistant to mechanical stress and temperature extremes than traditional ones, which use liquid or polymer electrolytes. To create them, it is necessary to use solid electrolytes with high ionic conductivity (10^{-3} - 10^{-1} S/cm), chemically and thermally stable over a wide temperature range. Thus, the search for new solid electrolytes remains an urgent problem of solid state ionics.

It is well known that the transition from individual compounds to composite solid electrolytes of the "ionic salt - inert oxide" (MX-A) type can increase the ionic conductivity of many common salts [1-2]. To date, there is a lot of experimental data on composite solid electrolytes with various oxide additives. On the other hand, there is practically no information on the effect of non-oxide heterogeneous dopants on the properties of ionic salts.

Nanodiamonds are a unique material with a number of unusual properties. At the same time, in terms of cost, nanodiamonds outperform such popular nanomaterials as, for example, nanographene, fullerene, and others. Recent studies have shown that nanodiamonds can be used to create nanocomposite materials, nanoelectronic elements, selective adsorbents and catalysts, and medical materials. The use of nanodiamonds improves the quality of microabrasive and polishing compounds, lubricating oils, abrasive tools, polymer compositions, rubbers, and makes it possible to grow diamond films on various substrates. Previously, there were no data in the literature on the use of nanodiamonds in power engineering for the synthesis of solid electrolytes. Nanodiamonds (ND) are characterized by a high specific surface area of 300 m² / g. In addition, the properties of the ND surface can be controlled by appropriate processing. Our studies show that nanodiamonds as additives in solid composite electrolytes lead to an increase in conductivity by 2-3 orders of magnitude with respect to the initial salt [3-5]. The work will carry out a comparative analysis of transport properties of various composite electrolytes type MX-ND.

The studies were supported by RFBR according to research project No. 18-29-11054-mk and Russian Science Foundation, project No. 20-13-00302.

References

1. Ivanov-Schitz, A.K., Murin, I.V., Solid state ionics (in Russian), St. Petersburg: S.-Peterburg. Univ, 2010. 1000 p.
2. N.F., Composite solid electrolytes (in Russian), Novosibirsk: Publishing House SB RAS, 2008. 258 p.
3. Mateyshina, Yu., Alekseev, D., Uvarov, N. The effect of the nanodiamonds additive on ionic conductivity of silver iodide, *Materials Today: Proceedings*, 2020, 25, p. 373.
4. Alekseev, D.V., Mateyshina, Yu.G., Komarov, V.Yu., Sevast'yanova, E.V., Uvarov, N.F., Synthesis and characterization of solid composite electrolytes LiClO₄ - Nanodiamonds, *MaterialsToday:Proceedings*, 2020, V.31, part 3, p. 576.
5. Mateyshina, Y.G., Alekseev, D.V., Uvarov, N.F., Ionic Transport in CsNO₂-Based Nanocomposites with Inclusions of Surface Functionalized Nanodiamonds. *Nanomaterials* 2021, 11, p. 414.

Evaluation the Amount of NV centers in 3-nm Detonation Nanodiamonds by Half Magnetic Field ESR Method

*Osipov V. Yu.*¹, *Takai K.*², *Ishiguro Y.*², *Romanyuk O.*³, *Stehlik S.*³

osipov@mail.ioffe.ru

¹ Ioffe Institute, St.Petersburg, Russian Federation

² Department of Chemical Science and Technology, Hosei University, Tokyo, Japan

³ Institute of Physics ASCR, Prague, Czech Republic

Introduction. X-band electron spin resonance (ESR) is a powerful tool for characterization paramagnetic defects in solids. Recently triplet NV centers were successfully identified in ordinary detonation nanodiamonds (DND) having the mean size ca. 5 nm. Such centers provide weak, but reliably detected photoluminescence in the red range of spectra. The intensity of such luminescence depends both upon the concentration of NV and their crystalline environment often working for quenching the main radiation recombination channel due to its high defectiveness. Recently the new technological approach permitting to reduce the mean size of DNDs down to 3-nm was proposed by Stehlik *et al* [1,2]. In this research we study the paramagnetic properties of these 3-nm DNDs mainly functionalized by oxygen-containing groups.

Results. Similarly to the ordinary commercially fabricated 5-nm DNDs the obtained 3-nm DNDs demonstrate two enough broad ESR signals located at the resonance magnetic field $H_{\text{res}} \approx 325$ mT ($\nu \approx 9.10$ GHz) and in the half-magnetic field range at $H \sim H_{\text{res}}/2$. First ESR signal of Lorentzian shape is related with dangling bond spins ($S=1/2$) and other intrinsic spin-half species (like paramagnetic nitrogen) in the interior of nanoparticles ($g=2.0027$). The second signal located in the half-magnetic field range consists of two single components ($g_1=4.27$ and $g_2=4.00$) separated by ~ 10 mT distance and caused by NV triplet centers ($S=1$) and spin-one multivacancies correspondingly. Double integration of the first component $g_1=4.27$ permits us to evaluate the concentration of NV in DND powder. In ordinary 5-nm DNDs this concentration is about ~ 1 ppm, although some researchers predict the value of one order of magnitude smaller. Careful comparison of $g_1=4.27$ and $g=2.0027$ ESR signals in both 3-nm DND and 5-nm DND shows that reducing the mean particle size down to 3-nm does not lead to the essential change in NV content although the concentration of main paramagnetic centers (both surface dangling bond spins and paramagnetic nitrogen) drops in two times. It probably means that the main spin-half paramagnetic defects of 5-nm DND particles are predominantly located in the thin sub-surface layer (<1.5 nm) of DND, whereas the NV centers are located in the sp^3 interior of nanoparticles. Etching the DND particles at 520°C in air to a great extent removes this defective layer and the new fresh surface becomes less defective and paramagnetic. This correlates well with the Raman spectra showing lower non-diamond carbon content in the 3 nm DND than in 5 nm DND. X-ray photoelectron spectroscopy (XPS) analysis of incorporated nitrogen (N 1s peak) revealed two bonding states of nitrogen (399 and 402.5 eV) in the DNDs whose ratio changed when DND size decreased from 5 to 3 nm. In contrast, only one bonding state of N in NV luminescent HPHT NDs was found at ~ 400 eV originating from sp^3 -C-N bonds.

Estimation the concentration of main paramagnetic agents with spin-half and spin-one in 3-nm DND gives us some clue about their original distribution in the parent 5-nm DNDs.

References

1. Stehlik et al., Scientific Reports 2016, 6:38419
2. Stehlik et al., ACS Appl. Mater. Interfaces 2017, 9, 38842-38853

Sonication assisted advanced oxidation process: hybrid method for deagglomeration of detonation nanodiamond particles

Shestakov M.S.¹, Shvidchenko A.V.¹, Yudina E.B.¹, Besedina N.A.², Koniakhin S.V.^{2,3}, Kirilenko D.A.¹, Dideikin A.T.¹

mikhail.shestakov@gmail.com

¹ Ioffe Institute, St.Petersburg, Russia

² Alferov University, Saint-Petersburg, Russia

³ Institut Pascal, PHOTON-N2, Universite Clermont AUvergne, CNRS, SIGMA Clermont, Clermont-Ferrand, France

A new approach for detonation nanodiamond (DND) deagglomeration is proposed. DND agglomerates of the size from 20 to 200 nm have been exposed to wet sonication assisted oxidative treatment with ozone under UV irradiation (Advanced Oxidation Process). Subsequent sonication and centrifugation gave a stable hydrosol of single crystal nanoparticles with negative zeta potential of -65mV. The yield of the desired 4 - 5 nm fraction reached 33%. Powder X-Ray Diffraction study showed no signs of DND crystalline core degradation, while the surface of particles was enriched significantly with carboxyl functional groups according to the data of Diffuse Reflectance Infrared Fourier Transform Spectroscopy, that gave boost to the stability of DND hydrosol. The approach provides relatively high yield deagglomeration of detonation nanodiamond without impact of high temperatures to the DND particles. It also allows to avoid gas phase processes sticking to wet-chemistry that could be useful for process scalability.

Influence of the size of detonation nanodiamond particles on their electrostatic properties in hydrosols

*Shvidchenko A.V.*¹, *Yudina E.B.*¹, *Zhukov A.N.*²

avshvid@mail.ioffe.ru

¹ Ioffe Institute, St.Petersburg, Russia

² St.Petersburg University, St.Petersburg, Russia

The electrostatic properties of deagglomerated particles of detonation nanodiamond (DND) with different sizes of monocrystals have been experimentally studied in aqueous electrolyte solutions. The acid-base potentiometric titration and laser Doppler electrophoresis have been employed to obtain the pH dependences of the surface charge density and electrophoretic mobility of the nanoparticles in hydrosols containing 0.001 M KCl within a pH range of 3.5-10.5.

Deagglomeration of DND particles was carried out using the method described in [1]. A fine separation of deagglomerated DND particles by size in hydrosols was carried out by centrifugation. Three samples were obtained with average sizes equal to 4.4 nm, 3.6 nm and 3.3 nm (from X-ray diffraction data).

It is shown that a decrease in the average size of DND nanoparticles leads to an increase in the absolute values of the density of their negative surface charge. The high surface potential values calculated for these DND samples are independent of the nanoparticle size. The absolute values of the electrokinetic charge density increase significantly with a decrease in the particle size [2].

References

1. Aleksenskiy A.E., Eydelman E.D., Vul' A.Ya. *Nanosci. and Nanotech. Lett.*, 2011, Vol. 3, No. 1, pp. 68-74.
2. Shvidchenko A.V., Yudina E.B., Zhukov A.N. *Colloid Journal*, 2020, Vol. 82, No. 4, pp. 369-375.

Dielectric spectroscopy study of detonation nanodiamonds self-organization in oil suspensions

Vdovichenko A.Yu.^{1,2}, *Kuznetsov N.M.*¹, *Shevchenko V.G.*², *Belousov S.I.*¹, *Yudina E.B.*³, *Chvalun S.N.*^{1,2}

vdartem@ya.ru

¹ National Research "Center Kurchatov Institute", Moscow, Russia

² Enikolopov Institute of Synthetic Polymeric Materials RAS, Moscow, Russia

³ Ioffe Institute, St. Petersburg, Russia

Detonation nanodiamonds in liquid media (such as water and silicone oil) have an increased viscosity and yield stress at extremely low concentrations (several wt%). This behavior was explained in terms of the percolation theory and the formation of chains from interacting nanodiamond particles [1,2]. Obviously, the electrophysical characteristics, in particular, the conductivity and permittivity, as well as the dependence of these parameters on concentration, are of great importance in the process of the particles self-organization in a liquid medium.

Broadband dielectric spectroscopy is a direct method for studying charge states and their dynamics. In this work, the electrophysical characteristics of nanodiamond particles were investigated in a non-polar mediums: low molecular weight polydimethylsiloxane and mineral oil with a filler concentration from 1 to 4 wt%. Two types of nanodiamond particles with different functional groups on the surface -CH and -COOH have been studied. It was found that the electrophysical properties of nanodiamond suspensions significantly depend on the chemical composition of the particle surface. Thus, the conductivity of hydrogenated nanodiamonds dispersions is almost two orders of magnitude higher than that of samples with a negative one. The effect of the particles surface functionalization on the electrophysical properties of suspensions was found and comprehended from the standpoint of their structural self-organization. The temperature dependences of the dielectric spectra show that nanodiamonds have a tendency to secondary agglomeration and the formation of extended structures. A model of self-organization of nanodiamond particles in a polydimethylsiloxane medium is proposed.

This work was funded by the Russian Foundation for Basic Research (grant 18-29-19117 mk).

References

1. Kuznetsov N.M., Belousov S.I., Bakirov A.V., Chvalun S.N., Kamyshinsky R.A., Mikhutkin A.A., Yudina E.B., Vasiliev A.L., Tolstoy P.M., Mazur A.S., Eidelman E.D., Yudina E.B., Vul, A.Y., Carbon (2020) **161**, 486
2. Kuznetsov N.M., Belousov S.I., Kamyshinsky R.A., Vasiliev A.L., Chvalun S.N., Yudina E.B., Vul A.Y. Carbon (2021) **174**, 138

Influence of nitrogen on the synthesis of diamonds during gas-jet HWCVD deposition.

Yudin I.B.¹, Emelyanov A.A.¹, Plotnikov M.Yu.¹, Rebrov A.K.¹, Timoshenko N.I.¹

yudinib@gmail.com

¹ Kutateladze Institute of Thermophysics of SB RAS, Novosibirsk, Russia

Nitrogen is ubiquitous in both natural and laboratory-grown diamonds, but the number and nature of nitrogen-containing defects can have a profound effect on a diamond material and its properties. The growing availability of diamond samples grown under well-defined conditions has made it possible to achieve significant advances in the characterization and understanding of nitrogen-containing defects in diamonds [1]. The appearance of nitrogen components in mixtures of precursor gases activated thermally and with hydrogen atoms affects both the gas-phase chemistry and the properties of the activating surfaces. In particular, the addition of nitrogen to the gas mixture makes it possible to control the crystal structure during growth by changing the growth ratio of the {100} and {111} faces, accelerating the growth in the direction of {100} up to 4 times [2]. All of the above stimulates the development of new approaches to the synthesis of diamond films using nitrogen additions.

Gas-phase deposition using thermal activation of precursor gases (HWCVD) is widely used for the synthesis of diamond structures. In recent years, a gas-jet modification of the method has been actively developing [3, 4]. The gas-jet method has a number of advantages, of which the main one is the possibility of wide variations in the parameters that determine the technological process, such as the specific mass flow of precursor gases, temperature, heat content, and pressure. The use of a supersonic gas flow expanding into a region with low pressure makes it possible to "freeze" active components. Another distinctive feature of the approach under consideration is that the activation of the components of a mixture of hydrogen with a carbon-containing gas is achieved with the use of a tungsten channel heated to high temperatures and providing a high degree of particle activation due to multiple collisions with the surface when the mixture flows through the channel.

The presented work is devoted to the study of the characteristics of the synthesis of diamond structures by the gas-jet method when a small amount of nitrogen is added to the mixture of precursor gases. In the course of the study, a number of experiments were carried out both with the supply of a mixture of hydrogen and methane without nitrogen additions and with nitrogen additions from 0.25 to 2 sccm. The pressure in the deposition chamber was maintained at 20 Torr. The deposition was carried out on a molybdenum substrate. A more detailed description of the experimental setup and experimental technique is given in [3]. The morphology of the synthesized diamond structures was analyzed using electron micrographs and Raman spectra. The performed analysis showed a significant effect of the addition of nitrogen on the structure and quality of synthesized crystals, as well as on the rate of their synthesis under the selected conditions. This encourages continued research on the effects of using nitrogen.

This work was carried out with partial support from the Russian Foundation for Basic Research (grant 19-08-00533) and the state contract with IT SB RAS (grant 121031800218-5).

References

1. N.R. Ashfold, J.P. Goss, B.L. Green, P.W. May, M.E. Newton, C.V. Peaker, *Chem. Rev.*(2020) **120**, 5745.
2. Yiming, F. Larsson, K. Larsson, *Theor. Chem. Ass.* (2014) **133**, 1432.
3. A. Emel'yanov, A.K. Rebrov, I.B. Yudin, *Tech. Phys.* (2016) **61(12)**, 1821.
4. K. Rebrov, M.N. Andreev, T.T. Bieiadovskii, K.V. Kubrak, *Surface & coatings technology* (2017) **325**, 210.
5. Firstauthorname, B. Second, Here Goes the Title of the Book (Publisher, City, year), p. 111.

Langmuir hydrogen atomization as a novel approach for nanodiamond treatment

Chernysheva M.G.¹, Badun G.A.¹, Popov A.G.¹, Egorov A.V.¹

chernysheva@radio.chem.msu.ru

¹ M.V. Lomonosov Moscow State University, Moscow, Russia

Hydrogen dissociation on the surface of hot tungsten filament with the formation of atoms was developed by I. Langmuir [1]. This approach has proven itself as a promising tool for hydrogen isotopes introduction into different organic substances including carbon-base nanomaterials. To prevent substances destruction under the influence of atomic hydrogen (or its isotopes) the reaction is performed during 10 – 30 s by 10 s exposures under low gas pressure providing free path-length from hot tungsten catalyst to the cooled target surface. Such technique allows introduction of hydrogen isotopes into molecules with preservation of its physical properties.

In our previous researches we have shown that this approach can be successfully used for tritium labeling nanodiamonds [2]. Unfortunately, the amount of tritium can be determined by liquid scintillation spectroscopy only, while the position of tritium besides that it is not in an exchangeable position in the composition of functional groups, cannot be determined. So, in present research we subjected nanodiamonds to the interaction with atomic hydrogen generated by Langmuir's technique for a long time to reveal the result of the reaction by means of FTIR-spectroscopy.

We used nanodiamond powder (Aldrich) as received and powder sample subjected to air annealing during 1 h at 450°C. Nanodiamond powder was suspended in water by sonication and equally distributed on the glass walls of the reaction vessel and lyophilized. The reaction with atomic hydrogen was performed by means of special device designed for gaseous hydrogen during 4 min by 10 s exposures under 1.0 Pa gas pressure. After the reaction the solid material was suspended in water and analyzed by means of dynamic light scattering and electrophoretic light scattering methods. It was found that in both cases (initial and preliminarily annealed samples) electrophoretic potential turned to lower values: from 30 mV to 15 mV and from -50 mV to -30 mV for non-annealed and air-annealed samples respectively, while particles diameter was increased.

Suspensions were lyophilized and solid materials were analyzed by FTIR for revealing changes in the surface functional composition and morphology of the material was analyzed by transmission electron microscopy. FTIR-spectroscopy results revealed that besides the increase in the intensity of the signals corresponding to C_{sp3}-H-bonds the decrease of the amount of bonded water for both initial and preliminarily air-annealed samples. Such data are correlates with the results of zeta potential changes. Moreover, several changes in CO-containing functional groups were observed indicated peculiarities of the mechanism of interaction of hydrogen atoms with nanodiamond surfaces. Note that widely used annealing in hydrogen atmosphere results in the reduction of carboxyl and carbonyl groups, while treatment with hydrogen atoms by few-seconds exposures results in selective reduction of oxygen containing groups and preserves functional development of nanodiamond surface. TEM images indicated the formation of long chains by nanodiamonds preliminarily subjected to air annealing even after interaction with atomic hydrogen, while initial nanodiamonds forms shorter chains and more viewable structures when subjected to atomic hydrogen treatment.

References

1. Langmuir, J. Am. Chem. Soc. (1912), **34**, 1310.
2. Y. Myasnikov, A. V. Gopin, I. V. Mikheev, M.G. Chernysheva, G.A. Badun, Mendeleev Commun. (2018), **28**, 495.

Possible mechanism for the formation of detonation nanodiamonds.

*Dolmatov V.Yu.*¹, *Ozerin A.N.*², *Vehanen A.*³, *Myllymaki V.*³, *Dorokhov A.O.*⁴, *Almazova N.S.*¹
diamondcentre@mail.ru

¹ Federal State Unitary Enterprise "Special Design and Technological Bureau "Technolog", St. Petersburg, Russia

² Federal State Budgetary Institution of Science Institute "Institute of synthetic polymeric materials named after N.S. Enikolopov RAS", Moscow, Russia

³ "Carbodeon Ltd. Oy", Vantaa, Finland

⁴ JSC "Plastmass" Plant", Kopeysk, Chelyabinsk region, Russia

It is assumed that a fractal carbon network with fluctuations in the density of carbon in the plasma of the chemical reaction zone (CRZ) occurs during the explosive decomposition of explosives (HE). At the "nodes" of this grid, the most dense carbon condensate has time to form a three-dimensional ordered core.

The carbon plasma behind the Chapman-Jouguet plane first becomes liquid carbon and then crystallizes into detonation nanodiamond (DND) crystallites. The crystallization process is completed in the range 1/3-3/4 of the diameter of the charge from the front of the detonation wave.

Conclusion:

1. It is assumed that condensed carbon in the zone of chemical reactions should have a density in the range of 2.5-3.2 g/cm³ in accordance with its determination in plasma by the SAXS method.
2. The appearance of a fractal carbon network with simultaneous fluctuations of the carbon density in the CRZ with the formation of a three-dimensional ordered nucleus at the nodes of the network is possible.
3. The time of chemical reactions in the CRZ is within the range of 0.1-0.3 μs, and the width of the CRZ is from 0.4 to 1.4 mm for the formation of DND.
4. The lifetime of a relative plateau for TNT-RDX compositions (the most preferred of mixed explosives for DND formation) is from ~ 1.8 μs to ~ 4.4 μs, which corresponds to a distance from the detonation wave front of 1/3 - 3/4 of the charge diameter. Next comes the decrease in the size of the DB particles.
5. A high DND yield (more than 6% wt.) is achieved when 20 ± 2% wt. is spent on its formation from the total carbon explosive.
6. The formation of DND from TATB, as in the case of RDX, takes only 5% wt. from the total carbon in the molecules of these individual HEs.

This work was carried out with partial support of the RFBR grant within the framework of scientific project № 18-29-19112.

Emission of GeV colour centre ensembles in HFCVD nanodiamonds

Grudinkin S.A.^{1,2}, *Feoktistov N.A.*¹, *Bogdanov K.V.*², *Baranov M.A.*², *Baranov A.V.*², *Golubev V.G.*¹

grudink.gvg@mail.ioffe.ru

¹ Ioffe Institute, St. Petersburg, Russia

² ITMO University, St. Petersburg, Russia

Impurity-vacancy color centers in nanodiamonds have attracted the attention of researchers as atom-like emitters for optical quantum technologies, biomedical markers, and temperature nanosensors [1, 2]. Among the most promising centers are negatively charged germanium-vacancy center (GeV) with zero phonon line (ZPL) at 602 nm. The GeV centers possess superior optical properties: a sharp ZPL (~5 nm at room temperature), high Debye-Waller factor (with nearly 80% of its emission is within ZPL), a short photoluminescence lifetime of 1.4-5.5 ns [1]. For quantum optics application it is important that nanodiamonds with embedded color centers can be integrated with photonic devices due to their small sizes.

In this work, we realized a top-down method to fabricate nanodiamonds with embedded GeV centers. The nanodiamonds were produced by reactive ion etching in oxygen plasma of heteroepitaxial diamond particles grown by Hot Filament Chemical Vapor Deposition (HFCVD) technique on silicon [3]. The size of diamond nanoparticles obtained after etching was within the range of 100 to 300 nm. Bulk crystalline germanium situated on the substrate holder during CVD growth was used as solid state source of Ge atoms [4]. The etching of the solid-state sources of Ge with atomic hydrogen gives rise to the volatile radicals GeH_x. Germanium atoms being incorporated into the diamond lattice from the gas phase promoted the formation of an ensemble of GeV center in nanodiamonds.

A linewidth of the diamond Raman line (at 1332.1 cm⁻¹) for nanodiamonds is about ~3.6 cm⁻¹. The photoluminescence spectra of nanodiamonds were measured in the temperature range of T=79-300 K. In the visible range the photoluminescence spectra of nanodiamonds have nearly no broad photoluminescence line, with strong ZPL of ensembles of GeV color centers with a linewidth of ~6 nm at T=300 K. At T=77 K the ZPL of GeV center split into the doublet due to lifting the orbital degeneracy of the ground and excited states [1]. It was found that at T=77 K high-resolution ZPL spectra of the ensembles GeV centers in the nanodiamonds consist of more than one doublets with different spectral positions. For various nanodiamonds the spectral positions of the ZPL doublets are dispersed in the range of ~600-604 nm. Such a spectral dispersion in the ZPL emission is owing to crystal strain inhomogeneity in the nanodiamonds. The strain response of a doublet structure of the ensembles of GeV ZPL and its analysis provides a way to optically image the strain distribution in CVD nanodiamonds.

This work was supported by the Russian Science Foundation (Agreement 21-12-00264).

References

1. C. Bradac, W. Gao, J. Forneris, M. Trusheim, I. Aharonovich, *Nat. Commun.* (2019) **10**, 5625.
2. J.W. Fan, I. Cojocar, J. Becker, I.V. Fedotov, M.H.A. Alkahtani, A. Alajlan, S. Blakley, M. Rezaee, A. Lyamkina, Y.N. Palyanov, Y.M. Borzdov, Y.P. Yang, A. Zheltikov, P. Hemmer, A.V. Akimov, *ACS Photon.* (2018) **5**, 765.
3. S. Grudinkin, N. Feoktistov, K. Bogdanov, A. Baranov, V. Golubev, *Tech. Phys. Lett.* (2020) **46**, 871.
4. S.A. Grudinkin, N.A. Feoktistov, K.V. Bogdanov, A.V. Baranov, V.G. Golubev, *Phys. Solid State* (2020) **62**, 919.

Electrorheological fluids filled by detonation nanodiamonds

*Kuznetsov N.M.*¹, *Belousov S.I.*¹, *Chvalun S.N.*^{1,2}, *Yudina E.B.*³, *Vul' A.Ya.*³

kyz993@yandex.ru

¹ National Research Center "Kurchatov Institute", Moscow, Russia

² Enikolopov Institute of Synthetic Polymeric Materials of the Russian Academy of Sciences, Moscow, Russia

³ Ioffe Institute, St. Petersburg, Russia

The electrorheological effect is a rapid and reversible change in the rheological behavior of fluids under an electric field. Typically, this effect is observed in suspensions of micro- or nanoparticles capable of polarization in a liquid dielectric medium. Such suspensions are called electrorheological fluids (ERFs), which are "smart" materials. The mechanism of the effect is in the polarization of the dispersed phase particles and the formation of columnar structures accompanied by a transition from the viscous behavior of the fluid to the elastic one. ERFs have numerous advanced applications in dampers, clutches, sensors, microfluidics, robotics, etc [1]. However, for extensive practical applications, ERFs must have a set of properties, such as a significant increase in the yield stress and storage modulus, as well as a contrast transition from viscous behavior to elastic under electric field, high operational stability in a wide range of electric field strengths, sedimentation stability. Therefore, the development of new compositions exhibiting electrorheological activity is an urgent task.

Detonation nanodiamonds (DNDs) are one of the modern nanocarbons. It is noteworthy that DNDs are capable of forming branched structures in liquid media [2,3], as well as polarizing in an electric field [4]. Therefore, DNDs were considered as promising filler for ERFs. DNDs suspensions in polydimethylsiloxane reveal electrorheological effect. It was found, that the chemical nature of DNDs surface has a crucial role on particles behavior in suspension under electric field. The hydrogenated particles polarize and form columnar structures, while the carboxylated ones migrate to one of the electrodes, exhibiting electrophoresis. Suspensions of hydrogenated DNDs show high electrorheological activity and stable operation in on/off mode [5]. Low filler concentration (< 5 wt%) and high sedimentation stability of fluids opens up the opportunity for wide practical application. The effect of dispersion media nature on electrorheological behavior of fluids depending on surface of DND particles is discussed as well.

This work supported by Russian Foundation for Basic Researches, project 18-29-19117 mk.

References

1. Z. Dong, Y. Seo, H.J. Choi. *Soft Matter* (2019) **15**, 3473.
2. M. Kuznetsov, S.I. Belousov, A.V. Bakirov, S.N. Chvalun, R.A. Kamyshinsky, A.A. Mikhutkin, A.L. Vasiliev, P.M. Tolstoy, A.S. Mazur, E.D. Eidelman, E.B. Yudina, A.Ya. Vul. *Carbon* (2020) **161**, 486.
3. L.Y. Chang, P. Reineck, D. Williams, G. Bryant, G. Opletal, S.A. El-Demrashed, P.-L. Chiu, E. Osawa, A.S. Barnard, C. Dwyer. *Nanoscale* (2020) **12**, 5363.
4. Yu. Vdovichenko, N.M. Kuznetsov, V.G. Shevchenko, S.I. Belousov, E.B. Yudina, S.N. Chvalun. *Diam. Relat. Mater.* (2020) **107**, 107903.
5. M. Kuznetsov, S.I. Belousov, R.A. Kamyshinsky, A.L. Vasiliev, S.N. Chvalun, E.B. Yudina, A.Ya. Vul. *Carbon* (2021) **174**, 138.

X-ray luminescent nanodiamonds modified by Eu diphthalocyanine

*Lebedev V.T.*¹, *Kulvelis Yu.V.*¹, *Fomin E.V.*¹, *Torok Gy.*², *Vul A.Ya.*³

lebedev_vt@pnpi.nrcki.ru

¹ Petersburg Nuclear Physics Institute named by B.P.Konstantinov, NRC "Kurchatov Institute", Gatchina, Leningrad distr., Russia

² Atomic Energy Research Institute, MTA, KFKI, Budapest, Hungary

³ Ioffe Institute, St. Petersburg, Russia

Detonation nanodiamonds of DND Z+ type (~ 4.5 nm in size, positive ζ -potential ~ 30-40 mV) [1] were modified by Eu diphthalocyanine molecules (DPC) to obtain photoactive catalysts with X-ray luminescent properties. The hydrophobic DPC molecules dissolved in dimethylformamide were transferred to aqueous dispersion of DND Z+ where the formation of binary complexes was detected by optical absorption and neutron scattering. Such stable complexes (DPC amounts $C_R = 0.1-1.0$ % wt. relative to DND) were organized into primary chain-like structures evolved to branched aggregates joint into gel network above the critical DPC concentration $C_R^* \sim 0.3$ % wt. Binary complexes with the luminescence at a wavelength $\lambda \sim 600$ nm (induced by X-ray irradiation, 0.154 nm) can serve as the catalysts generating singlet oxygen for air and water cleaning and for X-ray Photodynamic Therapy (PDT) to treat deep localized tumors, inaccessible for conventional PDT.

The work was supported by the Russian Foundation for Basic Researches (gr. No 18-29-19008).

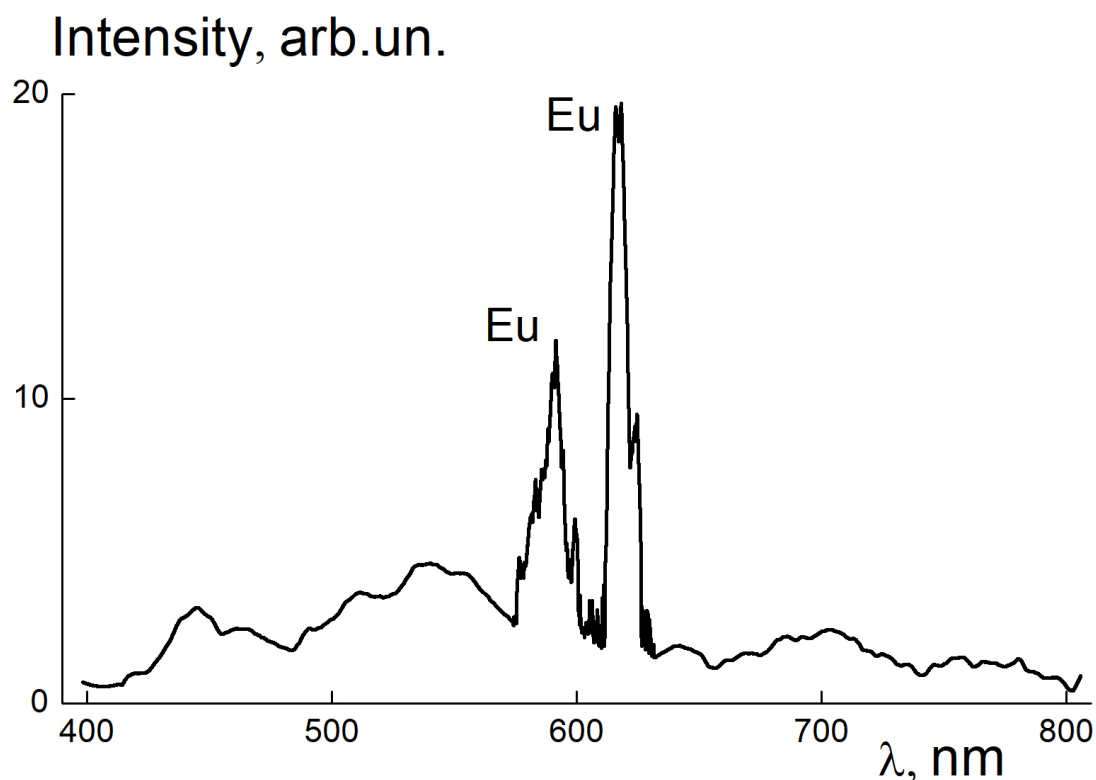


Fig.1. Spectrum of DND-DPC complexes powder luminescence $I(\lambda)$ in optical range induced by X-ray irradiation. The characteristic peaks of Eu atoms are revealed on the broad band $\lambda = 400-800$ nm of the luminescence from diamonds.

References

1. A.Ya. Vul, E.D. Eidelman, A.E. Aleksenskiy et. al. Carbon (2017) **114**, 242.

On mechanism of diamond growth: role of ethylene and acetylene

*Leshchev D.V.*¹, *Gorbachev Y.E.*²

dimvovich@narod.ru

¹ Center for Advanced Studies of Peter the Great Saint-Petersburg Polytechnic University, Saint-Petersburg, Russia

² Coddan Technologies LLC, Saint-Petersburg, Russia

The hot-filament HF CVD (HF-CVD) and microwave plasma enhanced CVD (MWCVD) techniques [1-3] are actively developed. Atomic hydrogen resulting on catalyst surface or in plasma source quickly converts hydrocarbon gas to methyl radical which is considered the main specie of deposited diamond. Further chain of chemical transformations converts methyl into atomic carbon as well as into hydrocarbons with a longer carbon chain. Such hydrocarbons as ethylene and acetylene can react with growing diamond surface and, therefore, contribute carbon deposition. In all the developed models of diamond growth this contribution has not been considered.

Gas-dynamic simulations including 86 gas-phase reactions under conditions close to the experimental [4] show that flux of acetylene to substrate can be significant. Here the parameters of reactions of ethylene and acetylene with different diamond sites are obtained as a result of quantum chemical simulations. It is shown that these reactions can cause the transformation of the growth process of diamond (sp³-phase) to growth of graphite or graphite-like shells. That may be the reason of diamond growth halting.

Those reactions were implemented into gas-dynamic simulations of diamond deposition. Comparison with experimental data was performed.

Acknowledgements. This work was partially supported by the Russian Foundation for Basic Research (project № 19-08-00533) and by the Ministry of Science and Education of Russian Federation (project № 0784-2020-0025).

References

1. May, Philos. Trans.R. Soc. (2000) **A 358**, 473.
2. A Rebrov, M Plotnikov, Y Mankelevich, I Yudin, Phys. Fluids (2018) **30**, 016106.
3. Rebrov, M. V. Isupov. A. Yu. Litvintsev, and V. F. Burov, Journal of Applied Mechanics and Technical Physics. (2018) **59**, 771.
4. A.Emelyanov, M.Y.Plotnikov, I.B.Yudin, Journal of Physics: Conference Series (2018) **1105**, 012120

Development of high-purity detonation synthesis nanodiamonds for slow neutron reflectors

Muzychka A.Yu.¹, Hramco C¹, Pavlov S.S.¹, Nezvanov A.Yu.¹, Lychagin E.V.^{1,2,3}, Nesvizhevsky V.V.⁴, Vul A.Ya.⁵, Dideikin A.T.⁵, Alexinskii A.E.⁵, Korobkina E.⁶

lychag@nf.jinr.ru

¹ Joint Institute for Nuclear Research, Dubna, Russia

² Dubna State University, Dubna, Russia

³ Lomonosov Moscow State University, Moscow, Russia

⁴ Laue-Langevin Institute, Grenoble, France

⁵ Ioffe Institute, St.Petersburg, Russia

⁶ North Carolina State University, Raleigh, NC, USA

Due to the unique combination of physical properties, nanodiamonds are a promising material for producing reflectors of very cold neutrons (VCNs) [1, 2]. To date, such reflectors do not exist as permanently used devices. Their development would make it possible to significantly increase the number of VCNs in the extracted neutron beams and, as a result, expand the range of neutron research both in the field of studying the physics of condensed matter and in the field of fundamental research.

The use of such reflectors in a real physical device requires nanodiamond powder in an amount measured in several kilograms or even tens of kilograms. Today, such quantities are available for detonation synthesis nanodiamonds (DND). The presence of impurity atoms with large neutron capture cross sections or activation cross sections can significantly deteriorate the property of such a material or make its use in intense neutron fields impossible for reasons of radiation safety. Earlier, a method was found for purifying nanodiamond powder from hydrogen atoms [3] - the main reason of VCN losses. Now an attempt has been made to deeply purify the deagglomerated DND powder from metallic impurities, which are both a reason of additional neutron losses and activation. The results of various stages of cleaning and the final results were monitored using neutron activation analysis.

The work is supported by grants: RFFI-18-29-19039, CREMLINplus agreement 871072, ERC INFRASUP P-2019-1/871072 and ANR-20-CE08-0034-04.

References

1. V. Nesvizhevsky, E.V.Lychagin, A.Yu.Muzychka, A.V.Strelkov, G. Pignol, K.V. Protasov "The reflection of very cold neutrons from diamond powder nanoparticles" // Nuclear Instruments and Methods in Physics Research Section A: Accelerators, Spectrometers, Detectors and Associated Equipment **595**, (2008) 631-636 DOI: 10.1016/j.nima.2008.07.149
2. Lychagin E.V., Muzychka A.Yu., Nekhaev G.V., Nesvizhevsky V.V., Pignol G., Protasov K.V., Strelkov A.V. "Storage of very cold neutrons in a trap with nano-structured walls" // Physics Letters B **679** (2009) 186-190 <https://doi.org/10.1016/j.physletb.2009.07.030>
3. V. Nesvizhevsky, U. Koester, M. Dubois, N. Batisse, L. Frezet, A. Bosak, L. Gines, O. Williams (2018). "Fluorinated nanodiamonds as unique neutron reflector." Carbon **130**: 799.

Gas-jet HWCVD synthesis of diamond from a mixture of hydrogen with ethylene.

*Yudin I.B.*¹, *Emelyanov A.A.*¹, *Plotnikov M.Yu.*¹, *Rebrov A.K.*¹, *Timoshenko N.I.*¹

yudinib@gmail.com

¹ Kutateladze Institute of Thermophysics of SB RAS, Novosibirsk, Russia

Gas-phase deposition using thermal activation of gas precursors (HWCVD) is widely used for the synthesis of diamond structures. In recent years, a gas-jet modification of the method has been actively developing [1,2]. The gas-jet method has a number of advantages, of which the main one is the possibility of wide variations in the parameters that determine the technological process, such as the specific mass flow of precursor gases, temperature, heat content, and pressure. The use of a supersonic gas flow expanding into a region with low pressure makes it possible to "freeze" active components. Another distinctive feature of the approach under consideration is that the activation of the components of a mixture of hydrogen with a carbon-containing gas is achieved with the use of a tungsten channel heated to high temperatures and providing a high degree of particle activation due to multiple collisions with the surface when the mixture flows through the channel.

In HWCVD synthesis of diamond, methane is most widely used as a carbon-containing gas [3]. At the same time, the problem of studying the possibilities of diamond structures synthesizing using active fragments formed by activation of gas mixtures of hydrogen with other hydrocarbons remains urgent.

The presented work is devoted to the study of the characteristics of the synthesis of diamond structures from a mixture of hydrogen with ethylene by the gas-jet method. The peculiarities of using ethylene for the synthesis of diamond by the HWCVD method have hardly been studied. Note that, in contrast to methane, ethylene on the surface of heated tungsten decomposes more actively [4], which can affect the results of deposition.

In the course of the study, a number of experiments were carried out using a mixture of hydrogen with ethylene. A mixture of hydrogen with methane was also used to synthesize diamond structures under similar conditions for the purpose of comparison. The morphology of the synthesized diamond structures was analyzed using electron micrographs and Raman spectra. Experiments on the diamond synthesis were carried out on activators of various lengths, allowing to obtain more (22mm) or less (11mm) activated hydrogen at the deposition surface. In the case with a long activator (22 mm), the use of ethylene leads to a decrease in the occupation of the substrate with diamonds, and the crystal size is smaller compared to the use of methane (although there are 2 times more carbon atoms supplied). The use of a short activator (11 mm) in the case of ethylene facilitates a higher occupation of the substrate with diamond crystals. In the same case for methane, an increased amount of amorphous carbon is observed in the deposition on a substrate.

The diamond structures obtained from a mixture of hydrogen and ethylene and the deposition rate differ from those obtained with methane. The comparison is complicated by the difference between the decomposition of methane and ethylene on the surface of hot tungsten. Experiments have shown that high deposition rates with a specific crystal structure are achievable. This encourages continued research using C₂H₄.

This work was carried out with partial support from the Russian Foundation for Basic Research (grant 19-08-00533) and the state contract with IT SB RAS (grant 121031800218-5).

References

1. A. Emel'yanov, A. K. Rebrov, I. B. Yudin, *Tech. Phys.* (2016) **61(12)**, 1821.
2. K. Rebrov, M.N. Andreev, T.T. Bieiadovskii, K.V. Kubrak, *Surface & coatings technology* (2017) **325**, 210.
3. W. May, *Phil Trans R Soc Lond A* (2000) **358**, 473.
4. F. Winters, H. Seki, R.R. Rye, M.E. Coltrin, *J. Appl. Phys.* (1994) **76(2)**, 1228.

Granular conductivity in boron rich diamond like carbon films

Zinin P.V.¹, Leksikov A.V.¹, Fominski V.Yu.², Romanov R.I.², Krasnoborodko S. Yu.¹, Vysokikh Yu. E.¹, Filonenko V.P.³, Buga S. G.⁴

zosimpvz@mail.ru

¹ Scientific and Technological Center of Unique Instrumentation, Russian Academy of Sciences, Moscow, Russia

² National Research Nuclear University MEPhI, Moscow, Russia

³ Institute for High Pressure Physics, Russian Academy of Sciences, Troitsk, Moscow, Russia

⁴ Technological Institute for Superhard and Novel Carbon Materials, Troitsk, Russia

In this report we present results of electrical property studies for BC_x films prepared by pulsed laser deposition on Si substrates at 770 K. Pulsed laser ablation of BC₃ and BC₇ targets was conducted under vacuum conditions to form the films with ~20 and ~300 nm thickness and two boron concentrations as described in Ref.[1]. The 20-nm-thick BC₇ films possessed a nearly metallic electrical resistivity, $3.6 \cdot 10^{-4}$ W·cm at room temperature. The lowest resistivity of $2.7 \cdot 10^{-5}$ W·cm was observed in the thin BC₃ film at 90 K. All the films exhibit metallic-type behavior: the resistivity decreases as the temperature drops below 250 K.

The nature of the low resistivity and metallic-type behavior of the resistivity in BC_x films was investigated by the atomic force microscopy with a conductive tip (CAFM) [2]. The CAFM images show that the resistivity of the films has a “granular” structure containing areas with high resistivity located inside grains of the film and areas with low resistivity coinciding with grain boundaries (Fig. 1). The CAFM measurements conducted on the surfaces of pyrolytic graphite and BC₃ film on Al₂O₃ substrate demonstrate that the contact-tip resistivity inside the area of low resistivity of the BC₃/Al₂O₃ films is 410 times lower than that of graphite.

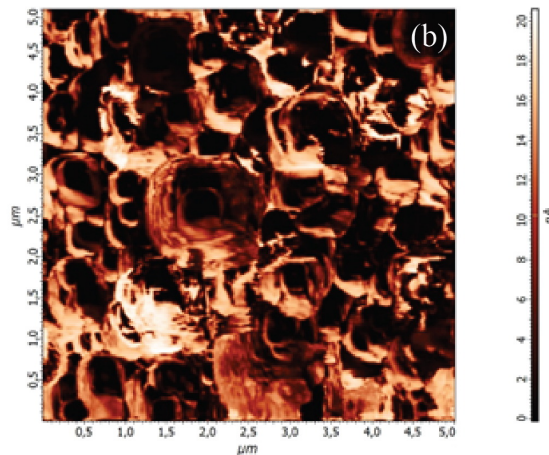


Fig. 1. Distribution of the electrical conductivity on the surface of the BC₃ films. The brightness of the contrast is proportional to the electrical current between the tip and specimen

References

1. Fominski V Y, Romanov R I, Solov'ev A A, Vasil'evskii I S, Safonov D A, Ivanov A A, Zinin P V, and Filonenko V P Tech. Phys. Lett. (2019) **45**, 446.
2. Fominski V Y, Romanov R I, Vasil'evskii I S, Safonov D A, Soloviev A A, Ivanov A A, Zinin P V, Krasnoborodko S Y, Vysokikh Y E, and Filonenko V P Diam Related Mater. (2021) **114**, 108336.

Organization in various small-angle x-ray scattering study of the detonation nanodiamonds structural media.

Kuznetsov N.M.¹, Belousov S.I.¹, Bakirov A.V.^{1,2}, Chvalun S.N.^{1,2}, Yudina E.B.³, Vul' A.Ya.³

serbell@gmail.com

¹ National Research Center Kurchatov Institute, Moscow, Russia

² Enikolopov Institute of Synthetic Polymeric Materials of the Russian Academy of Sciences, Moscow, Russia

³ Ioffe Institute, St. Petersburg, Russia

Detonation nanodiamonds (DNDs) produced from carbon-containing explosives have a great attention in numerous scientific and technological areas, due to their hardness, thermal conductivity, low toxicity, high surface area, etc [1]. The water-based suspensions of DNDs can be used for medical applications, for example drug delivery or magnetic resonance imaging [2,3]. Suspensions of nanodiamonds in various oils hold great promise as lubricants in tribology as well [4]. However, for many real practical applications of DNDs, it is important not only to obtain stable suspensions, but also to know the structural state of particles in various media.

In present research, suspensions of individual DND particles in water, silicone, and mineral oil in concentration range of 1-7 wt% were studied by the small angle X-ray scattering. Two types of particles terminated by hydrogen and carboxyl groups were used. Primary particle size of 4-5 nm was previously determined in an aqueous medium by dynamic light scattering. Suspension in oils were obtained during the mixing with DND powder by means of magnetic stirrer and following sonication.

Water, silicone and mineral oils have different chemical nature and dielectric permittivity. This, in turn, leads to different mechanisms of the dispersion medium molecules interaction with DNDs affecting the structural organization. Regardless of the type of dispersion medium and the functionalization of the DND surface, two slopes are observed on the X-ray scattering curves in double logarithmic scale. Such scattering indicates about complex particles organization and corresponds to scattering on the surface of compact particles and on a loose fractal structure of agglomerates. It is noteworthy that a more ordered structure is formed in aqueous suspensions than in silicone and mineral oils. Thus, at the smallest angles, a Bragg reflection appears even at a particle concentration of about 1 wt%, due to the scattering between ordered DNDs fractals.

This work supported by Russian Foundation for Basic Researches, project 18-29-19117 mk.

References

1. Detonation Nanodiamonds - Science and Applications. ed. A. Ya. Vul', O. A. Shenderova, Pan Stanford Publishing, 2013.
2. T. Uthappa, O.R. Arvind, G.Sriram, D. Losic, H.-Y.-Jung, M. Kigga, M.D. Kurkuri. J. Drug Del. Sci. Tech. (2020) **60**, 101993.
3. M. Panich, M. Salti, O. Prager, E. Swissa, Y.V. Kulvelis, E.B. Yudina, A.E. Aleksenskii, S.D. Goren, A.Ya. Vul', A.I. Shames. Magn. Reson. Med. (2021) <https://doi.org/10.1002/mrm.28762>.
4. Zhai, W. Lu, X Liu, L. Zhou. Tribol. Int (2019) **129**, 75.

Amplification of colour-centre luminescence using Getter-controlled nitrogen reduction for synthetic HPHT micro-diamonds.

*Bogdanov K.V.*¹, *Osipov V. Yu.*², *Baranov A.V.*¹

kirw.bog@gmail.com

¹ ITMO University, St. Petersburg, Russia

² Ioffe Institute, St. Petersburg, Russia

The neutral and negatively charged nitrogen-vacancy color centers in diamonds are well-known source of luminescence of zero-phonon and phonon-assisted lines. This material has wide possibilities for potential applications of NV- centre diamonds for bioimaging, sensing, and quantum-based technologies. [1-3]. It has recently been reported that simply increasing both the vacancy and substitutional nitrogen atom content in HPHT diamond microcrystals does not result in the expected increase in photoluminescence (PL) intensity. The production of diamonds in the atmosphere leads to the introduction of nitrogen in an amount equal to ~ 250 ppm. A number of works in which additional doping with nitrogen was carried out during the production of diamond particles show that exceeding this value leads to a sharp increase in nonradiative recombination and, accordingly, to a decrease in the intensity of luminescence. [4]. This work demonstrates the advantage of diamond particles production with a nitrogen concentration below the standard (atmospheric) synthesis.

A study of a sample of diamond particles with a concentration of ~ 90 ppm was carried out using the methods of Raman spectroscopy using low temperatures, EPR spectroscopy, lifetime spectroscopy, and IR spectroscopy. The effect of a decrease in nonradiative recombination centers and the quality of the structure of diamond particles on the luminescence intensity of nitrogen-vacancy color centers is shown. The possibility of controlled adjustment of the luminescence parameters and the achievement of maximum luminescence intensities by obtaining the optimal concentrations of interstitial nitrogen is shown.

This work was supported by the Russian Science Foundation (Agreement 21-12-00264).

References

1. I. Aharonovich, A. D. Greentree, and S. Praver, "Diamond photonics," *Nat. Photonics* **5**, 397–405 (2011).
2. J. J. L. Morton and J. Elzerman, "Three of diamonds QUANTUM COMPUTING," *Nat. Nanotechnol.* **9**, 167–169(2014).
3. S. A. Grudinkin, N. A. Feoktistov, A. V. Medvedev, K. V. Bogdanov, A. V. Baranov, A. Y. Vul, and V. G. Golubev, "Luminescent isolated diamond particles with controllably embedded silicon-vacancy colour centres," *J. Phys. D: Appl. Phys.* **45**(6), 062001 (2012).
4. A. I. Shames, V. Osipov, K. Bogdanov, A. Baranov, M. Zhukovskaya, A. Dalis, S. Vagarali, and A. Rampersaud, "Does progressive nitrogen doping intensify NV- emission from e-beam irradiated Ib type HPHT diamonds," *J. Phys. Chem. C* **121**, 5232–5240 (2017).

Influence of annealing atmosphere on DNDs' surface graphitization and impact on their colloidal stability in water

Ducrozet F.^{1,2}, *Girard H.A.*¹, *Brun E.*², *Sicard-Roselli C.*², *Arnault J.-Ch.*¹

florent.ducrozet@cea.fr

¹ NIMBE, UMR CEA-CNRS 3685, Université Paris-Saclay, CEA Saclay 91191 Gif-sur-Yvette, FRANCE

² Institut de Chimie Physique, UMR 8000, CNRS, Université Paris-Saclay, 91405 Orsay, FRANCE

In the past decades, research and engineering fields have developed an increased interest in nanodiamonds. Among them, nanodiamond synthesized by detonation (DNDs) are actively investigated, not only for their outstanding core properties but also for their high surface-to-volume ratio that leads to an exalted surface reactivity. DNDs are now considered as (photo)catalysts¹, radiosensitizers² and for antibacterial³ applications. To perform surface-related studies, a fine control of DND surface chemistry is of primary importance, and graphitized surface might be one of the most promising and yet intricate. If the formation of onion-like carbon structures is well documented⁴, primary steps of sp³-C/sp²-C transition at ND's surface remain less understood but crucial for catalytic⁵ or toward further functionalization⁶ studies. Furthermore, the consequences of graphitization treatments on the colloidal behavior of DND in aqueous suspensions is also of high interest. Indeed, their excellent colloidal stability previously reported⁷ with other surface chemistries could here be challenged by the hydrophobic behavior of graphite reconstructions.

The aim of the work is first to assess the increase of sp²-C carbon induced by annealing under vacuum or argon atmospheres in the 800°C-950°C temperature range that leads to different surface chemistries. Afterwards, the colloidal stability of these particles is studied in aqueous suspensions. Samples were characterized by a combination of techniques in order to have a complete overview of the induced modifications: surface chemistry (FTIR, TGA-DSC), carbon hybridization (XPS, Raman), crystalline structure (HRTEM) and colloidal properties (DLS, zetametry). For the first time, by working with the same initial DND and the same oven for both atmospheres, we can legitimately highlight differences between these protocols. Moreover, our study links the sp³-C/sp²-C ratio and the colloidal stability of these positively charged DNDs in water, allowing further surface reactivity studies of graphitized-DNDs in aqueous suspensions.

References

1. Mironova et al, *Russ Chem Bull*, (2013)
2. Brun et al, *Carbon*, (2020)
3. Wehling et al, *ACS Nano*, (2014)
4. Popov et al, *Synch. Investig.*, (2013)
5. Lin et al, *Soc. Rev.*, (2018)
6. Betz and Krueger, *ChemPhysChem*, (2012)
7. Hibson et al, *DRM*, (2008)

Composites of SiO₂ - aerogels with nanodiamonds

Lermontov S.A.¹, Gozhikova I.O.¹

innagozhik@gmail.com

¹ Institute of physiologically active compounds RAS, Chernogolovka, Russia

Detonation nanodiamonds (DND) are unique materials with very unusual properties. They possess a combination of biological (low toxicity, biocompatibility) [1], physicochemical (optical, magnetic, thermophysical, etc.) [2] and mechanical properties, which make them promising materials for nanotechnology. The size of the non-agglomerated DND particle lies in the range of 4-5 nm, the central part consists of sp³ carbon, and the outer layer consists of various forms of sp² carbon - graphite, graphene, fullerene, etc [3]. Stable DND suspensions exist in the form of hydrosols. The main difficulties when working with non-agglomerated DND particles arise from attempts to concentrate the hydrosol. DND particles form agglomerates, which make it impossible to study the properties of isolated primary DNDs.

By synthesizing a SiO₂ composite of aerogel and DND, we obtained immobilized primary detonation nanodiamonds with a size of 4-5 nm and investigated their properties - transparency, uniformity of DND distribution, aggregation of primary DND, etc. After isolation of nanodiamond particles in the cells of the SiO₂ matrix, they lose the ability to form aggregates, which makes it possible to study individual nanoparticles.

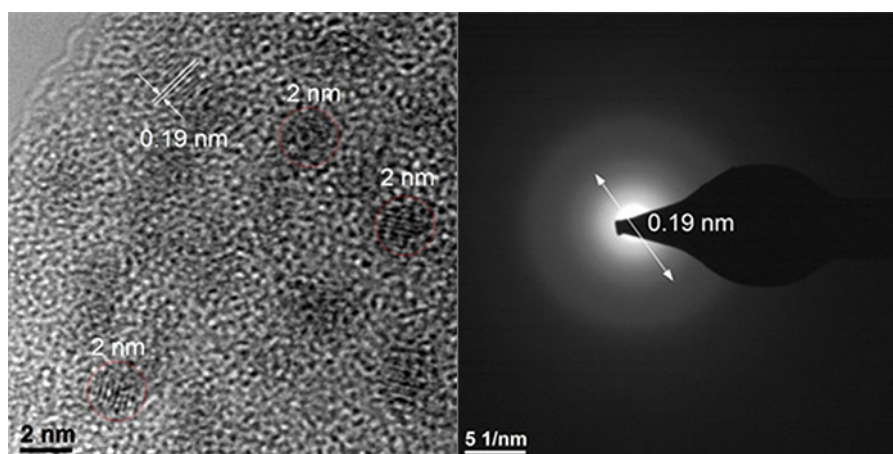


Figure 1. High resolution electron microscopy (HR TEM). Separate crystallites are visible inside the SiO₂ matrix. Figure 2. Electronic diffraction. The arrow indicates the radius of the diffraction ring corresponding to the first reflection in the diamond grating

References

1. Neburkova, J. Vavra, P. Cigler. (2017). Coating nanodiamonds with biocompatible shells for applications in biology and medicine // *Current Opinion in Solid State and Materials Science*. - 2017. - T. 21. - №. 1. - C. 43-53. <https://doi.org/10.1016/j.cossms.2016.05.008>
2. Roldán, A.M. Benito, E. García-Bordejé. Self-assembled graphene aerogel and nanodiamond hybrids as high performance catalysts in oxidative propane dehydrogenation // *Journal of Materials Chemistry A*. - 2015. - T. 3. - №. 48. - C. 24379-24388. <https://doi.org/10.1039/C5TA07404E>.
3. E. Aleksenskiy, E. Eydelman, A. Y. Vul. Deagglomeration of detonation nanodiamonds // *Nanosci Nanotechnol Lett.* - 2011. - T. 3. - №. 1. - C. 68-74. <https://doi.org/10.1166/nll.2011.1122>

Research of electrophysical properties of diamonds with NV-centres in a wide range of temperatures and frequencies

*Kapustin S. N.*¹, *Volkov A. S.*¹

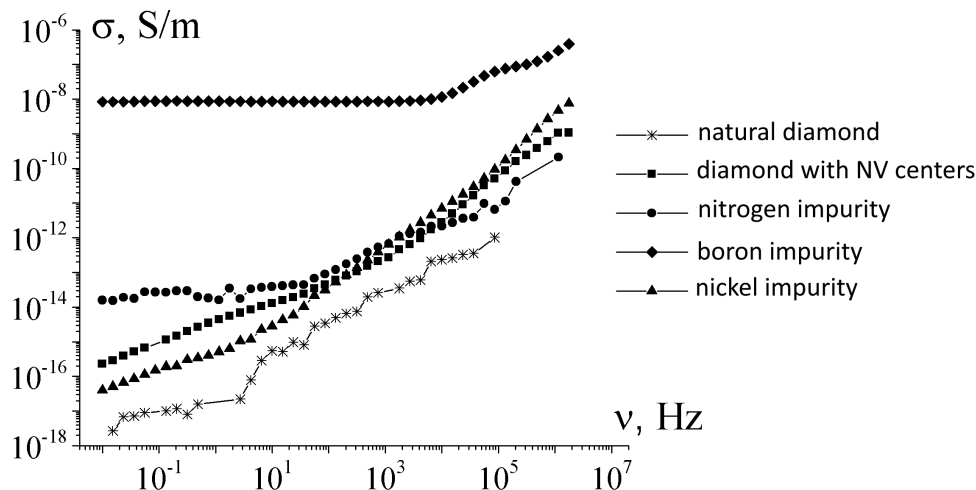
hare22@yandex.ru

¹ Arhangelsk, Russia, Northern (Arctic) Federal University named after M.V. Lomonosov

The artificial crystals were synthesized with the High Temperature High Pressure (HTHP) method and doped with nitrogen and boron. A proportion of diamonds with nitrogen impurities were developed using a beam of electrons with an energy of 3 MeV. In this way nitrogen-vacancy centers (NV-centers) were obtained. NV-centers are defects that have a great appeal during practical application in quantum calculations or various sensors.

Measurements of electrophysical properties of the artificial diamonds were taken. The research was conducted via dielectric and impedance spectroscopy [1], which allowed to provide extensive information on the dynamics of the main charge carriers and their changes caused by numerous factors such as frequency of the electric field, temperature, impurities etc. In the process temperature dependences of conductivity allowed to determine the activation energy and make conclusions about the nature of the main carriers in the matter.

The preliminary analysis of frequency dependences allowed to reveal the difference in the nature of the dependences upon doping the diamond structure with various impurities. Dependences for crystals with different concentrations of doped impurities at different temperatures (from 74 K to 374 K) will be presented.



Dependence of the conductivity of samples on the frequency of the electric field.

References

1. Kremer F., Schonhals A., Broadband Luck W. Dielectric Spectroscopy. — Springer-Verlag, 2002.

Improving the performance of PFSA membranes using sulfonated nanodiamonds

*Kulvelis Yu.V.*¹, *Primachenko O.N.*², *Odinokov A.S.*^{3,2}, *Shvidchenko A.V.*⁴, *Yudina E.B.*⁴, *Gofman I.V.*², *Marinenko E.A.*², *Lebedev V.T.*¹, *Vul A.Ya.*⁴, *Kuklin A.I.*⁵, *Skoï V.V.*⁵

kulvelis_yv@pnpi.nrcki.ru

¹ Petersburg Nuclear Physics Institute named by B.P. Konstantinov, NRC "Kurchatov Institute", Gatchina, Russia

² Institute of Macromolecular Compounds, Russian Academy of Sciences, St. Petersburg, Russia

³ Russian Research Center of Applied Chemistry, St. Petersburg, Russia

⁴ Ioffe Institute, St. Petersburg, Russia

⁵ Joint Institute for Nuclear Research, Dubna, Russia

Perfluorosulfonic acid (PFSA) membranes, having tetrafluoroethylene backbone and side chains with sulfonic acid $-SO_3H$ groups at the ends, play an important role working in hydrogen fuel cells (FC) in portable and stationary devices with various range of power. Long side chain (LSC) Nafion®-type membranes were first introduced to industry, however, short side chain (SSC) Aquivion®-type membranes have significant advantages due to higher proton conductivity and better thermal stability [1]. To improve the conductivity and mechanical properties of SSC PFSA membranes, being prepared by casting from copolymer solution in DMF (dimethylformamide), we used detonation nanodiamonds (DND, particle size 4-5 nm) with various surface functional groups as nanofillers. DND with carboxylic groups have demonstrated rise of proton conductivity at the increased temperatures (50°C), but low temperatures resulted in loss of conductivity because of the presence of low acidic $-COOH$ groups on the surface of DND [2]. The idea to use DND with $-SO_3H$ groups was realized by sulfonating the initial protonated DND in a reaction with oleum under increased pressure and temperature. Compositional membranes prepared with sulfonated DND demonstrated rise of conductivity at 0.5 – 2 wt.% of DND (Fig.1), accompanied by good mechanical properties, suitable for the use in fuel cells. Small-angle neutron scattering showed the saving of the basic structural elements in membranes – the conducting channels. We look forward to prepare DND, sulfonated at higher degrees, for the better performance.

The work was supported by the Russian Foundation for Basic Researches (gr. No 19-03-00249).

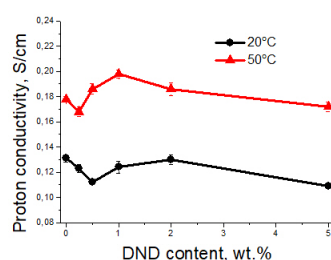


Fig.1. Proton conductivity of compositional SSC membranes with sulfonated DND vs DND content.

References

1. Primachenko O.N., Marinenko E.A., Odinokov A.S., Kononova S.V., Kulvelis Yu.V. Lebedev V.T. *Polymers for Advanced Technologies* (2021) **32**, 1386.
2. Kulvelis Yu.V., Primachenko O.N., Odinokov A.S., Shvidchenko A.V., Bairamukov V.Yu., Gofman I.V., Lebedev V.T., Ivanchev S.S., Vul A.Ya., Kuklin A.I., Wu B. *Fullerenes, Nanotubes and Carbon Nanostructures* (2020) **28**, 140.

Investigation of the Nitrogen-doped Diamond Defects by Positron Annihilation Spectroscopy

*Kuziv I.*¹

i-kuziv@yandex.ru

¹ Northern (Arctic) Federal University named after M.V. Lomonosov

Investigation of the defects in doped diamonds is important for solving different applied problems in X-ray optics and quantum sensorics.

Generation of the diamond test plates was conducted by HTHP method with addition of Nitrogen in different concentrations. Test plates were investigated by methods of IR-spectroscopy, UV-spectroscopy, Raman-spectroscopy and XRS-spectroscopy.

Crystalline structure of the test plates was studied with Positron Annihilation Spectroscopy (PAS). This is non-destructive method of detecting open-volume defects such as vacancies, vacancy clusters, dislocations and microvoids.

Doped diamond test plates were investigated with three different measuring PAS-methods. Each method used a radioactive isotope of sodium (Na22). First method is based on determination of the positron lifetime in the test plate. This method shows average lifetime of the positron, what in turn reveals defects in their type in the material. Dependence of Nitrogen concentration in test plate by positron's lifetime is represented in figure 1. Test plates in this study show typical vacancy-type defects from monovacancies up to large clusters. Second method investigates Doppler Broadening on Na22 source. Third method is Doppler Broadening on positron beam with energy of positrons from 0 to 20 keV. Second and third method allow to define defects in the near-surface layer.

This study reveals dependence between nitrogen concentration and appearance of the defects in the diamond plates. All the defects are of the vacancy-type. Dependence of the amount of such defects is also in accordance with the depth of the layer in diamond.

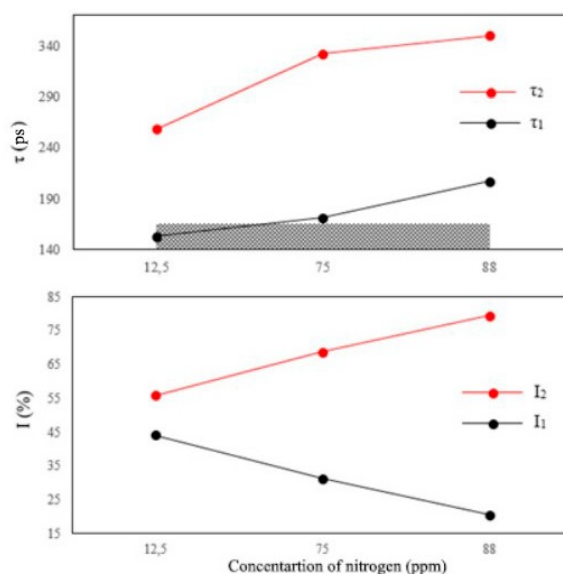


Figure 1. Dependence of the positron lifetime on nitrogen concentration

Dependence of the positron lifetime on nitrogen concentration

References

1. S. Dannefaer. Phys. Status Solidi C 4, 3605 (2007)
2. Uedono A, Watanabe M, Sabato T and Tanigawal S 1999 J. Phys.: Condens. Matter 12 719
3. Pu A, Bretagnon T, Kerr D and Dannefaer S 2000 Diamond Relat. Mater. 9 1450

The use of purified detonation nanodiamond in an anti-icing composition.

Ovchinnikov-Lazarev M.A.^{1,2}, *Spitsyn B.V.*², *Zavaleev V.A.*¹, *Korzhenevsky A.P.*³

13max94@gmail.com

¹ State Research Center of the Russian Federation Troitsk Institute for Innovative and Fusion Research (TRINITI) Rosatom, Moscow, Russia

² Frumkin Institute of Physical Chemistry and Electrochemistry RAS

³ NP CJSC "Sinta", Belarus, Minsk

At present, in the process of utilization of powerful explosives, a valuable intermediate product, a detonation charge, is formed. Its transformation into detonation nanodiamond under industrial conditions is carried out by the liquid method in superheated nitric acid (260°C, 90 atm). In this work, the development of a gas-phase method of phase and chemical purification of a detonation charge is carried out. The developed method, carried out in contrast to the industrial one in three stages, has technological and environmental advantages: no loss of a finer fraction of detonation nanodiamond (DNA) and the formation of only solid waste.

The DNA obtained by the laboratory method was applied as an active component to a previously developed anti-icing agent that prevents ice accumulation, especially in extreme weather conditions characterized by prolonged precipitation in the form of freezing rain, as well as critical thermodynamic parameters of the atmosphere. In the course of the work carried out, the positive effect of DNA on the operation of the anti-icing composition was revealed, within the framework of improving both the physical and chemical properties of the substance applied to the surface. A feature of the composition modified by DNA is that nanostructured particles of diamond and silicon oxide, in conjunction with polymers, create such a crystal lattice on the surface of the material to be coated that, compared to the composition without detonation nanodiamond content, the following properties are improved by more than 30%:

- Anti-icing effect,
- Oleophobicity,
- Hydrophobicity,
- Improved anti-corrosion properties,
- Surface protection from chemicals (salts, acids, alkalis),
- Protection from the effects of flora and fauna,
- Improved heat-resistant surface properties.

In addition, a high strength film is formed on the surface (10H on the Moss scale).



Fig.1 Sample of detonation nanodiamond grade "SHA-A": 1 - before processing; 2 - DNA obtained after gas-phase phase cleaning, used in de-icer

Nanodiamond batch enriched with B, P: Prospects for use in agriculture

Shilova O.A.^{1,2}, *Dolmatov V.Yu.*³, *Panova G.G.*⁴, *Khamova T.V.*¹, *Baranchikov A.E.*⁵, *Kopitsa G.P.*^{1,6}

olgashilova@bk.ru

¹ Institute of Silicate Chemistry of Russian Academy of Sciences, St. Petersburg, Russia

² Saint-Petersburg State Electrotechnical University "LETI", St. Petersburg, Russia

³ Special Design Bureau Technolog, Saint-Petersburg, Russia

⁴ Agrophysical Research Institute, Saint Petersburg, Russia

⁵ Kurnakov Institute of General and Inorganic Chemistry of the Russian Academy of Sciences, Moscow, Russia

⁶ Konstantinov Petersburg Nuclear Physics Institute NRC KI, Gatchina, Russia

It is known that detonation nanodiamond (DND) has bactericidal and fungicidal properties. The batch of detonation nanodiamond (DB) also has a scientific and practical interest, since it is much cheaper than nanodiamond, but at the same time, it can have a whole range of useful properties. Of particular interest is the DB, enriched with various elements that give it new useful properties. Recently, SKTB "Technolog" has obtained several variants of a DB, which contains impurities of P and B (DB-B, DB-P). The enriched DBs were obtained by explosion using both TNT with hexagon and tetryl as precursors. These DB-B and DB-P contained from 2.5 to 6 mass. % P or B. The content of DND in the resulting DBs variants varied from 25.5 to 53.8 wt.%, P - from 0.23 to 0.66 wt.%, and B - from 0.73 to 0.96 wt%. The morphological features, texture, and mesostructure of the obtained DB-B and DB-P nanopowders were investigated by SEM, SAXS, and low-temperature nitrogen adsorption. The influence of explosion precursors was clearly revealed.

In the last decade, nanoparticles of carbon materials have been actively studied for agriculture applications. It is known that aqueous suspensions of carbon nanotubes and fullerenols are successfully used for the seeds pre-sowing treatment and plant foliar treatment. These particles can act as growth promoters and biocide additives. They can carry herbicides, reducing their negative impact on the environment. The use of nanodiamonds (DND) in agriculture is less well known.

We tested both aqueous suspensions and silica sols containing 2.5 wt. % DND for the pre-sowing treatment of Chinese cabbage seeds. However, no clear positive effect was found. Besides, the diamond is quite expensive. Therefore, it was of interest to study the effect of a much cheaper carbon nanomaterial - the nanodiamond batch (DB). To enhance the positive effect, an innovative product was used a DB enriched with B (DB-B).

The DB-B, obtained from a mixture of TNT with hexagen (50/50), containing 0.96 wt. % B and 14.7 wt. % DND, was used to treat Peking cabbage seeds. As a result, the reliable positive effect of an aqueous suspension of DB-B (0.05-0.1 wt.%) was revealed on the following characteristics of seedlings (in relation to the control): the germination energy of Peking cabbage seeds and germination increased by ~ 50-60%, as well as the biomass of Peking cabbage increased by ~ 2-3 times (25 days after planting the treated seeds). A significant positive effect of DB-B on the morphological characteristics of Peking cabbage plants at the early stages of its development was revealed when using DB-B for pre-sowing seed treatment in combination with silica sol (an increase in the sprout length by ~ 20% and root length by ~ 50% in relation to the control).

This work was supported by the Russian Science Foundation (project 19-13-00442).

Detonation synthesis of carbon onions and their properties

Shevchenko N.V.¹, Gorbachev V.A.¹, Sigalayev S.K.², Vysotina E.A.², Efremov V.P.³

nanocentre@kerc.msk.ru

¹ AO "Petrovskiy scientific centre "FUGAS", Moscow, Russia

² Keldysh Research Centre, Moscow, Russia

³ Joint Institute for High Temperatures of the RAS, Moscow, Russia

Nano-sized carbon structures are one of the most promising investigated materials for wide application in the field of energy conversion and storage. Recent studies have shown that carbon bulbous formations - nano-onions (NO) are an ideal material used to create super capacitors electrodes. NO provide high power density and energy density in electric devices [1].

At present, the production of NO is carried out in several ways - with the help of an electric discharge, ion implantation, vacuum annealing of detonation nanodiamonds (ND) [2, 3]. In the latter case, the initial raw material is a batch containing detonation products of explosives. ND are extracted from the batch during chemical cleaning. Purification of detonation ND is an expensive and complex process, due to which the cost of ND exceeds \$ 1500/kg. Subsequent production of NO from ND further increases its price. At the same time, the primary detonation batch contains 10÷15% of onion-like structures, which are usually lost during chemical purification of ND. We proposed the technology for obtaining NO [4], consisting of the process of detonation synthesis, subsequent heat treatment of the batch, and the process of separating onions.

The aim of this work is to obtain a batch from explosives, to segregate onion-like nano-structures from the batch, to study their composition and properties, and to estimate their applicability as an active electrode material in super capacitors. During the detonation of the TNT-RDX mixture, two types of batch were formed - outside the coolant from the products of the vapor-gas phase of the batch (BVO) and in the volume of the coolant batch (BCO). Also, when utilizing of artillery gunpowder is in the volume of the vacuum chamber, the third batch was received (BGPO). A chemically purified detonation nanodiamond was used as a reference sample. To normalize the onions content, all three types of batch (BVO, BCO and BGPO) were preliminarily graphitized in an inert gas atmosphere for 3 hours at 1600 ° C.

Structural and morphological studies and measurements of electrochemical characteristics of all three types of batch showed the individual features of their structures, while the maximum content of onions was observed in the batch of BCO. The BCO batch has the highest specific surface area in comparison with the rest of the studied samples. A characteristic feature of the BVO batch was the maximum size of the contained onions. The presence of nano-sized ribbon structures was revealed in the BGPO charge. Also, it was found that the samples of BCO have the highest electrical conductivity at a specific capacity comparable to the values characteristic of BVO and BGPO, which is apparently due to the combination of a developed surface and a specifically organized ordered onion structure of sp²-hybridized carbon.

The electrochemical properties of the structures of BVO, BCO and BGPO and the ways of their modification in order to increase their efficiency in super capacitors have been studied.

References

1. D. Pech, M. Brunet, H. Durou, P. Huang, V. Mochalin, Y. Gogotsi, P. L. Taberna, and P. Simon, *Nature Nanotechnology*, , 2010, V.5, p. 651.
2. N. Sano, H. Wang, I. Alexandrou, M. Chhowalla, K.B.K. Teo, and K. Iimura, *J. Appl. Phys*, 2002, V.92, p. 2783.
3. V. Kuznetsov, I. Zilberberg, Yu. Butenko, A. Chuvilin, and B. Segall. *J. Appl Phys*, 1999, V. 86, p. 863.
4. N. Shevchenko, V. Gorbachev, V. Chobanyan, S. Sigalayev, R. Rizakhanov, E. Vysotina, V. Blank, A. Golubev. *Izv. Vyssh. Uchebn. Zaved. Khim. Khim. Tekhnol*, 2018, V. 61, N 11, p.25.

Tuning of the porous structure of detonation nanodiamond powders by pressure: SANS study

Tomchuk O.V.^{1,2,3}, Avdeev M.V.¹, Bulavin L.A.², Zabulonov Yu.L.³, Ivankov O.I.¹, Len A.⁴

tomchuk@jinr.ru

¹ Joint Institute for Nuclear Research, Dubna, Russia

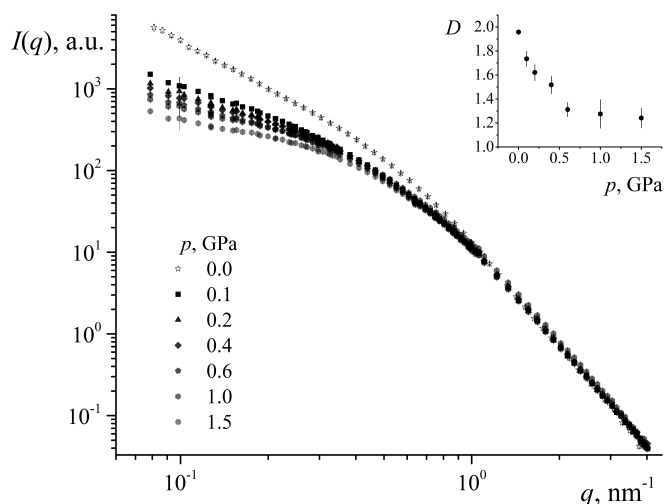
² Taras Shevchenko National University of Kyiv, Kyiv, Ukraine

³ Institute of Environmental Geochemistry of NASU, Kyiv, Ukraine

⁴ Centre for Energy Research, Budapest, Hungary

Nanodiamonds combine the unique mechanical, thermodynamic and optical properties of diamond with the peculiarities of colloidal dimensions and wide possibilities of chemical modification of their surface [1]. Of particular practical interest is the presence of a branched porous structure inside nanodiamond agglomerates in the initial powders. The porous structure was previously analyzed using small-angle neutron scattering [2]. The influence of high pressure allowed separating the contributions to the small-angle scattering from the micro- and nanosized pores [3]. In continuation of the above studies, the given research shows the possibilities of controlling the fractal structure of a porous system at the nanoscale by applying static pressure. For instance, the partial pore recombination in the range up to 1.5 GPa leads to the formation of the elongated pores, in contrast to the branched system characteristic of the initial industrial samples. This modification can have wide practical applications.

This work was supported by the Ministry of Education and Science of Ukraine through the project 20BF051-01 of the Taras Shevchenko National University of Kyiv.



Scattering curves (points) from the detonation nanodiamond powder for different pressure values. The curves refer to one density. The inset shows the dependence of the fractal dimension of the porous structure as a function of the applied static pressure.

References

1. M. Baidakova, A. Vul', J. Phys. D: Appl. Phys (2007) **40**, 6300.
2. M.V. Avdeev, V.L. Aksenov, L. Rosta, Diamond Relat. Mater. (2007) **16**, 2050.
3. L.A. Bulavin, O.V. Tomchuk, A.V. Nagorny, D.V. Soloviov, Ukr. J. Phys. (2021) **66**, in press.

Removal of several atomic layers in detonation nanodiamond particles

*Trofimuk A.D.*¹, *Sharonova L.V.*¹, *Shestakov M.S.*¹, *Kidalov S.V.*¹, *Dideikin A.T.*¹

trofimuk.ad@mail.ioffe.ru

¹ Ioffe Institute, Saint-Petersburg, Russia

Nanoscale diamonds, contrary to expectations, exhibit intense optical absorption, which makes nanodiamond powders and hydrosols look black and significantly limits the use of nanodiamonds and composites based on them in optical and luminescent systems. The generally accepted explanation for the absorption of visible light in nanodiamonds is the presence of the sp^2 -phase on the surface of diamond nanoparticles formed during the formation of nanocrystals [1, 2]. Thus, the successive removal of layers from the surface of diamond nanocrystals would make it possible to reduce optical absorption in systems based on nanodiamonds. In the presented work, an approach to solving this problem is developed.

The proposed technique is based on the formation of onion shells on the surface of diamond nanocrystals during heat treatment in vacuum and their subsequent removal by treatment with ozone in an aqueous medium.

The initial sample was a gray powder of DND agglomerates. The size of the diamond crystallite (according to the XRD data) was 4.77 nm. The size of agglomerates in an aqueous suspension (according to the the DLS data) was 37 nm. Sample electrical resistance was $2 \cdot 10^8$ Ohm·m. The aqueous suspension was white-gray. The original sample was treated for 1 hour in a vacuum chamber ($1 \cdot 10^{-5}$ Pa) at 1200°C. The obtained sample - DND with a shell of sp^2 -carbon - was a black powder. The crystallite size of the diamond core (according to the XRD data) was 4.25 nm. Sample electrical resistance was about $2 \cdot 10^3$ Ohm·m. The aqueous suspension was black. Finally, the resulting product was dispersed in an aqueous medium and treated in an aqueous medium by oxygen radicals according to the method described in [3].

For the initial sample (agglomerated DND) and for two samples obtained from it, optical absorption spectra in an aqueous medium were recorded. The concentration of all suspensions was 0.005 (\pm 0.001) wt.%; scattering was taken into account in the spectra. Upon annealing the diamond powder in vacuum, the nature of absorption changed: an absorption maximum appeared at 260 nm, and absorption in the visible region also increased significantly, which causes the powder and suspension to be black. After treatment of DND annealed in vacuum with oxygen radicals in an aqueous medium, the nature of the absorption changed again, and the absorption spectrum became close to the spectrum of the initial sample. Usually UV-absorption is attributed to diamond. Absorption in the visible range and a maximum at 220 nm clearly correlate with the appearance of the sp^2 -phase after vacuum annealing. The following conclusion can be drawn: the oxidation in aqueous medium (described in [3]) allows to remove the non- sp^3 -phase from the surface of a diamond core that has not undergone a phase transition.

The work was supported by Russian Foundation for Basic Research (grant №18-29-19125). X-ray diffraction patterns were obtained on the equipment of the Engineering Center of St. Petersburg State Institute of Technology.

References

1. Stelmakh, S., Skrobas, K., Gierlotka, S., Palosz, B. *Diam. Relat. Mater.* (2019) **93**, 139.
1. Knizhnik, A.A., Polynskaya, Y.G., Sinitza, A.S., Kuznetsov, N.M., Belousov, S.I., Chvalun, S.N., Potapkin, B.V. *Phys. Chem. Chem. Phys.* (2021) **23**, 674.
1. Shestakov, M.S., Vul', S.P., Dideikin, A.T., Larionova, T.V., Shvidchenko, A.V., Yudina, E.B., Shnitov, V.V. *J. Phys.: Conf. Ser.* (2019) **1400**, 055044

Nanodiamonds size, shape, and defectness determination using Raman spectroscopy

Utesov O.I.^{1,2,3}, *Koniakhin S.V.*⁴, *Yashenkin A.G.*^{1,2}

utiosov@gmail.com

¹Theory Division, Petersburg Nuclear Physics Institute NRC "Kurchatov Institute", Orlova roshcha, Gatchina, Russia

²Department of Physics, Saint Petersburg State University, St. Petersburg, Russia

³St. Petersburg School of Physics, Mathematics, and Computer Science, HSE University, St. Petersburg, Russia

⁴Nanobiotechnologies Laboratory, St. Petersburg Academic University, St. Petersburg, Russia

Nanoparticles (NP) in the forms of quantum dots arrays, powders, liquid suspensions, etc., are intensively studied now for various applications in, e.g., material science, biology. One of the possible experimental techniques for the characterization of NP including nanodiamonds is Raman spectroscopy. In NP Raman peak is redshifted and is asymmetrically broadened in comparison with bulk materials, which is related to the particle finite size.

Recently to closely connected approaches to NP powders Raman spectra (RS) were proposed. The first one combines the dynamical matrix method and the bond polarization model (DMM-BPM) [1]. The second one is the continuous reformulation of DMM-BPM, which we called EKFG [2]. Both approaches were shown to reproduce crystalline NP powders RS with excellent accuracy, beyond the famous phonon confinement model (PCM) possibilities.

In the present research, we focus on nanodiamonds and enhance DMM-BPM and nanoparticle shape-sensitive EKFG methods with the microscopic models of optical phonons damping, which was assumed to be determined mainly by elastic scattering on NP impurities, such as point-like defects (e.g., NV-centers), smooth finite-radius disorder, or random particle faceting - surface disorder. We theoretically describe phonon lines broadening, which depends on the line number, particle shape, and disorder strength S [3, 4]. In particular, our model yields $\Gamma \sim S/L$ under relevant to the experiments on nanodiamonds conducted by prof. Yoshikawa [5].

Understanding of microscopic mechanisms of the phonon lines broadening allows formulating the problem of extracting mean particle size, size distribution function standard deviation, disorder strength, and estimating the particle shape. Here one should make an assumption about the distribution function (e.g., Gaussian or log-normal). The obtained disorder strength can be recalculated to the defects (e.g. NV-centers) concentration in nanodiamonds if there is additional evidence that they are dominating impurities in the specimen. Using several concrete experimental examples, we show the applicability and robustness of our approach [6]. Our findings can be used for the treatment of Raman spectra of various crystalline nanoparticle ensembles and for reliable determination of their parameters: size distribution, shape, defect concentration.

This work is supported by the Russian Science Foundation (Grant No. 19-72-00031).

References

1. S.V. Koniakhin, *et al.*, J. Phys. Chem. C (2018) **122**, 19219.
2. O.I. Utesov, *et al.*, J. Phys. Chem. C (2018) **122**, 27738.
3. O.I. Utesov, *et al.*, Phys. Rev. B (2020) **102**, 205421.
4. S.V. Koniakhin, *et al.*, Phys. Rev. B (2020) **102**, 205422.
5. M. Yoshikawa, *et al.*, Appl. Phys. Lett.(1993) **62**, 3114.
6. A.G. Yashenkin, *et al.*, arXiv:2004.12631.

Nanodiamond deagglomerated by annealing under argon: infrared spectroscopy and mass-spectrometry study

*Yudina E.B.*¹, *Romanov P.A.*¹, *Shvidchenko A.V.*¹, *Aruev N.N.*¹

yudina@ioffe.mail.ru

¹ Ioffe Institute, St.Petersburg, Russia

Detonation nanodiamond (DND) is known to possess a tailored surface chemistry [1] that determines its colloidal properties [2]. In particular, hydrogenated nanodiamond exhibits positive surface charge. Meanwhile the issue on the origins of the positive charge is still arguable and intriguing. It was previously shown [3] that deagglomeration of DND, or obtaining colloids consisting of 4-5 nm particles, may be carried out by annealing under molecular hydrogen (DND-H) and vacuum (DND-vac). However the colloidal stability of DND-vac is confined by alkali medium in contrast to DND-H.

In this work we have stated that deagglomeration of DND may be implemented via annealing under argon (DND-Ar) as well. Pristine DND, DND-H and DND-Ar have been studied by time-of-flight mass-spectrometry (MS) and ex-situ FTIR. MS measurements have been implemented over a range of temperature from 100°C to 800°C.

DND-H and DND-Ar are occurred to exhibit almost the same colloidal behavior. While DND-Ar has significantly larger content of surface carbonyl and hydroxyl groups as revealed by MS and FTIR. Large water content is also observed in DND-Ar. MS spectra of both samples demonstrate nitrogen containing surface groups. Additionally, pristine DND possesses surface covered with hydrocarbons with length no more than C4. The presence of surface aliphatic amines, ketones, aldehydes, esters and alcohols is also discussed. The annealing under either hydrogen and argon results in elimination of most of these substances. Furthermore we show that mass-spectrometry along with FTIR is the effective tool in thorough investigation of the surface composition.

References

1. Nanodiamond, ed. by Jean-Charles Arnault, Elsevier, 2017, Chapter 8 by Anke Krueger, 183-242
2. A.V. Shvidchenko, E.D. Eidelman, A.Ya. Vul', N.M. Kuznetsov, D.Yu. Stolyarova, S.I. Belousov, S.N. Chvalun, *Advances in Colloid and Interface Science* (2019), **268**, 64-81
3. A.T. Dideikin, A.E. Aleksenskii, M.V. Baidakova, P.N. Brunkov, M. Brzhezinskaya, V. Yu. Davydov, V.S. Levitskii, S.V. Kidalov, Yu. A. Kukushkina, D.A. Kirilenko, V.V. Shnitov, A.V. Shvidchenko, B.V. Senkovskiy, M.S. Shestakov, A. Ya. Vul', *Carbon* (2017), **122**, 737-745

Density functional theory calculation for fullerene-lysine system

Abbas R.^{1,2}, Izotova S.G.¹

rashad88abbas@gmail.com

¹ Saint Petersburg State Institute of Technology, Saint Petersburg, Russia

² Al-Baath University, Homs, Syrian Arab Republic

Recently, computational chemistry software has been actively used for determining the structure of *natural products*. [1]. In this work we use it to explore the nature of the bond between C₆₀ and amino acid lysine in their adduct. This adduct has biological activity, being a subject to a wide range of applications [2,3].

We perform geometric optimization of the various structures of adducts and calculate their vibrational spectra using density functional theory method in the B3LYP/6-31G (*d, p*) approximation in the Gaussian 09 software package. IR spectra of the solid-phase samples in KBr is measured using a Shimadzu IRTracer-100 FT-IR spectrometer in the range of 400-4000 cm⁻¹.

Experimental data shows that the adduct consists of two lysine molecules and a fullerene. We explore how lysine binds to fullerene: through the α -NH₂, ϵ -NH₂ or COOH groups of lysine. Moreover, we investigate the effects of various factors, such as the number of methylene groups (-CH₂-), charge distribution, protonation-deprotonation and solvation.

The results show a good agreement between the calculated and experimental vibrational spectra of fullerene. We perform quantum-chemical calculations of protonated and deprotonated lysine structures with different charge distribution. We find that the proton transfer from COOH- to α -NH₂-group in a neutral-charged lysine molecule is energetically more favorable. The increase in the length of the hydrocarbon chain in the homologous series of lysine-related amino acids does not change significantly the position of the characteristic vibrations of adducts, but it slightly complicates the spectrum in the region of the wavenumbers of stretching vibrations of CH-groups. We determine characteristic vibrations of fullerene-lysine bond in the adduct. We also perform calculations, taking solvation into account, and conclude that the adduct in real systems is present in an unsolved form. We show that lysine can coordinate through the α -NH₂ and ϵ -NH₂ groups. The latter group is slightly more probable due to energy preference.

References

1. E. Nugroho, and H. Morita, J. Nat. Med. (2019) **73**, 687-695.
2. N. Semenov, N. A. Charykov, G. O. Iurev, N. M. Ivanova, V. A. Keskinov, D. G. Letenko, V. N. Postnov, V. V. Sharoyko, N. A. Kulenova, I. V. Prikhodko, and I. V. Murin, J. Mol. Liq. (2017) **225**, 767-777.
3. I. Lelet, K. N. Semenov, E.V. Andrusenko, N. A. Charykov, and I. V. Murin, J. Chem. Thermodyn. (2017) **115**, 7-11.

Study of temporal changes in the spectrum of fullerene C₆₀ in the presence of N-methylpyrrolidone

Andreev S.¹, Shershakova N.¹, Turetskyi E.¹, Shatilov A.¹, Timofeeva A.¹, Khaitov M.¹

sm.andreev@nrcii.ru

¹ NRC Institute of Immunology FMBA of Russia, Moscow

Fullerene C₆₀ is a highly demanded material due to its valuable biomedical properties. However, the only way to transfer unmodified C₆₀ into an aqueous medium is to obtain its aqueous dispersion. One of the promising method is based on the dissolution of fullerene in N-methylpyrrolidone (NMP), subsequent mixing with water and final exhaustive diafiltration to remove NMP [1]. One question that arises when obtaining a solution of C₆₀ in NMP is its spectral transformations, described earlier [2] as smoothing the spectral profile ("solution aging"), observed already in short time intervals (hours) and ascribed to aggregation processes. Surprisingly, the behavior of C₆₀ solutions in NMP was very different when we used the NMP of different grades. The spectrum of a solution of C₆₀ in anhydrous high pure NMP stored in the dark changed very slowly (obvious changes after 50-100 days), while water impurities and the presence of daylight quickly lead to the disappearance of characteristic peaks near 260 and 330 nm (color changed from purple to red-brown).

Other experiments analyzing the behavior of fullerene in hexane in the presence of an increasing excess of NMP without access to light demonstrated that its spectrum does not adhere to smoothing for a very long time (123 days), the spectrum demonstrates 3 sharp peaks and the solution remains purple (Fig.1). However, exposure the sample to daylight and air leads to a rapid smoothing of the spectrum. An interesting fact was that the previously reported solubility of C₆₀ in NMP, 0.8 mg / ml, was clearly overestimated, our experiments showed that its limit is 0.6 mg/ml (Fig. 2).

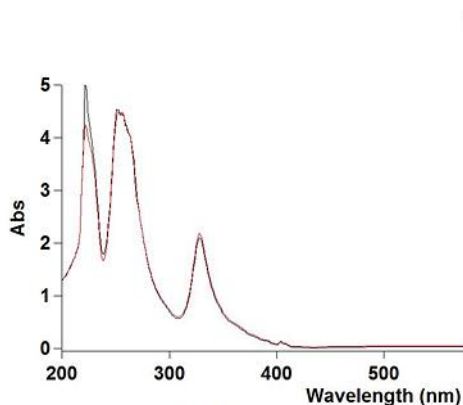


Fig. 1

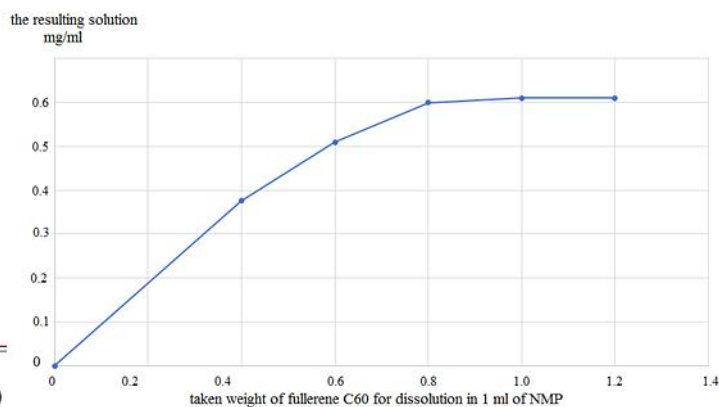


Fig. 2

References

1. S. Andreev, D. Purgina, E. Bashkatova, A. Garshev, A. Maerle, I. Andreev, N. Osipova, N. Shershakova, M. Khaitov. Study of Fullerene Aqueous Dispersion Prepared by Novel Dialysis Method: Simple Way to Fullerene Aqueous Solution, *Fullerenes, Nanotubes, Carbon Nanostruct.*, 2015. 23 (9), 792-800.
2. SV Snegir, TV Tropin, OA Kyzyma, MO Kuzmenko, VI Petrenko, V.M. Garamus, M.V. Korobov, M.V. Avdeev, L.A. Bulavin. On a specific state of C₆₀ fullerene in N-methyl-2-pyrrolidone solution: Mass spectrometric study. *Appl. Surf. Sci.*, 2019, 481, 1566-1572.

Inelastic Neutron Scattering of endofullerenes: $^3\text{HeC}_{60}$ study

*Aouane M.*¹

aouanem@ill.fr

¹ Institut Laue-Langevin - ILL

Endofullerenes are supramolecular complexes, consisting of a small (endohedral) atom/molecule enclosed by a fullerene (C_{60}) cage. Endofullerenes offer experimentalists with the molecular realisation of the ideal particle in a box model, enabling a direct observation of translational (atomic) quantisation. The resulting energy diagram is sensitive to the intermolecular interaction potential between the guest atom and the fullerene cage.

The aim of this study is firstly to observe transitions arising purely from atomic translational quantization due to confinement of a helium atom inside an almost spherical cage. The second aim is to obtain a detailed characterisation of the translational energy levels in an enlarged energy scale in order to derive experimentally the confining potential for the $^3\text{He@C}_{60}$ complex. In this talk, I will show that from neutron spectroscopy data, the potential function $V(r)$ is shown to be a superposition of r^2 , r^4 , and r^6 terms. Experiments of this kind provide high-quality experimental benchmarks for quantum chemistry calculations of non-bonded intermolecular and interatomic interactions.

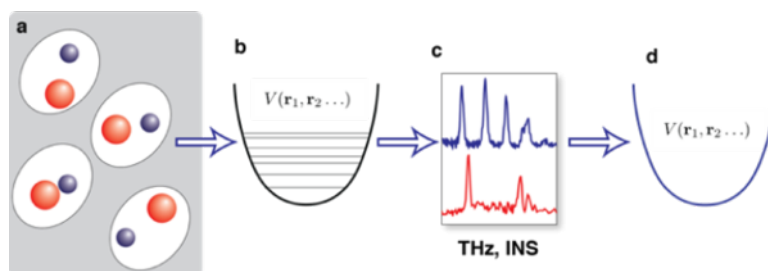
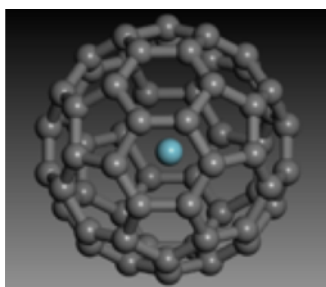


Fig.1 Analysis of the spectroscopic data allows determination of the potential energy function of the atom trapped in the C_{60}

References

1. S. W. Lovesey, *Theory of Neutron Scattering from Condensed Matter. Volume I: Nuclear Scattering*, Oxford University Press, New York, 1984.
2. K. S. K. Goh, M. Jimenez-Ruiz, M. R. Johnson, S. Rols, J. Ollivier, M. S. Denning, S. Mamone, M.H. Levitt, X. Lei, Y. Li, N. J. Turro, Y. Murata and A. J. Horsewill, *Phys. Chem. Chem. Phys.*, 2014,16,21330-21339.

Method for the extraction of EMF in a mechanical extractor

Elesina V.I.^{1,2}, *Vnukova N.G.*^{1,2}, *Churilov G.N.*^{1,2}

victes@iph.krasn.ru

¹ Kirensky Institute of Physics FRC KSC SB RAS, Krasnoyarsk, Russia

² Siberian Federal University, Krasnoyarsk, Russia

Fullerenes have a wide range of potential applications. In particular, molecular biology and medicine, where the prospects for the introduction of fullerenes and endometallofullerenes (EMF), for example, Gd@C82, Y@C82, for diagnostic (magnetic resonance imaging) and therapeutic purposes are important. Hydroxylated fullerenes (Gd@C82Ox(OH)_y) are highly biocompatible and have a wide spectrum of biological activity. To carry out studies, significant amounts of EMF are required. In this work, we demonstrate a method that has shown efficiency for the isolation of higher fullerenes and EMFs using mechanical action implemented in the Extractor developed by us [1].

The extraction of fullerenes from fullerene-containing carbon black on this apparatus was carried out using carbon disulfide, o-xylene, pyridine, and toluene. The total amount of fullerenes with Y recovered from soot was ≈ 5 wt%. Complex application of analytical methods (HPLC and atomic emission spectroscopy) allowed to unambiguously establish the quantitative content of EMF in fullerene extracts in a carbon disulfide, o-xylene, and pyridine. It averaged 3 wt%.

The total amount of extracted fullerenes from Gd toluene soot averaged only 1.3 wt% (the presence of Gd in mixtures has not been established). The amount of fullerene extracted with carbon disulfide from the soot treated with toluene using the Extractor - 1.2 wt%. In which a significant amount is C84 (3.26%). Complex application of HPLC and atomic emission spectroscopy showed the presence of EMF with Gd in amounts of 3.1 wt%. The HPLC results are shown in Figure 1.

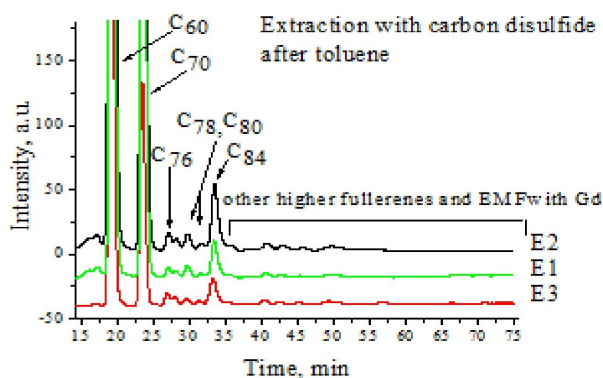


Fig.1. Typical general chromatograms of fullerene mixtures obtained from soot, first treated with toluene, then reprocessed with carbon disulfide in the Extractor, where: (E1) is the first extract most saturated in color; (E2) is a second extract less saturated in color; (E3) is a third, slightly colored extract.

References

1. Elesina, V. I.; Churilov, G. N.; Vnukova, N. G.; Dudnik, A. I.; Osipova, I. V. Filtration Process Combined with Mechanical Action, as a Method for Efficient Extraction of Endohedral Metallofullerenes from Carbon Soot. *Fullerenes, Nanotubes and Carbon Nanostructures* (2019) **27(10)**, 803-807.

The reported study was funded by RFBR according to the research project № 18-29-19003.

Theory of electron states in cone made of graphene or other multivalley 2D systems.

*M.V. Entin*¹, *Magarill L.I.*^{1,2}

entin@isp.nsc.ru

¹ Rzhanov Institute of Semiconductor Physics, SB RAS, Novosibirsk, Russian Federation

² Novosibirsk State University, Novosibirsk, Russian Federation

Electron states in 2D many-valley systems rolled into a cone (see Fig.1) are theoretically studied. Such materials as zero-gap graphene and modified gapped graphene are meant. The dependence of the valley center local momentum $\mathbf{K}(\mathbf{r})$ on coordinates on the conic surface \mathbf{r} is taken into account. We show that $\mathbf{K}(\mathbf{r})$ acts as the vector potential of effective magnetic field. The localized electron states are found by mapping the problem to 2D Coulomb problem.

Unexpectedly, the influence of the multivalley structure via the center of valley position turned to be strong.

We have determined optical transitions probabilities between the discrete electron states. The valley-selectivity of optical transitions is discussed.

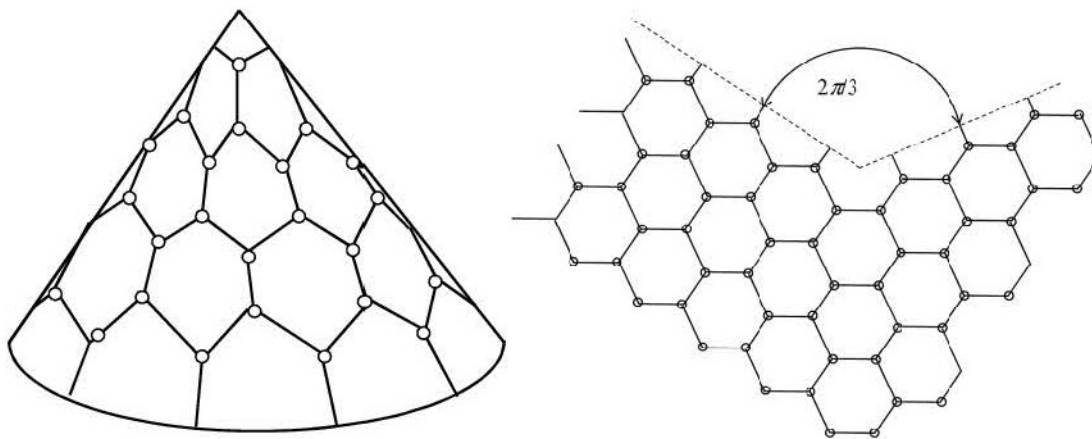


Fig.1. The graphene cone (left panel) is formed from a sheet (right panel) by a connection of rays shown by dashed lines, what guarantee the absence of extended defects.

Solubility of rare earth chlorides in ternary water-salt systems in the presence of a fulleranol - $C_{60}(OH)_{24}$ nanoclusters at 25°C

Charykov N.A.^{1,2}, Gerasimova L.V.¹, Keskinov V.A.¹, Tsvetkov K.A.¹, Kanbar A.¹, Semenov K.N.^{3,1}, Shaimardanov Zh. K.⁴, Shaimardanova B.K.⁴, Kulenova N.A.⁴

liubov.g.v@gmail.com

¹ Saint-Petersburg State Technological Institute (Technical University), Saint-Petersburg, Russia

² Saint-Pretersburg Electrotechnical University (LETI), Saint-Petersburg, Russia

³ Pavlov First Saint Petersburg State Medical University, Saint Petersburg, Russia

⁴ East Kazakhstan State Technical University, Ust-Kamenogorsk 070004, Kazakhstan

This work continues the cycle of studies, devoted to the study of solubility diagrams in systems, containing simultaneously water-soluble nanoclusters—light fullerenols. The solubility of $NdCl_3$, $PrCl_3$, YCl_3 , $TbCl_3$ in ternary water-salt systems containing water-soluble fulleranol $C_{60}(OH)_{24}$ at 25°C was studied by isothermal saturation in ampoules: $PrCl_3 - C_{60}(OH)_{24} \cdot H_2O$, $NdCl_3 - C_{60}(OH)_{24} \cdot H_2O$, $YCl_3 - C_{60}(OH)_{24} \cdot H_2O$, $TbCl_3 - C_{60}(OH)_{24} \cdot H_2O$. Saturation was conducted for 6 hours under the conditions of a shaker thermostat (temperature control accuracy $\Delta T \leq 0.05$ K, shaking frequency $\nu = 1.5$ Hz). After that, the saturated solutions were settled for 30 minutes, after which samples were taken from the ampoules for analysis.

The analysis for the content of rare earth elements was carried out by atomic absorption spectroscopy (Perkin Elmer PinAAcle 500 atomic absorption spectrometer), the analysis on the content of fulleranol were carried out by electron spectrophotometry, according to the Bouguer-Lambert-Ber law (spectro-photometer UV 1280) the by the optical density at the wavelength $\lambda = 400$ nm.

Obtained solubility diagrams in four ternary systems are simple eutonic. They consist of two branches, corresponding to the crystallization of fulleranol crystal-hydrate and rare-earth chloride crystal-hydrates, and contain one eutonic nonvariant point corresponding to saturation with both solid phases [1-2]. On the long branches of $C_{60}(OH)_{24} \cdot 18H_2O$ crystallization, a pronounced salting-out effect is observed - the solubility of $C_{60}(OH)_{24} \cdot 18H_2O$ decreases by almost 2 orders of magnitude compared to the solubility of fulleranol in pure water. On very short branches of crystallization of $NdCl_3 \cdot 6H_2O$, $PrCl_3 \cdot 7H_2O$, $YCl_3 \cdot 6H_2O$, $TbCl_3 \cdot 6H_2O$, the effect of salting-in is clearly observed, the solubility of crystal-hydrates of four chlorides increases markedly. The long crystallization curves themselves $C_{60}(OH)_{24} \cdot 18H_2O$ in both cases have a rare concave-convex σ -id character with an inflection point:

$$dm_{C_{60}(OH)_{24}}/dm_{REMCl_3} = 0 \text{ and } d^2m_{C_{60}(OH)_{24}}/dm_{REMCl_3}^2 = 0$$

The all diagrams are fairly accurately approximated by classical one-parameter Sechenov equation and very accurately approximated by the three-parameter modified Sechenov equation in the whole concentration range up to 4-7 molalities of electrolytes.

Acknowledgements: The work was supported by the Ministry of Science and Higher Education of the Russian Federation (institution 785.00.X6019, mnemonic code of the application topic 0785-2021-0002) and Russian Scientific Foundation, project application № 22-23-00013.

References

1. M.V.Charykova, N.A.Charykov, Thermodynamic modeling of the process of evaporate sedimentation (Science, St-Petersburg, 2003), p. 262.
2. N.A. Charykov, M.V. Charykova, K. N. Semenov, V.A. Keskinov, A.V. Kurilenko, Zh. K. Shaimardanov, B. K. Shaimardanova, Multiphase Open Phase Processes Differential Equations, Processes (2019) v.7, n.3, p. 148-167.

The peculiarities of molecular structure of low-symmetry isomers of non-IPR fullerene C₇₆

*Khamatgalimov A.R.*¹, *Gerasimova T.P.*¹, *Burganov T.I.*¹, *Kovalenko V.I.*¹

ayrat_kh@iopc.ru

¹ Arbuzov Institute of Organic and Physical Chemistry, FRC Kazan Scientific Center, Russian Academy of Sciences, Kazan, Russia

C₇₆ fullerene has 19 151 cage isomers, among which two isomers satisfy the isolated pentagon rule (IPR) and only one IPR isomer 19150 (D₂) have been produced and characterized as empty molecule. However, fullerene cages, including non-IPR ones, are often become stable as exohedral or endohedral derivatives. So, crystallographic analysis revealed that recently produced U@C₇₆ was assigned to non-IPR U@C₁(17418)-C₇₆ [1]. The experimentally produced exohedral fullerene C₇₆Cl₂₄ with non-IPR isomer 18917 (C₂) having five pairs of fused pentagons was a first case of non-degradative skeletal rearrangement in fullerenes [2]. In this report, we investigated the molecular structures of non-IPR isomers 17418 (C₁), 17894 (C₁), 18917 (C₂) of fullerene C₇₆ according the approach developed early by us [3] to establish their structures and reasons of stabilizations.

The distributions of single, double and delocalized π-bonds are presented for the first time as well as their molecular formulas and supported by DFT calculations. According the approach [3,4], it is revealed that structures of studied isomers can be described as having either closed or open electronic shells and require additional analysis of the results of quantum-chemical calculations. So, isomers 17418 (C₁) and 17894 (C₁), in addition to the one pentalene fragment, can contain different numbers of perylene-like (closed shell) or phenalenyl-radical (open shell) substructures. The isomer 18917 (C₂), besides five pentalenes, contain 2 coronene substructures, that can be reason of local overstrain of isomer molecules. These assumptions were verified during the quantum chemical DFT calculations. It is shown the chains of π-bonds delocalization passing through some cycles are appeared, which to be unusual for IPR higher fullerenes. The stability of these isomers was also evaluated in accordance with local strains in the molecule. It was shown that the instabilities of the studied isomers are caused by a significant local overstrain due to the excessive folding of pentagons in pentalene fragments, which typically are planar molecules. Their stabilizations in the form of endohedral U@17418-C₇₆ or exohedral C₇₆(18917)Cl₂₄ are explained by strain relaxation due to coordination of endohedral atom or exohedral addends with pentalene fragments.

The reported study was funded by Russian Foundation for Basic Research, research project No.18-29-19110mk.

References

1. W. Cai, L. Abella, J. Zhuang, X. Zhang, L. Feng, Y. Wang, R. Morales-Martínez, R. Esper, M. Boero, A. Metta-Magaña, A. Rodríguez-Forteza, J.M. Poblet, L. Echegoyen, and N. Chen, *J. Am. Chem. Soc.* 2018, **140**, 18039-18050.
2. I.N. Ioffe, A.A. Goryunkov, N.B. Tamm, L.N. Sidorov, E. Kemnitz, and S.I. Troyanov, *Angew. Chem., Int. Ed.*, 2009, **48**, 5904-5907.
3. A.R. Khamatgalimov, and V.I. Kovalenko, *Russ. Chem. Rev.* 2016, **85(8)**, 836-853.
4. A.R. Khamatgalimov, and V.I. Kovalenko, *Int. J. Mol. Sci.* 2021, **22**, 3760.

Observation of singlet oxygen in polysiloxan block-sopolimer, modified C60

*Kudoyarova V.Kh.*¹, *Vozniyakovskiy A.P.*¹, *Kudoyarov M. F.*¹, *Patrova M.Ya.*¹

kudoyarova@yandex.ru

¹ Ioffe Institute, St.Petersburg, Russia

Track membrane (TM) is widely researched and has already found use in medicine [1]. To expand its use, work is under way to modify it in order to give new properties. Previously, work was carried out on covering TM with a thin layer of polysiloxan block-sopolimer (PSBS) with fullerene additives. C60. It has been shown that fullerene C60 supplements in PSBS (siloxane) affect the mechanical properties of siloxane [2]. It is known that fullerene molecules under the influence of radiation visible or UV light contribute to the transformation of triplet sord milk into singlet, thus acting as a "generator" of singlet oxygen[3]. In the presented work, studies were carried out on the formation of singlet oxygen in the composite membrane (TM, covered with a thin layer of PSBS, modified C60). The possibility of using the iodometry method was tested for quantitative or relative quantification of the number of singlet oxygen molecules.

The method involves the use of liquid environments in which KJ is dissolved. Active singlet oxygen, generated by an object when illuminated by light with a certain wavelength, restores J to a molecular state, which changes the optical density of the solution

Various samples were irradiated by light: a composite membrane, a track membrane and a separate thin layer of PSBS in ditch filled with KJ water solution and KJ solution in acetonitril, the formula of which does not contain oxygen. KJ's water 5-mole solution was prepared in advance and was not exposed to light or contact with samples. Various samples were illuminated in ditches filled with KJ solutions in water and acetonitril. The same volumes of solutions were then placed in the ditch to measure optical density

All experiments with different samples in acetonitril, i.e. without oxygen in the solution, found a much faster and significantly greater increase in optical density from the time of exposure of samples than experiments with water solution KJ. It seems to play a role interaction with solvents that affect the life time of the excited state. Depending on the environment, it is possible to "generation" fullerene C60 of various active forms of oxygen (AFC). It is planned to continue research in order to increase the quantum output of singlet oxygen. To do this, you should use

- large concentrations of C60 (in our experiments the concentration of C60 was 4 masses) and
- use a more intense light source with a wavelength of 550 nm to increase the quantum output of singlet oxygen.

References

1. Kudoyarov M.F., A.P. Voznyakovskiy A.P., Basin B.Y. Russian Nanotechnology (2007) **2** (9-10), 90.
2. Kudoyarov M.F., Wishnewski B.I., Manicheva O.A., Myakotina E.N., Mukhin S.A., Patrova M.Y., Vedmetsky J.V. . Technical Physics Letters (2011) **37**, 81
3. Wozniakovskiy A.P., Kudoyarova V.Kh., Kudoyarov M.F., Patrova M.Ya.. FTT (2017) **59**, 1632

Algorithm for enumeration and generation of regioisomeric fullerene cycloadduct structures

*Sabirov D.Sh.*¹, *Zakirova A.D.*¹

diozno@mail.ru

¹ Institute of Petrochemistry and Catalysis UFRC RAS

Enumerating isomers is a fundamental question of organic chemistry. It started importantly sounding in the fullerene chemistry in the aspect of the materials science applications of fullerene cycloadducts $C_{60}X_n$. As is known, such compounds can exist in various isomeric forms, which are hardly separable and usually used as mixtures, *e.g.*, in organic solar cells. However, recent works have demonstrated that the use of the isolated bis- or polyadducts of C_{60} and C_{70} enhances photovoltaic output parameters [1,2].

We have designed an algorithm for enumerating and generating all possible isomers of [2+1] fullerene cycloadducts and applied it to compounds with empirical formulae $C_{20}X_n$ and $C_{60}X_n$. Fullerene C_{20} , the first representative of the fullerene family with the smallest number of double bonds ($n_{\max} = 10$), has been chosen as a test model for constructing the algorithm. To analyze $C_{20}X_n$, each regioisomer has been described with the matrix $n \times (n - 1)$ of shortest topological distances between the functionalized chemical bonds. If the elements in the strings of the matrices are equal

$$P'_{ij} = P'_{i+kj} \text{ and } P'_{ij+1} \geq P'_{ij}$$

the corresponding regioisomers are identical.

Further, the algorithm has been tested on the C_{60} fullerene adducts. In this case, the fullerene core has larger number of bonds (30). The matrix of the shortest topological distances corresponding to the weighted graph has been used to describe the chemical structures. Dijkstra's algorithm has been applied to find the shortest paths between the functionalized double bonds.

The proposed algorithm has been used in the program that enumerates and generates Cartesian coordinates of regioisomeric fullerene cycloadducts (Fig. 1). For full regioisomeric sets of $C_{60}O_3$, $C_{60}O_4$, $C_{60}(CH_2)_3$, and $C_{60}(CH_2)_4$ have been further investigated within the density functional theory computational techniques to reveal the trends of total energy and polarizability.

This research was funded by the Council of the Grants of the President of RF, grant number MD-874.2021.1.3 and Russian Foundation for Basic Research, grant number 19-03-00716.

<i>n</i>	2	3	4	5	6
$C_{20}X_n$	5	8	16	16	16
$C_{60}X_n$	8	45	262	1255	5112

The numbers of regioisomeric C_{20} and C_{60} cycloadducts found with the proposed algorithm.

References

1. T. Umeyama, H. Imahori, *Acc. Chem. Res.* (2019) **52**, 2046.
2. D. Sabirov, *J. Phys. Chem. C* (2016) **120**, 24667.
3. A. Zakirova, D. Sabirov, *J. Chem. Inf. Model.* (*in press*).

Comparative characteristics of $\text{Sc}_2\text{C}_2@\text{C}_{82}$ and C_{84} polymerization under high pressure

Vnukova N.G.^{1,2}, Churilov G.N.^{1,2}, Popov Yu.M.³, Glushenko G.A.^{1,2}

churilov@iph.krasn.ru

¹ Kirensky Institute of Physics, Krasnoyarsk, Russia

² Siberian Federal University, Krasnoyarsk, Russia

³ Technological Institute for Superhard and Novel Carbon Materials, Troitsk, Moscow, Russia

Even though fullerenes have been discovered more than 30 years ago [1], the behavior of fullerenes under high pressure is still not fully clear. For example, under the high pressure and high-temperature conditions, C_{60} undergoes a series of phase transitions and transform to the polymer which final structure depends on the exact processing conditions [2]. The polymers obtained from fullerenes are of considerable interest due to their wide range of applications (from solar cells to ultra-hard materials). The transfer of electrons leads to a reduction of the HOMO-LUMO gap in the EMF and an increase in their chemical activity.

This work is the first investigation of a unique material obtained in macroscopic quantities consisting of endofullerenes containing Sc atoms [3]. It was shown that there are differences in the processes of polymerization of $\text{Sc}_2\text{C}_2@\text{C}_{82}$ (Fig. 1a) and C_{84} (Fig. 1b) under high pressure, which was shown by the observed various phase transitions recorded by the XPS method.

The reported study was funded by RFBR according to the research project № 18-29-190080.

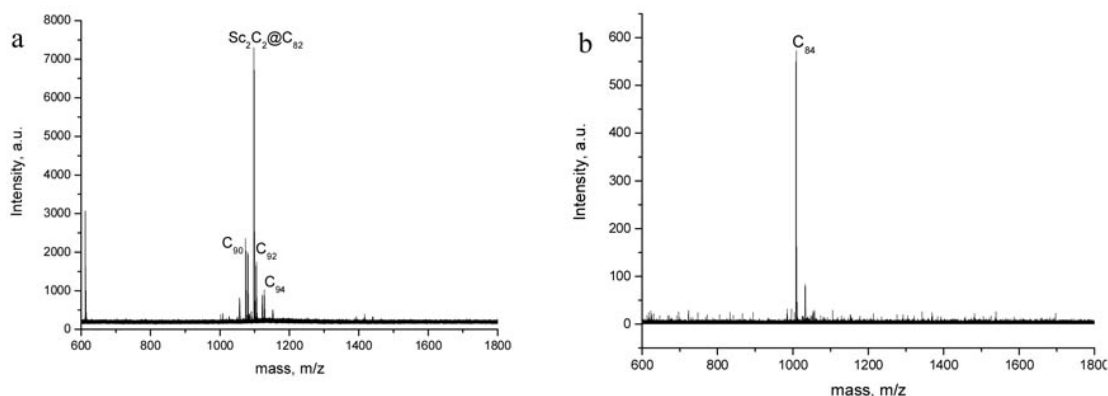


Fig. 1. Mass-spectra of $\text{Sc}_2\text{C}_2@\text{C}_{82}$ (a) and C_{84} (b)

References

1. Kroto, H. W.; Heath, J. R.; O'Brien, S. C.; Curl, R. F.; Smalley, R. E. C_{60} : Buckminsterfullerene. *Nature* 1985, 318, 162-163
2. Blank, V. D.; Buga, S. G.; Dubitsky, G. A.; Serebryanaya, N. R.; Popov, M. Y.; Sundqvist, B. High-Pressure Polymerized Phases of C Carbon 1998, 36 (4), 319-343. [https://doi.org/10.1016/S0008-6223\(97\)00234-0](https://doi.org/10.1016/S0008-6223(97)00234-0).
3. G.N. Churilov, W. Kratschmer, I.V. Osipova, G.A. Glushenko, N.G. Vnukova, A.L. Kolonenko, A.I. Dudnik Synthesis of fullerenes in a high-frequency arc plasma under elevated helium pressure // *Carbon*, 2013, V.62, P.389-392.

Role of fullerenes shell in time delay of photoelectrons from endohedrals

Amusia M.Ya.^{1,2}, *Chernysheva L.V.*²

amusia@012.net.il

¹ Racah Institute of Physics, the Hebrew University, Jerusalem, Israel

² A. F. Ioffe Physical-Technical Institute, St. Petersburg, Russian Federation

In this Presentation, we investigate the time delay of photoelectrons by the fullerenes shell in endohedrals. We present general formulas in the frame of the random phase approximation with exchange (RPAE) applied to endohedrals $A@C_N$ that consist of an atom A located inside of a fullerenes shell that consist of N carbon atoms C.

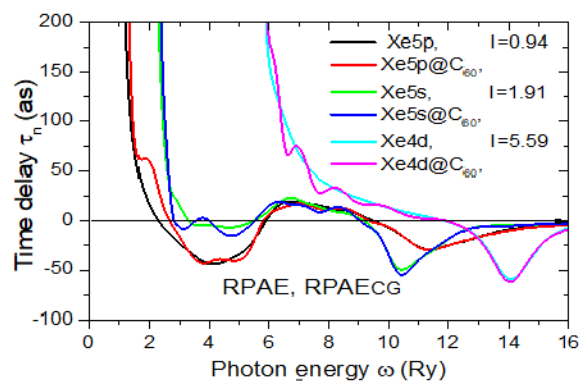
We calculate the time delay of electrons that leave the inner atom A in course of $A@C_N$ photoionization. Our aim is to clarify the role that is played by C_N shell. As concrete examples, of A we have considered Ne, Ar, Kr and Xe, and as fullerene we consider C_{60} .

The presence of the C_{60} shell manifests itself in powerful oscillations of the time delay $\tau_n(\omega)$ of an electron that is ionized from a given subshell n by a photon with energy ω . Calculations are performed for outer, subvalent and d -subshells.

The time delay of a photoionization process τ_n as a function of the photon energy ω in atomic units is connected to the phase of the amplitude $f_n(\omega)$ of the process under consideration by the following relation (see [1] and references therein)



Phases, their energy derivatives and partial cross sections are obtained in RPAE for an isolated atom and in RPAE with account of fullerenes static C potential and dynamic polarization G, denoted as RPAECG [2]. Fig.1 presents results of calculations for Xe atom and $Xe@C_{60}$ endohedral. Note that the variation of time delay is much stronger than that of the partial cross sections. The dipole photoionization of nl subshell permits to obtain from experiment only phase differences. Time delay depend upon phases itself, thus supplying in principle new information about the photoionization amplitude.



Time delays for 5p, 5s and 5d-subshell of Xe and $Xe@C_{60}$.

References

1. M.Ya. Amusia and L.V. Chernysheva, JETP Letters (2020) **111**, 1, 12.
2. M.Amusia, L. Chernysheva, V. Yarzhemsky, Handbook of theoretical Atomic Physics, Data for photon absorption, electron scattering, and vacancies decay (Springer, Berlin, 2012), Chap.1.

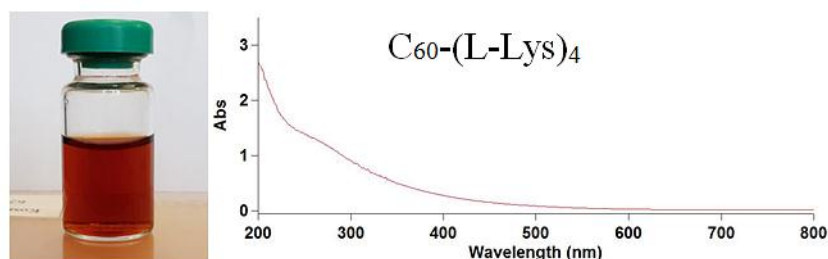
Facile organosilicon-based route for synthesis of fullerene amino acid adducts

Andreev S.¹, Shershakova N.¹, Turetskyi E.¹, Shatilov A.¹, Timofeeva A.¹, Khaitov M.¹

sm.andreev@nrcii.ru

¹ NRC Institute of Immunology FMBA of Russia, Moscow

Fullerene C₆₀ is a promising substance for the development of high-tech materials and new pharmaceuticals. Here we report the application of trimethylsilyl (TMS)-amino acids as components for straightforward preparation of water-soluble fullerene C₆₀ adducts. Such substances obtained earlier are characterized by low toxicity, good transport activity across mammalian cell membranes, and have antiviral activity [1, 2]. A significant problem in the synthesis of such substances is the incompatibility of the reaction components in terms of their solubility: fullerene requires an aprotic non-polar environment for dissolution while amino acids are prone to an aqueous environment. Due to the heterogeneity of the reaction, the reaction rate is significantly reduced. For example, the reaction of C₆₀ with condensed lysine in water-toluene, even in the presence of a phase transfer catalyst (TBAH) medium, proceeds with a very low yield. TMS-amino acids (these are liquids) are readily soluble in aprotic solvents and are resistant to light and atmospheric oxygen. When mobile protons (water) are added in reaction mixture, they easily cleave the TMS group to the starting compounds. Moreover, it is known that silylation of primary amines increases their nucleophilicity due to the electron donor properties of the TMS group. Using N,O-bis (trimethylsilyl) acetamide as donors of the TMS group, C₆₀ adducts of L-arginine, L-lysine, L-cysteine and 1,6-diamino-hexan were obtained from the corresponding amino acid hydrochlorides. The silylation of amino acids was carried out in the medium of N-methylpyrrolidone at room temperature, followed by dropwise introduction (e) of a solution of fullerene in toluene. Finally, the products were purified by exhaustive dialysis. The resulting substances are products of multiple additions of amino acids to fullerene, content of amino acid per mole of C₆₀ ranged from 4 to 9. Their behavior in terms of solubility was similar to that of amino acids with hydrophobic side residues; they are good soluble in neutral and acidic pH ranges and worse in alkaline ones. Their aqueous solution (orange-red) is dispersion with a particle size of 100 to 300 nm and a positive zeta potential. The substances were characterized by FTIR, UV spectroscopy and elemental analysis. Cytotoxicity test (MTT, 4 cell lines) did not reveal significant toxicity.



References

1. Andreev I. M., Romanova V. S., Petrukhina A. O., Andreev S. M. Amino acid derivatives of fullerene C₆₀ behave as lipophilic ions penetrating through biomembranes. *Phys. Solid State*, 2002, 44(4):683-685. doi: 10.1134/1.1470559.
2. Klimova R., Andreev S., Momotyuk E., Demidova N., Fedorova N., Chernoryzh Y., Yurlov K., Turetskyi E., Baraboshkina E., Shershakova N., Simonov R., Kushch A., Khaitov M., Gintsburg A.. Aqueous fullerene C₆₀ solution suppresses herpes simplex virus and cytomegalovirus infections. *Fullerene, Nanotubes, Carbon Nanostr.*, 2020, 28 (6): 487-499.

The structure of water-soluble derivatives of endohedral metallofullerenes and features of their self-organization in aqueous solutions

Fokin N.S.^{1,2}, *Suyasova M.V.*^{1,3}, *Sedov V.P.*¹, *Orlova D.N.*¹, *Shilin V.A.*¹, *Artemyev A.N.*⁴, *Ivanov A.V.*⁵

fokin_ns@pnpi.nrcki.ru

¹ Petersburg Nuclear physic institute named by B.P. Konstantinov of national research center Kurchatov Institute, Gatchina, Russia

² Saint-Petersburg State Institute of Technology, Saint-Petersburg, Russia

³ Saint-Petersburg university of state fire service of emercom of Russia, Saint-Petersburg, Russia

⁴ National research center Kurchatov Institute, Moscow, Russia

⁵ Saint-Petersburg university of state fire service of emercom of Russia, Saint-Petersburg, Russia

Assuming the possibility of biological and medical application of derivatives of endohedral metallofullerenes, an important aspect is the study of the features of their structure and ability to aggregate in aqueous solutions. The relationship between the structure of such systems and their properties provides complete information about the prospects for their application in biomedicine. In earlier structural studies [1-2] of aqueous solutions of endofullerenols with 4*f*- and 3*d*-elements, it was found that hydroxy derivatives of endofullerenes tend to form branched clusters with a characteristic radius of gyration $R_g \sim 25$ nm. Also, a relationship was revealed between the nature of intermolecular interactions and the structural properties of endometallofullerenes (EMF). The aim of this work was a comprehensive structural study of hydroxy derivatives of endometallofullerenes 4*f*- and 3*d*-elements in aqueous solutions, as well as an assessment of the influence of the structural features of the obtained compounds on the tendency to aggregation.

The synthesis of endohedral metallofullerenes was carried out by the method of electric arc evaporation with subsequent extraction of EMF from electric arc soot, treatment of the dry EMF extract with hydrogen peroxide to obtain hydroxy derivatives of endohedral metallofullerenes $\text{Me}@C_{2n}(\text{OH})_{38-40}$ (Me=Pr, Sm, Eu, Gd, Tb, Dy, Ho, Tm). The study of the obtained compounds was carried out by IR, Raman, EXAFS-spectroscopy. The cluster sizes and structural features of EMF aqueous solutions were studied by atomic force microscopy (AFM) and small-angle neutron scattering (SANS).

In order to establish the position of the metal atom relative to the carbon cage, we analyzed EXAFS data on samples of lanthanide oxides, powders and aqueous solutions of endofullerenols (C=1.5 wt%, pH=3, pH=7, T=20°C). It was found that the radii of the first coordination spheres vary within the range: 0.16 - 0.24 nm for powdered samples and 0.16 - 0.21 nm for aqueous solutions. Based on the AFM and SANS data, the general character of the structuring of endofullerenols $\text{Me}@C_{2n}(\text{OH})_{38-40}$ in aqueous solutions with a concentration of 1.5 wt% in acidic (pH=3) and neutral media (pH=7) at temperatures of 20 and 37°C was revealed. Variations in temperature and pH have almost no effect on the size of aggregates $R_g \sim 25$ nm and their fractal dimension. The effect of distance between the encapsulated metal and the carbon shell in EMF molecules to the nature of the interaction of hydroxy derivatives of endohedral metallofullerenes in aqueous solutions is discussed.

References

1. Xing G.M., Zhang J., Zhao Y.L. et al. Influences of Structural Properties on Stability of Fullerenols // J. Phys. Chem. B. 2004. V. 108. No. 31. P. 11473-11479.
2. Lebedev V. T., Szhogina A. A., Suyasova M. V. Neutron studies of paramagnetic fullerenols' assembly in aqueous solutions // Journal of Physics: Conference Series. - IOP Publishing, 2018. - T. 994. - No. 1. - S. 012005.

Catalytic fulleranol action on chlorella growth in the conditions of limited resource base

*Gerasimova L.V.*¹, *Charykov N. A.*¹, *Keskinov V.A.*¹, *Kanbar A.*¹, *Shaimardanov Zh. K.*²,
*Shaimardanova B.K.*², *Kulenova N.A.*²

liubov.g.v@gmail.com

¹ Saint-Petersburg State Technological Institute (Technical University), Saint-Petersburg, Russia

² East Kazakhstan State Technical University, Ust-Kamenogorsk, Kazakhstan

This article continues the cycle of articles, concerning the synthesis, identification and properties investigation of fullerolenols [1-2].

We report about the investigation of fulleranol of light fullerene $C_{60} - C_{60}(OH)_{24}$ in bio-testing, using as test micro-organism "Chlorella vulgaris beijer" – very popular alga for bio-testing. We shall report about the kinetics in the system: chlorella vulgaris beijer (bio-component)-fullerenol (catalyst-inhibitor)-water (solvent) in the presence of light (visional region wavelength) and CO_2 (dissolved in water solution).

Chlorella growth or oppression were investigated in open transparent in the visible area cylindrical polystyrene test tubes at room temperature under illumination by standard incandescent lamp (Phillips E27 – 40 Wt) for the period of 9 days. Catalyst concentrations were varied in the range 0.01 – 1.0 g/dm³. Chlorella Vulgaris concentrations were determined by the method of turbidimetry – by the determination of optical density of scattered light in the direction of propagation of the incident beam at wavelength $\lambda = 664 \text{ nm} - D_{664}$. The spectrum was obtained relative to the comparison solution – water solution of $C_{60}(OH)_{24}$ with the same concentraion, that was in test suspension without fulleranol (fullerenol was not consumed during the growth of Chlorella). All suspensions before turbidimetrical determination were thoroughly shaken.

The best way for describe kinetics of Chlorella Vulgaris growth is Verhulst model. It gives information about population growth in the conditions of intraspecific competition. We processed obtained data Chlorella Vulgaris concentrations (C_{chl}) at different catalyst – fulleranol concentrations with the help of Verhulst equation.

Calculations showed that fulleranol has negative catalytic activity or inhibitor activity in chlorella growth, with exception of the cases of low concentrations ($C_{fullerenol}$ is hundredths or less than 0.1 g/dm³). For this cases fulleranol possesses real positive catalyst activity. Moreover, for the longer the observation time, positive catalyst fulleranol activity manifests stronger.

References

1. K.N. Semenov, A.A. Meshcheriakov, N. A. Charykov, M. E. Dmitrenko, V. A. Keskinov, I. V. Murin, G. G. Panova, V. V. Sharoyko, E. V. Kanashc, Yu. V. Khomyakovc, Physico-chemical and biological properties of $C_{60} - L$ -hydroxyproline water solutions, RSC Advances (2017), v. 7, p. 15189.
2. G.G. Panova, I. N. Ktitorova, O. V. Skobeleva, N. G. Sinjavina1, N. A. Charykov, K. N. Semenov, Impact of polyhy-droxy fullerene (fullerol or fulleranol) on growth and biophysical characteristics of barley seedlings in favorable and stressful conditions, Plant Growth Regulation, International Journal on Plant Growth and Development (2015), v. 77, p. 309.

Is there a molecular symmetry lowering in open-shell IPR higher fullerenes?

*Khamatgalimov A.R.*¹, *Kovalenko V.I.*¹

ayrat_kh@iopc.ru

¹ Arbuzov Institute of Organic and Physical Chemistry, FRC Kazan Scientific Center, Russian Academy of Sciences, Kazan, Russia

A row of fullerenes that obey the isolated pentagon rule (IPR) are unstable due to their open-shell molecules [1,2]. According to some theoretical studies, the molecular symmetry of such a pristine fullerene falls; usually the quantum-chemical study stops after two steps: calculations of closed shell ($M = 1$) and triplet ($M = 3$).

Indeed, the symmetry reductions were shown for IPR molecules of open-shell isomers: 2 (T_d) of the fullerene C_{76} , isomers 6 (D_{5h}) and 7 (I_h) of the fullerene C_{80} , as well as isomers 7 (C_{3v}), 8 (C_{3v}), and 9 (C_{2v}) of the fullerene C_{82} , etc. [2]. For example, the molecular symmetry of the isomer 2 of the pristine IPR fullerene C_{76} is T_d , but after calculations it falls to D_{2d} ($M = 1$) and to C_{3v} ($M = 3$).

The typical explanation for this symmetry reduction is the Jahn-Teller effect that claims that a geometric distortion removes a spatially degenerate electronic ground state and leads to a decrease in the total energy, but it is questionable for fullerenes [3].

In accordance with developed by us the analysis of fullerene molecular structure [1,2], isomer 2(T_d) of fullerene C_{76} is unstable due to presence of four phenalenyl-radical substructures [4]. The C_3 symmetry axes go through central triple hexagon junction of each of them. It is obvious that one can suppose the existence of four unpaired electrons of this molecule. As a matter of fact, this isomer has the T_d symmetry when multiplicity is 5 (four unpaired electrons), which is corresponding to the structure with four phenylenyl-radical substructures. Despite the high relative energies of such state our assumption was supported by the experimental results of monocrystal X-ray analysis indicating the equal distribution pattern of addends on each of phenalenyl-radical substructures in exohedral derivative $C_{76}(CF_3)_{12}$ [5] and a dynamic arrangement of endohedral atoms inside the cage for endohedral fullerene $Lu_2@C_{76}(T_d)$ [6]. In our view the seeming molecular symmetry lowering of open-shell fullerene reflects a discrepancy between real symmetry of molecule and wrong choice of its multiplicity i.e. real number of unpaired electrons.

The reported study was funded by Russian Foundation for Basic Research, research project No.18-29-19110mk.

References

1. R. Khamatgalimov, and V.I. Kovalenko, Russ. Chem. Rev. 2016, **85(8)**, 836-853.
2. I. Kovalenko, and A.R. Khamatgalimov, Structure and Stability of Higher Fullerenes (Publ. Russ. Acad. Sci., Moscow, 2019), 212 p. (in Russian).
3. Schwerdtfeger, L.N. Wirz, and J. Avery, WIREs Comput. Mol. Sci. 2015, **5**, 96-145.
4. R. Khamatgalimov, and V.I. Kovalenko, Fuller. Nanotub. Carbon Nanostruct. 2015, **23**, 148-152.
5. B. Shustova, I.V. Kuvychko, R.D. Bolskar, K. Seppelt, S.H. Strauss, A.A. Popov, and O.V. Boltalina, J. Am. Chem. Soc. 2006, **128**, 15793-15798.
6. Umemoto, K. Ohashi, T. Inoue, N. Fukui, T. Sugai, and H. Shinohara, Chem. Commun. 2010, **46**, 5653-5655.

Quantum chemistry simulation of halogenated fullerene. Regiochemistry and vibrational spectra.

Kopeuw A.J.^{1,2}, *Izotova S.G.*³

agkopeuw@gmail.com

¹ Saint-Petersburg State Institute of Technology (Technical University), Saint-petersburg, Russia

² University of Cenderawasih Jayapura, Papua, Indonesia.

³ Saint-Petersburg State Institute of Technology (Technical University) Saint-Petersburg, Russia

The bulk of the molecule C₆₀ contains 30 reactive double bonds between two C6 rings that can engage in various addition reactions. As a consequence, there can emerge different regioisometric fullerene adducts.^[1-2]

The simulation of fullerene-halogen adducts has been performed as a function of the type, number of halogen atoms and of how they are distributed over the fullerene surface. The simulation is performed using Gaussian09 at the level B3LYP / 6-31G (d) based on the density functional theory (DFT). We have constructed various C₆₀-X_n isomers (X-halogen, n = 2, 4, 6, and 8). For all the adducts geometrical optimization has been performed and vibrational spectra have been calculated.

We have noticed the common regiochemical pattern that the bonds tend to form. The distance between the halogen atoms on the fullerene surface has a big impact on the stability of halogenated fullerene bond. Moreover, the number of atoms on the fullerene surface, type of halogen, as well as their spatial distribution, affect the stability of the bond. The latter is decreased for fluorine, chlorine, bromine and iodine halogens. The formation of the bond with iodine is extremely difficult.

The stability of adducts has been examined, depending on the position of halogen: between C6 and C6 rings, on the same C6 ring and between C5 and C6 rings.

The assignment of vibrations in calculated spectra has been performed. We have also analyzed how common structural features of C₆₀-X_n adducts, type, number of halogen atoms and their distribution on the surface of fullerene affect the shape of spectra and wave numbers of characteristic vibrations of fullerene-halogen bond.

References

1. Hirsch A., Lamparth I., Grosser T., J. Am. Chem. Soc. (1994) 9385-9386.
2. D.Sh. Sabirov et al, J. Molecular Graphics and Modelling (2008) **27**,124-130

Antioxidant properties of water-soluble fullerene derivatives

Lyutova Zh.B.^{1,2}, *Borisenkova A.A.*^{1,2}, *Sedov V.P.*¹, *Titova A.V.*^{1,2}

borisenkova_aa@pnpi.nrcki.ru

¹ Petersburg Nuclear Physics Institute named by B.P. Konstantinov of NRC "Kurchatov Institute", Gatchina, Russia

² Saint-Petersburg State Institute of Technology, Saint-Petersburg, Russia

The accumulation of free radicals in the human body is considered as one of the reasons for the progression of many dangerous diseases. In this regard, an active search for biologically active substances with high antioxidant activity is being continued. It is known that Fullerene C₆₀ exhibits remarkable reactivity towards free radicals, which makes it a very attractive antioxidant. However, its potential use in personal care products or biomedicine is limited due to inherent hydrophobic properties and poor water solubility.

In this regard, this work was aimed to study the antioxidant properties of water-soluble fullerene derivatives - fullerlenols C₆₀(OH)₃₀, C₇₀(OH)₃₀ and C₁₂₀O(OH)₄₄, obtained by the original two-step method [1]. The structure of the obtained water-soluble derivatives was confirmed by IR-spectrometry, elemental and thermal analysis. The antioxidant activity (AA) of water-soluble derivatives in concentrations from 10⁻² to 10⁻⁷ mg/ml was evaluated by their ability to inhibit the adrenaline autooxidation and thereby prevent the appearance of reactive oxygen species [2]. The kinetics of free radicals absorption by water-soluble fullerene derivatives in the reaction of their interaction with the stable free radical 2,2'-diphenyl-1-picrylhydrazyl (DPPH) was also investigated [3].

It was found that the AA of water-soluble fullerene derivatives nonlinearly depends on their concentration: the highest antioxidant activity is manifested at concentrations of 10⁻³-10⁻⁴ mg/ml. Fullerlenols do not interact directly with adrenaline and its oxidation products, and inhibition of the autooxidation reaction of adrenaline is achieved due to the interaction of fullerlenols with superoxide anion radicals.

Analysis of the kinetic curves of the interaction of DPPH with fullerlenols showed that their interaction occurs in three stages. It is assumed that the first stage of the kinetics can be associated with the rapid detachment of a hydrogen atom from the -OH groups of fullerlenol, which leads to the formation of epoxy bonds. Then, at a second, slower stage, DPPH reacts with a conjugated double bond, followed by electron transfer to the DPPH radical. The interaction of the radicals with the C = C bond is hindered by the low availability of reaction centers due to steric hindrances on the part of the hydroxyl group, which determines the presence of a third, even slower stage of the reaction.

References

1. Bolshakova O., Borisenkova A., Suyasova M., Sedov V., Slobodina A., Timoshenko S., Varfolomeeva E., Golomidov I., Lebedev V., Sarantseva S., Aksenov V. *Materials Science and Engineering: C*. 2019. V. 104. P. 109945.
2. Ryabinina E.I., Zotova E.E., Vetrova E.N., Ponomareva N.I., Ilushina T.N. *Chemistry of vegetable raw materials*. 2011. No. 3. P.117
3. Awan, F., Bulger, E., Berry, R. M., & Tam, K. C. *Cellulose*. 2016. V. 23. No. 6. P. 3589.

Aqueous fullerene dispersions: preparation techniques, characterization, and applications

*Mikheev I.V.*¹, *Volkov D.S.*¹, *Kareev I.E.*², *Korobov M.V.*¹, *Proskurnin M.A.*¹

mikheev.ivan@gmail.com

¹ Chemistry Department, Lomonosov Moscow State University, Moscow, Russia

² Institute of Problems of Chemical Physics of the RAS, Chernogolovka, Russia

Stable aqueous fullerene dispersions (AFD) are very promising for many applications dealing with antioxidant activity and MRI contrast agents. Water is an excellent dispersant for all these issues but preparing purified aqueous dispersions of pristine fullerenes and endofullerenes is not an easy task due to its intrinsically hydrophobic nature.

For the last decade, the laboratories' collaboration of the Chemistry Department has been dealing with preparation, complete investigations, and analysis of AFD. We recently switched to assessing the effectiveness of dispersions in different biological systems and estimating their toxicity. In the report, we would be reviewing the achievements of the past ten years in AFD chemistry.

To date, the stable (over nine years) AFDs of C₆₀ and C₇₀ (~100 ppm) were obtained using a solvent-exchange ultrasound-assisted technique. Direct sonication using a high-energy ultrasound probe was recently proposed for rapid and green preparation of any AFD of both pristine and functionalized AFDs. Techniques for purification from organic and inorganic impurities are proposed. The report will summarize the proposal of general principles and approaches to prepare highly-concentrated and pure AFDs.

A methodology for the analysis of AFD has been developed, including the compulsory use of spectroscopy and chromatography methods. Procedures for determining the main component in a wide range of concentrations from ppb to ppm have been developed. Using MALDI and FTIR spectroscopy, we confirmed the functional composition and presence of surface groups. However, the exact mechanism of stabilization of colloidal solutions is unknown still. Surface hydroxylation of the initially hydrophobic fullerene molecules deals with the perceived stabilization mechanism.

The biomedical application of AFD deals with studying their effect on reactive oxygen species homeostasis. The reactivity of AFDs and Gd@C₈₂ endofullerene AFD has been studied for superoxide in the xanthine/xanthine oxidase chemiluminescence system. It was found that C₆₀ and C₇₀ in AFD react with superoxide as scavengers by a similar mechanism. However, in the cell model, Gd@C₈₂ showed the lowest activity than C₆₀ and C₇₀. It can be accounted for by its higher affinity for the lipid phase.

Acknowledgments. The Russian Science Foundation has supported this work under Contract No. 19-73-00143.

References

1. I.V. Mikheev, E.S. Khimich, A.T. Rebrikova, D.S. Volkov, M.A. Proskurnin, M.V. Korobov, *Carbon* 2017, **111**, 191.
2. Mikheev, M. O. Pirogova, L. O. Usoltseva, A. S. Uzhel, T. A. Bolotnik, I. E. Kareev, V. P. Bubnov, N. S. Lukonina, D. S. Volkov, A. A. Goryunkov, M. V. Korobov, M. A. Proskurnin, *Ultrasonics Sonochemistry* 2021, **73**, 105533.
3. I.V. Mikheev, I.E. Kareev, V.P. Bubnov, D.S. Volkov, M.A. Proskurnin, M.V. Korobov, *J Anal Chem* 2018, **73**, 837.
4. I.V. Mikheev, M. M. Sozarukova, E. V. Proskurnina, I. E. Kareev, M. A. Proskurnin, *Molecules* 2020, **25**, 2506.

Bader's bond ellipticity as a reactivity index in the stepwise [2+1] cycloaddition reactions to the C₆₀ fullerene

Sabirov D.Sh.¹, Tukhbatullina A.A.¹

diozno@mail.ru

¹ Institute of Petrochemistry and Catalysis UFRC RAS, Ufa, Russia

The C₆₀ molecule is a truncated icosahedron, in which all carbon atoms are chemically equivalent. The cycloaddition reduces the C₆₀ symmetry, so the reactive chemical bonds become inequivalent. This causes difficulties for both experimental and theoretical chemistry of C₆₀ polyadducts. Indeed, the theoretical description of the competing reactions requires assessing energy parameters (heat effects and/or activation barriers) of parallel addition paths to determine the most preferable one.

A theoretical description is simplified with the use of reactivity indices: bond orders, pyramidal angles, and curvatures *etc.* However, the bond order, a widely used parameter in physical organic chemistry, does not work well in the case of stepwise polyaddition reactions of C₆₀ because it varies in a very narrow and uninformative range.

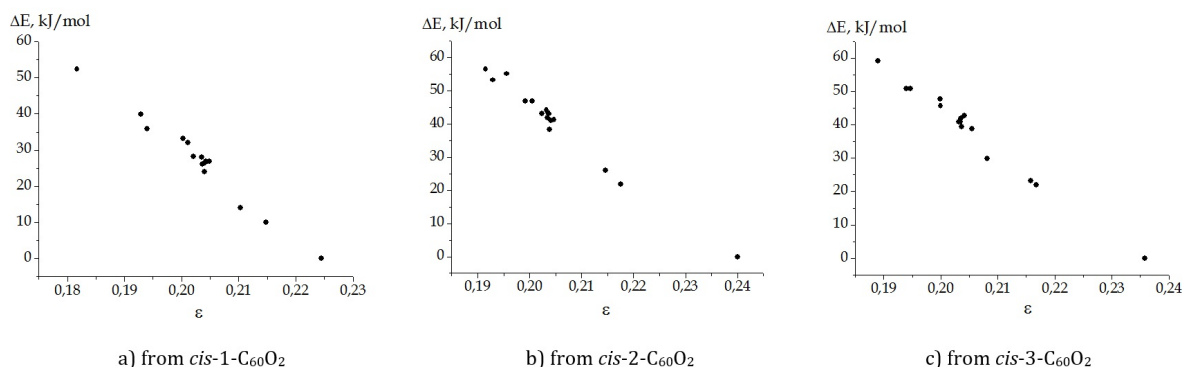
We have found that the Atoms-in-Molecules analysis (AIM) accurately quantifies the reactivity of 6.6-bonds upon multiple cycloaddition to fullerene. The analysis provides the ellipticity ε for each of the nonequivalent chemical bonds defined as:

$$\varepsilon = \lambda_1/\lambda_2 - 1,$$

where λ_1 and λ_2 are the eigenvalues of the Hessian of the electron density at the bond critical point corresponding to the considered double bond. Ellipticity characterizes the anisotropy of the electron density between the bonded atoms and considered as an analogue of the bond order.

We have found that the thermodynamic favorability of the cycloadducts C₆₀X_n correlate with the bond ellipticities in their precursors C₆₀X_{n-1}. This conclusion we have made based on the corresponding DFT/AIM calculations on the series of adducts C₆₀X_n with epoxide (X = O) and cyclopropane (X = CH₂) addends and n up to 3. The orders of 6.6 bonds in C₆₀ and C₆₀X_n are usually almost equal being 1.44–1.46. In contrast, ellipticities vary in a large range that allows designing correlations with thermodynamic favorability of C₆₀X_n (Figure shows examples of such trends).

This research was funded by the Council of the Grants of the President of RF, grant number MD-874.2021.1.3 and Russian Foundation for Basic Research, grant number 19-03-00716.



Correlations between relative energies of C₆₀O₃ fullerene epoxides and bond ellipticities in their precursors C₆₀O₂.

References

1. A. A. Tukhbatullina, E. M. Khamitov, D. S. Sabirov, *Comput. Theor. Chem.* (2019) **1149**, 31.
2. D. S. Sabirov, *Mendeleev Commun.* (2020) **30**, 91.

Structural features of new fullerene derivatives according to IR-, Raman- and UV/Vis-spectroscopy

Suyasova M.V.^{1,2}, *Sedov V.P.*¹, *Orlova D.N.*¹, *Ivanov A.V.*², *Titova A.V.*¹, *Ryabokon I.S.*¹, *Shabunina A.V.*¹, *Borisenkova A.A.*^{1,3}

marina.suyasova@mail.ru

¹ Petersburg Nuclear Physics Institute named by B.P. Konstantinov of NRC Kurchatov Institute, Gatchina, Russia

² Saint-Petersburg university of state fire service of emercom of Russia, Saint-Petersburg, Russia

³ Saint-Petersburg State Institute of Technology, Saint-Petersburg, Russia

More than three decades have passed since the discovery of buckminsterfullerene, which allowed scientists to study in depth the mechanisms of C₆₀ solubility in various solvents [1]. The highest solubility of fullerene C₆₀ is observed in solvents, the molecules of which are related in structure to the five- and six-membered cycles of the carbon frame. Such solvents are aromatic hydrocarbons and their derivatives [2]. Polar solvents, such as N,N-dimethylformamide (DMFA), can also be used to dissolve polar fullerenes and endometallofullerenes (EMF), but the solubility of fullerenes remains quite low. The addition of hydrazine hydrate to the DMFA solution can significantly increase the solubility of both hollow fullerenes and EMF [3]. Presumably, the fullerenes dissolved in this way are adducts of fullerenes with hydrazine-hydrazine and DMFA. However, the mechanism of formation of these adducts is not completely clear. In this regard, the aim of this work was to study the interaction of individually pure C₆₀, C₇₀ fullerenes and C_{2n} mixture of fullerenes in DMFA with the addition of hydrazine hydrate. Fullerene powders C₆₀ (≥99.5% HPLC), C₇₀ (98.4 ÷ 99.0% HPLC) and fullerene extract C_{2n} (C₆₀ - 88% HPLC, C₇₀ - 12% HPLC) isolated from electric arc soot using ortho-xylene were used for the studies. The obtained compounds were studied by HPLC, IR, Raman, and UV-Vis spectroscopy. The IR spectra of C₆₀, C₇₀, and C_{2n} adducts, which were dried in vacuum at a temperature of 80 C, contain the following bands, cm⁻¹: 565, 570, 612 - 618, 672, 750 - 800, 1133, 1378 - 1386, 1413 - 1454, 1653, 1680, 2350, 3350 - 3840. In addition to the absorption bands of the C₆₀ (565 and 1422 cm⁻¹) and C₇₀ (570, 672, 794 and 1427 cm⁻¹) fullerenes themselves, the 1378 and 1680 cm⁻¹ bands characteristic of DMFA were found. In addition, the bands 612-618 cm⁻¹ appear, indicating the formation of new covalent bonds of fullerene molecules. The Raman spectra of the studied powder samples of adducts reflects a general trend: most of the allowed modes of the initial C₆₀ or C₇₀ fullerenes are absent, and two broad bands appear at 1360-1370 and 1580-1590 cm⁻¹. The detected intense bands are close to the D and G modes of disordered graphite, as well as to the modes of 3D C₆₀ polymers. The presence of these bands may indicate the intermediate nature of hybridization between sp² and sp³ for most of the valence C-C bonds in the resulting adducts. The analysis of the IR, Raman, and UV-Vis spectra suggests that the presence of hydrazine hydrate in the water may lead to two parallel reactions. DMFA can react with hydrazine hydrate to form hydrazones or azines of DMFA. The interaction of hydrazine hydrate with fullerene can occur with the formation of hydrazine and pyrazole addends on the surface of the fullerene cage. The interaction most likely follows the mechanism of nucleophilic addition, but cycloaddition is also possible. The mechanism of the expected reactions is discussed.

References

1. Mchedlov-Petrosyan, N. O. Journal of Molecular Liquids. — 2011. — V. 161. — №. 1. — P. 1-12. DOI: 1016/j.molliq.2011.04.001
2. Mchedlov-Petrosyan, N. O. Chem. Rev. — 2013. — V. 113. — №. 7. — P. 5149-5a193. DOI: 1021/cr3005026
3. Sedov, V. P. et al. Russian Journal of Applied Chemistry. - 2020. - V. 93. - P. 527-539. DOI: 10.1134/S1070427220040072

Kinetics of cluster growth in C₆₀-toluene solutions: DLS study and theoretical evaluation

*Tropin T.V.*¹, *Selyshchev P.A.*², *Petrenko V.I.*^{3,4}, *Avdeev M.V.*¹, *Aksenov V.L.*^{1,5}

ttv@jinr.ru

¹ Frank Laboratory of Neutron Physics, Joint Institute for Nuclear Research, Dubna, Russia

² Department of Physics, University of Pretoria, Pretoria, South Africa

³ BCMaterials, Basque Centre for Materials, Applications and Nanostructures, Leioa, Spain

⁴ Ikerbasque, Basque Foundation for Science, Bilbao, Spain

⁵ National Research Centre Kurchatov Institute, Moscow, Russia

Kinetics of cluster growth in various systems is an interesting subject both from scientific point of view, and for the applications, where control of this process is often important. In this sense, fullerene nanoparticles present an outstanding object, due to their solubility in various solvents and the occurrence of aggregation processes in most of them. The properties of fullerenes cluster state and the dynamics of its formation depends on the solvent type [1]. Up to now, the clear understanding in this field is not reached, thus a need for further research remains.

In this work we revisit the kinetics of aggregation in fullerene C₆₀ solutions in toluene by utilizing dynamic light scattering for a continuous investigation, as well as develop new models for description via a set of kinetic equations. As a basic assumption, we suppose that fullerene oxides form in the solution after exposure to light [2], and that they are the centres for cluster processes to occur. Thus, cluster growth will proceed via several stages resulting in a multi-level structure of aggregates (as detected by structural methods, for example in [3]). The kinetic equations for the first stage of cluster growth were solved analytically, the solution in general forms is presented and reaffirmed by numerical calculations. Stage II, on the other hand, being a more complex subject is investigated by a phenomenological approach and numerical schemes.

This work is supported by JINR-SA grant (28/2020 #4).

References

1. M.V. Avdeev, V.L. Aksenov, T.V. Tropin, *Rus. J. Phys. Chem. A* (2010), **83** (8), 1273.
2. R. Dattani, K.F. Gibson, S. Few, A.J. Borg, P.A. DiMaggio, J. Nelson, S.G. Kazarian, J.T. Cabral, *J. Colloid Interface Sci.*, (2015), **446**, 24.
3. S.V. Snegir, T.V. Tropin, O.A. Kyzyma, M.O. Kuzmenko, V.I. Petrenko, V.M. Garamus, M.V. Korobov, M.V. Avdeev, L.A. Bulavin, *Appl. Surf. Sci.* (2019), **481**, 1566.

Day 5: Applications of Nanocarbons.

Exfoliated graphite-based carbon ink for screen-printing applications

*Gryaznova M.I.*¹, *Lugvishchuk D.S.*¹, *Gryaznov K.O.*¹, *Mitberg E.B.*^{1,2}, *Karaeva A.R.*¹, *Mordkovich V.Z.*^{1,2}

mig@tisnum.ru

¹ Technological Institute for Superhard and Novel Carbon Materials, Troitsk, Moscow 108840, Russia

² INFRA Technology Ltd., Moscow 125009, Russia

Screen-printing technology development for the past three decades is proven to be a cheaper and more productive manufacturing method for carbon electrodes production. There are spectra of promising nanomaterials used for preparation of carbon inks (single and multiwalled nanotubes, graphene and others) with some benefits to the classical conductive additive - natural graphite. But the production cost of such new materials is still relatively high to make large production of cost-efficient carbon-based biosensors [1].

Complexity of the screen-printing technology is defined not only by the conductive material, but by the combination of many factors and parameters such as polymer binder/solvent composition, solid additives rheological behavior, substrate and its flexibility, screen mesh etc. There is some optimal composition of mass concentration of each component for preparation of carbon-based inks. The world leading commercially available pastes from the companies such as GWENT, Dupont, EMS have composition carbon-based ink with solid phase concentration around 35-40 mass. % [2]. Such large amount of conductive graphite particles in a typical σ -bonded polymer (or any inert binder) is needed to achieve high bulk conductivity. All relationships between structure of particles and bulk conductivity is the province of percolation theory.

In order to make conductive carbon ink more economically feasible percolation threshold need to be decreased. Highly conductive exfoliated graphite is promising carbon material to decrease the concentration of solid components of carbon ink.

This work presents the way to produce exfoliated graphite-based carbon ink for screen-printing application with low specific bulk electric resistance (0,00045 Ohm×m) and excellent physical properties of resulting carbon electrodes. Optimization of exfoliated graphite/polymer ratio, as well as investigation of solvent/binder compositions were carried out. The use of exfoliated graphite allows to reduce mass concentration of solid conductive particles up to 4 time in contrast to the commercially available carbon inks, which will result in a cost-efficient carbon biosensors manufacturing via screen-printing process.

References

1. Chu Z., Peng J., Jin W. Advanced nanomaterial inks for screen-printed chemical sensors // *Sensors Actuators B Chem.* (2017) **Vol. 243**, P. 919-926.
2. Fletcher S. Screen-Printed Carbon Electrodes // *Advances in Electrochemical Science and Engineering.* (2015) P. 425-444.

Thermodynamics of xenon adsorption on nanoporous SiC-derived carbon affected by adsorption-induced and thermal strain

*Menshchikov I.E.*¹, *Shkolin A.V.*¹, *Khozina E.V.*¹, *Fomkin A.A.*¹

i.menshchikov@phycha.ac.ru

¹ A.N. Frumkin Institute of Physical and Electrochemistry of the Russian Academy of Sciences, M.M. Dubinin Laboratory of sorption processes, Moscow, Russia

Xenon adsorption processes are of great current interest for gas separation, medical, nuclear power, and other industrial applications. The efficiency of these processes depends on the porous structure of adsorbents, chemical state of the surface, P,T -conditions, heat effects (heat of adsorption) described by variations in the thermodynamic state functions of an adsorption system, namely the enthalpy, entropy, and heat capacity. Nanoporous activated carbons are considered to be the most appropriate for Xe adsorption systems. In this work, a nanoporous carbon (SiC-AC) obtained from silicon carbide by the thermochemical synthesis in chlorine flow at 1173 K was investigated as an adsorbent for Xe, taking in account the influence of its adsorption- and thermal non-inertness on the thermodynamics of the SiC-AC/Xe adsorption system.

Low-temperature N_2 adsorption, XRD, and SEM methods were employed to examine the textural properties and morphology of the SiC-AC. Experimental measurement of Xe adsorption and the adsorption-induced strain of Si-AC were carried out in the temperature range of 178–393 K and at pressures up to 6 MPa using a purpose-built experimental setup [1]. It was found that in the early adsorption stage, the SiC-AC adsorbent contracted as a result of interactions between the first adsorbed molecules and the walls of micropores (to -0.01%), and upon further pore filling with xenon molecules, relaxation of the solid was observed, being followed by its expansion (to $+0.59\%$). The thermal expansion coefficient of SiC-AC was also calculated from the thermal deformation data measured in the range of 260–575 K.

The thermodynamic functions of the SiC-AC/Xe adsorption system were calculated taking into account the thermal and adsorption non-inertness of the adsorbent and the non-ideality of the gas phase using the approach proposed by Bakaev [2-3]: differential molar isosteric heats of adsorption, changes in the entropy, enthalpy, and heat capacity of the adsorption system. The contributions of these corrections to the final values of the thermodynamic parameters of the system were estimated. The variations in the thermodynamic functions with the amount of adsorbed xenon and temperature provided a possibility to evaluate the correlations with changes in the state of adsorbed Xe molecules, confined in nanopores of SiC-AC.

It was shown that the Xe gas-phase non-ideality and the adsorption- and thermally-induced deformation of the adsorbent changed the heat of adsorption by 32, 1.3 and 0.1 % respectively. These findings are of fundamental and practical importance for developing new adsorption-based technologies for Xe separations and storage.

The research was carried out within the State Assignment of the Russian Federation No. 0081-2019-0018.

References

1. Men'shchikov I.E., Shkolin A.V., Fomkin A.A., *Measurement Techniques* (2018), **80**, 578.
2. Bakaev V.A., *Bull. Acad. Sci. USSR Div. Chem. Sci.* (1971), **20**, 2516.
3. Fomkin A.A., *Adsorption* (2005), **11**, 425.

In vitro evaluation of fullerenes and endofullerenes in aqueous dispersions as superoxide scavengers and their toxicity

*Mikheev I.V.*¹, *Kareev I.E.*², *Sozarukova M.M.*¹, *Savinova E.A.*³, *Kostyuk S.V.*³, *Proskurnina E.V.*³, *Korobov M.V.*¹, *Proskurnin M.A.*¹

mikheev.ivan@gmail.com

¹ Chemistry Department, Lomonosov Moscow State University, Moscow, Russia

² Institute of Problems of Chemical Physics of the RAS, Chernogolovka, Russia

³ Research Centre for Medical Genetics, Laboratory of Molecular Biology, Moscow, Russia

Aqueous fullerene dispersions (AFD) are very promising for many applications dealing with enzyme inhibition, antiviral activity, photothermal and photodynamic therapies, electron transfer, and various other *in vitro* and *in vivo* biological techniques. Most promising applications dealing with endohedral metal fullerene contain gadolinium(III), e.g., Gd@C₈₂ for potential nanopharmaceuticals: contrast agents for MRI intracellular labeling and T₁ enhancement. Thus, it is essential to study their effect on reactive oxygen species (ROS) homeostasis. Superoxide anion radical is one of the essential ROS. The MTT colorimetric assay is a well-known procedure for determining viable cell numbers in proliferation and cytotoxicity studies. It is crucial to conduct a survival assay for further *in vivo* AFDs application.

The present study examined the AFDs of C₆₀, C₇₀, and Gd@C₈₂ in superoxide dismutase (SOD) scavenging activity and analysis of post-treatment survival in MTT assay. We applied the safest, rapid technique for AFD preparation, which contains the minimum amount of impurity components. The technique involves a high-power continuous ultrasonic probe. The concentration of the obtained dispersions was at the ppm level; the cluster size was about 100 nm. Stable dispersions are shown for up to 20 months [1].

The reactivity of aqueous dispersions of pristine (non-functionalized) fullerenes and Gd@C₈₂ have been studied concerning superoxide in the xanthine/xanthine oxidase chemiluminescence system [2]. It was found that C₆₀ and C₇₀ in aqueous dispersions react with superoxide as scavengers by a similar mechanism; Gd@C₈₂ is characterized by a significantly higher—one-and-a-half to two orders of magnitude—reactivity and is likely to exhibit nanozyme (SOD-mimic) properties. However, in the cell model, Gd@C₈₂ showed the lowest activity than C₆₀ and C₇₀. It can be accounted for by its higher affinity for the lipid phase. Slightly higher antioxidant activity of aqueous fullerene dispersions by solvent-exchange preparation techniques is most likely due to the effect of benzoic acid adsorbed at the fullerene clusters.

We used the MTT assay for cytotoxicity to obtain a quantitative measurement of cell death for all produced AFD. Incubation of human fibroblasts with AFD of various concentrations was carried out. The studied concentration range of C₆₀, C₇₀, and Gd@C₈₂ AFDs was in a ppt or ppb-level. All the systems studied have shown relatively low cytotoxicity. Cell survival rates of 90% or higher were demonstrated.

Acknowledgments. The Russian Science Foundation has supported this work under Contract No. 19-73-00143.

References

1. Mikheev, M. O. Pirogova, L. O. Usoltseva, A. S. Uzhel, T. A. Bolotnik, I. E. Kareev, V. P. Bubnov, N. S. Lukonina, D. S. Volkov, A. A. Goryunkov, M. V. Korobov, M. A. Proskurnin, *Ultrasonics Sonochemistry* 2021, **73**, 105533.
2. I.V. Mikheev, M. M. Sozarukova, E. V. Proskurnina, I. E. Kareev, M. A. Proskurnin, *Molecules* 2020, **25**, 2506.

Ni catalysts on N-doped and N-free porous carbon materials for hydrogen production from formic acid

*Nishchakova A.D.*¹, *Bulushev D.A.*², *Trubina S.V.*¹, *Stonkus O.A.*², *Bulusheva L.G.*¹

nishchakova@niic.nsc.ru

¹ Nikolaev Institute of Inorganic Chemistry SB RAS, Novosibirsk, Russia

² Borekov Institute of Catalysis SB RAS, Novosibirsk, Russia

Hydrogen is an environmentally friendly raw material, but its use is hindered by the difficulties associated with storage and transportation. In this regard, the production of hydrogen from various organic compounds is promising. From a variety of options, formic acid can be selected, which contains 4.4 wt% hydrogen and can be obtained by processing biomass or by hydrogenation of CO₂. Also, this acid decomposes relatively easily to hydrogen and carbon dioxide in the presence of catalysts.

Catalyst carriers have a significant effect on their activity. Among a various support materials, porous carbon materials can be preferred due to their unique combination of a high accessible surface area, an opportunity of its development and a presence of specific sites. These materials could be considered as good catalyst carriers, since they possess thermal, mechanical, and chemical stability, and cheap to synthesize. Palladium is widely used as an active phase for catalysts, but its high price is the reason for the search for cheaper, but no less effective analogs.

The object of our study was the synthesis of N-doped and N-free porous carbon supports for nickel, which is active in the reaction of hydrogen production from formic acid. These supports were synthesized by CVD decomposition of acetonitrile and ethanol vapors on template Fe@CaO particles in an inert atmosphere at 800°C. The specific surface area of the samples was 443 and 966 m²/g for N-containing and N-free samples, respectively. The study of the electronic state of nitrogen was carried out using XPS and revealed four forms: "pyridinic" (398.3 eV), "pyrrolic" (399.9 eV), "graphitic" (401 eV) and "oxidized" (402.5 eV), and the total amount of nitrogen was 4.4 at%. Nickel in the amount of 1, 3, and 6 wt% was deposited on the surface of the synthesized supports by impregnation with nickel acetate followed by reduction in a 2.5% HCOOH/Ar flow at 350°C before each experiment. This same mixture was used to carry out the reaction. The experimental technique was described earlier [2].

Catalysts were studied by XPS, HAADF/STEM, XRD and EXAFS. Summarizing the results of abovementioned techniques, Ni in N-free catalyst is presented in the form of clusters, on the surface of which Ni have been oxidized by oxygen and water from the air. In case of N-doped catalysts, no sign of Ni particles was seen. The kinetic studies of synthesized catalysts indicated independence of the specific Ni mass-based reaction rates on the concentration of Ni for the same type of the carbon support (N-doped or N-free). The apparent activation energy was 106 kJ/mol for N-doped catalysts vs 76 kJ/mol for N-free.

This work was supported by the Ministry of Science and Higher Education of the Russian Federation within the governmental orders for Borekov Institute of Catalysis (project AAAA-A21-121011390007-7, 0239-2021-0005) and for Nikolaev Institute of Inorganic Chemistry.

References

1. A.D. Nishchakova, D.A. Bulushev, O.A. Stonkus, I.P. Asanov, A.V. Ishchenko, A.V. Okotrub, L.G. Bulusheva, Effects of the Carbon Support Doping with Nitrogen for the Hydrogen Production from Formic Acid over Ni Catalysts, *Energies*. 12 (2019), 4111.

Deformation of nanoporous carbon adsorbent induced by methane adsorption in wide range of pressures and temperatures

*Shkolin A.V.*¹, *Menshchikov I.E.*¹, *Fomkin A.A.*¹

shkolin@phych.ac.ru

¹ A.N. Frumkin Institute of physical chemistry and electrochemistry of Russian academy of sciences (IPCE), Moscow, Russia

Effect of deformation of porous solid occurs due to its interaction with adsorbed molecules which has significant influence on adsorption process. This effect is especially noticeable for the high-pressure adsorption systems with microporous materials, when the process runs according to the volume filling mechanism [1-3].

Nanoporous carbon adsorbent Sorbonorit-4 with a wide pore size distribution was used as object of study in this work. The structure-energy characteristics were determined for the Sorbonorit-4 nanoporous adsorbent from the standard nitrogen adsorption isotherm at 77 K using the Dubinin theory of volume micropore filling (TVMF) [4]: micropore volume $W = 0.49 \text{ cm}^3/\text{g}$, characteristic adsorption energy $E = 21.8 \text{ kJ/mol}$, and effective micropore width $X = 1.10 \text{ nm}$. Relative linear strain of the material, induced by methane adsorption at temperature range 212-393 K was measured as a function of pressure up to 10 MPa - $Dl/l = f(p)$. It was shown, that $Dl/l(p)$ functions have strong dependence on temperature.

At initial range of pressures a contraction of the adsorbent is observed due to interactions between first adsorbed molecules and walls of the pores. Maximal contraction was found for 213 K, which reached -0.15% . At the same time with an increase in temperature, the contraction region becomes less pronounced and at temperatures above 303 K strain of the material becomes fully positive. Sharp expansion of adsorbent with values of 0.04 and 0.08% is observed at initial adsorption fillings at temperatures of 333 and 393 K respectively. At pressures in the range from 0.8 to 1.2 MPa, a region of inversion of the curves of adsorption-induced deformation is observed. Increasing the pressure up to 10 MPa demonstrated expansion of Sorbonorit-4 with maximal value for 213 K (about 0.45%) and minimal for 393 K (about 0.10%).

A semiempirical method based on a generalized potential of intermolecular interactions (6, n) [5] was developed to describe adsorption-stimulated deformation of microporous adsorbents. The equations agreed qualitatively with experimental data. It was shown that the best alignment between the calculated and experimental data for the Sorbonorit-4 adsorbent is observed in the range of intermediate and high micropore loading at temperatures less than 333 K, when molecules adsorb in accordance with the mechanism of volume micropore filling.

Obtained results can be used for development of advanced adsorption processes for separation and storage of normal hydrocarbons in gas-processing systems and increasing the durability and reliability of the adsorbent.

This work was carried out in frames of the State Assignment of the Russian Federation № 0081-2019-0018.

References

1. Shkolin A.V., Fomkin A.A. Colloid Journal. 2009. V. 71. № 1. pp. 119-124.
2. Gor G.Y., Huber P., Bernstein N. Applied Physics Reviews. 2017. V. 4. № 1. pp. 011303.
3. Shkolin A.V., Potapov S.V., Fomkin A.A. Colloid Journal. 2015. V. 77, №. 6. pp. 812-820.
4. Dubinin M.M. Progress Surface Membrane Sci. 1975. V. 9. pp. 1-70.
5. Shkolin A.V., Fomkin A.A. Protection of Metals and Physical Chemistry of Surfaces. 2016. V. 52, № 2, pp. 193-198.

Ab initio study of fluorinated fullerenes as drug delivery systems

Kalika E.^{1,2}, Katin K.^{2,3}, Kaya S.⁴, Maslov M.^{2,3}

KPKatin@yandex.ru

¹ Moscow Institute of Physics and Technology (National Research University), Moscow, Russia

² Research Institute for the Development of Scientific and Educational Potential of Youth, Moscow, Russia

³ National Research Nuclear University MEPhI, Moscow, Russia

⁴ Cumhuriyet University, Sivas, Turkey

Targeted drug delivery (TDD) based on the nanoparticles ensures the release of the drug in a specific place of the organism (for example, in a cancerous tumor) and reduces unwanted side effects. The accumulation of nanoparticles in the tumor is provided by specific functional groups that are sensitive to cancer cells, as well as the roughness of the inner surface of the vessels in the tumor. The trigger for the drug release is the increased acidity characteristic of the tumor (i.e., $\text{pH} < 6$), or special heating of nanoparticles by means of the electromagnetic field. Here we studied the interaction of common doxorubicin anti-cancer drug (DOX) with the fluorinated fullerene. Effect of fluorination on the efficiency of fullerene as a drug delivery system was studied in details. Fluorination of carbon nanoparticles provides a number of advantages when creating TDD systems. Firstly, fluorine provides the ability to detect a nanoparticle in the organism using nuclear magnetic resonance [1]. Secondly, fluorine provides absorption of radiation near the infrared range, which is necessary for photo-thermal anti-cancer therapy [2]. Thirdly, fluorine has a strong electronegativity, which contributes to the non-covalent interaction of the nanoparticle with drugs. Recently, TDD systems based on the fluorinated graphene have been successfully synthesized and tested [3]. Therefore, fluorinated carbon fullerenes seem to be a promising basis for TDD systems. Despite this, their adsorption capacity with respect to the drugs has not yet been studied by quantum chemistry. As a first step, we applied genetic algorithm combined with the density functional theory to understand the regularity of the fullerenes fluorination. Then we investigated effective interaction between fluorine atoms and other functional groups (OH, COOH, NH_2), adsorbed on the same cage to provide solubility and biocomparability. Based on our findings, we proposed atomic models of fullerenes simultaneously functionalized with fluorine atoms and OH groups with different concentrations of fluorine. Since the interaction between fluorine atom and OH-group is stronger than F to F interaction, we observed alternation of F and OH as the main regularity of functionalization. IR and UV-visible spectra of such molecules were calculated and DOX loading on them was investigated. It was confirmed that fluorine provides stronger binding between carrier cage and drug molecule.

The reported study was supported by the Russian Science Foundation, project no. 20-73-00245.

References

1. R. Romero-Aburto, T.N. Narayanan, Y. Nagaoka, T. Hasumura, T.M. Mitcham, T. Fukuda, P.J. Cox, R.R. Bouchard, T. Maekawa, D.S. Kumar, S.V. Torti, S.A. Mani, P.M. Ajayan, *Adv. Mater.* (2013) **25**, 5632-5637.
2. L. Sun, P. Gong, X. Liu, M. Pang, M. Tian, J. Chen, J. Du, Z. Liu, *J. Mater. Chem. B.* (2017) **5**, 6128-6137.
3. P. Gong, L. Zhang, X. Yuan, X. Liu, X. Diao, Q. Zhao, Z. Tian, J. Sun, Z. Liu, J. You, *Dyes and Pigments* (2019) **162**, 573-582.

Development of delivery systems based on fullerene C₆₀ and application prospects

Litasova E.V.¹, Ilyin V.V.¹, Safonova A.F.¹, Piotrovsky L.B.¹

llitasova@mail.ru

¹ Institute of Experimental Medicine, St.Peterburg, Russia

The blood-brain barrier (BBB), as a natural defense of the brain against polar foreign molecules, makes it impossible to use many drugs for the treatment of disorders in the central nervous system. Fullerenes have a number of properties that suggest that they can be used to create systems for the delivery of drugs through the BBB. This could open up prospects for the treatment of many neurological diseases such as Alzheimer's and Parkinson's.

We have synthesized a number of complexes of carboxy derivatives of fullerene C₆₀ with the bis-cation of hexamethonium to establish the possibility of delivering a low-molecular-weight charged compound to the central nervous system.

Earlier, we conducted studies of this series of compounds *in vivo* in laboratory animals and showed the suppression of seizures induced by nicotine [1] and *in vitro* on model lipid membranes, showed directly the permeability of the barrier [2]. Thus, we confirmed hexonium penetration of these complexes in the CNS via the BBB.

In this work, we investigated the acute toxicity of this series of complexes. The work was performed on white male mice. To assess acute toxicity, the Prozorovsky method was used. Complexes with hexonium based on fullerene C₆₀ derivatives with amino acids and fullerenemalonic acids (IEM-2143, IEM-2144, IEM-2197, IEM-2214, and IEM-2222) were studied. Hexamethonium was used as a reference drug.

The results indicate the absence of toxicity of these compounds at the doses used in the experiment. The effective dose is several orders of magnitude less than the lethal dose in all complexes, and all complexes were also less toxic than the reference drug Hexamethonium itself.

Thus, we have shown that it is possible to develop drug delivery systems based on C₆₀. And this is of obvious interest for further research.

References

1. L.B. Piotrovskiy, E.V. Litasova, M.A. Dumpis, et.al. Doklady Biochemistry and Biophysics (2016) **468**,173-175
2. S.S. Efimova, D.A. Khaleneva, E.V. Litasova, et.al. BBA - Biomembranes 1862. (2020) 183433

The model of adsorption/desorption process on nanoporous carbon materials under the thermal insulation conditions

*Shkolin A.V.*¹, *Strizhenov E.V.*^{2,1}, *Menchshikov I.E.*¹, *Chugaev S.S.*^{2,1}

shkolin@phych.e.ac.ru

¹ Frumkin Institute of Physical Chemistry and Electrochemistry, Russian Academy of Sciences

² Research Institute of Power Engineering, Bauman Moscow State Technical University

In research, we considered a model heat- mass transfer in adsorption process on nanoporous carbon materials with lumped parameters, which did not take into account the thermal and diffusional gradients in an adsorbent bed, and between the adsorbent and the adsorber walls. These simplifications were justified because we considered slow adsorption/desorption processes.

The model is based on the mass and energy balance equations. The equations were solved using successive approximations at every time step. Assuming constant pressure of supplied or delivered gas after the reducer, we did not take account technical work. The flow rates of supplied and delivered gas were assumed to be constant during initial periods of filling and emptying the tank with nanoporous carbon materials until the pressure reaches the maximum and minimum values. This assumption is close to realistic experimental conditions when gas supply and delivery rates are determined by a compressor capacity.

The amount of heat transferred ΔQ_{he} upon heat exchange in the period $\Delta\tau$ is given by the following equation:

$$\Delta Q_{he} = k_e \cdot F_e \cdot (T_f - T) \cdot \Delta\tau = K_e \cdot (T_f - T) \cdot \Delta\tau,$$

where k_e is the effective heat transfer coefficient related to the heat transfer surface area F_e and the difference between the ambient or coolant temperature T_f and average adsorber temperature T . The coefficient $K_e = k_e \cdot F_e$, [W/K] characterizes the intensity of cooling or heating of the total ANG system. The coefficients k_e and K_e are assumed to be constant, although their magnitudes depend on many parameters, primarily on the pressure in the adsorber. This simplification is permissible since the pressure (and the gas density) in the adsorber changes significantly only in the short initial periods of the adsorption/desorption cycle.

The mass of gas stored in the adsorber m_{acc} is calculated by the equation:

$$m_{acc} = a \cdot \rho_g \cdot (1 - x) \cdot V_{tank} + \varepsilon \cdot \rho_g,$$

where: a is the adsorption value reduced to a "pure" adsorbent without the binder; ρ_g is the gas density at the average temperature and pressure of the adsorber; x is the mass content of a binder in the monolithic nanoporous carbon; V_{tank} is the internal volume of the tank with nanoporous carbon; ε is the porosity, i.e., fractional void space of the tank.

Following the method the investigations of the adsorption/desorption processes were carried out for the system loaded with the microporous carbon (nanopore volume is about 0.65 cm³/g) under two different conditions: 1. thermal insulation regime realized by thermal insulation and in the absence of forced heating and cooling. The initial period of charge and discharge proceeds under nearly adiabatic conditions; 2. thermal regulation regime realized by forced cooling and heating using a coolant with a temperature close to the ambient.

The results of modeling are consistent with the experimental data. The experimental data combined with the mathematical model enabled evaluating the integral heat-exchange characteristics, which determined the duration and efficiency of charge/discharge processes. The forced thermal regulation made it possible to accelerate the adsorption/desorption processes by 2/4 times and to obtain slightly larger amounts of delivered methane compared to the thermal insulation process. The mathematical model can be directly used in elaborating the optimal heat-exchange facilities of the adsorption system with nanoporous carbon to maximize its performance.

Funding: The research was supported by a grant from the Russian Science Foundation (project No. 20-19-00421).

Comparative structural and in vitro toxicity study of C₆₀-lysine and C₆₀-piperazine aqueous solutions for biomedical purposes

Tomchuk A.A.¹, Avdeev M.V.¹, Shershakova N.N.², Turetskiy E.A.², Andreev S.M.², Khaitov M.R.², Voiteshenko I.S.³

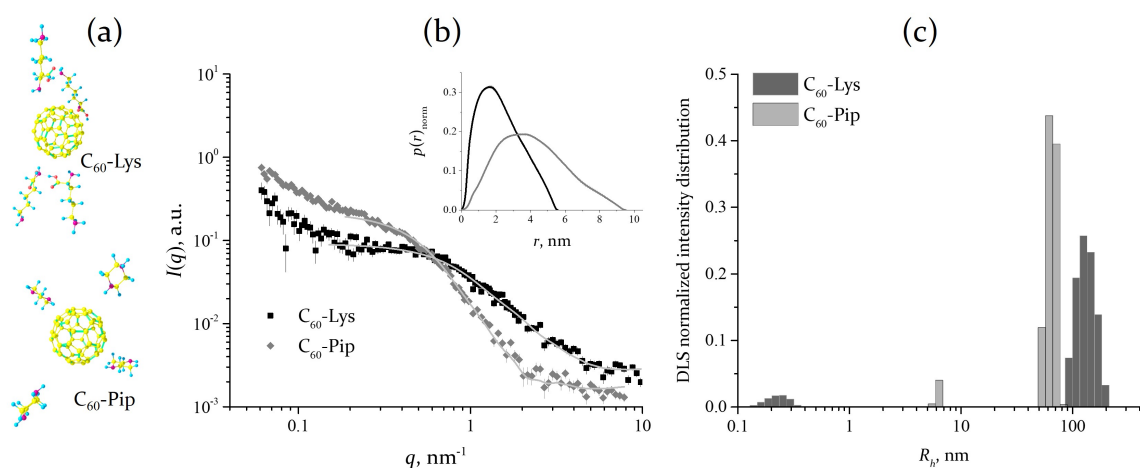
a.a.tomchuk@gmail.com

¹Joint Institute for Nuclear Research, Dubna, Russia

²NRC Institute of Immunology, FMBA of Russia, Moscow, Russia

³Taras Shevchenko National University of Kyiv, Kyiv, Ukraine

Fullerene C₆₀ is a promising therapeutic agent due to its antioxidant properties and low toxicity. In current research small-angle X-ray and neutron scattering, UV-Vis absorption spectroscopy and dynamic light scattering were applied for the structural characterization of aqueous solutions of C₆₀-lysine and C₆₀-piperazine conjugates prepared by dialysis method [1, 2]. Two-level aggregation, as well as the difference in the structural organization for the systems under study, were observed. The density functional theory calculations show the higher dissociation energy of the C₆₀-lysine complexes in comparison with the C₆₀-piperazine case that is in accord with the difference in the size of primary aggregates. Experiments on the cytotoxicity of these systems on the various cells showed no toxic effects of the solutions.



(a) Optimized geometrical structures of the molecular complexes composed of a single C₆₀ with four lysine/piperazine molecules. Small-angle X-ray scattering (b) and dynamic light scattering data for aqueous solutions of C₆₀ with lysine and piperazine.

References

1. A.A. Tomchuk, N.N. Shershakova, S.M. Andreev, E.A. Turetskiy, O.I. Ivankov, O.A. Kyzyma, O.V. Tomchuk, M.V. Avdeev, Fuller. Nanotub. Car. Nanostruct. (2020) **28**, 245.
2. R. Klimova, S. Andreev, E. Momotyuk, N. Demidova, N. Fedorova, Y. Chernoryzh, K. Yurlov, E. Turetskiy, E. Baraboshkina, N. Shershakova, R. Simonov, A. Kushch, M. Khaitov, A. Gintsburg, Fuller. Nanotub. Car. Nanostruct. (2020) **28**, 487.

Fullerene C₆₀ exhibits no subacute toxicity in mice after repeated administration

Turetskiy E.^{1,2}, Andreev S.¹, Shershakova N.¹, Kamyshnikov O.¹, Timofeeva A.¹, Shatilov A.¹, Khaitov M.¹

ea.turetskiy@nrcii.ru

¹ NRC Institute of Immunology FMBA of Russia

² I.M. Sechenov first Moscow state medical university (Sechenov university)

Fullerenes and their derivatives are regarded by scientists as promising agents for a variety of bio-medical applications. Despite that, safety of their biological application is yet to be fully evaluated. Previously, we have reported lack of toxicity of fullerene in aqueous dispersions, as well as a number of its derivatives, in *in vitro* experiments [1]. In this study, we show the effects of repeated administration of fullerene C₆₀ in aqueous dispersions in an *in vivo* model.

For this study, adult female balb/c mice, weighing 20-22 g at the start of experiment, received daily intraperitoneal injections of fullerene C₆₀ aqueous colloidal solution for a period of 30 days. After that period, a necropsy was performed, to collect blood, heart, thymus, lungs, liver, spleen, small and large intestines, pancreas, kidneys, adrenal glands, uterus, ovaries, lymphatic nodes, adipose tissue samples and tissue samples from injection site. Complete blood count was performed in collected blood. Collected organs were weighed, suspended in paraffin and cut using microtome. The samples were stained with hematoxylin-eosin stain and studied under 50-600x magnification.

No pathological changes in blood cell count could be observed and organ weights were found to be within normal parameters. Histological study did not reveal any pathological changes, but some observations could be made. In the injection site in the abdominal cavity, some granuloma-like formations of macrophages, containing intracellular inclusions of fullerene, could be observed. Those formations were localized, primarily, in adipose tissues, surrounding abdominal organs (ovaries, intestines, kidneys). In experimental animals, macrophages containing fullerene inclusions could also be found in lung alveoli (see fig. 1) and parathyroid lymph nodes.

Overall, the study demonstrates lack of sub-acute toxicity of fullerene C₆₀ in mammals.

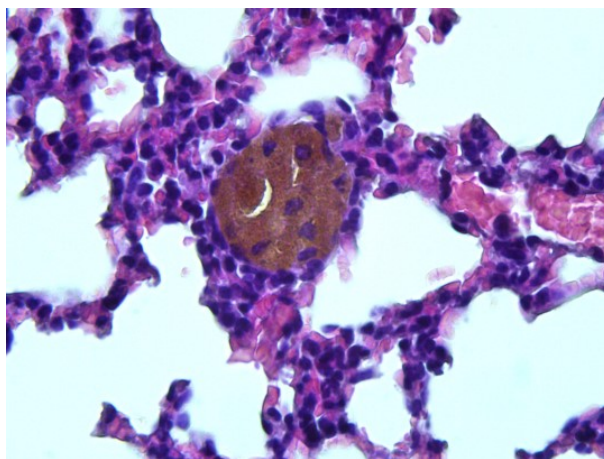


Fig.1. Lung sample, showing macrophage with xenobiotic inclusions, H&E stain, 600x magnification

References

1. Alina A. Tomchuk, Nadezhda N. Shershakova, Sergey M. Andreev, Evgeniy A. Turetskiy, Oleksandr I. Ivankov, Olena A. Kyzyma, Oleksandr V. Tomchuk & Mikhail V. Avdeev (2020) C60 and C60-arginine aqueous solutions: In vitro toxicity and structural study, *Fullerenes, Nanotubes and Carbon Nanostructures*, 28:4, 245-249

Full Contents

Timetable	6
Invited Lectures	7
I-01 Gruen D.M. Solar cells based on graphene's quantum electrodynamic properties	8
I-02 Ewels C.P. Forming the Void: Folding, Twisting and Collapsing Carbon	9
I-03 Arenal R. Structural and chemical analyses at the atomic scale of carbon nanomaterials	10
I-04 Tomanek D. Water! Water! *2	11
I-05 Yakobson B.I. 1D-carbon nanotubes and 2D-layers synthesis, insights from thermodynamics to kinetics	12
I-06 Vins V.G. Engineering of atomic defects in the crystal structure of diamond	13
I-07 Dolmatov V.Yu. Theory and practice of detonation synthesis of nanodiamond, its properties and application.	14
I-08 Lermontov S.A. Carbon Aerogels - Synthesis, Properties, Application	15
I-09 Lychagin E.V. Neutron activation analysis for diagnostics of advanced carbon nanomaterials	16
I-10 Siklitskaya A. Modelling the carbonaceous nanostructures: modern advances	17
I-11 Vasiliev A.L. Transmission electron microscopy in the study of carbon-based nanostructures.	18
I-12 Knizhnik A.A. Theoretical modeling of structure and properties of detonation nanodiamonds	19
I-13 Stehlik S. Smaller than usual: preparation, properties, and size effects in sub-5 nm nanodiamonds	20
I-14 Haenen K. Doping of diamond: Importance for nanodiamond particles and nanocrystalline CVD diamond films	21
I-15 Cami J. The Hidden Life of Cosmic Fullerenes	22
I-16 Menard-Moyon C. Multifunctionalized carbon nanotubes for applications in diagnosis and therapy	23
Day 1: Graphene & Related Materials.	25
O1-1-01 Chernysheva M.G. Structural peculiarities of lysozyme-graphene oxide adsorption complexes	26
O1-1-02 Chichkan A.S. Nitrogen-doped graphene with high specific surface area	27
O1-1-03 Danilov E.A. Synergetic effect in graphene/silver nanowire composite suspensions electrical conductivity	28
O1-1-04 Gurianov K.E. Investigation of alcohols transport through graphene oxide membranes.	29

01-1-05 Kalashnikova E.I.	Thermal conductivity and heat capacity of nanofluid based on water modified by hybrid material of composition detonation nanodiamonds-carbon nanotubes	30
01-1-06 Klimenko I.V.	Hybrid structures based on oxygen-free graphene and aluminum phthalocyanine chloride	31
01-1-07 Okotrub A.V.	Effect of iron and nickel metal films on graphitization of the diamond surface during high-temperature annealing	32
01-1-08 Safargaliev R.F.	Formation of fractal filaments under the influence of thermocapillary waves at the hydrocarbon-nanofluid interface.	33
01-1-09 Struchkov N.S.	Sensor set based on spray coated carbon nanomaterials for selective detection of ammonia and hydrogen sulfide	34
01-2-01 Baryshnikov K.A.	Superlattice and nonlinear screening problem in graphene	35
01-2-02 Kidalov S.V.	New way of synthesis of few-layer graphene (FLG) by the self-propagating high-temperature synthesis (SHS) method from biopolymers.	36
01-2-03 Komarov I.A.	AFM investigation of polygonal wrinkles on thin UV-irradiated graphene oxide films for biosensor applications	37
01-2-04 Kvitsinskiy A.	Polarization-resolved terahertz spectroscopy of graphene-based films	38
01-2-05 Sadilov I.S.	Light-responsive membranes based on graphene oxide modified by azo-group molecules	39
01-2-06 Smirnova V.E.	Mechanical and thermophysical properties of polymer composites with few-layer graphene obtained by laser stereolithography 3D printing	40
01-2-07 Rukhov Ar.V.	Features of the effect of graphene nanoplates on the properties of grease lubricants	41
01-2-08 Vozniakovskii A.A.	Low-threshold field electronic emission from two-dimensional carbon structures	42
01-2-09 Voznyakovskii A.P.	Determination of Stone-Wales Structural defects in 1D and 2D nanocarbons	43
01-3-01 Evlashin S.A.	Role of heteroatoms and defects on the obtained electrochemical characteristics of carbon materials	44
01-3-02 Kalashnikova E.I.	Thermal properties of water-based nanofluids modified with few-layer graphene	45
01-3-03 Komarov I.A.	Spin-coating deposition of graphene oxide from mixed water-organic solutions	46
01-3-04 Niftalieva V.V.	Nanoscale structures formed on SiC substrates for field emission devices	47
01-3-05 Pavlov S.V.	Influence of defects in graphene on the non-adiabatic electron transfer kinetics	48
01-3-06 Podlozhnyuk N.D.	Hardness and thermal conductivity of a composite based on aluminum modified with a hybrid material detonation nanodiamond/few-layer graphene	49
01-3-07 Rabchinskii M.K.	On the relationship between chemistry, optical properties and electronic structure of graphene derivatives: revisiting the puzzling complexity	50
01-3-08 Soltamov V.A.	Creation of optically addressable spin-triplet defects in hexagonal Boron Nitride by electron irradiation	51

01-3-09 Yankova T.S.	Spin probing of graphene oxide by 4-aminoTEMPO	52
01-4-01 Bokai K.A.	Highly ordered and polycrystalline graphene/Co interfaces intercalated by oxygen	53
01-4-02 Butko A.V.	Interfacial phenomena in electrical transport in graphene/molecular ions hybrid nanostructures	54
01-4-03 Gudkov M.V.	Processes of low-temperature functional restructuring and gas evolution of the GO from room temperature to 90 °C	55
01-4-04 Morozova J.V.	Application for gas sensing graphene	56
01-4-05 Nechaev Yu.S.	Methodology and results of studying the states of hydrogen in graphene structures	57
01-4-06 Novikau U.	Graphene-like carbon functionalization	58
01-4-07 Ryzhkov S.A.	Aminated graphene: From synthesis to applications	59
01-4-08 Saveliev S.D.	On the synthesis of carboxylated graphene derivative and its application as a transducer in aptasensors	60
01-4-09 Trofimuk A.D.	Specific surface area studying of reduced graphene oxide - detonation nanodiamond compounds	61
01-5-01 Belenkov M. E.	Computer simulation of the three-dimensional structure of fluorinated graphene crystals	62
01-5-02 Colin M.	The first free-standing transparent fluorinated graphene film	63
01-5-03 Korobov M.V.	Sorption of polar liquids by GO powders and membranes	64
01-5-04 Kulvelis Yu.V.	Structure of graphene oxide aerogels	65
01-5-05 Potapov D.O.	Mechanisms of graphene oxide reduction under ultrafast laser irradiation: insights from reactive molecular dynamics	66
01-5-06 Rabchinskii M.K.	Graphene chemical derivatives as gas sensing layers: From the synthesis to the theory behind	67
01-5-07 Seliverstova E.	Long-lived luminescence and transient absorption of graphene oxide quantum dots, prepared by laser ablation	68
01-5-08 Usol'tseva N.V.	Influence of different types of low-layer graphite fragments on tribological and rheological properties of plastic lubricants	69
01-5-09 Voznyakovskiy A.P.	Photovoltaic 2D graphene structures for safe explosion	70
01-6-01 Abramenko N.D.	Structure and properties of pseudo-graphene	71
01-6-02 Bugrov A.N.	Composite materials based on reduced graphene oxide and their magnetic properties	72
01-6-03 Chernova E.A.	Graphene oxide membranes: tuning the microstructure for gas dehumidification	73
01-6-04 Chumakova N.A.	Spin probe method for investigation of graphite oxide materials - possibilities and perspectives	74

01-6-05 Gudkov M.V.	An approach to the preparation of aerogels with ultra-high molecular weight polymers using the rGO template on the example of UHMWPE	75
01-6-06 Novikau U.	Graphene-like carbon additive to negative electrodes of lead-acid battery	76
01-6-07 Ryzhkov S.A.	Guiding the chemistry of GO via the use of $\text{KMnO}_4/\text{K}_2\text{Cr}_2\text{O}_7$ oxidizing agents	77
01-6-08 Saveliev S.D.	Unveiling graphene N-doping upon Hummers oxidation and its effect on electrical properties	78
01-6-09 Shnitov V.V	Valence Band Electron Structure of Graphene Derivatives: Study by XPS measurements and DFT modeling	79
Day 2: Carbon Nanostructures. Carbon Nanotubes.		81
02-1-01 Digurova A.I.	Complexes "boron+vacancy" on the hydrogenated C(100)-(2×1) diamond surface	82
02-1-02 Fedoseeva Y.V.	Synthesis and chemical activation of porous nitrogen-doped carbon materials for sodium-ion batteries	83
02-1-03 Jalolov F.N.	The mechanical properties of diamond nanopolycrystals by machine learning interatomic potentials	84
02-1-04 Oliva Gonzalez C.M.	Synthesis of hydrophobic carbon sponges from MOF type HKUST and melamine-formaldehyde sponges for the absorption of oil dispersed in water.	85
02-1-05 Laptinskiy K.A.	Vibrational spectroscopy of carbon nanoparticles interactions with biomacromolecules	86
02-1-06 Popov V.V.	Magnetic properties of birch biocarbon	87
02-1-07 Rodin E.A.	Evaluation of the in-plane electronic conjugation in carbon nanobelts	88
02-1-08 Ibrayev N. Kh.	Optical properties of N- and S-doped carbon quantum dots	89
02-1-09 Shlyakhova E.V.	Effect of metal dopant in structure and supercapacitor property of templated-assisted porous nitrogen carbon	90
02-1-10 Stolyarova S.G	Brominated porous carbon materials for sodium-ion batteries	91
02-2-01 Belenkov E.A.	Ab initio calculations of layered compounds consisting of sp^3 or $\text{sp}+\text{sp}^2$ hybridized carbon atoms	92
02-2-02 Dyachkova T.P.	Features of carbon nanostructures modification by stearic acid	93
02-2-03 Cedeno M.E.	Gold decorated MOF-derived CuO, ZnO and NiO for CO_2 photoreduction.	94
02-2-04 Klimenko I.V.	Morphology of graphene obtained in DMF and DMF-aqua media	95
02-2-05 Laptinskiy K.A.	Heavy metal nanosensor based on fluorescent carbon dots	96
02-2-06 Nelson D. K.	Properties of carbon dot luminophores studied by polarized luminescence experiments	97
02-2-07 Orlova T.S.	Structural characterization and magnetic behavior of nickel nanoparticles encapsulated in monolithic wood-derived porous carbon	98

O2-2-08 Popov V.V.	Magnetic properties of polymerized exfoliated graphite	99
O2-2-09 Rodin E.A.	Influence of the p-electrons concentration in carbon nanobelts on their emission properties	100
O2-2-10 Vervald A.M.	Difference between oxygen-containing groups on sp^2 and sp^3 carbons: deprotonation	101
O2-3-01 Arutyunyan N.R.	High-temperature synthesis of linear carbon chains confined in carbon nanotubes	102
O2-3-02 Belenkov M.E.	Modeling the structure and interlayer interactions of twisted bilayer graphene	103
O2-3-03 Chernogorova O.P.	Tribological properties of carbon-containing composite materials prepared by high-pressure high-temperature synthesis	104
O2-3-04 Fazlitdinova A.G.	Structural transformations of graphite during dispersion	105
O2-3-05 Moshnikov I.A.	Electrical conductivity of carbon films obtained by thermal sputtering of shungite	106
O2-3-06 Petrova O.V.	Characterization of new functional materials based on graphitized bath sponge scaffold	107
O2-3-07 Rodionova E.V.	Emission properties of $C_x(BN)_y$ nanobelts	108
O2-3-08 Semavin K.D.	The evaporation study of 1-Ethyl-3-methylimidazolium chloride	109
O2-3-09 Tchougreeff A.L.	Deductive molecular mechanics of carbon materials	110
O2-3-10 Ushakova E.V.	Chiral carbon dots synthesized via room temperature surface modification and one-pot carbonization	111
O2-3-11 Yakovleva V. V.	Distribution of nitrogen-vacancy NV^- centers in cubic diamond crystals revealed by ODMR and PL tomography	112
O2-4-01 Dyachkova T.P.	Novel methods of carbon nanotubes suspensions stabilizing	113
O2-4-02 Gnedova E. A.	Thermogravimetry study of selected surfactants annealing from single-wall carbon nanotube films	114
O2-4-03 Ichkitidze L.	Bend sensor based on biocompatible composite nanomaterials	115
O2-4-04 Ivanov P.D.	Electronic structure of a metal-decorated carbon nanotube (8,0): first-principles modelling	116
O2-4-05 Kotsun A.A.	Single-walled carbon nanotube additive for improvement of lithium-ion storage performance of nanostructured MoS_2	117
O2-4-06 Kulakov R.A.	Improving the frost resistance of concrete reinforced with carbon nanotubes	118
O2-4-07 Latypov R.M.	Current-voltage characteristics of a carbon nanotube (6,6): first principle calculations	119
O2-4-08 Khamidullin T.L.	Simple and cost-efficient method for sorting single-wall carbon nanotubes with modified cotton.	120
O2-4-09 Osotova O.I.	Influence of defectiveness of carbon nanotubes on their piezoelectric response	121

O2-4-10 Ryzhkov I.	Experimental and theoretical study of carbon nanotube growth inside porous anodic alumina membranes	122
O2-4-11 Vorfolomeeva A.A.	Electrochemical properties of phosphorus-filled single-walled carbon nanotubes	123
O2-5-01 Manohar R.	Ion trapping effect and enhancement of orientational order parameter in nematic liquid crystals dispersed with a dilute amount of carbon nanotube	124
O2-5-02 Elbakyan L.S.	Strengthening of polymeric materials based on polypropylene by doping with carbon nanotubes.	125
O2-5-03 Gaidamavichute V.V.	Simulation of supramolecular microporous structures on the basis of carbon nanotubes and toluene coordinator molecules	126
O2-5-04 Khantimerov S.M.	Electrical properties of low-doped carbon nanotubes/epoxy resin composite material hardened in an electric field	127
O2-5-05 Il'in O.I.	Effect of the growth temperature on parameters of vertically aligned carbon nanotubes	128
O2-5-06 Il'ina M.V.	Vertically aligned carbon nanotubes for piezoelectric nanogenerator	129
O2-5-07 Mozhayko A.A.	Aluminum Based Composite Materials with Carbon Nanofibers Obtained by Hot Extrusion and Rolling	130
O2-5-08 Nechaev Yu.S.	On the "intercalation" of 7 wt.% hydrogen into graphite nanofibers	131
O2-5-09 Polozkov R.G.	Ab-initio study of electronic properties of 2D and 3D regular arrays of carbon nanotubes	132
O2-5-10 Sozykin S.A.	Li-decorated carbon nanotubes: charge analysis	133
O2-5-11 Vilkov I.V.	Hybrid nanomaterial TiC/MWCNTs: synthesis, application as strengthening components in aluminum alloys	134
Day 3: School for Young Scientists.		135
Y3-1-01 Alekseev D.V.	The use of nanodiamonds in solid composite electrolytes	136
Y3-1-02 Kotsun A.A.	Nanostructures VS _x /reduced graphene oxide materials for energy storage applications	137
Y3-1-03 Nishchakova A.D.	Synthesis, functionalization and electrochemical properties of N-free and N-doped porous carbon materials	138
Y3-1-04 Rezvanova A.E.	Influence of additives of multi-walled carbon nanotubes on the porosity and macrostresses in the composite «hydroxyapatite - MWCNTs»	139
Y3-1-05 Semenukha O.V.	Organosilicon polymer compositions based on carbon nanotubes in tensoresistive applications	140
Y3-1-06 Vorfolomeeva A.A.	Influence of the synthesis temperature on electrochemical properties of porous nitrogen-containing carbon in sodium-ion batteries	141
Y3-2-01 Chizhikova A.S.	Synthesis of a suspension of detonation nanodiamonds modified with nickel ions	142

Y3-2-02 Popov D.S.	Phase transition in the system "BGO - CH ₃ CN" - dependence on characteristics of the material	143
Y3-2-03 Shiyanova K.A.	Adjustment of the functional composition of graphene oxide at the synthesis stage	144
Y3-2-04 Tudupova B.B.	Formation and properties of structures based on Graphene Oxide and Detonation Nanodiamonds in water	145
Y3-2-05 Zhirov M.S.	Solid-state fluorinating agents for fluorination of graphene	146
Y3-3-01 Bunyaev V.A.	Tritium labeled graphene oxide as a component of a nuclear battery	147
Y3-3-02 Dubovenko R.R.	Impact of C ₆₀ based star macromolecules & ionic liquid as novel membrane modifiers on pervaporation performance in lactic acid dehydration	148
Y3-3-03 Kulbina A.S.	3D ultrashort optical pulses in anisotropic optical medium with carbon nanotubes and an order parameter	149
Y3-3-04 Lobanova E.Yu.	Iron- and silicon-intercalated graphene on silicon carbide	150
Y3-3-05 Sinolits A.V.	Preparation and properties of Myramistin-hyaluronic acid coatings on the nanodiamond surface	151
Day 4: Nanodiamond Particles. Fullerenes.		153
04-1-01 Dolmatov V.Yu.	Influence of modification of tetryl detonation nanodiamonds on the combustion process of model pasty rocket fuels (RF)	154
04-1-02 Lebedev V.T.	Complexes of nanodiamonds with Gd-fullerenols for biomedicine	155
04-1-03 Leshchev D.V.	On mechanism of diamond growth: role of atomic carbon	156
04-1-04 Mateyshina Yu.G.	Nanodiamonds as a component for composite solid electrolytes	157
04-1-05 Osipov V. Yu.	Evaluation the Amount of NV centers in 3-nm Detonation Nanodiamonds by Half Magnetic Field ESR Method	158
04-1-06 Shestakov M.S.	Sonication assisted advanced oxidation process: hybrid method for deagglomeration of detonation nanodiamond particles	159
04-1-07 Shvidchenko A.V.	Influence of the size of detonation nanodiamond particles on their electro-surface properties in hydrosols	160
04-1-08 Vdovichenko A.Yu.	Dielectric spectroscopy study of detonation nanodiamonds self-organization in oil suspensions	161
04-1-09 Yudin I.B.	Influence of nitrogen on the synthesis of diamonds during gas-jet HWCVD deposition.	162
04-2-01 Chernysheva M.G.	Langmuir hydrogen atomization as a novel approach for nanodiamond treatment	163
04-2-02 Dolmatov V.Yu.	Possible mechanism for the formation of detonation nanodiamonds.	164
04-2-03 Grudinkin S.A.	Emission of GeV colour centre ensembles in HFCVD nanodiamonds	165

04-2-04 Kuznetsov N.M.	Electrorheological fluids filled by detonation nanodiamonds	166
04-2-05 Lebedev V.T.	X-ray luminescent nanodiamonds modified by Eu diphthalocyanine	167
04-2-06 Leshchev D.V.	On mechanism of diamond growth: role of ethylene and acetylene	168
04-2-07 Lychagin E.V.	Development of high-purity detonation synthesis nanodiamonds for slow neutron reflectors	169
04-2-08 Yudin I.B.	Gas-jet HWCVD synthesis of diamond from a mixture of hydrogen with ethylene.	170
04-2-09 Zinin P.V.	Granular conductivity in boron rich diamond like carbon films	171
04-3-01 Belousov S.I.	Organization in various small-angle x-ray scattering study of the detonation nanodiamonds structural media.	172
04-3-02 Bogdanov K.V.	Amplification of colour-centre luminescence using Getter-controlled nitrogen reduction for synthetic HPHT micro-diamonds.	173
04-3-03 Ducrozet F.	Influence of annealing atmosphere on DNDs' surface graphitization and impact on their colloidal stability in water	174
04-3-04 Gozhikova I.O.	Composites of SiO ₂ - aerogels with nanodiamonds	175
04-3-05 Kapustin S. N.	Research of electrophysical properties of diamonds with NV-centres in a wide range of temperatures and frequencies	176
04-3-06 Kulvelis Yu.V.	Improving the performance of PFSA membranes using sulfonated nanodiamonds	177
04-3-07 Kuziv I.	Investigation of the Nitrogen-doped Diamond Defects by Positron Annihilation Spectroscopy	178
04-3-08 Ovchinnikov-Lazarev M.A.	The use of purified detonation nanodiamond in an anti-icing composition.	179
04-3-09 Shilova O.A.	Nanodiamond batch enriched with B, P: Prospects for use in agriculture	180
04-3-10 Sigalayev S.K.	Detonation synthesis of carbon onions and their properties	181
04-3-11 Tomchuk O.V.	Tuning of the porous structure of detonation nanodiamond powders by pressure: SANS study	182
04-3-12 Trofimuk A.D.	Removal of several atomic layers in detonation nanodiamond particles	183
04-3-13 Utesov O.I.	Nanodiamonds size, shape, and defectness determination using Raman spectroscopy	184
04-3-14 Yudina E.B.	Nanodiamond deagglomerated by annealing under argon: infrared spectroscopy and mass-spectrometry study	185
04-4-01 Abbas R.	Density functional theory calculation for fullerene-lysine system	186
04-4-02 Andreev S.	Study of temporal changes in the spectrum of fullerene C ₆₀ in the presence of N-methylpyrrolidone	187
04-4-03 Aouane M.	Inelastic Neutron Scattering of endofullerenes: ³ HeC ₆₀ study	188

04-4-04 Elesina V.I.	Method for the extraction of EMF in a mechanical extractor	189
04-4-05 Magarill L.I.	Theory of electron states in cone made of graphene or other multivalley 2D systems.	190
04-4-06 Gerasimova L.V.	Solubility of rare earth chlorides in ternary water-salt systems in the presence of a fulleranol - C ₆₀ (OH) ₂₄ nanoclusters at 25°C	191
04-4-07 Khamatgalimov A.R.	The peculiarities of molecular structure of low-symmetry isomers of non-IPR fullerene C ₇₆	192
04-4-08 Kudoyarova V.Kh.	Observation of singlet oxygen in polysiloxan block-sopolimer, modified C 60	193
04-4-09 Sabirov D.Sh.	Algorithm for enumeration and generation of regioisomeric fullerene cycloadduct structures	194
04-4-10 Vnukova N.G.	Comparative characteristics of Sc ₂ C ₂ @C ₈₂ and C ₈₄ polymerization under high pressure	195
04-5-01 Amusia M.Ya.	Role of fullerenes shell in time delay of photoelectrons from endohedrals	196
04-5-02 Andreev S.	Facile organosilicon-based route for synthesis of fullerene amino acid adducts	197
04-5-03 Fokin N.S.	The structure of water-soluble derivatives of endohedral metallofullerenes and features of their self-organization in aqueous solutions	198
04-5-04 Gerasimova L.V.	Catalytic fulleranol action on chlorella growth in the conditions of limited resource base	199
04-5-05 Khamatgalimov A.R.	Is there a molecular symmetry lowering in open-shell IPR higher fullerenes?	200
04-5-06 Kopeuw A.J.	Quantum chemistry simulation of halogenated fullerene. Regiochemistry and vibrational spectra.	201
04-5-07 Lyutova Zh.B.	Antioxidant properties of water-soluble fullerene derivatives	202
04-5-08 Mikheev I.V.	Aqueous fullerene dispersions: preparation techniques, characterization, and applications	203
04-5-09 Sabirov D.Sh.	Bader's bond ellipticity as a reactivity index in the stepwise [2+1] cycloaddition reactions to the C ₆₀ fullerene	204
04-5-10 Suyasova M.V.	Structural features of new fullerene derivatives according to IR-, Raman- and UV/Vis-spectroscopy	205
04-5-11 Tropin T.V.	Kinetics of cluster growth in C ₆₀ -toluene solutions: DLS study and theoretical evaluation	206
Day 5: Applications of Nanocarbons.		207
05-1-01 Gryaznova M.I.	Exfoliated graphite-based carbon ink for screen-printing applications	208
05-1-02 Menshchikov I.E.	Thermodynamics of xenon adsorption on nanoporous SiC-derived carbon affected by adsorption-induced and thermal strain	209
05-1-03 Mikheev I.V.	In vitro evaluation of fullerenes and endofullerenes in aqueous dispersions as superoxide scavengers and their toxicity	210

O5-1-04 Nishchakova A.D.	
Ni catalysts on N-doped and N-free porous carbon materials for hydrogen production from formic acid	211
O5-1-05 Shkolin A.V.	
Deformation of nanoporous carbon adsorbent induced by methane adsorption in wide range of pressures and temperatures	212
O5-2-01 Katin K.	
Ab initio study of fluorinated fullerenes as drug delivery systems	213
O5-2-02 Litasova E.V.	
Development of delivery systems based on fullerene C ₆₀ and application prospects	214
O5-2-03 Shkolin A.V.	
The model of adsorption/desorption process on nanoporous carbon materials under the thermal insulation conditions	215
O5-2-04 Tomchuk A.A.	
Comparative structural and in vitro toxicity study of C ₆₀ -lysine and C ₆₀ -piperazine aqueous solutions for biomedical purposes	216
O5-2-05 Turetskiy E.	
Fullerene C ₆₀ exhibits no subacute toxicity in mice after repeated administration	217

Author Index

A

Abbas R. - 186
Aborkin A.V. - 134
Abramenko N.D. - 71
Adilov V.F. - 100
Afzal A.M. - 95
Aksenov V.L. - 206
Alekseev D.V. - 136, 157
Alexinskii A.E. - 169
Almazova N.S. - 164
Amanzholova G. - 89
Amusia M.Ya. - 196
Andreev S. - 187, 197, 217
Andreev S.M. - 216
Anisimov A. N. - 112
Anosov A.A. - 75
Antonov G.A. - 59, 60, 77
Aouane M. - 188
Arefina I.A. - 111
Arenal R. - 10
Arnault J.-Ch. - 174
Artemyev A.N. - 198
Aruev N.N. - 185
Arutyunyan N.R. - 102, 114
Avdeev M.V. - 182, 206, 216
Avramenko N.V. - 64

B

Badun G.A. - 26, 147, 151, 163
Baidakova M.V. - 50, 59, 65, 67, 75, 77, 78, 79, 144
Bakirov A.V. - 172
Bakunin E.S. - 41
Barabashko M.S. - 139
Baranchikov A.E. - 180
Baranov A.V. - 165, 173
Baranov M.A. - 165
Baranov P. G. - 112
Baryshnikov K.A. - 35
Belenkov E.A. - 92, 103
Belenkov M. E. - 62, 103
Belonenko M.B. - 149
Belousov S.I. - 161, 166, 172
Berezkin V.I. - 99
Besedina N.A. - 159
Beskachko V.P. - 133
Bets K.V. - 12
Bogdanov K. - 38, 165, 173
Bokai K.A. - 53
Bolshakova O.I. - 155
Borisenkova A.A. - 202, 205

Boytsova O.V. - 73
Breev I. D. - 112
Brevnov P.N. - 75
Brotsman V.A. - 73
Brun E. - 174
Brunkov P.N. - 50, 59, 60, 67, 77, 78
Brusko V.V. - 120
Brzhezinskaya M. - 50, 78, 79, 103
Buga S. G. - 171
Bugrov A.N. - 72
Bulavin L.A. - 182
Bulushev D.A. - 211
Bulusheva L.G. - 32, 83, 90, 91, 117,
123, 137, 138, 141, 211
Bunyaev V.A. - 26, 147
Burakova E.A. - 41, 93
Burganov T.I. - 192
Burikov S.A. - 86, 96
Burkov A.A. - 69
Butko A.V. - 54
Butko V.Y. - 54

C

Cami J. - 22
Cedeno M.E. - 94
Chapaksov N.A. - 113
Charykov N. A - 191, 199
Chen X. - 63
Cheretaeva A.O. - 57, 131
Chernogorova O.P. - 104
Chernov V. M. - 62
Chernova E.A. - 73
Chernysheva L.V. - 196
Chernysheva M.G. - 26, 147, 151, 163
Chesnokov V.V. - 27
Chichkan A.S. - 27
Chilingorov N.S. - 109
Chizhikova A.S. - 142
Chugaev S.S. - 215
Chugreeva G.N. - 96
Chumakov A.P. - 73
Chumakova N.A. - 52, 74, 143
Churilov G.N. - 189, 195
Chuvilin A.L. - 32
Chvalun S.N. - 161, 166, 172
Colin M. - 63

D

Danilov D.V. - 111
Danilov E.A. - 28
Danilova E.A. - 46

Darkhanov E.V. - 28
Das A. - 111
Davydov V.Y. - 51, 54
Denisenko E.I. - 46
Denisov E.A. - 57, 131
Desyatov S.V. - 154
Dideikin A.T. - 61, 72, 159, 169, 183
Digurova A.I. - 82
Dimiev A.M. - 120
Dmitriev A.P. - 35
Dolenko T.A. - 86, 96, 101
Dolmatov V.Yu. - 14, 154, 164, 180
Dorokhov A.O. - 164
Drozdova E.I. - 104
Dubois M. - 63
Dubovenko R.R. - 148
Ducrozet F. - 174
Dyachkova T.P. - 41, 93, 113
Dzhanabekova R.Kh. - 89

E

Efremov V.P. - 181
Egorov A.V. - 163
Ehrlich H. - 107
Ekimov E.A. - 104
Elbakyan L.S. - 125
Elesina V.I. - 189
Eliseev A. A. - 73
Eliseev A.A. - 29, 39
Eliseev Ar. A. - 73
Eliseyev I.A. - 54
Emelyanov A.A. - 162, 170
Entin M.V. - 190
Eremina E.A. - 64, 143
Eurov D. A. - 97
Evlashin S.A. - 44, 66
Ewels C.P. - 9
Ezdin B. S. - 33

F

Fazlitdinova A.G. - 105
Fedorov A.V. - 111
Fedorov D.L. - 97
Fedorov M.V. - 48
Fedoseeva Y. V. - 83, 90, 91, 138, 141
Fedotov A.A. - 128
Feoktistov N.A. - 165
Filipovich S. - 58, 76
Filonenko V.P. - 171
Fokin N.S. - 198
Fomenko V.V. - 154
Fomin E.V. - 167
Fominski V.Yu. - 171
Fomkin A.A. - 126, 209, 212

Fursei G. N. - 42

G

Gaidamavichute V.V. - 126
Galyaltdinov S.F. - 120
Garipov R.R. - 127
Gavrilov Yu.V. - 131
Gerasimenko A.Y. - 115
Gerasimova A.V. - 113
Gerasimova L.V. - 191, 199
Gerasimova T.P. - 192
Girard H.A. - 174
Glushenko G.A. - 195
Gnedova E. A. - 114
Gofman I.V. - 177
Golubev V. G. - 97
Golubev V.G. - 165
Gonzalez Lucy T. - 85
Gorbachev V.A. - 181
Gorbachev Y.E. - 156, 168
Gorenberg A.Ya. - 75
Gorodetskii D.V. - 32
Goshev A.A. - 118
Gozhikova I.O. - 175
Greibenkina M.A. - 83, 90, 91, 141
Grebnyuk G.S. - 150
Greshnyakov V.A. - 92, 103
Grudinkin S.A. - 165
Gruen D.M. - 8
Gryaznov K.O. - 208
Gryaznova M.I. - 208
Gudilin E.A. - 64
Gudkov M.V. - 55, 65, 75, 77, 78, 79, 144
Guerin K. - 63
Gurianov K.E. - 29
Guzei D. - 122

H

Haenen K. - 21
Hramco C - 169

I

Ibrayev N. - 68
Ibrayev N. Kh. - 89
Ichkitidze L. - 115
Il'in O.I. - 121, 128, 129
Il'ina M.V. - 121, 128, 129
Ilyin V.V. - 214
Ilyushin M.A. - 70
Ionov A.N. - 72
Ishiguro Y. - 158
Ismagilov A.O. - 111
Istomin A.M. - 41
Ivan'kova E.M. - 72

Ivankov O.I. - 182
Ivanov A.V. - 198, 205
Ivanov P.D. - 116
Izotova S.G. - 186, 201

J

Jalolov F.N. - 84
Jurina L.V. - 95

K

Kalashnikova E.I. - 30, 40, 45
Kalika E. - 213
Kalyada V. V - 33
Kamyshnikov O. - 217
Kanbar A. - 191, 199
Kapitanova O.O. - 73
Kaplin A.V. - 64, 143
Kapustin S. N. - 176
Karaeva A.R. - 208
Kareev I.E. - 203, 210
Katin K. - 213
Kaya S. - 213
Keskinov V.A. - 191, 199
Kessler I.O. - 47
Ketkov S.Yu. - 134
Khaitov M. - 187, 197, 216, 217
Khamatgalimov A.R. - 192, 200
Khamidullin T.L. - 120
Khamova T.V. - 180
Khantimerov S.M. - 127
Kharchenko I. - 122
Kharisov B.I. - 85, 94
Kharissova O.V. - 85
Khozina E.V. - 209
Kidalov S.V. - 30, 36, 40, 43, 45, 49, 183
Kirilenko D.A. - 50, 59, 60, 67, 77, 78, 98, 159
Kislenko S.A. - 48
Kislenko V.A. - 48
Kitsyuk E.P. - 115
Klimenko I.V. - 31, 95
Klimin V.S. - 47, 56
Knizhnik A.A. - 19
Kolesnikova A.L. - 71
Komarov I.A. - 37, 46, 60, 144
Koniakhin S.V. - 159, 184
Konobeeva N.N. - 149
Kopeuw A.J. - 201
Kopitsa G.P. - 180
Kornev A.Y. - 41
Korobkina E. - 169
Korobko A. - 122
Korobov M.V. - 64, 74, 203, 210
Koroleva A.V. - 111

Korzhenevsky A.P. - 179
Kostikova E.K. - 57
Kostyuk S.V. - 210
Kotsun A.A. - 117, 137
Kovalenko V.I. - 192, 200
Kovalevski V.V. - 106
Kozhushnyi K.A. - 101
Kozlov A.S. - 154
Kozlova S. - 122
Krasheninnikov V.G. - 75
Krasnoborodko S. Yu. - 171
Ksenofontov A.L. - 26
Kubas A. - 17
Kudoyarov M. F. - 193
Kudoyarova V.Kh. - 193
Kuklin A.I. - 177
Kukushkina Yu.A. - 61
Kulakov R.A. - 118
Kulbina A.S. - 149
Kulenova N.A. - 191, 199
Kulvelis Yu.V. - 65, 155, 167, 177
Kumzerov Y.A. - 54
Kupreenko S.Y. - 93
Kurdyukov D. A. - 97
Kuziv I. - 178
Kuznetsov N.M. - 161, 166, 172
Kuznetsova V.A. - 111
Kvashnin A.G. - 84
Kvitsinskiy A. - 38

L

L'vov S.G. - 127
Laptinskiy K.A. - 86, 96
Latypov R.M. - 119
Lebedev A.A. - 54
Lebedev S.P. - 54
Lebedev V.T. - 155, 167, 177
Leksikov A.V. - 171
Len A. - 182
Lermontov S.A. - 15, 175
Leshchev D.V. - 156, 168
Lewandowska-Andralojc A. - 17
Litasova E.V. - 214
Litvin A.P. - 111
Lobanov A.V. - 31
Lobanova E.Yu. - 150
Lomonosov V. - 58, 76
Longoria Rodriguez F.E. - 85
Lugvishchuk D.S. - 208
Lukina I.N. - 104
Lvova N.A. - 82
Lychagin E.V. - 16, 169
Lyutova Zh.B. - 202

M

Magarill L.I. - 190
Malkov M. N. - 60
Mamin G.V. - 51
Manohar R. - 124
Marchenko D. - 53
Marchukov V.A. - 154
Marinenko E.A. - 177
Markovskii Yu.A. - 106
Maslov M. - 213
Mateyshina Yu.G. - 136, 157
Mavrinskii V.V. - 92
Melezhik A.V. - 113
Melnikov V.P. - 55, 75, 144
Memetov N.R. - 113
Menard-Moyon C. - 23
Menchshikov I.E. - 215
Mendez-Rojas M.A. - 94
Menshchikov I.E. - 126, 209, 212
Menshova E. - 68
Mikhailenko E.K. - 150
Mikhailovskii V.Yu. - 53
Mikheev I.V. - 203, 210
Mikhlina E. - 122
Minakov A. - 122
Mithberg E.B. - 208
Molodtsov S. - 107
Mordkovich V.Z. - 208
Morozova J.V. - 47, 56
Moshnikov I.A. - 106
Mozhayko A.A. - 130
Mumdzhi I.E. - 51
Murzakhanov F.F. - 51
Muzychka A.Yu. - 169
Myakishev A.Y. - 108
Myllymaki V. - 164

N

Naryzhny S.Yu. - 154
Nechaev Yu.S. - 57, 131
Nekipelov S.V. - 107
Nelson D. K. - 97
Nemtsev I. - 122
Nesvizhevsky V.V. - 169
Neverovskaya A.Yu. - 42, 43
Nezvanov A.Yu. - 169
Niftalieva V.V. - 47
Nikolaev V.V. - 139
Nikolaeva M.N. - 72
Nishchakova A.D. - 90, 138, 211
Novikau U. - 58, 76
Novokshonova L.A. - 75

O

Ob'edkov A.M. - 134
Obraztsova E. - 38
Obraztsova E. D. - 102, 114
Obraztsova E.Y. - 41
Odinokov A.S. - 177
Okotrub A.V. - 32, 83, 90, 91, 117, 123, 137, 141
Oliva Gonzalez C.M. - 85
Orekhov N.D. - 66
Orlinskii S.B. - 51
Orlova D.N. - 198, 205
Orlova T.S. - 87, 98
Osipov V. Yu. - 158, 173
Osotova O.I. - 121, 129
Ovchinnikov E.V. - 30, 45
Ovchinnikov-Lazarev M.A. - 179
Ozerin A.N. - 164

P

Pakharukov Yu. V. - 33
Palyanov Y.N. - 32
Panova G.G. - 180
Parfenov A.S. - 69, 93, 113
Parfenov P.S. - 111
Pasko A.A. - 93
Patrova M.Ya. - 193
Pavlov A.V. - 132
Pavlov S.I. - 50, 59, 60, 65, 67, 77, 78
Pavlov S.S. - 169
Pavlov S.V. - 48, 79
Peretiyagin V.G. - 46
Peters G.S. - 155
Petrenko V.I. - 206
Petrova O.V. - 107
Petrova V.I. - 151
Petukhov D.I. - 29, 39, 73
Petukhov V.A. - 34
Piotrovsky L.B. - 214
Plotnikov M.Yu. - 162, 170
Podlozhnyuk N.D. - 49
Polotskaya G.A. - 148
Polozkov R.G. - 132
Polyakov M. A. - 42
Polyvyanova O.R. - 128
Ponomarev A.N. - 139
Ponomarev D.A. - 87, 98
Popov A.G. - 163
Popov D.S. - 143
Popov V.V. - 87, 98, 99
Popov Yu.M. - 195
Popova M.V. - 155
Portnoi M.E. - 132
Potapov D.O. - 66
Potorochin D.V. - 75

Primachenko O.N. - 177
Prokopenko D.A. - 104
Proskurnin M.A. - 203, 210
Proskurnina E.V. - 210
Pulyalina A.Yu. - 148

R

Rabchinskii M.K. - 34, 37, 46, 50, 55, 59, 60, 65,
67, 75, 77, 78, 79, 144
Razanau I. - 58, 76
Rebrikova A.T. - 64, 74, 143
Rebrov A.K. - 162, 170
Rezvan A.A. - 47, 56
Rezvanova A.E. - 139
Rodin E.A. - 88, 100, 108
Rodionova E.V. - 88, 100, 108
Rogach A.L. - 111
Romanov A.E. - 71
Romanov P.A. - 185
Romanov R.I. - 171
Romanyuk O. - 158
Romashkin A.V. - 34
Rostovtseva V.A. - 148
Rozhkov M.A. - 71
Rudyk N.N. - 128
Rukhov An.V. - 41
Rukhov Ar.V. - 41
Runov V.V. - 72
Ryabkov Ye.D. - 75
Ryabokon I.S. - 205
Rybin M. - 38
Ryzhkov I. - 122
Ryzhkov S.A. - 59, 60, 77, 78

S

Sabirov D.Sh. - 194, 204
Sadilov I.S. - 39
Safargaliev R.F. - 33
Safonova A.F. - 214
Sarantseva S.V. - 155
Saveliev S.D. - 59, 60, 78
Savilov S.V. - 69, 93
Savinova E.A. - 210
Sedov V.P. - 198, 202, 205
Seliverstova E. - 68
Selyshchev P.A. - 206
Semashkin G.V. - 154
Semavin K.D. - 109
Semenov K.N. - 191
Semenukha O.V. - 140
Serrano Quezada T.E. - 85
Shabiev F. K. - 33
Shabunina A.V. - 205
Shaimardanov Zh. K. - 191, 199

Shaimardanova B.K. - 191, 199
Sharonova L.V. - 183
Shashkin D.P. - 144
Shatilov A. - 187, 197, 217
Shchegolikhin A.N. - 95
Shelykh I.A. - 132
Shershakova N. - 187, 197, 217
Shershakova N.N. - 216
Shestakov M.S. - 159, 183
Shevchenko N.V. - 181
Shevchenko V.G. - 161
Shilin V.A. - 198
Shilov M.A. - 69
Shilova O.A. - 180
Shiyanova K.A. - 75, 77, 144
Shkolin A.V. - 126, 209, 212, 215
Shlyahova E.V. - 141
Shlyakhova E.V. - 83, 90
Shnitko A.V. - 26
Shnitov V.V. - 79
Shnitov V.V. - 50, 67
Shugalei I.V. - 70
Shvidchenko A.V. - 61, 145, 159, 160, 177, 185
Shyrygina N.A. - 57
Sicard-Roselli C. - 174
Sigalayev S.K. - 181
Sikarwar S. - 124
Siklitskaya A. - 17
Simunin M. - 122
Simunin M.M. - 140
Singh B.P. - 124
Sinolits A.V. - 151
Sivkov V.N. - 107
Skoi V.V. - 177
Skokan E.V. - 109
Skvortsova A.N. - 130
Smirnov A.N. - 51
Smirnov A.V. - 70
Smirnov D.A. - 79, 144
Smirnova A.I. - 41, 69, 113
Smirnova V.E. - 40
Smitnova A.I. - 93
Smyslov R.Y. - 72
Sokura L.A. - 144
Soldatova V.I. - 88
Solomatin M.A. - 67
Soltamov V.A. - 51
Sozarukova M.M. - 210
Sozykin S.A. - 116, 119, 133
Spitsyn A.A. - 87, 98
Spitsyn B.V. - 179
Staritsyn M.V. - 130
Starukhin A. N. - 97
Stehlik S. - 20, 158
Stolbov D.N. - 69

Stolyarova D.Yu. - 50, 59, 60, 67, 78, 79, 144
Stolyarova S.G. - 83, 91, 117, 123, 137
Stonkus O.A. - 211
Stovpiaga E. Yu. - 97
Strizhenov E.V. - 215
Struchkov N.S. - 34, 37, 67
Suleimanov N.M. - 127
Suyasova M.V. - 198, 205
Sysoev V.V. - 67

T

Takai K. - 158
Tchougreeff A.L. - 110
Telyshev D.V. - 115
Timofeeva A. - 187, 197, 217
Timofeeva V.A. - 144
Timoshenko N.I. - 162, 170
Titkov S. V. - 112
Titova A.V. - 202, 205
Tkachenko M.V. - 139
Tkachev A.G. - 93
Tomanek D. - 11
Tomchuk A.A. - 216
Tomchuk O.V. - 182
Tomilin O.B. - 88, 100, 108
Tomkovich M.V. - 61, 99
Tomskaya A. E. - 96, 114
Torok Gy. - 167
Trofimuk A.D. - 61, 144, 183
Tropin T.V. - 206
Trubina S.V. - 211
Trusova E.A. - 31, 95
Tsvetkov K.A. - 191
Tudupova B.B. - 145
Tukhbatullina A.A. - 204
Turetskiy E. - 187, 197, 216, 217
Tyumentsev V.A. - 105

U

Usachov D.Yu. - 53
Ushakova E.V. - 111
Usol'tseva N.V. - 41, 69, 93, 113
Utesov O.I. - 184
Uvarov N.F. - 157

V

Valeev R.G. - 73
Varezchnikov A.S. - 67
Vasiliev A.L. - 18
Vasilyev Yu.B. - 35
Vdovichenko A.Yu. - 59, 161
Vedernikov Y.N. - 70
Vehanen A. - 164
Verbetsky V.N. - 147

Veretennikov M.R. - 28
Vervalde A.M. - 101
Verzhichinskaya S.V. - 131
Vilkeeva D.E. - 125
Vilkov I.V. - 134
Vilkov O.Yu. - 53
Vinogradova L.V. - 148
Vins V.G. - 13
Vnukova N.G. - 189, 195
Voiteshenko I.S. - 216
Volkov A. S. - 176
Volkov D.S. - 203
Volkov M.P. - 72
Volochaev M. - 122
Vorfolomeeva A.A. - 83, 91, 123, 141
Vorobiev A.Kh. - 52, 74
Voronina S.Yu. - 140
Votyakova V.S. - 151
Vozniakovskii A.A. - 40
Vozniakovskii A.A. - 30, 36, 42, 43, 45, 49, 70
Vozniakovskiy A.P. - 193
Voznyakovskii A.P. - 30, 36, 40, 42, 43, 45, 49, 70, 193
Vul' A.Ya. - 155, 166, 167, 169, 172, 177
Vul S.P. - 61
Vysokikh Yu. E. - 171
Vysotina E.A. - 181

Y

Yakobson B.I. - 12
Yakovleva V. V. - 112
Yankova T.S. - 52
Yashenkin A.G. - 184
Yavkin B.V. - 51
Yudin I.B. - 162, 170
Yudina E.B. - 142, 159, 160, 161, 166, 172, 177, 185

Z

Zabulonov Yu.L. - 182
Zaitsev A. - 38
Zakirov I. I. - 42
Zakirova A.D. - 194
Zaporotskova I.V.. - 125
Zarvin A. E. - 33
Zavaleev V.A. - 179
Zhirov M.S. - 146
Zhizhin E.V. - 111
Zhukov A.N. - 160
Zinin P.V. - 171
Zykov D. - 38



FUND FOR INFRASTRUCTURE AND EDUCATIONAL PROGRAMS

RUSNANO Group

<http://www.fiop.site>

Fund for Infrastructure and Educational Programs (part of RUSNANO Group)

A non-profit organization that promotes the creation of infrastructure for the Russian nanotechnology industry and is part of the "innovation lift" system of Russian development institutions. The Fund is financed by the Russian federal budget.

The Fund works in seven main areas:

- (1) Development of technology infrastructure.
- (2) Building human resources for the nanoindustry:
- (3) Development of the market for innovative products.
- (4) Standardization, certification and safety assessment of nanotechnology products.
- (5) Metrological support for the nanoindustry.
- (6) Improvement of legislation in the innovation sphere.
- (7) Popularization of nanotechnologies.

10a Prospect of the 60th Anniversary of October, Moscow, 117292, Russia,

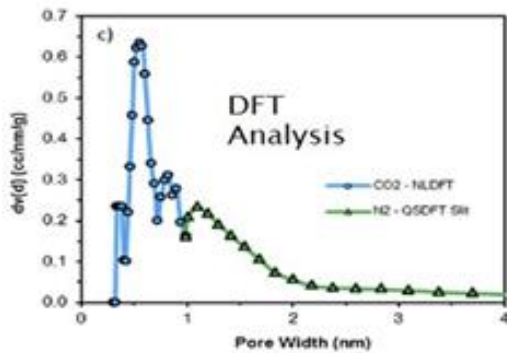
Telephone: +7 (495)988 53 88

E-mail: info@rusnano.com

www.fiop.site

Analysis of carbon materials by Anton Paar

Analysis of the size of micropores in porous carbon by CO₂ adsorption at 273.15 K (0° C) on analyzers from Anton Paar Quantatec Inc. (former Quantachrome Instruments)



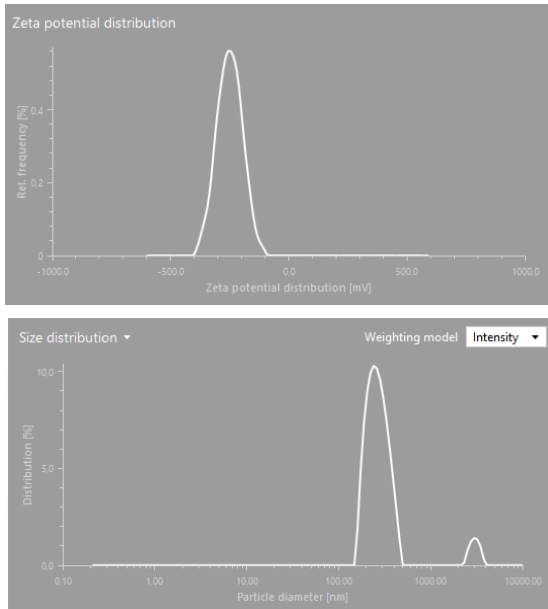
The CO₂-adsorption method provides access to the initial part of the adsorption isotherm for calculating the micropore size of carbon materials:

- analysis time 3-4 hours
- no more complex and expensive micropore analyzer required

Combining with nitrogen sorption makes it possible to obtain micro- and mesoporous characteristics of carbon materials.

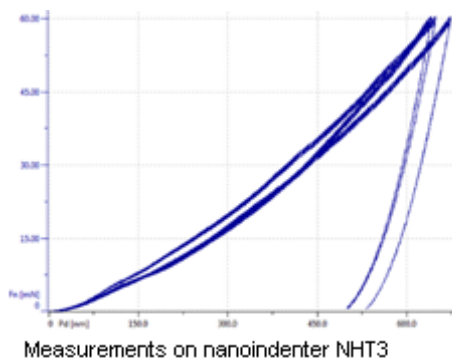
Instruments: NOVA, NOVAtouch with option of CO₂ - sorption

Black as the Night: Zeta Potential and Particle Size Measurements of Carbon Black Dispersed in Organic Solvents using Anton Paar Litesizer® 500 Dynamic Light Scattering Analyzer



The Litesizer® 500 particle analyzer provides the possibility to determine particle size (including polydispersity index and size distribution plots), zeta potential, average molecular weight of particles, as well as the determination of the refractive index of the solvent and real-time monitoring of the optical transmission of the sample. Due to high-precision optics with automatic selection of measurement parameters, the Litesizer® 500 allows you to examine the widest range of samples, including highly concentrated and very cloudy. Variety of cuvettes allows measurements in both aqueous and organic media. The graphs on the left represent the zeta potential and particle size of carbon black dispersed in various organic solvents. More detailed information can be found at the [link](#), as well as on the website paar.ru.

Determination of the mechanical properties of coatings using scratch analysis, indentation and tribological tests on Anton Paar TriTec equipment (former CSM Instruments)



The mechanical properties of a DLC coating are determined by nanoindentation methods (hardness and elastic modulus), scratch tests (adhesion force, friction force), tribological tests (friction force, coefficient of friction, wear assessment) and coating thickness measurement. It is possible to combine modules on one platform for complex analysis of samples.

Partners and Sponsors



**FUND FOR INFRASTRUCTURE
AND EDUCATIONAL
PROGRAMS**

RUSNANO Group

AVRORA
MEASURING TECHNOLOGIES

ISBN 978-5-93634-069-7



9 785936 340697 >